Functional Modules in the flocculus of the rabbit cerebellum

Functional Modules in the flocculus of the rabbit cerebellum

Functionele modules in de flocculus van het cerebellum van het konijn

PROEFSCHRIFT

Ter verkrijging van de graad van doctor
aan de Erasmus Universiteit Rotterdam
op gezag van de rector magnificus
Prof. dr. P.W.C. Akkermans M. Lit.
en volgens besluit van het College van Dekanen.
De openbare verdediging zal plaatsvinden op
woensdag 15 december 1993 om 15.45 uur.

door

Tjiauw Hok Marinus Tan

geboren te Jogjakarta, Indonesie

Promotiecommissie

Promotoren:	Prof. dr. J. Voogd
	Prof. dr. J.I. Simpson
Overige leden:	Prof. dr. H.J. Groenewegen
	Dr. J. van der Steen

Index **page**

Aan

pap en mam

Zonal patterns in the cerebellum

Many studies, using different anatomical and physiological techniques, have aimed at subdividing the cerebellum into distinctive parts that exert control over specific motor systems for reflex and voluntary movements, posture, and muscle tone. In view of the homogeneity of the cerebellar cortex, delineation can not be based on cytoarchitectonic differences as in the cerebral cortex. In the first half of this century the macroscopic subdivision of the cerebellum into lobes, lobules, and folia was used to distinguish functional units. The comparative anatomical studies of Bolk (1906) stressed the importance of the subdivision of the mammalian cerebellum into vermis and hemispheres. Bolk considered the vermis and hemispheres as continuous, relatively independent "folial chains", separated by the paramedian sulcus. Each of the folial chains can be subdivided into lobules, separated by deep, transverse fissures, and/or changes in the direction of the folial chain. In the anterior lobe and the adjoining part of the posterior lobe (the simple lobule) the transverse fissures continue uninterrupted from the vermis into the hemisphere. The separation into vermis and hemisphere is more complete in the caudal posterior lobe. In some regions the cortex between vermis and hemisphere is completely interrupted and white matter comes to the surface in the paramedian sulcus. Bolk (1906) used the variation among species in the size of different segments of the folial chains of vermis and hemispheres, in combination with differences in motor behaviour, to relate parts of the cerebellum to the control of specific motor behaviours. The comparative studies by Larsell (1934, 1937) showed the constancy in the development of the transverse lobular pattern throughout many mammalian species. This approach eventually culminated in the subdivision of the cerebellum into ten, transverse lobules, each of which was given a Roman numeral (Larsell, 1952).

Other concepts on the functional organization of the cerebellum

were based on the connectivity of different parts of the cerebellum. In the early fourties a series of tracing studies using the Marchi method by Jansen and Brodal (1940, 1942) demonstrated that each half of the cerebellum could be subdivided into 3 longitudinal zones that extended perpendicularly to the transverse fissures and continued from one lobule to the next. This subdivision was based on the projections of the Purkinje cells of the cerebellar cortex to their target nuclei. They distinguished a medial (vermal), an intermediate and a lateral (hemispheral) zone projecting to the fastigial, interposed, and lateral (dentate) cerebellar nuclei, respectively. This longitudinal zonation concept was supported by the findings of Chambers and Sprague (1955a, 1955b), who found that lesions in different longitudinal zones resulted in different patterns of deficiencies in motor behaviour, and they consequently concluded that this zonation reflected a differentiated arrangement of motor control.

The longitudinal subdivision was later found to be far more detailed. In the sixties the collective results of a series of anatomical tracing and myelin stain studies led Voogd (1964, 1969) to the conclusion that the cerebellum was subdivided into 7 longitudinal compartments and zones. By using the Häggqvist stain (Häggqvist, 1936), which reveals the axonal myelin sheaths, Voogd (1964) demonstrated that the cerebellar white matter is not homogeneous. In transverse sections, accumulations of thin fibers (the so-called "raphes") were observed. They run as longitudinal sheets across the transverse fissures and alternate with bundles of rather coarse fibers. These raphes subdivide the cerebellar white matter into compartments, each of which consists of a bundle of coarse fibers delimited on either side by a narrow sheet of thin fibers (the raphes). Recently, it has been shown that these raphes stain more densely for acetylcholinesterase (AChE) than the compartments they delimit (Hess and Voogd, 1986; Voogd et al., 1987). An explanation for the preference of AChE for the raphes has not yet been found.

The zonal organization of the cerebellar cortex is also reflected by the presence in the molecular and Purkinje cell layer of a longitudinal zonal arrangement of certain enzymes such as 5'-nucleotidase (Scott, 1963, 1964), and acetylcholinesterase (Marani and Voogd, 1977),

neurotransmitters such as motilin (Nilaver et al., 1982) and taurin (Chan-Palay et al., 1982) and Purkinje cell markers such as zebrin mabQ 113 (Hawkes and Leclerc, 1987).

The compartments contain the olivocerebellar climbing fiber afferents and the efferent axons of Purkinje cells that are distributed in discrete, longitudinal zones, which extend perpendicular to the transverse fissures. The axons from the Purkinje cells of a zone (or a combination of zones) terminate in a specific cerebellar or vestibular target nucleus. These Purkinje cells and their target nucleus both receive afferents from a particular subnucleus of the inferior olive (Voogd, 1964, 1969; Groenewegen and Voogd, 1977; Groenewegen et al., 1979; Voogd and Bigaré, 1980). A reciprocal nucleo-olivary pathway connects the target nucleus within this olivary subnucleus (Ruigrok and Voogd (1990). The ensemble of a Purkinje cell zone (or combination of zones), together with its target nucleus, its climbing fiber afferents, and it nucleo-olivary pathway constitutes an efferent cerebellar module (Voogd and Bigaré, 1980).

The modular organization of the cerebellum is characteristic for its output systems, but does not apply to the organization of its mossy fiber input. Terminal fields of mossy fiber systems and the axons of their target cells (the granule cells and the parallel fibers) are transversely oriented. The mossy fiber input of the cerebellum, therefore, is closely related to the transverse lobular subdivision of the cerebellum advocated by Larsell. The modular organization of the output systems of the cerebellar cortex can be considered as an elaboration of the concepts of Bolk and Jansen and Brodal on the longitudinal subdivision of the cerebellum.

Studies of the function of longitudinal zones or cerebellar modules are rare. The demonstration that acetylcholinesterase (AChE) stains the borders of compartments in the white matter of the flocculus (Hess and Voogd, 1986) and the interest of Dr. J.I. Simpson, who occupied the Tinbergen chair at the Erasmus University in 1989, in oculomotor control by the flocculus prompted us to undertake a combined anatomical and physiological study of compartments and Purkinje cell zones in the flocculus of the rabbit.

According to Bolk (1906; see also Voogd, 1975) the flocculus and the paraflocculus are the last two segments of the folial chain of the hemisphere. Between lobules IX and X of the caudal vermis and the paraflocculus and flocculus the cortex is interrupted and white matter comes to the surface at the bottom of the paramedian sulcus and the interparafloccular sulcus in the center of the folial loop of the paraflocculus. The paraflocculus and flocculus constitute a curved, foliated band that is delimited on its inner side by an extension of the white matter in the paramedian sulcus and on its outer border by the white matter of the cerebellar peduncles. The paraflocculus can be arbitrarily subdivided into dorsal and ventral limbs, which are known as the dorsal and ventral paraflocculus (Stroud, 1895). In some species a part of the paraflocculus, known as the petrosal lobule, is lodged in the subarcuate fossa of the petrosal bone.

The flocculus (Bolk's uncus terminalis) is a well-demarcated lobule that is located at the end of the folial chain of the hemisphere. Its border with the paraflocculus is formed by the posterolateral fissure, the earliest fissure to appear during ontogeny (Larsell, 1937). In the depth of the posterolateral fissure, the cortex of the flocculus and the paraflocculus are continuous. The gross anatomy of the flocculus and paraflocculus of the rabbit was described by Brodal (1940) and their morphogenesis was traced by Larsell (1972). Yamamoto and Shimoyama (1977) gave a detailed account of the foliation of the rabbit flocculus (fig. 0.1).

A zonal pattern has been identified for the climbing fiber afferent input and efferent output of the flocculus by numerous anatomical studies (see introduction of chapters 2 and 3) and physiological studies (see introduction of chapter 4). However, the number and extent of the zones, described in these studies vary considerably. Histological results from different experiments were compared by the use of positioning relative to the floccular folia. However, these folia show individual variation in size and number, which complicates matching histological results from different experiments.

Aim of the present study

To accurately compare histological results obtained in different experimental paradigms a framework, independent of any individual variation of the gross anatomy of the flocculus, is necessary. In chapter 1 AChE histochemistry is used to determine whether this technique shows a consistent compartmentalization pattern in the white matter that could then serve as the required independent framework. The distribution of AChE in the floccular cortex and white matter, in the lateral cerebellar nucleus and group y, and in the course of the floccular peduncle will be described.

The possibility that the compartments in the white matter of the flocculus correspond to anatomically and physiologically definable functional modules was investigated in studies reported in chapters 2, 3, and 4. The AChE chemoarchitecture of the floccular white matter, as described in chapter 1, could serve as an intrinsic framework that can be used to correlate the position of labeled Purkinje cells and climbing fibers with recording and stimulation sites in different sets of experiments. This approach would allow the correct matching of histological data obtained in anterograde (chapter 2) and retrograde tracing (chapters 3) and microstimulation (chapter 4) experiments in the rabbit flocculus. In chapter 2, studies on the origin, course and target zones of the afferent climbing fiber input to the flocculus and nodulus are reported. Chapter 3 concentrates on the differential efferent projection of the floccular zones to the vestibular and cerebellar nuclei. Chapter 4 considers the functional significance of this differential efferent projection by describing the types of eye movement elicited by stimulation of circumscribed compartments in the floccular white matter.

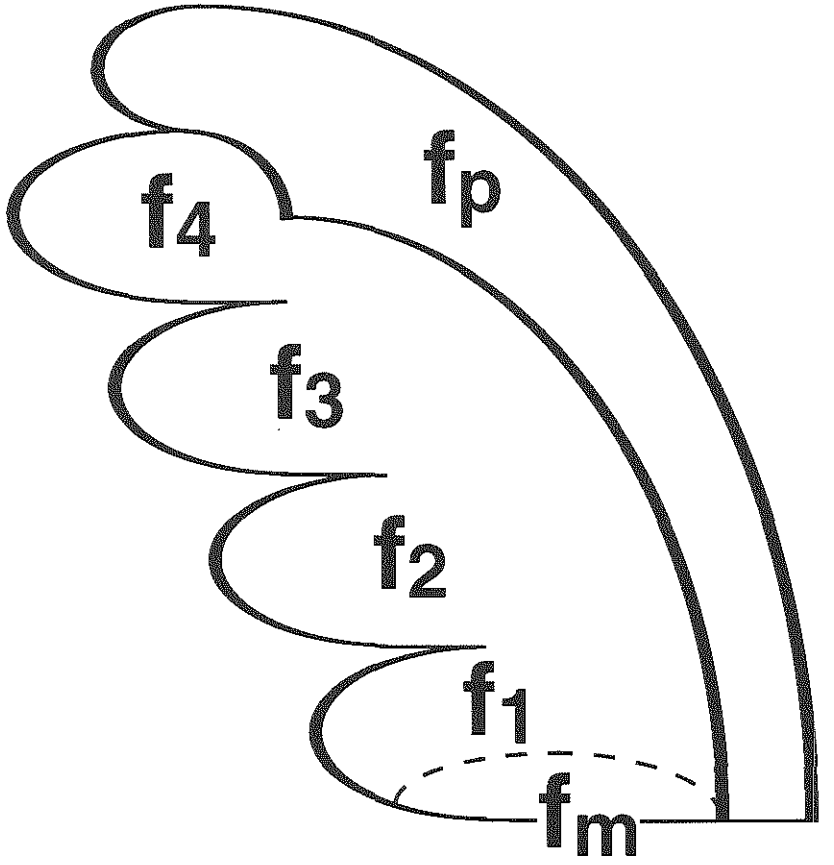

fig. 0.1 Schematic drawing of a lateral view of the flocculus showing the most common configuration of folia labeled according to Yamamoto and Shimoyama (1977).

Chapter 1

Anatomical compartments in the white matter of the rabbit flocculus.

1.1 Introduction

The subdivision of the cerebellum into longitudinal zones which extend perpendicularly to the transverse fissures and continue from one lobule to the next supplements the traditional subdivision of the cerebellum into lobes, lobules, and folia. These zones have been defined as longitudinal strips of Purkinje cells projecting to a particular cerebellar or vestibular target nucleus (Voogd, 1964, 1969; Voogd and Bigaré, 1980) or by the origin of their olivocerebellar climbing fiber afferents (Courville et al., 1974; Groenewegen and Voogd, 1977; Groenewegen et al., 1979; Brodal and Kawamura, 1980; Voogd, 1982; Bernard, 1987). A longitudinal zonal arrangement also has been demonstrated for Purkinje cells containing specific markers (Nilaver et al., 1982; Chan-Palay et al., 1981, 1982; Ingram et al., 1985; Hawkes and Leclerc, 1987) and for the distribution of enzymes, including acetylcholinesterase (AChE) in the molecular layer of the cerebellar cortex (Scott, 1963, 1964; Marani and Voogd, 1977a,b).

The zonal pattern of the cerebellar cortex is expressed in the cerebellar white matter as a system of compartments that contain the efferent axons and the climbing fiber afferents of the Purkinje cells of the longitudinal zones (Voogd, 1969; Voogd, 1989). These compartments can be distinguished with the Häggqvist myelin stain as bundles of rather coarse Purkinje cell fibers separated by narrow strips of thin fibers, the so-called "raphes" (Voogd, 1964, 1969). Since then, it has been shown that these raphes stain strongly for AChE (Hess and Voogd, 1986). The co-localization of axons of the Purkinje cells of a zone and their climbing fiber afferents in a particular white matter compartment and the termination of these Purkinje cell axons and collaterals of their climbing

fiber afferents in one of the cerebellar or vestibular nuclei formed the basis for the concept of the modular organization of the cerebellum (Voogd, 1969; Groenewegen and Voogd, 1977; Groenewegen et al., 1979; Voogd and Bigaré, 1980). In this concept a module consists of a discrete strip of Purkinje cells, its target nucleus and the olivocerebellar afferents to these two structures. Anatomical and electrophysiological studies that correlated climbing fiber afferents with the output of the cerebellar cortex of the anterior lobe in the cat generally supported the modular organization of this part of the cerebellum (Voogd, 1969, 1989; Oscarsson, 1973; Andersson and Oscarsson, 1978a,b; Trott and Armstrong, 1987a,b). Three compartments have been distinguished in the white matter of the paraflocculus in Häggqvist-stained sections of the cerebellum of cat and ferret (Voogd, 1964, 1969). The C_2 compartment is related to the posterior interposed nucleus, the D_1 and D_2 compartments access different parts of the dentate nucleus. Climbing fibers from the rostral medial accessory olive (MAO) use the C_2 compartment to terminate on Purkinje cells of the C_2 zone; the principal olive projects to the D_1 and D_2 zones of the paraflocculus (Groenewegen et al., 1979). Compartments in the white matter of the flocculus have until now only been observed in the cerebellum of the monkey by Hess and Voogd (1986) using AChE histochemistry.

Anatomical tracing and electrophysiological studies have shown that the afferent climbing fiber and the efferent connections of the flocculus are characterized by a zonal organization. Climbing fibers from the dorsal cap (dc), adjacent ventrolateral outgrowth (vlo) and the rostral medial accessory olive (MAO) terminate in the flocculus in a pattern of alternating longitudinal zones (Groenewegen and Voogd, 1977; Yamamoto, 1979a; Gerrits and Voogd, 1982, 1989; Sato et al., 1983; Ruigrok et al. 1992). The climbing fiber zones distinguished by Yamamoto (1979a) in the rabbit and by Sato et al. (1983) in the cat seem to coincide with Purkinje cell zones projecting to specific vestibular and cerebellar nuclei as delineated by the same authors (Yamamoto and Shimoyama, 1977; Yamamoto, 1978; Sato et al., 1982a,b). Seven and five climbing

fiber zones were distinguished in the flocculus of cat (Gerrits and Voogd, 1982) and rat (Ruigrok et al. 1992), respectively.

According to Bolk (1906, see also Voogd, 1975), the flocculus and the paraflocculus are the last two segments of the folial chain of the hemisphere. Between lobules IX and X of the caudal vermis and the paraflocculus and flocculus the cortex is interrupted and white matter comes to the surface at the bottom of the paramedian sulcus and the interparafloccular sulcus in the center of the folial loop of the paraflocculus. The paraflocculus and flocculus thus constitute a curved, foliated band of cortex, which is delimited on its inner side by an extension of the white matter in the paramedian sulcus and on its outer border by the white matter of the cerebellar peduncles. The paraflocculus can be arbitrarily subdivided into dorsal and ventral limbs, which are known as the dorsal and the ventral paraflocculus (Stroud, 1895). In some species a part of the paraflocculus, known as the petrosal lobule, is lodged in the subarcuate fossa of the petrosal bone.

The flocculus (Bolk's uncus terminalis) forms a well-demarcated lobule located at the end of the folial chain of the hemisphere. Its border with the paraflocculus is formed by the posterolateral fissure, one of the earliest fissures to appear during ontogeny (Larsell, 1937). The gross anatomy of the paraflocculus and the flocculus of the rabbit was described by Brodal (1940) and their morphogenesis was traced by Larsell (1972). The most detailed account of the foliation of the rabbit flocculus stems from Yamamoto and Shimoyama (1977).

Some of the Purkinje cell zones projecting to the vestibular and cerebellar nuclei (Yamamoto and Shimoyama, 1977; Yamamoto, 1978; Bigaré, 1980; Voogd and Bigaré, 1980), and some of the climbing fiber zones (Yamamoto, 1979a), including the C_2 zone which receives climbing fibers from the rostral half of the medial accessory olive (Gerrits and Voogd, 1982, 1989), extend across the posterolateral fissure into part of the ventral paraflocculus. This part of the ventral paraflocculus is known as the medial extension of the ventral paraflocculus (ME, Gerrits and Voogd, 1982) in the cat and corresponds to folium p in the rabbit (Yamamoto and Shimoyama, 1977).

For this paper the white matter compartmentation of the rabbit flocculus was studied using Häggqvist's myelin stain and enzyme histochemistry for AChE. Visualizing the borders of compartments with AChE enzyme histochemistry is particularly easy and can be used to compare the zonal distribution of the Purkinje cells with their climbing and mossy afferents and to correlate electrophysiological and anatomical data (Robertson and Logan, 1986; Tan et al., 1989; Van der Steen et al., 1991; see also Chapter 4).

1.2 Material and methods

Forty-five sectioned and AChE-stained brains of pigmented Dutch belted rabbits were prepared. Some of these rabbits were also used for axonal tracing or electrophysiological experiments to be reported in subsequent papers. For AChE histochemistry the rabbits were deeply anaesthetized with Nembutal and perfused intracardially first with 1 L of saline at room temperature, followed by 2 L of a solution containing 1-3% paraformaldehyde and 0.5-1.25% glutaraldehyde in 0.1 M phosphate buffer (pH 7.2-7.4) at room temperature, and finally with 10% sucrose in 0.1 M phosphate buffer (pH 7.2-7.4) at 4°C. The brainstem and cerebellum were removed, rinsed in 10% sucrose phosphate buffer, and embedded in a solution of 10% gelatin and 10% sucrose, which was hardened in 10% formalin. The embedded tissue was stored overnight in 30% sucrose phosphate buffer, after which it was cut into 30 or 40 μm transverse, horizontal or sagittal sections and processed for AChE. We used a standard thiocholine method to demonstrate AChE activity in the cerebellum (Geneser-Jensen and Blackstad, 1971). Acetylthiocholine acted as a substrate and ethopropazine as a blocking agent for non-specific cholinesterases (Hess and Voogd, 1986). Incubation times of 6-9 hours were used to obtain optimal staining of the AChE-positive fibers of the raphes. The sections were developed in a solution of 10% ferricyanide for 10 minutes, then rinsed in water, coverslipped and examined with a light microscope.

Alternate sections for the Häggqvist (1936) staining procedure

were stored in 10% formaldehyde for several weeks. After mounting, the slides were immersed in a solution of 10% potassium bichromate and 1% calcium chloride at room temperature for 4-5 days, then rinsed in distilled water and left in 96% alcohol for one day. Before staining in the Häggqvist solution (methylblue and eosin, 1-24 hr) the slides were immersed for 30 minutes in 10% phosphomolybdenic acid. A complete set of transversely sectioned Häggqvist-stained, celloidin embedded 40 µm sections through the rabbit cerebellum was also used (see Voogd and Feirabend (1981) for details on the Häggqvist stain). Three-dimensional reconstructions of the flocculus and its white matter compartments were prepared from styrofoam sheets or with the aid of the MacReco® program (by E. Luitjens, University of Groningen) running on an Apple Macintosh II computer.

1.3 Results

1.3.1 *The morphology of the flocculus and the paraflocculus.*

The flocculus is applied to the lateral surface of the middle cerebellar peduncle. It consists of three to four rostrolaterally facing folia, which are numbered f1-4 from ventral to dorsal (fig. 0.1). A short stretch of cortex of f1 that is folded back on the surface of the middle cerebellar peduncle (folium m of Yamamoto and Shimoyama, 1977) serves as the attachment of the roof of the lateral recess. Folia f3 and f4 are often fused, as was the case in the cerebellum depicted in fig. 1.1. Caudally the folia of the flocculus taper into a single folium. Caudally f3 and f4 taper and disappear and folium m, f1, and f2 fuse into a single folium. The posterolateral fissure demarcates the flocculus from the ventral paraflocculus. This fissure runs obliquely along the medial side of folium f4 to the caudomedial pole of the flocculus, where it opens on the ventral surface of the cerebellum.

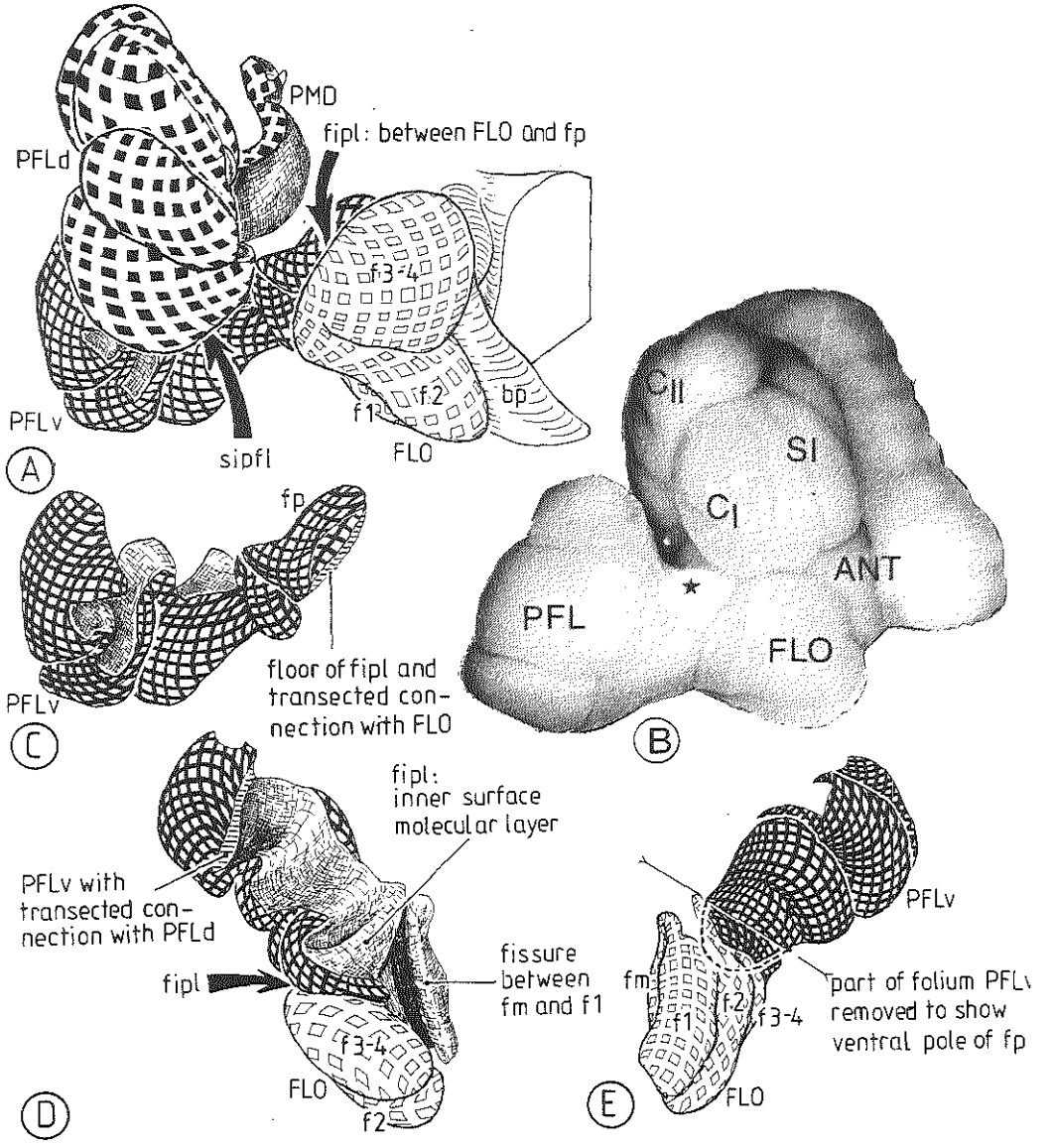
PMD
fipl: between FLO and fp
PFLd
f3-4
f2
f1
bp
PFLv
sipfl
FLO
A
fp
floor of fipl and transected connection with FLO
PFLv
C
CII
SI
CI
ANT
PFL
FLO
B
fipl:
inner surface
molecular layer
PFLv with
transected connection with PFLd
fipl
fissure
between
fm and f1
f3-4
FLO
f2
D
PFLv
fm
f1
f2
f3-4
part of folium PFLv
removed to show
ventral pole of fp
FLO
E

The folium of the ventral paraflocculus bordering on the flocculus (folium p of Yamamoto and Shimoyama, 1977) occupies a similar, oblique position. The cortices of f4 (or the fused folia f3 and f4) and folium p are continuous across the posterolateral fissure (figs. 1.2 nrs. 9-18). The posterolateral fissure is rather wide in this region and a narrow strip of cortex is found in the bottom between f4 and folium p (figs. 1.1 C; 1.9 A, C). More caudally, where the ventral paraflocculus starts to deviate laterally, white matter coming to the surface in the posterolateral fissure, separates folium p from the caudal pole of the flocculus (figs. 1.1 D; 1.2 nrs. 19-31). The cortex of the ventral paraflocculus covers the ventral surface of the paraflocular stalk and forms a rosette of three folia on the ventrocaudal aspect of the petrosal lobule, which in the rabbit consists of the entire paraflocculus. The two rosettes on the dorsal and caudomedial aspect of the petrosal lobule belong to the dorsal paraflocculus (fig. 1.1 A).

The folial chain of the paraflocculus and flocculus is reflected on the ventrolateral surface of the cerebellum. As a consequence, the mediolateral position of these lobules is reversed when compared to the proximal part of the chain, with their outer border facing medially.
Caudally, the cortex of the paraflocculus is continuous with the cortex of the paramedian lobule. More rostrally, white matter extending from the surface of the middle cerebellar peduncle separates the cortex of the paraflocculus and the flocculus from the anterior lobe and the simple, ansiform and paramedian lobules (asterisk in fig. 1.1 B).The white matter that borders the cortex of flocculus and paraflocculus on the lateral side is an extension of the white matter at the bottom of the paramedian sulcus

fig. 1.1 Drawing of a computer-reconstruction of the rabbit's right flocculus and paraflocculus. This specimen is also depicted in fig. 1.9. Only the molecular layer was reconstructed. *A)* Rostrodorsolateral view. Flocculus and ventral and dorsal paraflocculus are indicated with different symbols. For border between dorsal and ventral paraflocculus see text and fig. 1.6. *B)* Photograph of the rabbit cerebellum. Rostrodorsolateral view. Asterisk indicates white matter on dorsal surface of paraflocular stalk. *C)* The ventral paraflocculus, same view as in A. *D)* Dorsal view of the flocculus and the ventral paraflocculus. *E)* Ventral view of the flocculus and the ventral paraflocculus.

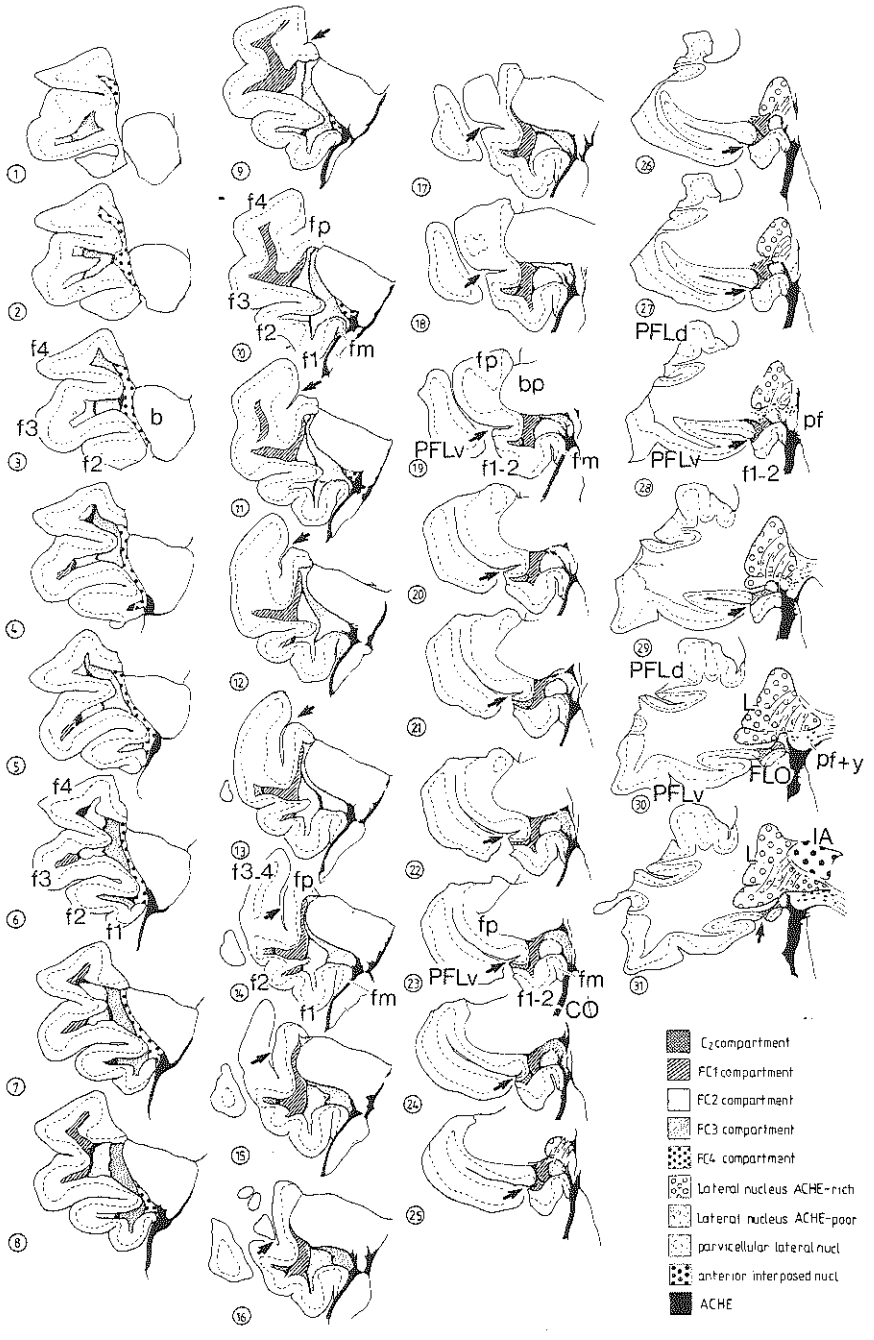
f4
f3
f2
b
f1
fp
fm
bp
PFLv
f1-2
PFLd
pf
L
FLO
pf+y
IA
f3-4
CO
C2 compartment
FC1 compartment
FC2 compartment
FC3 compartment
FC4 compartment
Lateral nucleus ACHE-rich
Lateral nucleus ACHE-poor
parvicellular lateral nucl
anterior interposed nucl
ACHE

between vermis and hemisphere. It extends from lobules IX and X of the caudal vermis, along the caudal border of the paramedian lobule over the petrosal lobule, where it radiates over the caudomedial surface of the folia of the flocculus and paraflocculus.

1.3.2 *AChE-staining of the cerebellar cortex.*

The granular layer of the cerebellar cortex of the rabbit stains more intensely for AChE than the molecular layer. The two layers are separated by the AChE-negative Purkinje cells. The staining in the granular layer is irregular with strongly reactive patches scattered between less reactive granule cells and neuropil. The AChE-positive patches were identified as glomeruli and Golgi cells, first by Gerebtzoff (1959) and later by many others (Csillik et al., 1963; Altman and Das, 1970; Brown and Palay, 1972). Generally the staining increases in the superficial part of the granular layer, next to and in between the Purkinje cells. Strong and more uniform AChE staining is present in the entire granular layer of the flocculus. The staining of the granular layer of folium p and its transition into the flocculus is particularly dense (fig. 1.3 D). Intense staining of the granular layer is also present in the vermis, in the depth of the fissures and in lobules IX and X, where it extends farther apically. The molecular layer of the flocculus and the ventral paraflocculus can be subdivided into two layers. The lower one third of the molecular layer, next to the Purkinje cell layer, is more densely stained than the superficial two thirds.

fig. 1.2 Schematic drawing of 31 transverse sections through the flocculus and ventral paraflocculus showing the location and course of AChE-positive raphes. The white matter compartments (C_2, FC_1-FC_4) and cerebellar nuclei are indicated with different symbols. Arrow points at the posterolateral fissure. Between the caudal pole of the flocculus and folium p the cortex is interrupted.

The AChE staining in the lower one third disappears abruptly at the proposed border of the ventral with the dorsal paraflocculus[1] .(fig. 1.6 A, arrow). The molecular layer of the dorsal paraflocculus is poor in AChE. Medium-sized AChE positive cells are found scattered over the lower half of the molecular layer in all lobules of the rabbit cerebellum (fig. 1.6 B, C). According to Spaçek et al. (1973) these AChE-stained cells correspond to the displaced Golgi cells of Cajal (1911).

1.3.3 *Topography of the flocculus and the floccular peduncle.*

In sections incubated for AChE a narrow strip of intensely stained fibers marks the border between the white matter of the flocculus and the middle cerebellar peduncle (figs. 1.2; 1.3; 1.10; 1.11; 1.13). Ventrally, the flocculus borders on the cochlear nuclei with the granular layer of its most ventral folium (folium f1 or m, figs. 1.2; 1.3 nrs. 4-29 and 1.3). The border between the dorsal cochlear nucleus and the granular layer, both of which react strongly for AChE, is sometimes difficult to establish. More caudally, where the medial cerebellar peduncle has entered the cerebellum, the fibers of the flocculus assemble in the floccular peduncle located between the flocculus and the restiform body, with the lateral cerebellar nucleus on its dorsal side and the dorsal cochlear nucleus more ventrally (figs. 1.2 nrs. 25-31; 1.6). The cells and the neuropil of group y, which stain strongly for AChE, appear in this area. Still more caudally the entire complex of the floccular peduncle and group y arches medially over the restiform body and merges with the superior and medial vestibular nuclei (fig. 1.7 B-D). The floccular peduncle and group y are located next to the cochlear nuclei and the dorsal acoustic stria, which follow a similar curve over the restiform body at a slightly more ventral and caudal level (fig. 1.7 C-E).

[1] A dorsal and a ventral paraflocculus have been distinguished in the cerebellum of the rabbit by several authors (Brodal, 1940; Larsell, 1970), but the precise border between the lobules was never indicated. It is proposed that this border is situated at the transition in the chemoarchitecture of the molecular layer of the two division of the para-flocculus (see fig. 1.6).

1.3.4 *Compartments and raphes in the white matter of the flocculus and paraflocculus.*

AChE histochemistry reveals narrow strips of densely stained fibers in the white matter of the cerebellum (figs. 1.2; 1.10; 1.11; 1.13). The strips separate more lightly stained fiber compartments. In serial sections the AChE-positive strips can be traced as sheets throughout the white matter of the flocculus and the paraflocculus (fig. 1.3). In a drawing of a computer reconstruction of the white matter of the flocculus the compartments appear as oblique slabs that taper towards the caudal pole of the flocculus (fig. 1.5). AChE positive fibers of the raphes coincide with accumulations of dark blue, small diameter fibers found in Häggqvist stained sections, at the borders (the so-called raphes) of white matter compartments containing larger diameter fibers (fig. 1.4). At the sites where the raphes meet the granular layer, this layer often stains more intensely. At these points the granular layer also shows a characteristic bulging into the white matter. These bulges form strictures in the white matter. In the vermis and hemispheres, concentrations of AChE-positive glomeruli are obvious in the midline and at certain parasagittal positions. Such a regular glomerular staining pattern is not seen in the flocculus or the paraflocculus.

In the white matter of the flocculus four raphes usually can be distinguished. They subdivide the white matter into five compartments (figs. 1.3; 1.5). The most lateral compartment corresponds to the C_2 compartment of Voogd (1964, 1969). The other four are numbered from lateral to medial and indicated as (floccular compartment) FC_1-FC_4 The raphes are named after the compartments they border.

Raphe $C_2/1$, the most lateral and one of the most intensely staining AChE raphes, can be traced from the white matter of the paraflocculus into the flocculus. It delimits a white matter compartment located on the caudal side of the stalk of the paraflocculus. In horizontal and sagittal sections (fig. 1.9; 1.12) reveal how this raphe becomes applied to the caudal border of the lateral cerebellar nucleus and continues as the border between the lateral and posterior interposed nuclei (fig. 1.7

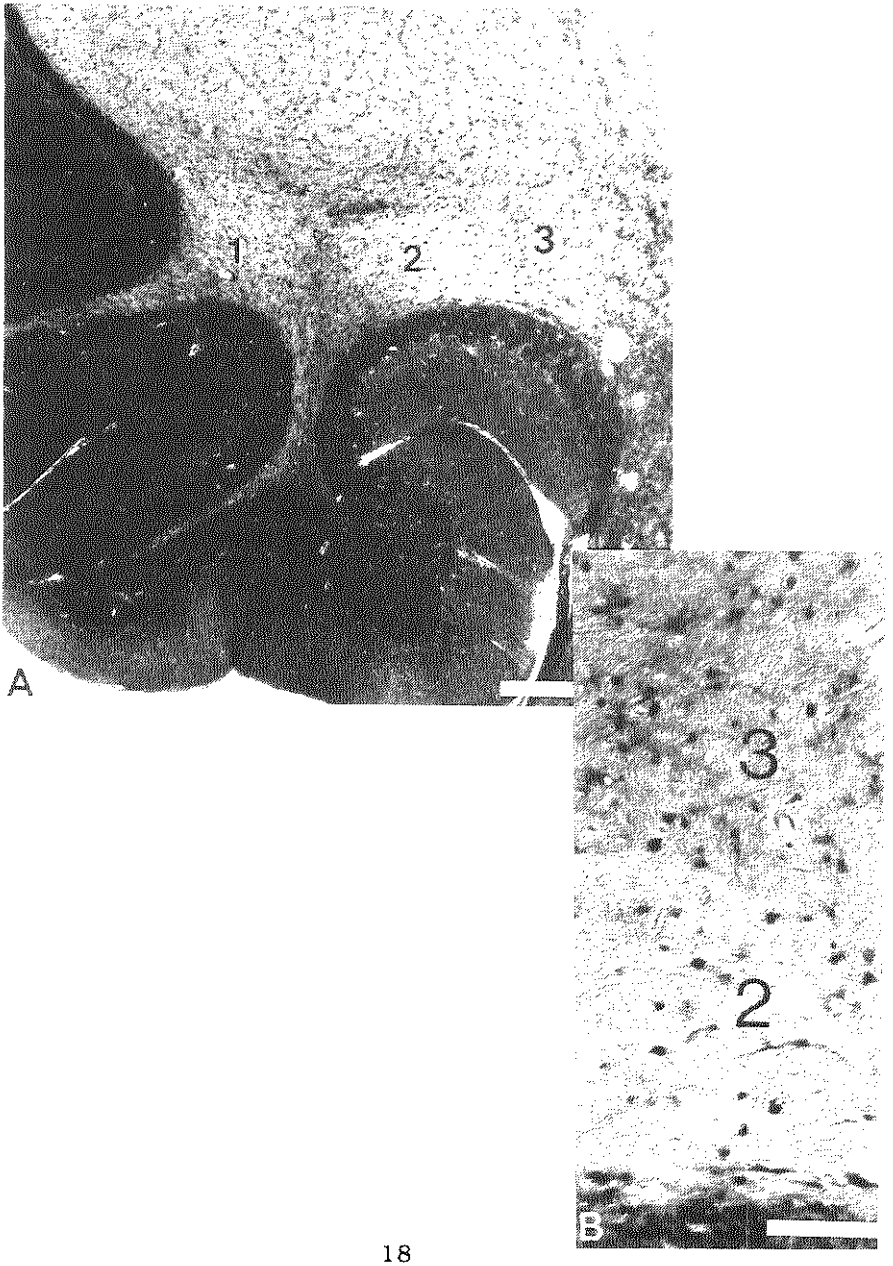
1
2
3
A
3
2
B

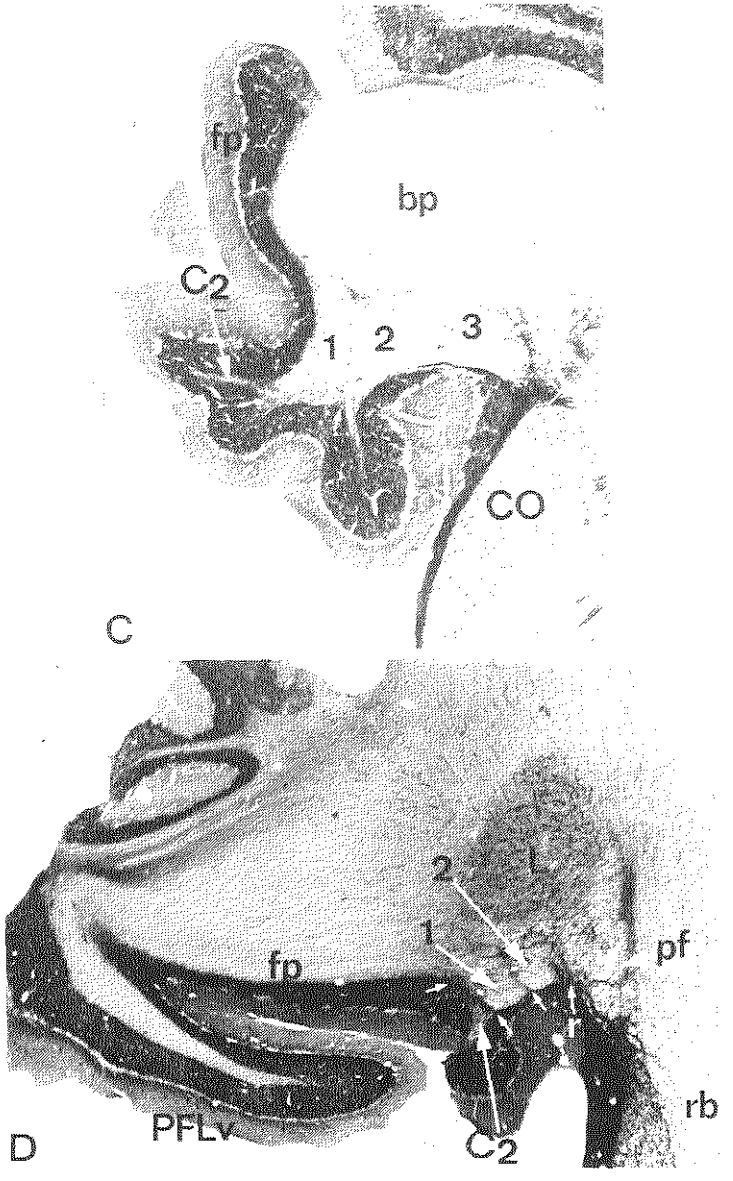

fig. 1.3 Photomicrographs of four AChE-stained transverse sections (A-D) through the left flocculus, corresponding respectively to sections 4, 11, 16, and 27 of figure 1.2. Small arrows indicate AChE-positive raphes between the compartments.

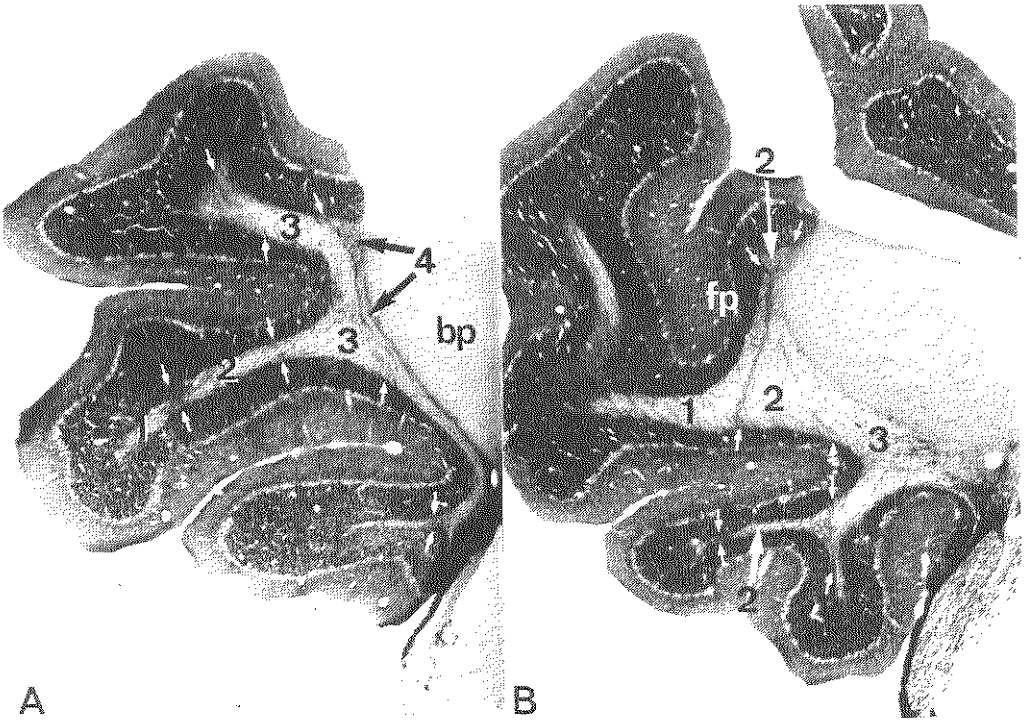

fig. 1.4 Photomicrographs of a Häggqvist-stained transverse section through the flocculus (A) and a high power view of the border area between compartments FC_2 and FC_3 (B). The level of the section approximately corresponds to fig. 1.3 C. Note the relatively coarse fibers in FC_2. Bar in A = 500 μm, and in B = 75 μm.

E-F). The caudal compartment of the paraflocculus, which contains the posterior interposed nucleus, therefore, can be identified as the C_2 compartment (Voogd, 1964, 1969). The C_2 compartment continues from folium p into the white matter of the caudal pole of the flocculus, from where it can be traced for a short distance into the white matter of f1-3 (figs. 1.2; 1.3; 1.7; 1.9-1.13). The large, rostral compartment of the paraflocculus supposedly corresponds to the D-compartment, but it does not show clear signs of a subdivision into D_1 and D_2 compartments as present in cat, ferret and monkey (Voogd, 1964, 1969, Voogd et al, 987, see, however, asterisk in fig. 1.11 A). Compartment C_2 stains rather

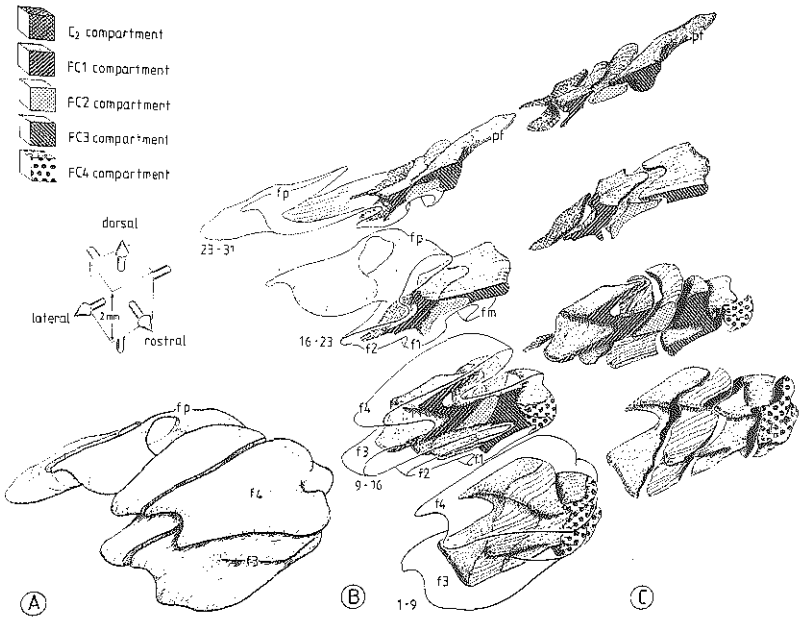

fig. 1.5 Drawing of a rostrolateral view of a computer reconstruction of the flocculus (A), the cortex and the five white matter compartments (B) and the white matter compartments pulled slightly apart (C). Note the oblique position of the compartments. In the caudal flocculus compartment FC_4 has disappeared, and FC_1 and FC_3 cover the FC_2 compartment. The reconstruction was generated from the sections depicted in fig. 1.2. The numbers in B refer to these sections.

densely for AChE. Compartments FC_1, FC_2, and FC_3 are present in all folia of the flocculus and in folium p. FC_2, FC_3, and FC_4 appear in the rostralmost sections of the transverse series depicted in fig. 1.2, FC_1 appears next and C2 is only present in the caudal half of the flocculus. When traced caudally the compartments shift medially and ventrally (figs. 1.2; 1.3; 1.5).

Raphe 1/2 is distinct and delimits FC_1 on its lateral side. FC_2 is

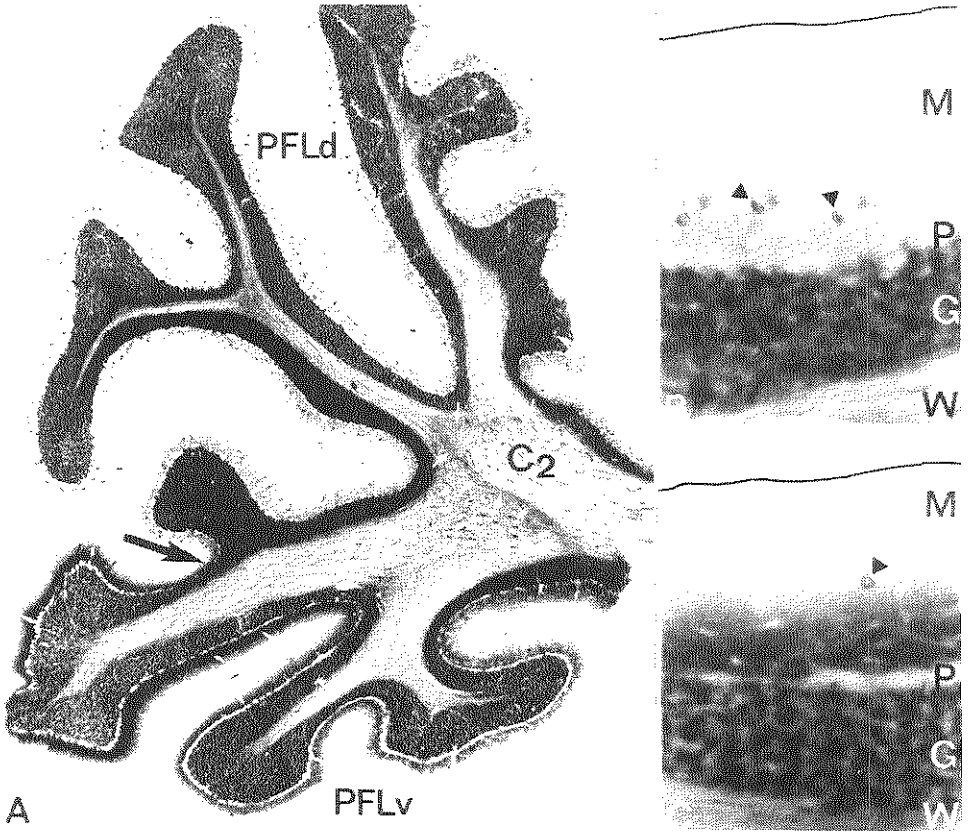

fig. 1.6 Photomicrograph of an AChE-stained transverse section through the dorsal and ventral paraflocculus and high power views of the cortical layers of the dorsal (B) and the ventral paraflocculus (C). Note the abrupt change in staining density of the inner third of the molecular layer of the dorsal paraflocculus at its border with the ventral paraflocculus (large arrow in A) and the displaced Golgi cells in the molecular layer (triangles in B and C). Small white arrows indicate the raphe bordering the C_2 compartment.

characterized by its pale appearance in comparison with the adjoining compartments FC_1 and FC_3 (fig. 1.3 C; 1.5). From Häggqvist-stained sections the impression is gained that the fibers contained in the FC_2 compartment are of a slightly larger calibre than those in the adjoining compartments (figs. 1.3 C; 1.4 A). The number of large fibers decreases and the amount of AChE increases in the lateral half of FC_2, towards the

intensely stained raphe 1/2 (figs. 1.4 A; 1.10 A). Raphes 1/2 and 2/3 fuse in the caudal half of the flocculus, dorsal to FC_2, which now has the shape of a triangle, with its base resting on the granular layer of folium f1 and its apex pointing dorsally. The point of fusion of the two raphes around the apex of FC_2 can always be recognized by intense staining for AChE (figs. 1.4 A; 1.10 A). The fused raphe 1/3 extends dorsally as the border between FC_1 and FC_3 and terminates at the granular layer of folium p. (fig. 1.2 nrs. 11-15; 1.3 B).

Compartment FC_3 is located between the raphes 2/3 and 1/3 laterally and raphe 3/4 and the medial border of the flocculus with the middle cerebellar peduncle medially. Raphe 2/3 stains less intensely for AChE than the other raphes, but can be identified because it separates the dense staining in FC_3 from the pale area of FC_2. Compartment FC_4 is narrow and located parallel to the border of the flocculus with the middle cerebellar peduncle. FC_4 can be distinguished as a separate compartment only in the rostral one-third of the flocculus (figs. 1.2 nrs. 1-11; 1.3 A; 1.10 C; 1.13 B). Raphe 3/4 fuses with the medial border of the flocculus and the fibers of FC_4 disappear into a meshwork of AChE-positive cells, located between the cochlear nuclei, the middle cerebellar peduncle, and the restiform body (figs. 1.2 nrs. 8-11; 1.3 C, D).

Compartment FC_1 straddles the posterolateral fissure over most of its extent and continues for some distance into the white matter of folium p (fig. 1.2 nrs. 9-23). FC_2 is only represented in the rostral pole of folium p (fig. 1.2 nrs. 9-11). FC_3 is narrow in the rostral white matter of folium p and widens more caudally (fig. 1.2 nrs. 9-15). Its caudal extent and its relation with the D compartment of the paraflocculus could not be determined.

An additional raphe, which subdivides compartment FC_1, is sometimes present in an intermediate position between the intensely stained raphe $C_2/1$ and the raphe 1/2, which itself can be recognized by its fusion with raphe 2/3. This raphe is present in the horizontally

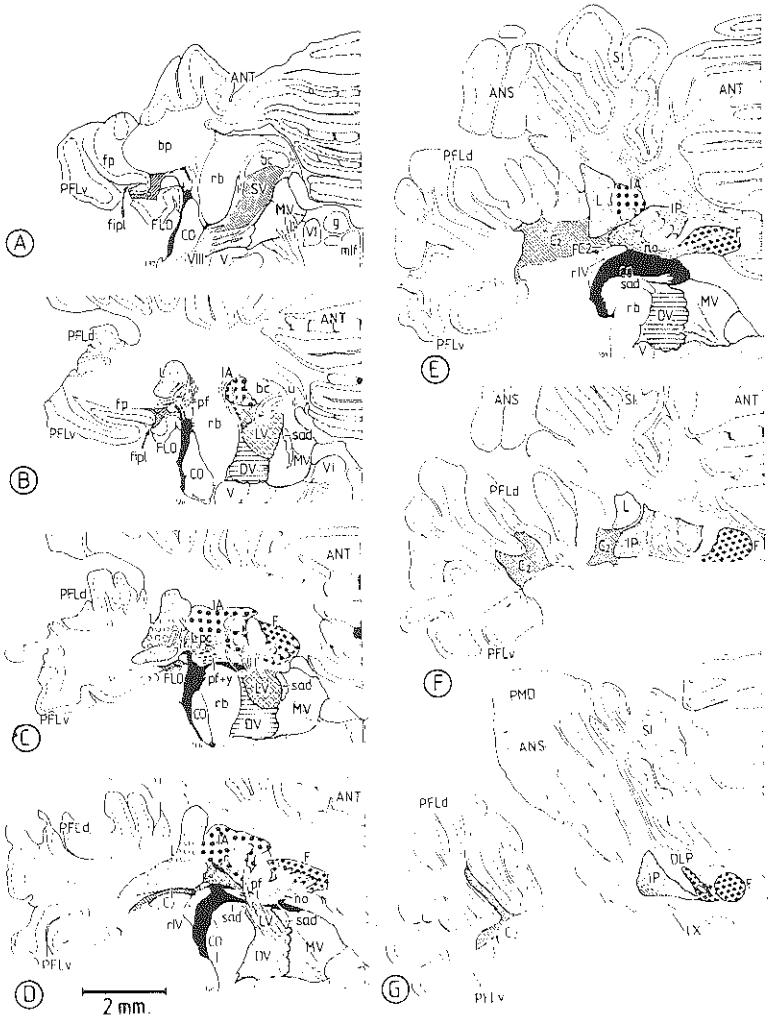

fig. 1.7 Drawing of AChE-stained transverse sections through the cerebellum showing the close relationship between flocculus, floccular peduncle, group y and the cerebellar and vestibular nuclei. Note the extent of compartment C_2. For explanation of symbols used to indicate floccular compartments and cerebellar nuclei see fig. 1.12. The distribution of AChE in deep parts of the molecular layer is indicated by stippling.

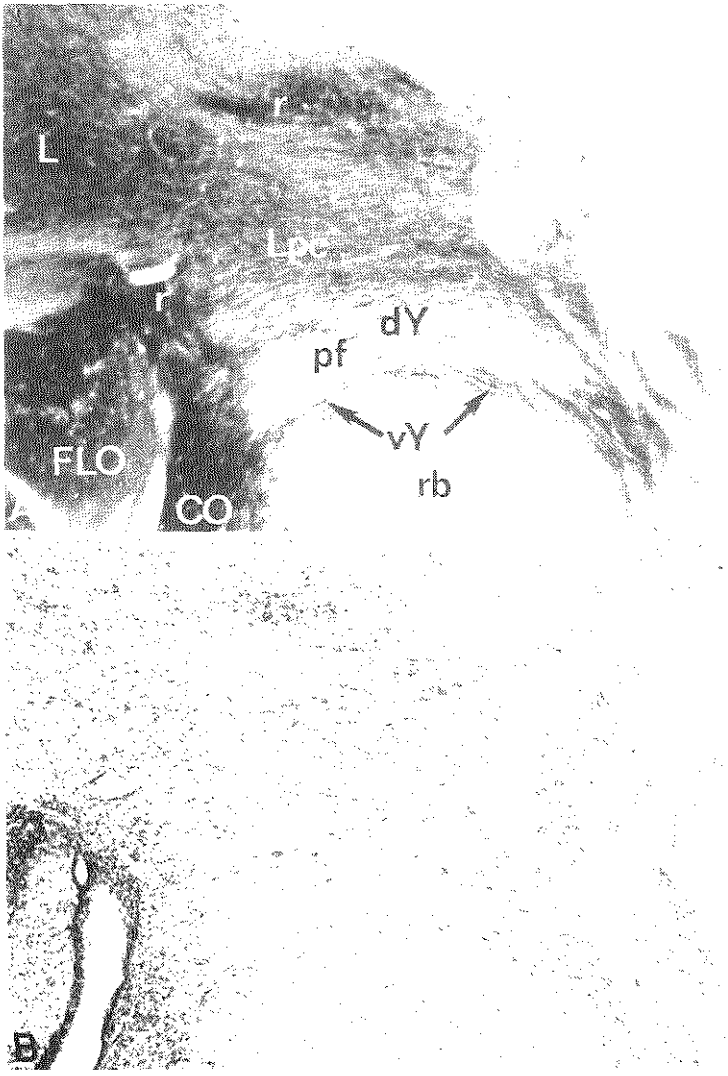

fig. 1.8 Photomicrographs of adjacent transverse AChE- (A) and Nissl-stained (B) sections through group y and floccular peduncle. Small, densely ACHE-stained cells constitute the ridge indicated with r. Ventral group y (vY) consists of small cells (mean 24 x 6 μm) in a densely AChE-stained matrix; the cells of dorsal group y (dY) are larger (mean 32 x 12 μm) and located between the fibers of the floccular peduncle. Lpc contains small neurons (mean 12 x 12 μm), and the lateral cerebellar nucleus contains large cells (mean 26 x 22 μm).

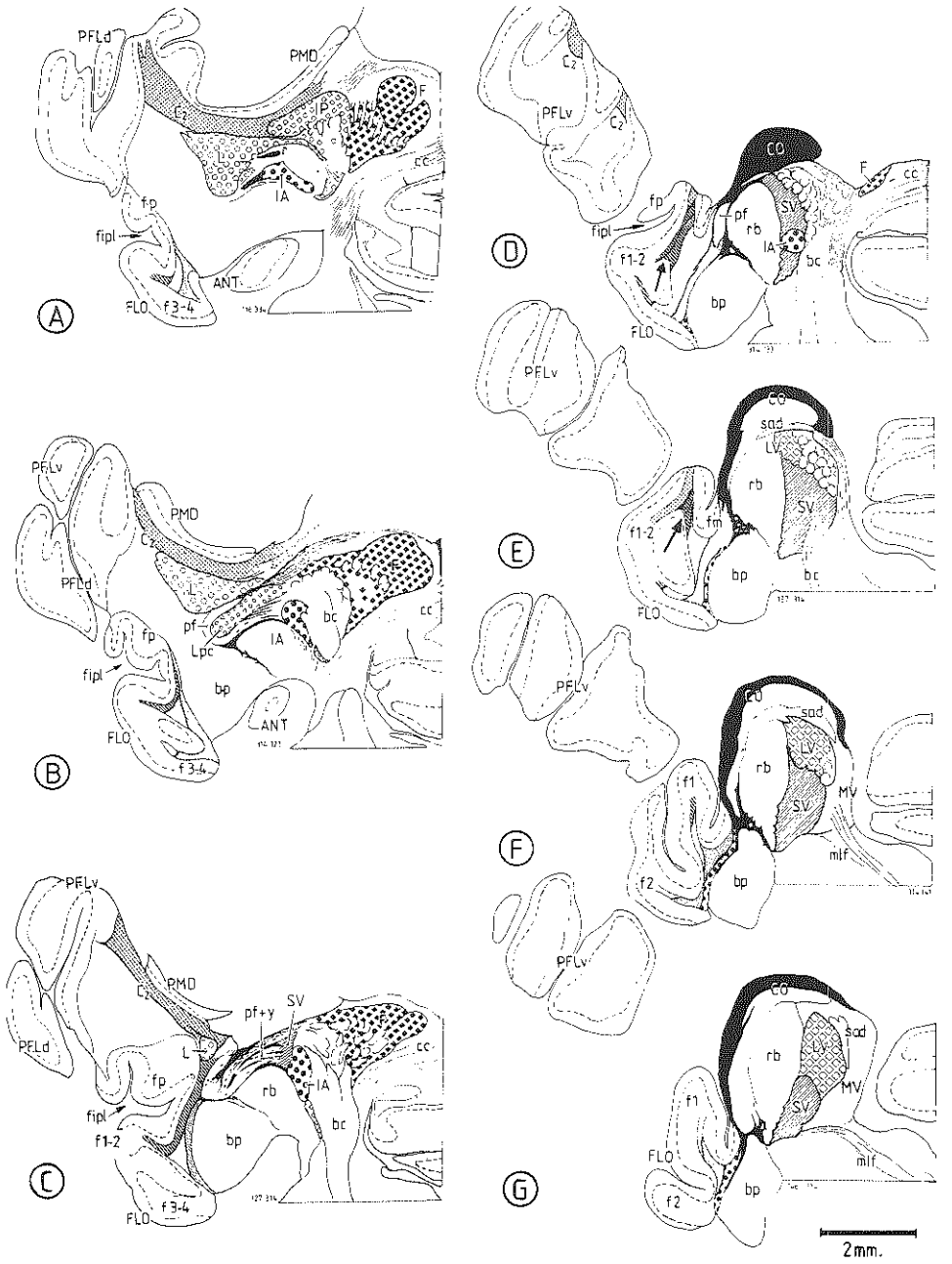
A
PFLd
PMD
C2
F
cc
IA
fp
fipl
ANT
FLO
f3-4
B
PFLv
PMD
C2
PFLd
pf
Lpc
IA
bc
cc
fp
fipl
bp
ANT
FLO
f3-4
C
PFLv
C2
PMD
pf+y
SV
PFLd
L
fp
rb
IA
cc
fipl
f1-2
bp
bc
FLO
f3-4
D
C2
PFLv
C2
CO
F
cc
fp
fipl
pf
rb
SV
IA
f1-2
bc
bp
FLO
E
PFLv
CO
sad
LV
rb
SV
f1-2
fm
bp
bc
FLO
F
PFLv
CO
sad
LV
rb
f1
MV
SV
mlf
f2
bp
PFLv
G
CO
sad
rb
LV
MV
f1
SV
FLO
mlf
f2
bp
2mm.

sectioned specimen of fig. 1.9 D,E (arrows) and 1.10 C (small white arrows), but it cannot be recognized in the transverse sections of the case illustrated in figs. 1.2 and 1.3.

1.3.5 *The floccular peduncle, topographical relations with group y and the cerebellar nuclei.*

The fibers contained in the compartments of the flocculus enter the cerebellar nuclei and the floccular peduncle, but in this process some of the borders between the compartments can no longer be distinguished. The unique relation of the C_2 compartment with the posterior interposed nucleus has been described above. Caudally, raphe 1/3, dorsal to FC_2, becomes less distinct (fig. 1.2 nrs. 23-25). Fibers of FC_1, FC_2 and FC_3 enter the ventral region of the lateral cerebellar nucleus and/or shift medially to constitute the incipient floccular peduncle in the area ventromedial to the lateral cerebellar nucleus, dorsal to the cochlear nucleus and medial to the restiform body. The conglomerate of fibers travelling in different directions imparts a patchy appearance to the AChE-staining in caudal compartment FC_3 (fig. 1.3 C). Much reduced compartments FC_1 and FC_2, flanked by the C_2 compartment, can be traced through the caudal pole of the flocculus, into the roof of the lateral recess (figs. 1.3 D; 1.13 B), and farther along the attachment of the roof of the fourth ventricle in the direction of lobule X of the caudal vermis. At this point, the border of compartment FC_2 with the floccular peduncle is formed by an AChE-positive cellular ridge, which may be continuous with the dorsal cochlear nucleus (r in figs. 1.3 D; 1.7 B,C; 1.11 A; 1.13 C). Similar small, AChE-positive cells invade the raphes and compartments in the caudal pole of the flocculus and the incipient floccular peduncle.

fig. 1.9 Drawings of AChE-stained horizontal sections through the flocculus. A is the most dorsal, G the most ventral section. Compartment FC_1 is subdivided by an additional raphe in medial and lateral parts (arrow in D and E). For explanation of symbols indicating compartments and cerebellar nuclei see fig. 1.12.

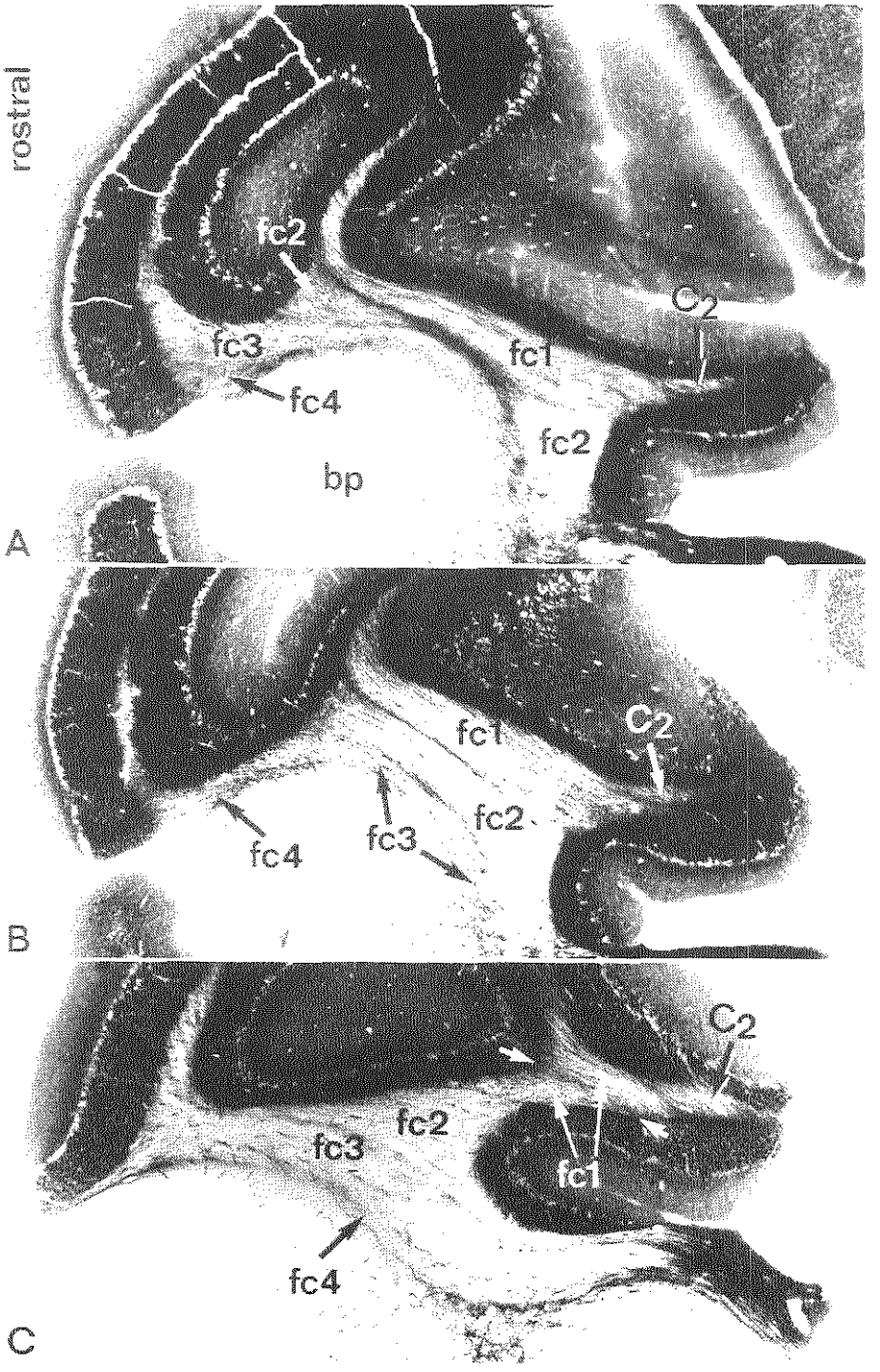
rostral
fc2
fc3
fc4
fc1
C2
fc2
bp
A
fc1
C2
fc4
fc3
fc2
B
C2
fc2
fc3
fc1
fc4
C

Group y can be considered as the bed nucleus of the floccular peduncle. Dorsal and ventral subdivisions of group y can be distinguished. The dorsal division consists of both strands and single, AChE-positive neurons, lying between the fibers of the floccular peduncle, ventral to the parvicellular extension of the lateral cerebellar nucleus (fig. 1.9). These fusiform cells are much larger than those of ventral group y (see legend fig. 1.8). The small cells of the ventral subdivision constitute a dense, AChE-positive cap over the restiform body at its border with the floccular peduncle. The floccular peduncle and the cells of group y arch over the restiform body, ventral to the parvicellular extension of the lateral cerebellar nucleus, to merge with the rostral pole of the superior vestibular nucleus (fig. 1.10 E).

The relations and the composition of the floccular peduncle are most distinct in horizontal and sagittal sections. Laterally, the peduncle is separated from the FC_2 compartment in the caudal pole of the flocculus by the AChE-positive cellular ridge (figs. 1.9; 1.12 D). This ridge still separates the peduncle from a narrow offshoot from FC_2, located in the wall of the lateral recess and penetrating between group y and the dorsal cochlear nucleus (figs. 1.12 E,F; 1.13 C,D). Before the peduncle enters the caudal pole of the superior vestibular nucleus, it divides into rostral and caudal bundles. The caudal bundle stains more intensely for AChE and corresponds to Löwy's (1928) bundle (1.9 C; 1.13 E,F; 1.14 C,D). It passes the lateral angle of the fourth ventricle, where it is located dorsal to the medial vestibular nucleus and turns rostrally. The rostral bundle of the floccular peduncle becomes lost in the superior vestibular nucleus.

fig. 1.10 Photomicrographs of three horizontal sections through the flocculus. In the dorsalmost section (A) compartment FC_2 has disappeared from the middle part of the flocculus and the 1/2 and 2/3 raphes have fused. Note the presence of an additional raphe (indicated with an arrow in C) which subdivides FC_1 into lateral and medial halves. Compare fig. 1.9 D, E.

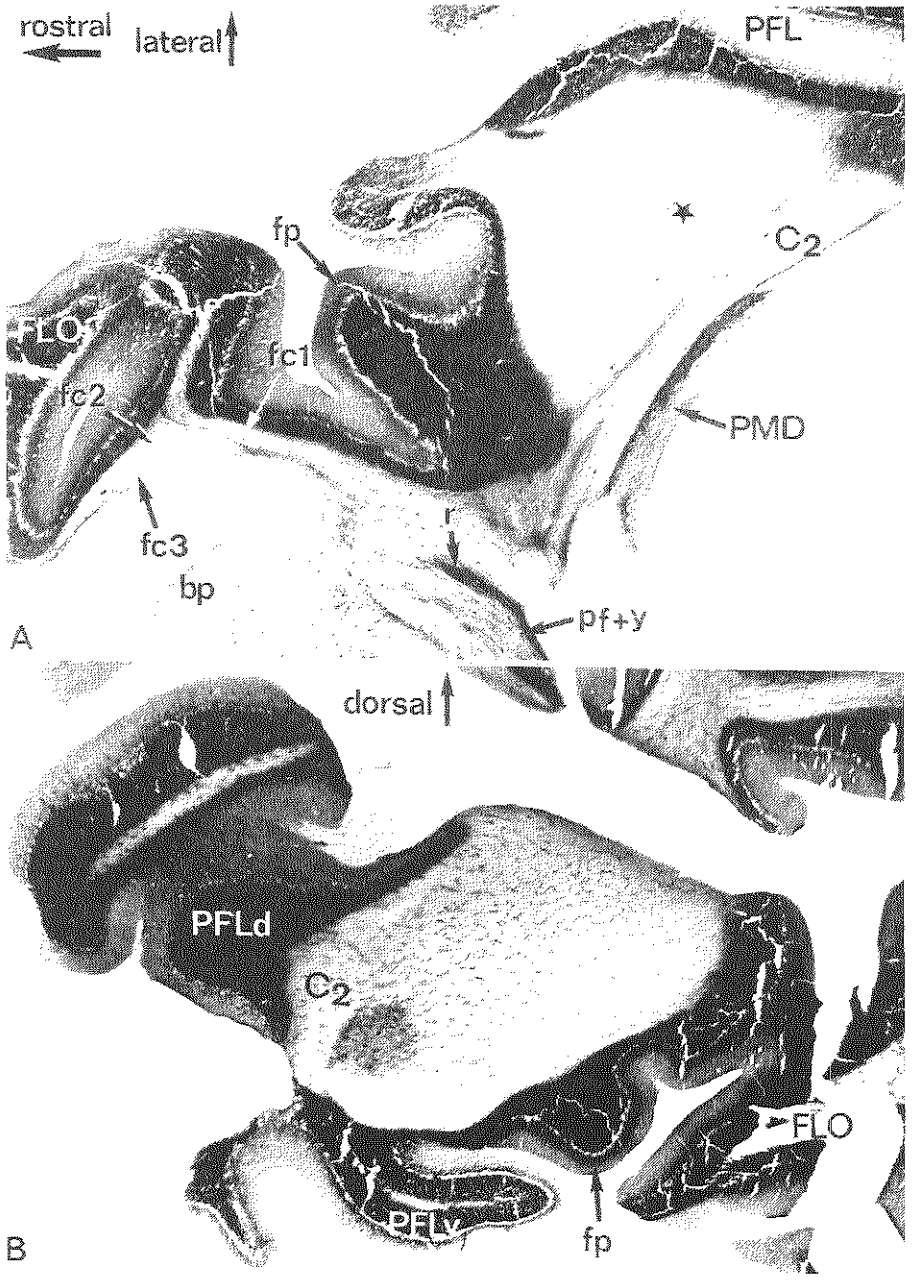
rostral
lateral
PFL
fp
C2
FLO
fc1
fc2
PMD
fc3
r
bp
pf+y
A
dorsal
PFLd
C2
FLO
PFLv
fp
B

The subdivision of the cerebellar nuclear complex in the rabbit can best be appreciated from the illustrations of horizontal and sagittal AChE-stained sections. The lateral cerebellar nucleus is fairly compact with a lateral tail extending into the stalk of the paraflocculus and a medially-directed hilus. This nucleus consists of two groups of large neurons in an AChE-poor neuropil in the rostromedial and caudolateral parts of the nucleus, separated by an area with somewhat smaller cells in a strongly AChE-reactive neuropil (figs. 1.3 D; 1.7; 1.9; 1.13). Like most neurons of the cerebellar nuclei they contain AChE. The caudolateral group of large cells constitutes the lateral tail and the caudal pole of the lateral nucleus. Medially, the lateral nucleus borders on the anterior interposed nucleus. Fibers from the white matter of the flocculus enter the ventral aspect of the lateral nucleus and traverse its AChE rich border region (figs. 1.2 nr. 28-31; 1.3 D; 1.7 B,C). These fibers separate the ventromedial extension of the lateral nucleus, which contains small- and medium-sized neurons in a moderately AChE-reactive neuropil, from the lateral and caudal magnocellular shell of the lateral nucleus. This subnucleus is indicated as the parvicellular part of the lateral nucleus (Lpc, fig. 1.8 A). The floccular peduncle abuts the Lpc on its ventral and rostral side. A conspicuous AChE-positive patch of small round cells is located along the caudal and dorsal border of the Lpc (r in figs. 1.8; 1.9 B; 1.12 D,E; 1.13 C). This cell group may be continuous with the AChE-positive ridge separating the floccular peduncle from the flocculus. Medially, the Lpc joins the vestibular nuclei, while ventrally it merges with the fibers of the floccular peduncle and group y.

fig. 1.11 Photomicrographs of a horizontal (A) and a sagittal (B) section through the flocculus and paraflocculus. Note position of C_2 compartment in the paraflocculus stalk in A and B. A densely AChE-positive cellular ridge (r) separates the caudal white matter of the flocculus from the floccular peduncle (pf + y) in A. Asterisk in A indicates a vague raphe subdividing compartment D.

The anterior interposed nucleus is located on the medial side of the lateral nucleus. It can be distinguished from the latter by its medium-sized neurons in a pale, non-AChE reactive neuropil. Lateral to the superior cerebellar peduncle it extends far ventrally, bordering on the highly AChE-reactive superior vestibular and parabrachial vestibular nuclei (figs. 1.7 B-E; 1.9 A-D). The posterior interposed nucleus is found in a rather medial and caudal position. Its ventrolateral pole reacts strongly for AChE and is sharply delimited by a fiber lamella from the lateral nucleus (figs. 1.7 F; 1.9 A; 1.12; 1.13). The dorsal part of the nucleus contains large cells in a pale neuropil. A meshwork of cells separates the posterior interposed nucleus from the medial cerebellar nucleus. This meshwork is traversed by the efferent fibers of the posterior interposed nucleus, which continue as the medial one third of the brachium conjunctivum, and by bundles of corticovestibular (perforating) fibers.

1.4 Discussion

1.4.1 *AChE and its distribution.*

AChE is present in neuronal as well as in non-neuronal tissues (Silver 1974). In the brain, AChE is associated with the hydrolysis of acetylcholine in the synaptic cleft of axonal terminals of cholinergic neurons and "cholinoceptive" cells. Other possible functions of AChE in the brain have been discussed by Greenfield (1984) and Appleyard and Jahnson (1992). Pseudocholinesterase, which converts other substrates (Marani, 1982), is present in endothelial and glial cells (Barth and Ghandour, 1983), but was inhibited in our experiments by ethopropazine.

fig. 1.12 Drawings of AChE-stained sagittal sections through the left flocculus, showing compartments in the flocculus, paraflocculer stalk, and emerging floccular peduncle. Compare photomicrographs of figs. 1.11 B and 1.13.

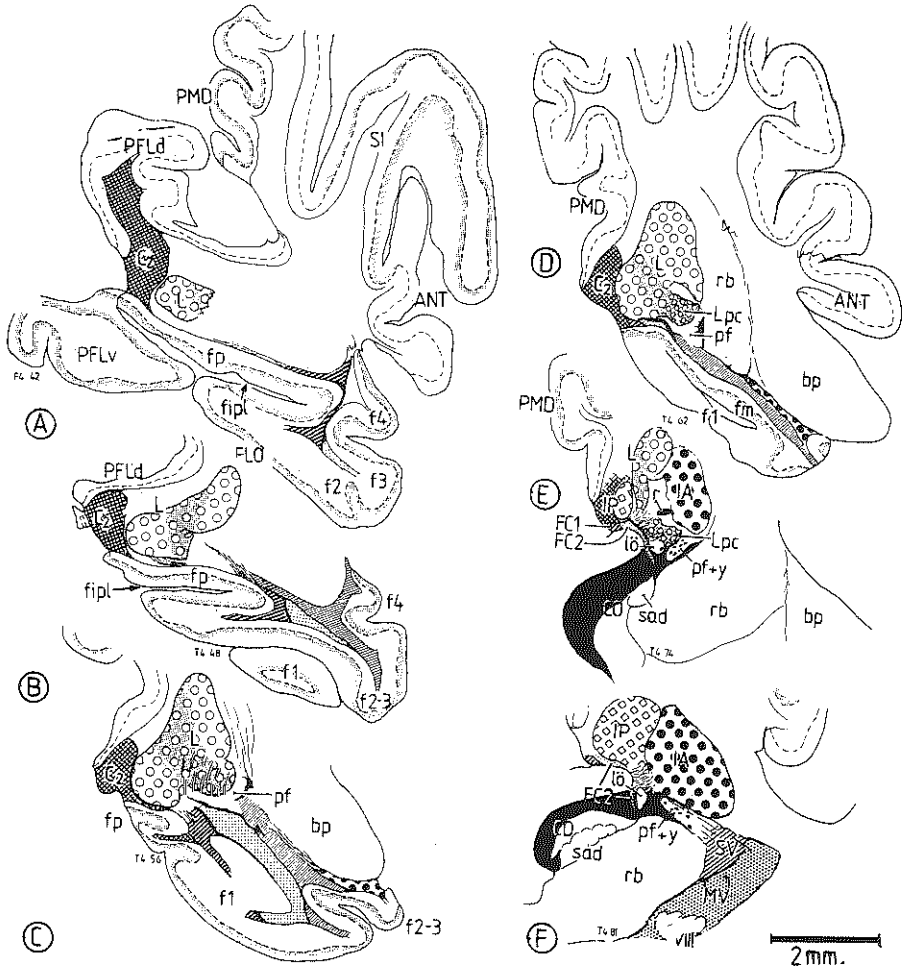
PMD
PFLd
SI
ANT
PFLv
fp
fipl
f4
A
PFLd
FLO
f2
f3
L
fipl
fp
f4
f1
f2-3
B
L
pf
fp
bp
f1
f2-3
C
PMD
L
rb
Lpc
pf
ANT
bp
D
PMD
f1
fm
E
IP
IA
FC1
FC2
Lpc
pf+y
CD
sad
rb
bp
IP
IA
FC2
CD
pf+y
sad
SV
rb
MV
F
VIII
2 mm.
L / L AChE-rich
Lpc
IP / IP AChE-rich
IA
F / F AChE-rich
AChE in the lower molecular layer
FC1
FC2
FC3
FC4
C2
SV
MV
DV
LV
AChE

Recently, pseudocholinesterase was demonstrated in certain Purkinje cells in lobules IX and X of the cerebellum of the rat, but the flocculus was not investigated (Gorenstein et al. 1987). In this paper, AChE was distributed in sheets of thin fibers at the borders of compartments in the white matter of the flocculus and the paraflocculus. AChE-staining within the compartments shows characteristic differences. Compartment FC_2 lacks AChE, especially medially where large diameter fibers accumulate. The other compartments, particularly C_2, stain more intensely. The subdivision of the white matter into compartments is not reflected in a zonal distribution of AChE over the cortex of the flocculus and the paraflocculus.

1.4.2 *Distribution of AChE in the cortex of the flocculus.*

Strong staining for AChE, with the highest reactivity in patches between less reactive granule cells, is observed in the entire granular layer of the flocculus and folium p. The deep stratum of the molecular layer also reacts intensely for AChE, but this type of staining extends beyond the flocculus and folium p to include (by our definition) the entire

fig. 1.13 Photomicrographs of sagittal sections through the flocculus.
A) Lateral section through folium p and the lateral pole of the flocculus with the compartments FC_1-FC_3. Arrow indicates the raphe bordering the C_2 compartment.
B) More medial section. The incipient floccular peduncle is separated from compartments FC_1, and FC_2, and C_2 in the white matter of the flocculus by a densely AChE-stained ridge of small cells (r). FC_3 joins the floccular peduncle and FC_4 appears in the rostral flocculus.
C) Section through the lateral pole of the posterior interposed nucleus (IP). The floccular peduncle is divided into the AChE-rich bundle of Löwy (lö) and a rostral, AChE-poor portion, which contains the neurons of dorsal group y. Note the densely stained ridge of small cells (r) dorsal to the parvicellular lateral nucleus.
D) Higher magnification of the floccular peduncle and the ventral and dorsal group y.

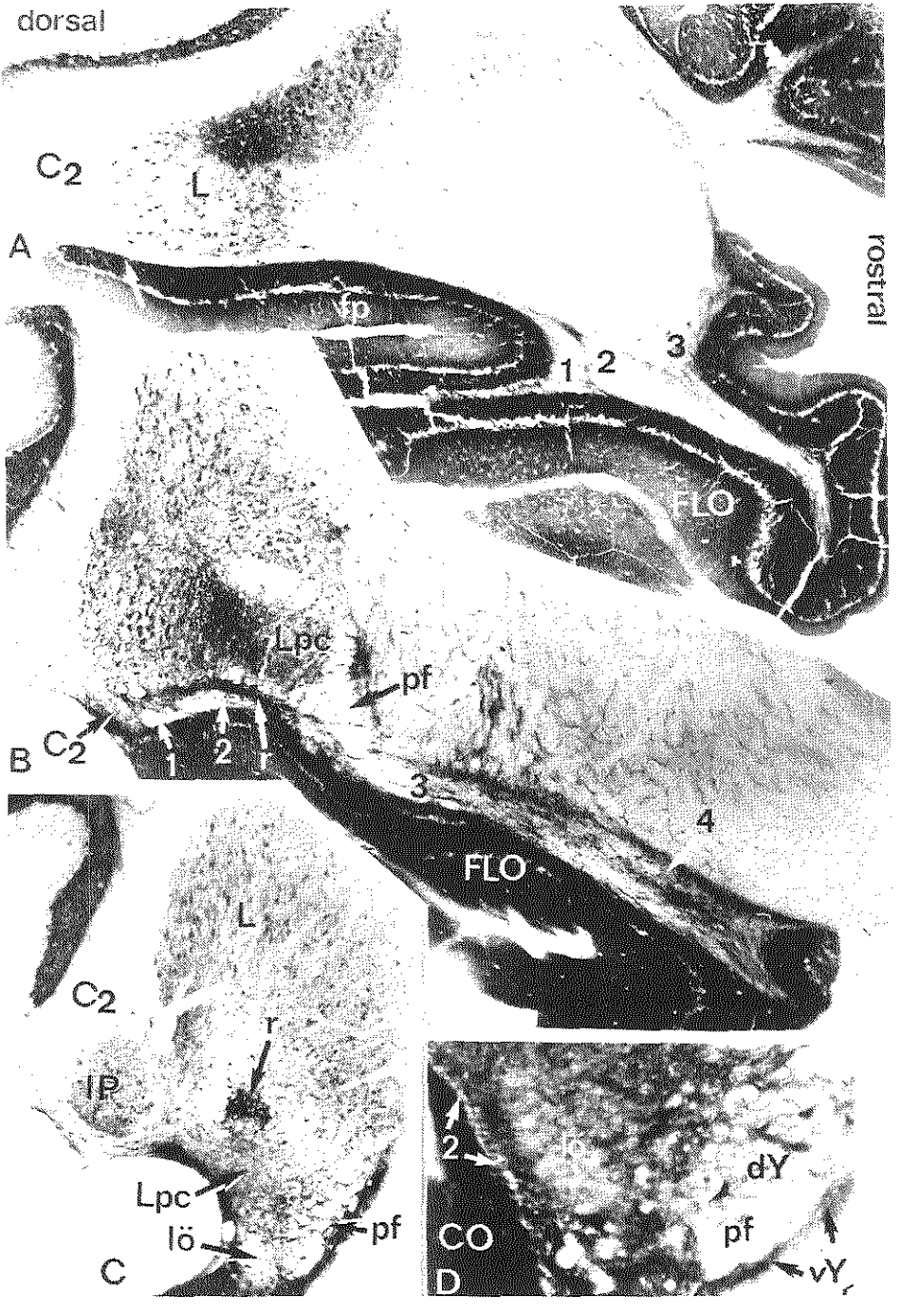
dorsal
rostral
A
B
C
D
C2
L
fp
1
2
3
FLO
Lpc
pf
r
4
IP
lö
CO
dY
vY

ventral paraflocculus. Strong staining of the granular layer is also observed in the cortex of the vermis at the bottom of the fissures. This staining extends further apically in the ventral part of the anterior lobe and the caudal vermis, including the entire lobule X and the ventral lobule IX. In other parts of the cerebellum staining is most intense in the superficial granular layer, next to the Purkinje cells, which always are left unstained. AChE is also present in the deep stratum of the molecular layer of the vermis, the hemisphere of the anterior lobe, and the simple and paramedian lobules. More laterally, the molecular layer of the hemisphere, including the ansiform lobule and the entire dorsal paraflocculus, is entirely AChE- negative.

According to many authors the patchy distribution of AChE in the granular layer is due to staining of cerebellar glomeruli and Golgi cells (Gerebtzoff 1959; Csillik et al., 1963; Brown and Palay, 1972; Altman and Das, 1970). Glomerular staining for AChE may be indicative of cholinergic transmission because choline-acetyl transferase (ChAT, the synthesizing enzyme of acetylcholine) immunoreactive mossy fiber rosettes were found in the granular layer in rat, guinea pig, cat, rabbit, monkey and man (Kan, 1978, 1980; Illing, 1990; Ojima et al., 1990; Ikeda et al., 1991; Barmack et al., 1992a; De Lacalle et al., 1993). In the rat a plexus of thin, beaded ChAT-immunoreactive fibers pervades all layers of the cortex. ChAT-immunoreactive mossy fibers were mostly restricted to lobules X and ventral lobule IX and the flocculus (Ojima et al., 1990; Barmack et al., 1992a). The plexus of beaded ChAT-immunoreactive fibers could not be detected in the cerebellum of the rabbit. In this species, ChAT-containing mossy fibers were present in lobules I and II of the anterior lobe and the portions of lobules X and IX facing the posterolateral fissure. They were rather scarce in the flocculus, but the ventral paraflocculus of the rabbit was densely innervated (Barmack et al., 1992a).

The resemblance between the distribution of the vestibulocerebellar mossy fiber projections (Gerrits et al., 1989; Epema et al., 1990; Tan and Gerrits, 1992; Thunnissen et al., 1989) and the regions with strong AChE reactivity of the granular layer in the rabbit is very close indeed. Barmack et al. (1992b) traced the cholinergic mossy fiber projections to lobules X

and IX and the flocculus in rat and rabbit from ChAT-immunoreactive neurons in the caudal medial vestibular nucleus and the nucleus prepositus hypoglossi with a double-labeling HRP retrograde axonal transport-immunohistochemical technique. A projection to the ventral paraflocculus of the rabbit took its origin from ChAT-immunoreactive cells in the nucleus prepositus hypoglossi.

AChE staining of the molecular layer is more variable among different species and is therefore more difficult to interpret (Friede and Fleming, 1964; Silver, 1967, 1974; Karczmar, 1969; Marani and Voogd, 1977a,b; Marani, 1982, 1986; Hess and Voogd, 1986). The presence of AChE in the deep stratum of the molecular layer of the flocculus and ventral paraflocculus and its absence (by definition) in the dorsal paraflocculus of the rabbit does not appear to be related to the distribution of cholinergic terminals, which could not be demonstrated in the molecular layer of the rabbit cerebellum (Barmack et al., 1992a). The AChE-positive displaced Golgi cells of Cajal (1911) and Spaçek et al. (1973) cannot be responsible for the differential distribution of AChE over the molecular layer of the ventral and dorsal paraflocculus of the rabbit cerebellum, because these cells are distributed ubiquitously over the cortex. ChAT-immunoreactive Golgi cells, some of which of which were found in the cat (Illing, 1990; Ikeda et al., 1991), were not observed in the rabbit (Kan et al., 1978; Barmack et al., 1992a). The distribution of nicotinic cholinergic receptors (Hunt and Schmidt, 1978) and muscarinic (M2) receptors (Mash and Potter, 1986) over the granular layer of the rat cerebellum corresponds well with the punctate AChE-staining and the ChAT-immunoreactivity of the mossy fiber rosettes. Muscarinic receptor distribution over the molecular layer is more variable, with multiple bands in the molecular layer of the caudal vermis, flocculus, and paraflocculus of the rabbit, less distinct zonation in rat and guinea pig and a uniform distribution in the mouse (Yamamura and Snyder, 1974; Kuhar and Yamamura, 1975; Gulya and Kása, 1983; Mallol et al., 1984; Rotter et al, 1979a,b; Neustadt et al., 1988).

1.4.3 *Compartmental organization of the floccular white matter.*

An AChE subdivision of the cerebellar white matter has previously been observed in the anterior lobe of the cat (Voogd et al., 1986) and in the cerebellum of the monkey, including the flocculus and paraflocculus (Hess and Voogd, 1986; Voogd et al., 1986; Voogd et al., 1987). Both in the cerebellum of cat and monkey, and in the flocculus of the rabbit, the AChE-positive fiber bundles correspond to accumulations of thin myelinated fibers (raphes) in Häggqvist-stained sections. Raphes usually separate bundles of coarser Purkinje cell axons arising from longitudinal cortical zones on their way from the cortex to their target nuclei. The nature of the AChE-positive fibers of the raphes is puzzling. They may represent AChE-positive mossy fibers, which have become concentrated at the borders of sheets of Purkinje cell axons having a different destination. A possible correlation between concentrations of AChE positive mossy fiber rosettes in the granular layer and the presence of fascicles of strongly stained fibers in the white matter was noticed by Boegman et al. (1988) for the vermis and paravermis of the rat cerebellum. These authors described a close correspondence between the localization of bands of MAB-Q113 (zebrin) immunoreactive Purkinje cells and the zonal AChE pattern. MAB-Q113 positive Purkinje cells in the flocculus of the rabbit are not distributed in a clear zonal pattern, but rather in patches; moreover MAB-Q113 immunoreactivity was absent from the axons of Purkinje cells in the white matter of the flocculus (Tan et al., 1989). Another factor that may determine the staining of the raphes of the flocculus is their invasion by small, strongly AChE-positive cells. Concentrations of such cells are found as a ridge at the lateral border of the floccular peduncle, where it separates from the flocculus, and as strongly AChE-reactive patches, dorsal to the parvicellular lateral cerebellar nucleus. The scattered, AChE-positive cells in the white matter of the flocculus may correspond to part of the basal interstitial nucleus of primates (Langer, 1985). The AChE-positive neurons of the floccular white matter and group y of the rat are ChAT-negative (Komei et al., 1983).

Four compartments were tentatively identified in the white matter of the flocculus and the ventral paraflocculus of macaques (Hess and Voogd 1986; Voogd et al., 1987). Both in the monkey and in the rabbit the most lateral C_2 compartment extends into the petrosal lobule and the dorsal paraflocculus and includes the posterior interposed nucleus. Rostrally, compartment C_2 continues into the ventral paraflocculus in both species. No equivalent of compartment FC_4 was found in primates.

1.4.4 *Zones and compartments in the flocculus.*

Anatomical as well as physiological studies have indicated the presence of longitudinal zonation in the flocculus. In an anterograde tracing study in the cat Gerrits and Voogd (1982) showed that climbing fibers from the dorsal cap and the adjoining ventrolateral outgrowth, the bend of the principal olive, and the rostral pole of medial accessory olive terminate in longitudinal strips in the molecular layer. In the flocculus and the adjacent folia of the ventral paraflocculus, they observed seven climbing fiber zones (F1-F6, C_2) in the molecular layer derived from different parts of the inferior olive. An additional zone (F7) was observed in the adjacent ventral paraflocculus. The fibers travelled in bundles in adjacent longitudinal white matter compartments. However, they did not correlate the location of these fiber bundles to matching AChE or Häggqvist-stained material. A lateral C_2 zone, receiving climbing fibers from the rostral pole of the medial accessory olive was clearly present in the cat, and the fusion of the F2+3 and the F5+6+7 zones around F4 (a zone which receives climbing fibers from the caudal part of the dorsal cap, Gerrits and Voogd 1982) may correspond to the fusion of compartments FC_1 and FC_3 in folium p of the flocculus of the rabbit. The topographical relations of the five climbing fiber zones that were traced by Ruigrok et al. (1992) with anterograde transport of Phasaeolus vulgaris lectin to the flocculus and the paraflocculus of the rat closely resemble the compartmentation of AChE in the flocculus of the rabbit. A C_2 zone, innervated from the rostral pole of the medial accessory olive, is present

in the lateral and caudal region of the flocculus of the rat. The dorsal cap and the ventrolateral outgrowth each project to two discrete zones in the flocculus of the rat[2]. The FD and FD' zones receive their climbing fibers from the ventrolateral outgrowth. They continue in the ventral paraflocculus, where they are innervated by the ventral leaf of the principal olive. Two other zones (FE and FE') receive climbing fibers from the dorsal cap. The FE' zone is found at the rostral pole of the flocculus and does not extend into the ventral paraflocculus and may correspond to FC_4 of the rabbit flocculus. The FE zone continues for a short distance into the ventral paraflocculus, where the FD and FD' zones fuse around it. This fusion can be considered as the equivalent of the fusion of FC_1 and FC_3 around FC_2 in folium p of the rabbit.

The observations of Yamamoto and Shimoyama (1977) on Purkinje cell zones in the flocculus and folium p of the rabbit are very similar to our observations on compartments, with respect to their number and extent. Originally Yamamoto and Shimoyama (1977) distinguished two pairs of Purkinje cell zones that were retrogradely labeled from the medial vestibular nucleus and the superior vestibular nucleus, respectively. The Purkinje cell zones that project to the medial vestibular nucleus interdigitated with the two zones projecting to the superior vestibular nucleus. The most rostromedial of these zones projected to the medial vestibular nucleus. In later papers (Yamamoto, 1978, 1979a, b), the existence of the most rostral one of the two zones, projecting to the medial vestibular nucleus was ignored. Purkinje cells in the caudal flocculus projected to the lateral cerebellar nucleus and those from an intermediate region of folium p to the nucleus prepositus hypoglossi (Yamamoto, 1978).

Sato et al. (1982a,b) distinguished three Purkinje cell zones in the flocculus of the cat: the rostral zone projected to the superior vestibular

[2]The dorsal cap and the ventrolateral outgrowth are segments of a continuous cell column. Rostrally, this column is continuous with the principal olive. The morphological and functional criteria used to subdivide this cell column are discussed in chapter 2. In the rabbit and cat, the column is subdivided into two subnuclei that comprise the caudal dorsal cap and the rostral dorsal cap with the ventrolateral outgrowth. In the rat, these subnuclei correspond to the dorsal cap and the ventrolateral outgrowth.

nucleus, the middle zone projected to the medial vestibular nucleus, and the caudal zone projected to group y and the parvicellular part of the lateral cerebellar nucleus. Three similar, if not identical zones received projections from the rostral dorsal cap and ventrolateral outgrowth (rostral and caudal zones), and the caudal dorsal cap (middle zone) (Sato et al.,1983). Sato's findings are difficult to reconcile with the data from the literature and our study on the subdivision of the rabbit flocculus, and with the more detailed analysis of the olivocerebellar projection to the cat flocculus by Gerrits and Voogd (1982). Neither Yamamoto (1978) nor Sato et al. (1982b) reported a zone corresponding to the floccular C_2 zone found in the present study to be related to the posterior interposed nucleus. Instead, they advocated a projection to the lateral cerebellar nucleus from Purkinje cells in this region. Their injections of the lateral cerebellar nucleus, however, may have included the posterior interposed nucleus. Yamamoto (1979a) reported a projection from the rostral pole of the MAO to the caudal flocculus in the rabbit, a projection that is in accordance with the presence of the C_2 zone in this region.

Yamamoto and Shimoyama (1977), Yamamoto (1978,1979a), Gerrits and Voogd (1982) and Ruigrok et al. (1992) traced their Purkinje cell and climbing fiber zones from the flocculus into the adjoining part of the ventral paraflocculus. Gerrits and Voogd (1982) found an extension of the climbing fiber zones from the dorsal cap, the ventrolateral outgrowth, and the MAO into their medial extension of the ventral paraflocculus (ME) and an exclusive projection of the principal olive to the ME and the ventral paraflocculus. Similar connections from dc, vlo, and caudal principAl olive were described by Yamamoto (1978, 1979a) for folium p of the rabbit cerebellum and by Ruigrok et al. (1992) for the ventral paraflocculus of the rat. We also found that compartments C_2 and FC_1-FC_3 extended into the white matter of folium p. FC_2 and FC_3 were only represented in the rostral pole of folium p. FC_4 did not enter folium p.

1.4.5 *Group y and parvicellular part of the lateral cerebellar nucleus.*

Group y can be considered the bed nucleus of the floccular peduncle. Unfortunately, a definition of this cell group that can be applied to all species is lacking. Brodal and Pompeiano (1957) first described it as a subgroup of the vestibular nuclei of the cat, containing small cells, capping the restiform body dorsally. It was situated between Deiters' nucleus medially and the cochlear nucleus laterally. Scattered cells connected it with the lateral cerebellar nucleus. Group y was further subdivided by Gacek (1977;1979) and Highstein and Reisine (1979), both in the cat. Highstein and Reisine (1979) distinguished a dorsal group y, located within the floccular peduncle where it arches over the restiform body (corresponding to the infracerebellar nucleus of Gacek) from more ventrally located, small and tightly packed cells of the ventral group y (corresponding to group y of Gacek). The two nuclei differed in their connections, the dorsal group y projecting to the oculomotor nucleus, while the ventral group y is part of the commissural vestibular system. No descriptions of group y are available for the rabbit. We distinguished dorsal and ventral subdivisions of group y in AChE-reacted material of the rabbit. Ventral group y corresponds to the densely, AChE-stained parvicellular layer that caps the restiform body. The larger, AChE-positive cells of dorsal group y are scattered between the fibers of the floccular peduncle. Epema et al. (1988), Gerrits et al. (1989), Epema et al., (1990) and Thunnissen (1990) included a variable portion of Lpc in the rabbit in their group y (sometimes indicating it as the "dorsal group y"), because the Lpc participated both in the vestibulo-oculomotor and commissural projections. The position of Lpc in rabbit corresponds to that of the parvicellular part of the lateral cerebellar nucleus of the rat (Korneliussen, 1968; Voogd et al., 1985; Ruigrok and Voogd, 1990). The border between the AChE-positive Lpc and the strongly reactive group y is not sharp and both nuclei merge with the AChE-positive caudal pole of the superior vestibular nucleus, which was indicated as a separate subnucleus (group l) by Brodal and Pompeiano (1957) in the cat. In our subdivision of the cerebellar nuclei we closely followed Ono and Kato (1938). The main

divergence from these authors is the identification of the "pars a" of the posterior interposed nucleus of Ono and Kato (1938), and also of Van Rossum (1969), as the dorsolateral protuberance of the fastigial nucleus, first described by Goodman, Hallett and Welch (1963) in the rat.

The explanation for the presence of AChE at the borders of white matter compartments of the rabbit flocculus and paraflocculus still eludes us, but as an independent method of reliably subdividing that part of the cerebellum it has proven useful to correlate the connections, immunohistochemistry and electrophysiology of the rabbit flocculus (Tan et al., 1989; Van der Steen et al., 1991, Chapter 4).

Chapter 2

Zonal organization of the climbing fiber projection to the flocculus and nodulus of the rabbit.

2.1 Introduction

The flocculus and nodulus are involved in control of motor systems relayed by the vestibular nuclei. Best known is the role of the flocculus in the adaptive control of eye movements (Robinson, 1976; Ito, 1982, 1984; Ito et al., 1972, 1982a, b; Nagao, 1983, 1988; Ito 1990). The flocculus receives a visual input via climbing fibers from the inferior olive. The nodulus receives climbing fibers both from visually-dominated and vestibular subnuclei of the inferior olive. The main output of the flocculus and the nodulus is directed, through their Purkinje cell axons, to the vestibular nuclei.

Climbing fibers terminating in the flocculus originate from the dorsal cap (dc) and adjoining ventrolateral outgrowth (vlo) of the inferior olive (Maekawa and Simpson, 1972, 1973; Alley et al., 1975; Maekawa and Takeda, 1976, 1977; Hoddevik and Brodal, 1977; Groenewegen and Voogd, 1977; Kawamura and Hashikawa, 1979; Walberg et al., 1979; Yamamoto, 1979a; Brodal and Brodal, 1982; Gerrits and Voogd, 1982, 1989; Blanks et al., 1983; Sato et al., 1983; Whitworth et al., 1983; Balaban, 1984; Takeda and Maekawa 1984a, 1989a,b; Langer et al., 1985; Bernard, 1987; Blanks, 1990; Ruigrok et al., 1992) and the rostral pole of the medial accessory olive (MAO) (Brodal, 1940; Alley et al., 1975; Hoddevik and Brodal, 1977; Walberg et al., 1979; Yamamoto, 1979a; Brodal and Brodal, 1982; Gerrits and Voogd, 1982; Blanks et al., 1983; Langer et al., 1985; Ruigrok et al., 1992). Climbing fibers to the nodulus and the adjoining part of the uvula take their origin from the dc and vlo, the subnucleus β, the dorsomedial cell column (dmcc), rostral and caudal parts of the MAO and the ventral leaf of the principal olivary nucleus

(Brodal, 1940; Alley et al., 1975; Brodal, 1976; Groenewegen and Voogd, 1977; Groenewegen et al., 1979; Kawamura and Hashikawa, 1979; Voogd and Bigaré, 1980; Brodal and Kawamura, 1980; Brodal and Brodal, 1981, 1982; Whitworth et al., 1983; Furber and Watson, 1983; Eisenman, 1984; Sato and Barmack, 1985; Walberg et al., 1987; Bernard, 1987; Katayama and Nisimaru, 1988; Balaban and Henry, 1988; Kanda et al., 1989; Kano et al., 1990). Some of the neurons of the dc and the vlo distribute their axons to both the flocculus and the nodulus and uvula (Takeda and Maekawa, 1984, 1989a,b; Maekawa et al., 1989).

Visual signals are sent to the dc/vlo via the nucleus of the optic tract (NOT), the nuclei of the accessory optic system (AOS) and the visual tegmental relay zone (VTRZ). The projection of the optic nerve to the NOT and the nuclei of the AOS is mainly crossed. The caudal part of the dc receives afferent projections from the dorsal (DTN) and interstitial terminal nucleus (ITN, i.e. the interstitial nucleus of the superior fascicle of the AOS, Giolli et al., 1984, 1985, 1988 and the NOT (Mizuno et al., 1973, 1974; Takeda and Maekawa, 1976; Holstege and Collewijn, 1982). This projection is mainly uncrossed and also involves the group ß (Holstege and Collewijn, 1982). The rostral part of the dc and the vlo receive afferent projections from the medial terminal nucleus of the accessory optic system (MTN) and the VTRZ (Maekawa and Takeda, 1977, 1979; Giolli et al., 1984, 1985; Simpson et al., 1988). The major projection from these nuclei is ipsilateral and derived from the VTRZ. The VTRZ does not receive direct afferents from the optic tract, but it receives a crossed projection from the MTN, passing through the posterior commissure (Giolli et al., 1984). Physiologically, the dc/vlo complex can also be subdivided into caudal and rostral parts on the basis of laterality of retinal signals (Maekawa and Takeda, 1976, 1977; Ito et al., 1978; Takeda and Maekawa, 1980), their connectivity with different vestibulo-ocular reflexes (Ito et al., 1978, 1982b) and their preferred axis in responses to rotating visual patterns (Simpson and Alley 1974; Simpson et al., 1981; Leonard et al., 1988).

The dc also receives a projection from the pontine paramedian reticular formation (Gerrits and Voogd, 1986). Afferents from the

vestibular nuclei terminate in different subnuclei of the olive including subnucleus b of the caudal MAO, subnucleus ß and the dmcc (Saint-Cyr and Courville, 1979; Martin et al., 1980; Gerrits et al., 1985; Nelson et al., 1986; Nelson and Mugnaini, 1989; Kaufman et al., 1991). The nucleus prepositus hypoglossi projects both to visual and vestibular subnuclei of the inferior olive (Gerrits et al., 1985, McCrea and Baker, 1985). This projection is partially GABAergic (De Zeeuw et al., 1993), partially cholinergic (Barmack et al., 1993).

A zonal pattern in the olivocerebellar projection to the flocculus, consisting of a central zone from the caudal dc and two flanking zones from the rostral dc and the vlo, was first demonstrated with autoradiography of axonal transport of tritiated leucine by Groenewegen and Voogd (1977) in the cat. These results were confirmed in retrograde tracing studies in rabbit (Yamamoto, 1979a) and cat (Kawamura and Hashikawa, 1979; Sato et al., 1983). The three climbing fiber zones seem to coincide with three Purkinje cell zones that were delineated in the rabbit (Yamamoto and Shimoyama, 1977) and the cat (Sato et al., 1983) on the basis of their projection to different vestibular and/or cerebellar nuclei. A more complicated pattern with seven climbing fiber zones was described by Gerrits and Voogd (1982) for the olivocerebellar projection to the flocculus of the cat. They identified the caudalmost zone of the flocculus as an extension of the C_2 zone, which receives its climbing fibers from the rostral pole of the MAO. Gerrits and Voogd (1982) stressed the extension of some of the floccular zones (including the C_2 zone) into the adjoining part of the ventral paraflocculus (the medial extension of the caudal ventral paraflocculus or ME). The ME differs from the flocculus in receiving an additional projection from the principal olive. A projection of the principal olive to folium p, which is the equivalent in the rabbit of the ME, was also described by Yamamoto (1979a).

A zonal arrangement in the olivocerebellar projection to the flocculus and the adjacent ventral paraflocculus is also present in the rat (Ruigrok et al., 1992). Five climbing fiber zones were distinguished, including a C_2 zone in the caudal flocculus and two pairs of alternating

zones, innervated by the caudal dc and the rostral dc with the vlo respectively. All but the most medial, which is innervated by the caudal dc, extended into the paraflocculus. Parasagittal zonal patterns in the olivonodular projection were found by several authors; the most detailed pattern was presented by Katayama and Nisimaru (1988) and Balaban and Henry (1988), both in the rabbit.

It is clear that not all of these studies agree on the location and number of climbing fiber zones in the flocculus. Still, a pattern has emerged of discrete zones (Ito, 1984) or modules (Voogd and Bigaré, 1980) consisting of subsets of Purkinje cell receiving specific climbing fiber input and projecting to distinctive parts of the vestibular and cerebellar nuclei. These modules may constitute the anatomical circuitry used by the vestibulo-ocular (Ito et al., 1977; Ito et al., 1982b; Sato and Kawasaki, 1990b) and eye movement related zones in the flocculus to control eye muscle activity (Dufossé et al., 1977; Balaban et al., 1984; Nagao et al., 1985; Sato and Kawasaki, 1984, 1990a, 1991). An intrinsic framework for revealing these zones, such as the one revealed by the AChE-positive raphes that subdivide the white matter of the flocculus (Hess and Voogd, 1986; Voogd et al., 1987), has never been used to correlate anatomical and physiological data. Such a framework became available with our recent subdivision of the white matter in AChE-stained sections of the rabbit flocculus into five compartments (see Chapter 1).

This study addresses the following questions:

a) Do the afferent climbing fibers from different parts of the dc/vlo complex travel in specific white matter compartments in the flocculus and nodulus ?

b) What is the relationship between the white matter compartments and the climbing fiber termination zones ?

2.2 Materials and methods

In 20 pigmented Dutch belted rabbits small quantities (5-15 nl) of a 7% solution of horseradish peroxidase coupled to wheat germ agglutinin (WGA-HRP, Sigma type VI) were injected with air pressure through micropipettes, placed in the inferior olive. A dorsal approach through the fourth ventricle avoided the cerebellum. In nine cases optimal sites for injection were located by electrophysiological recording, using the method and the criteria for the responses of dc/vlo neurons to rotatory stimuli of Leonard et al. (1988). Recordings and injections were made through the same glass pipette filled with the WGA-HRP solution. Neurons in the caudal dc can be recognized by their preference for rotation of the visual surround about the vertical axis, rostral dc/vlo neurons prefer rotation about specific horizonal axes. Eye dominance can also be used to distinguish caudal dc and rostral dc/vlo responses during visual stimulation. Flash stimuli to the ipsilateral and contralateral eye were used to determine the relative rostrocaudal position of the tip of the injection pipette. Flash potentials from caudal dc neurons were optimal when the stimulus was delivered to the contralateral eye. Rostral dc neurons responded optimally with flash stimulus to the ipsilateral eye, while vlo neurons and the most rostral neurons in the rostral dc hardly showed any response to flash stimulation.

After a survival time of 36-48 hours the rabbits were deeply anaesthetized and perfused transcardially with 1 L of saline at room temperature, followed by 2 L of a solution containing 1-3% paraformaldehyde and 0.5-1.25% glutaraldehyde in 0.1 M phosphate buffer (pH 7.2-7.4) at room temperature, and finally with 1 L of 10% sucrose in 0.1 M phosphate buffer (pH 7.2-7.4) at 4°C. The brainstem and cerebellum were removed, rinsed in 10% sucrose phosphate buffer, and embedded in a solution of 10% gelatin and 10% sucrose. The embedded tissue was stored overnight in 30% sucrose in 0.1 M phosphatebuffer (pH 7.2-7.4) and then cut into 40 μm transverse sections. Adjacent serial sections were processed with diaminobenzidine as a chromogen in the histochemical reaction for horseradish peroxidase (one series, DAB,

Graham and Karnovsky, 1966) or tetramethyl benzidine (two series, TMB, Gibson et al., 1984) as the chromogen and acetylcholinesterase (one series, AChE). A standard thiocholine method (Geneser-Jensen and Blackstad, 1971) was used with acetylthiocholine iodide as a substrate and ethopropazine as a non-specific acetylcholinesterase blocker (Hess and Voogd, 1986). The extent of the injection site was assessed in DAB reacted sections with light microscopy. The climbing fibers in the white matter and molecular layer were plotted from TMB reacted sections and their position was compared to the AChE-stained raphes in adjacent sections. The serial DAB- and TMB-processed sections of one case with an injection of WGA-HRP in the rostral MAO (B 2202) was put at our disposal by Dr. C. Yeo and J. van Ham, MD from the neurobiology group of the Department of Anatomy, University College, London U.K.

In three rabbits (C 914, C 1134, C 1135) tritiated leucine was injected in the caudal inferior olive. A stock solution of L(4,5-^{3}H)-leucine (specific activity about 140 Ci/mM, concentration 1 μCi/μl; Radiochemical Centre, Amersham, UK) was evaporated to dryness under a gentle flow of nitrogen at 40°C and redissolved in saline to a final concentration of 75 μCi/μl. Injections were performed with a 1 μl Hamilton syringe with a 25 gauge needle. To reduce unwanted spread of tritiated leucine delivery started 5 minutes after placing the needle in position. The injections were made at a rate of 0.1 μl per 10 minutes. After the injection the needle was left in place for an additional 15 minutes. Following a survival time of 4-7 days the animal was transcardially perfused under deep anaesthesia with 0.5 L of saline and 2 L of 4% formaldehyde. The brainstem and cerebellum were removed and embedded in 10% gelatin and transversely sectioned at 30 μm on a freezing microtome. Sections were mounted on slides prepared with a chrome-alum gelatin solution, defatted in xylene, dipped in Ilford G5 emulsion, and exposed for 6 weeks at 4°C. The sections then were developed in Kodak D19 at 16-18°C for 4 minutes, rinsed in distilled water, fixed in 24% sodium thiosulphate for 8 minutes, and counterstained with cresyl violet. Criteria previously described by Groenewegen and Voogd (1977) were used to delineate the effective injection site. All injection sites are illustrated in selected

sections and in graphical reconstructions of the inferior olive, prepared according to Brodal (1940) and Gerrits and Voogd (1982). The caudal dc and the rostral dc are separated by a narrow neck (Leonard et al., 1988). The border between the rostral dc and the vlo is arbitrary. The vlo is continuous with the dorsal leaf of the principal olive.

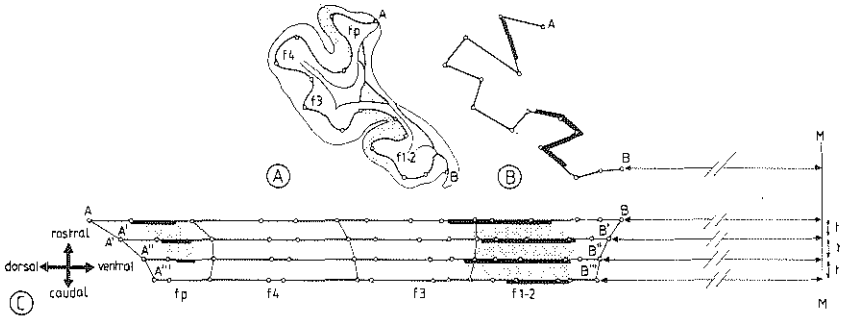

fig. 2.1 Diagram illustrating the unfolding of the Purkinje cell layer used to prepare maps of the unfolded surface of the flocculus. The Purkinje cell layer A-B is straightened; the position of labeled climbing fibers (in this case FZ_{II}) is indicated. Sections are aligned using the distance between the midline (M) and the most ventromedial point of the Purkinje cell layer (B). Four sections (A-B to A''' to B''') are reconstructed in C. The distance between the reconstructed sections (t) is obtained by multiplying the distance between the sections by the magnification factor.

The labeling of the climbing fibers was represented in diagrams of the unfolded Purkinje cell layer of the flocculus and the adjacent ventral paraflocculus. The length of the unfolded Purkinje cell layer in a single transverse section was indicated as a straight line (fig 2.1 A, B). Segments of this line representing the portions of the molecular layer containing the labeled climbing fibers were demarcated. The sections were aligned using the distance between the midline (M) and the most ventromedial point of the floccular Purkinje cell layer (B in fig. 2.1). The distance

between the reconstructed sections (t) corresponds to the distance between the sections multiplied by the magnification factor. Finally, the points on the lines representing the borders between the folia and the climbing fiber zones were interconnected (fig. 2.1).

The folial rosette of the flocculus usually consists of four or five folia which fuse caudally. They are indicated from ventral to dorsal as folium m and f1-f4. The cortices of the flocculus and the adjoining folium of the ventral paraflocculus (folium p) are continuous in the bottom of the posterolateral fissure (Yamamoto and Shimoyama,1977), but sometimes interrupted by surfacing white matter (figs. 1.2, 1.3 D). The compartments of the white matter of the flocculus are numbered from lateral to medial as C_2 and FC_1-FC_4. Raphes are indicated with the numbers of the compartments they separate (e.g. 1/2). Climbing fiber zones are indicated with the prefix FZ (floccular zone) and the Roman numeral of the corresponding compartment. Compartments in AChE-stained sections containing lobule X, and the corresponding climbing fiber zones, are indicated as XC_1-XC_4 and XZ_I-XZ_V respectively. The distribution of retrograde labeling in the AOS nuclei and VTRZ in experiments with injections of WGA-HRP into the inferior olive was determined and compared with the rostrocaudal extent of the injection site in the dc and the vlo (fig. 2.8).

2.3 Results

2.3.1 *Projections of the caudal dorsal cap (caudal dc).*

In six rabbits the targeted injection site was in the caudal half of the dorsal cap (caudal dc). In four cases (K 324, K 369, K 426, C 914) the injection site did not extend beyond the narrow neck separating the caudal dc from the rostral dorsal cap (rostral dc). In two other cases (K 314 and K 325) the injection site included the caudal part of the rostral dc. One experiment out of each of these two groups will be described in some detail.

The injection site in case K 369 (fig. 2.2 B) includes in addition to the caudal dc, the medial part of the caudal MAO and subnucleus ß. Retrogradely labeled neurons in the AOS are limited to the nucleus of the optic tract (NOT), dorsal (DTN) and interstitial (ITN) terminal nuclei (fig. 2.8 A). Climbing fibers from the caudal dc cross the midline, pass lateral to the spinal tract of the trigeminal nerve and accumulate along the medial border of the restiform body and more rostrally along the dorsal border (fig. 2.3 j). Many labeled fibers enter the cerebellum along the superior cerebellar peduncle. Within the cerebellum they pass rostral and dorsal to and through the anterior interposed nucleus to be distributed to the white matter of the vermis and the medial part of the hemisphere (fig. 2.3 d-m). Labeled fibers from the caudal dc enter the floccular white matter medially. Some of these fibers arch through or around group y and the ventromedial extension of the lateral cerebellar nucleus (Lpc). Within the flocculus they separate into two streams. One stream passes through the medial compartment FC_3 to accumulate in compartment FC_2 (figs. 2.3 h; 2.4 H). Within FC_2 the fibers are densely packed, especially medially. Their distribution in FC_2 is complementary to the AChE-staining, which is more concentrated in the lateral part of compartment (fig. 2.4 H). From this compartment labeled fibers enter the granular layer to terminate as climbing fibers in a continuous strip in the molecular layer of folia f1-4, and also the rostral pole of folium p (fig. 2.2 A; 2.3 b-g; 2.4 A-D). The border between labeled and unlabeled parts of the cortical layers is sharp. Climbing fiber zone FZ_{II}, composed of the terminals of olivocerebellar fibers from FC_2, gradually shifts laterally in more rostral sections (fig. 2.3 a-i; 2.4).

Labeled fibers of the second fiber stream accumulate at the border of the white matter of the flocculus with the restiform body and the brachium pontis along the AChE-positive cell strands in this region (fig. 2.3 f-h). Where the raphe between FC_3 and FC_4 can be clearly distinguished in the rostral flocculus they become located in FC_4, where they travel in a rostrodorsal direction (fig. 2.3 a-f; 2.4 A-C). They terminate as the climbing fiber zone FZ_{IV} in the medial parts of f3 and f4

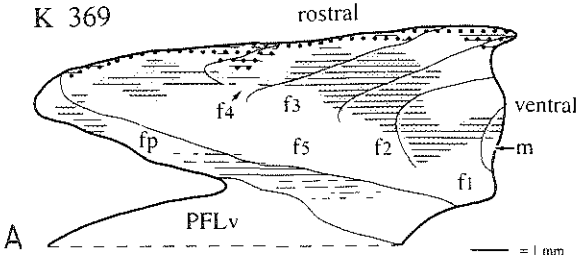
K 369
rostral
ventral
f4
f3
f2
f5
fp
f1
m
PFLv
A
= 1 mm

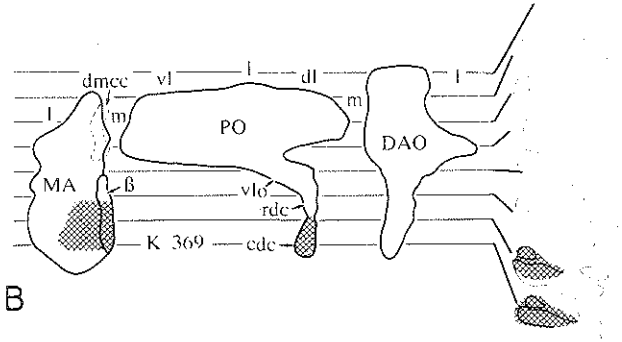
dmcc
vl
l
dl
m
PO
DAO
MA
ß
vlo
rdc
K 369
cdc
B

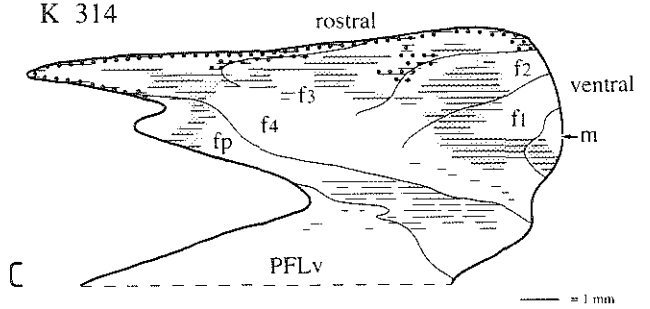
K 314
rostral
ventral
f2
f3
f4
f1
fp
m
PFLv
C
= 1 mm

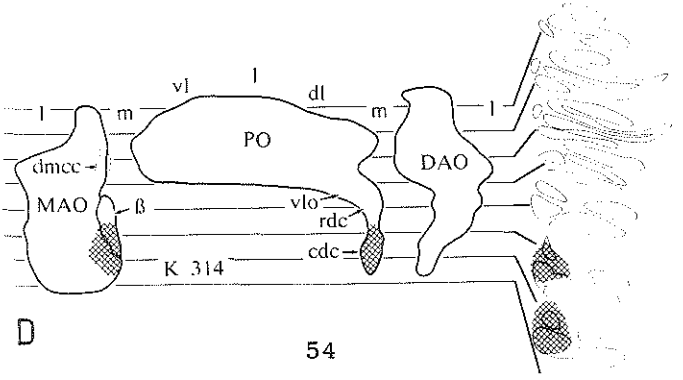
vl
l
dl
m
PO
DAO
dmcc
MAO
ß
vlo
rdc
cdc
K 314
D

(fig. 2.2 A). FZ_{IV} does not extend into folium p. FZ_{II} and FZ_{IV} are separated from each other by an empty strip of molecular layer corresponding to FZ_{III}, which is innervated from FC_3 (see next paragraph). Labeled climbing fibers from this injection site terminate in isolated patches in caudal folium p without a clear zonal pattern. This labeling cannot be associated with a specific compartment or climbing fiber zone (fig. 2.2 A).

Labeled olivocerebellar fibers in FC_2 can be traced caudally in the roof of the lateral recess, ventral to the lateral cerebellar nucleus. They continue their course in the roof of the fourth ventricle, near the attachment of the posterior medullary velum to enter the nodulus at its lateral side (fig. 2.3 i-k). Here they terminate in two climbing fiber strips, one in the medial and one in the lateral part of this lobule.

Four compartments can be distinguished in the white matter of the nodulus in adjacent AChE-stained sections (fig. 2.3 k-m; 2.7; 2.11 k-l; 2.12 m-n). Rather wide compartments XC_1 and XC_2 are present in the medial two thirds of the lobule. A distinct AChE-positive raphe delineates XC_3, which is only present in the dorsal white matter of the nodulus (fig. 2.7 A,C). It corresponds to a similar, but wider compartment in the lateral white matter of the uvula. Compartment XC_4 is narrow and occupies the lateral white matter of the nodulus. Labeled fibers are located in XC_4 and XC_1 (figs. 2.6 a; 2.7 G, H). Those contained in XC_4 terminate in two concentrations of climbing fibers on the ventrolateral aspect of the nodulus and in a narrow single strip on the dorsal aspect of this lobule. Labeled fibers in XC_1 innervate the XZ_I zone, flanking the

fig. 2.2 Drawings of the distribution of labeled climbing fibers in the unfolded flocculus and ventral paraflocculus and the injection sites in the caudal dorsal cap. The presence of labeled climbing fibers in the sections used to prepare the unfolded flocculus is indicated by horizontal lines. Climbing fibers of the FZ_{IV} zone are indicated with large dots, those belonging to FZ_{II} with small dots. Climbing fibers in caudal folium p cannot be allocated to these zones. Injection sites are indicated in a diagram of the unfolded inferior olive and in assorted transverse sections. A and B: case K 369; C and D: case K 314.

midline. This zone continues from the ventral side of the lobule X onto its dorsal side and farther into lobule IX. A rostrolateral triangular area, indicated with a question mark in fig. 2.6 a, is clearly separated from the rest of XZ_I.

Other fibers head for the midline dorsal to the cerebellar nuclei and constitute a parasagittal band of labeled fibers in the molecular layer of the vermis close to the midline. They correspond to the A zone of Groenewegen and Voogd (1977). Labeled olivocerebellar fibers enter the white matter of the paramedian, ansiform, and simple lobules from the region of the dorsolateral protuberance of the fastigial nucleus. They terminate as a continuous climbing fiber zone in the medial part of the molecular layer of these lobules (fig. 2.3 h-k) and correspond to the lateral A zone of Buisseret-Delmas (1988). The medial A zone and the lateral A are innervated from the subnuclei b and c of the caudal MAO, which are included in the injection site in this case.

Retrogradely labeled cells are present mainly in the medial part of the fastigial nucleus. A few labeled cells are located in the lateral cerebellar nucleus. Retrogradely labeled cells in the vestibular complex are found in the caudal descending vestibular nucleus (DV) bilaterally and in the ventral part of the ipsilateral medial magnocellular vestibular nucleus (MVmc). Very few labeled neurons are present in the SV, none are located in group y (fig. 2.3 d-k).

The injection site in case K 314 includes the caudal MAO, caudal DAO, subnucleus ß, and the caudal dc, and a bit of the caudal part of the rostral dc (fig. 2.2 C). The distribution of retrogradely labeled neurons in the AOS nuclei is similar to cases K 369 and K 426, but in addition a

fig. 2.3 Drawings of AChE-stained sections through the flocculus and the caudal vermis (left columns) and of adjacent sections incubated for HRP through the flocculus and the cerebellum (right columns) in case K 369. Note the presence of labeled olivocerebellar fibers in the FC_2 and FC_4 compartments of the flocculus and the XC_1 and XC_4 compartments of the nodulus and the termination of these fibers in corresponding zones. In addition, olivocerebellar fibers terminate in the A zone of the anterior vermis (A) and in the lateral A zone (dlp) of Buisseret-Delmas (1988).

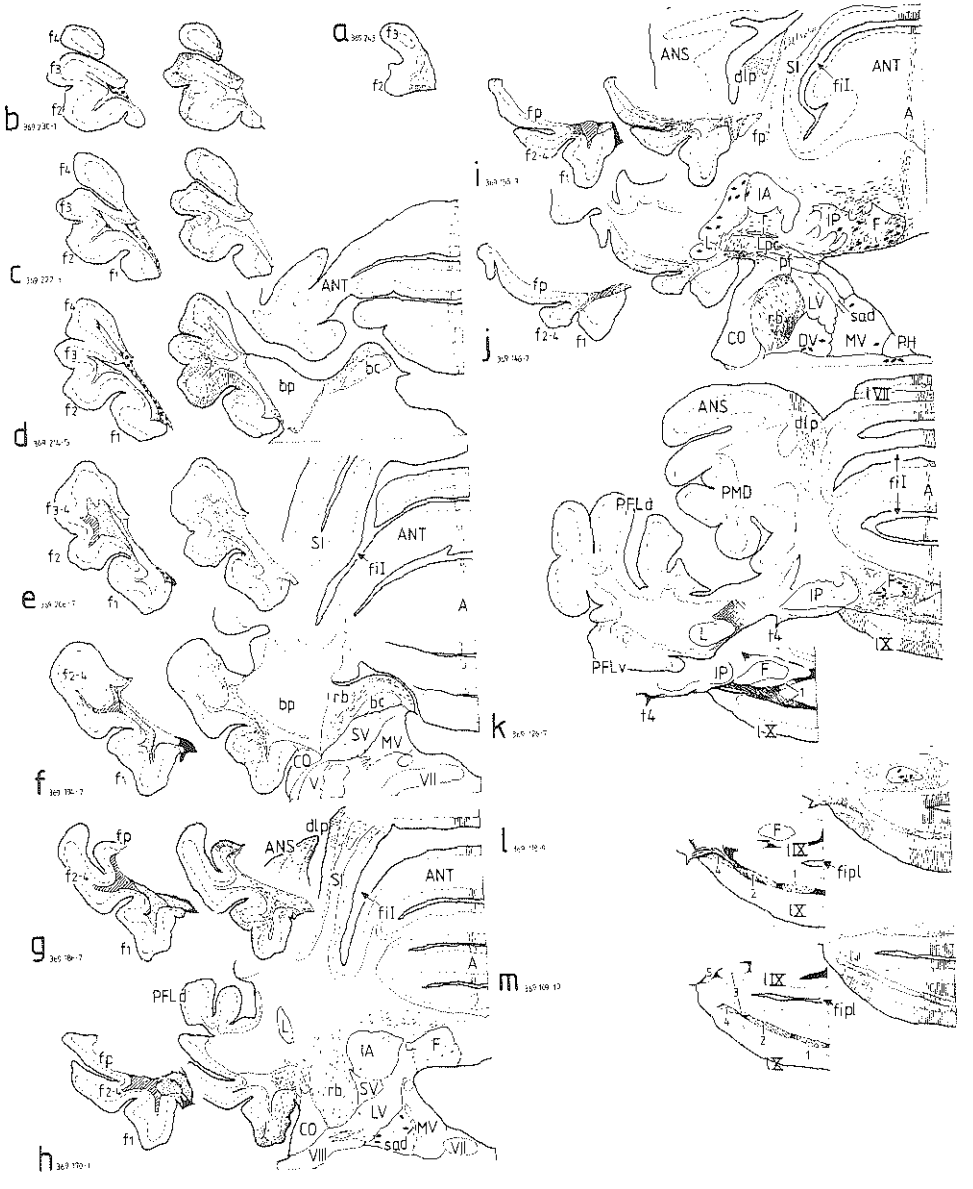
a
b
c
d
e
f
g
h
i
j
k
l
m
ANS
dlp
SI
ANT
filI
A
fp
f1
f2-4
IA
IP
F
Lpc
Lpl
LV
sad
rb
CO
DV
MV
PH
bp
bc
SV
V
VII
VIII
IX
PMD
PFLd
PFLv
t4
fipl

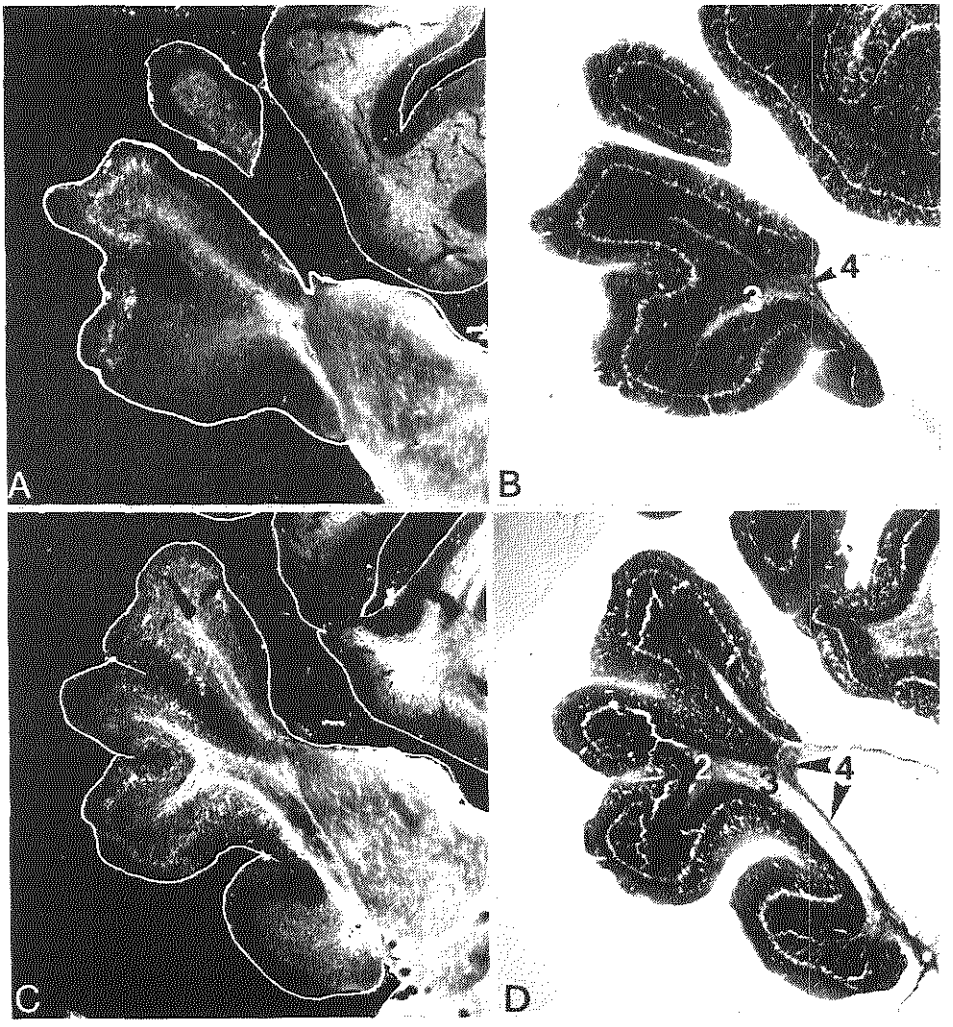

fig. 2.4 Darkfield photomicrographs of four sections through the flocculus in case K 369 (A, rostral; G, caudal) and brightfield photomicrographs of adjacent AChE-stained sections (B-H).


E
F
1
2
3
4
G
H
1
2
3

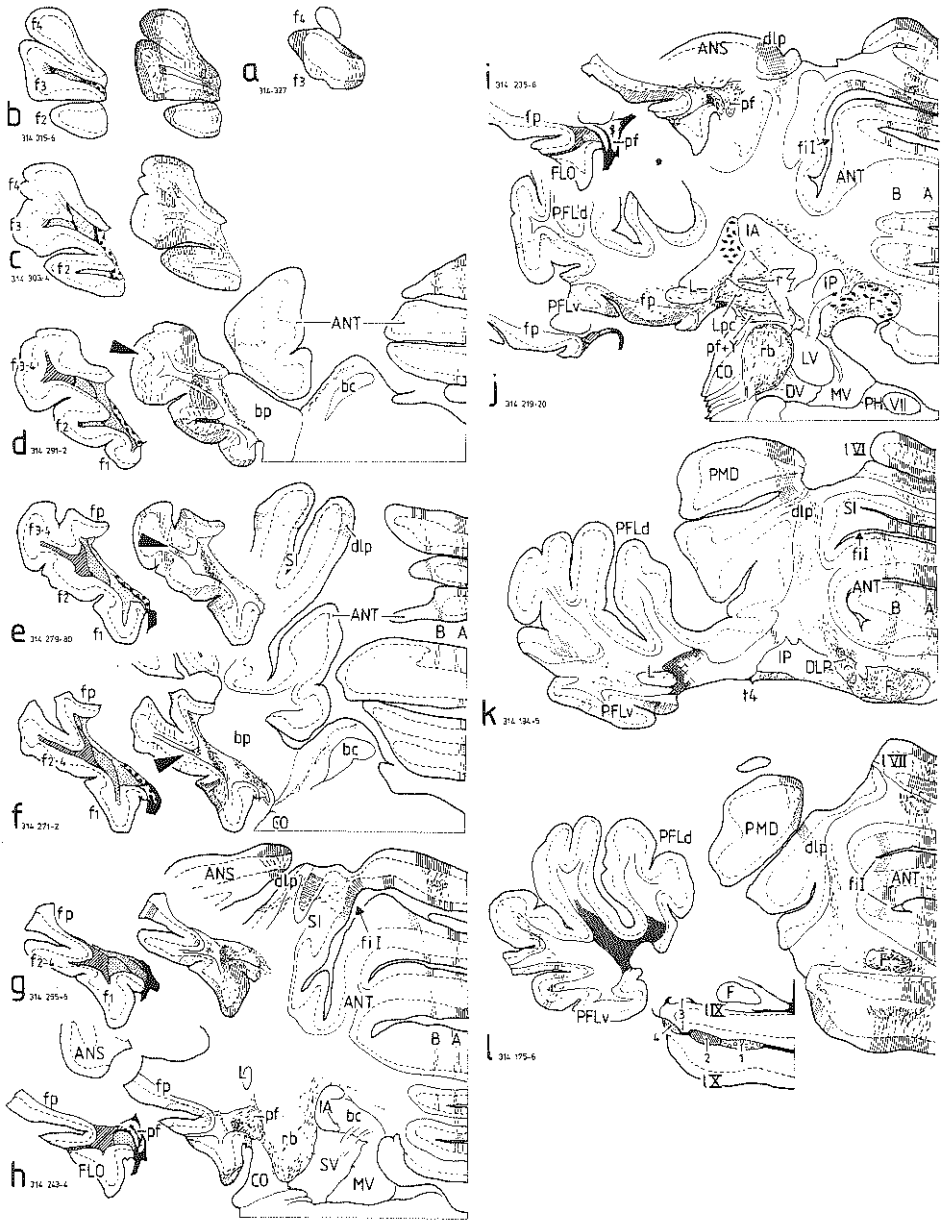
a
b
c
d
e
f
g
h
i
j
k
l
f4
f3
f2
f1
f3-4
f2-4
ANS
dlp
SI
fil
ANT
B A
fp
pf
FLO
PFLd
PFLv
IA
IP
Lpc
pf+rb
rb
CO
LV
DV
MV
PH
VII
bp
bc
SV
PMD
DLP
t4
F
IX
X
1
2
3
4

small number of weakly labeled neurons was observed in the VTRZ. Labeled fibers are located in compartments FC_2 and FC_4 and terminate in the corresponding climbing fiber zones FZ_{II} and FZ_{IV} (fig. 2.5; 2.10 A-B, D). In this case a third fiber stream is present. It separates from the second fiber stream in the caudal flocculus and travels in FC_1 in a lateral direction towards folium f2 and f3 to terminate in the most lateral parts of the molecular layer of these folia (figs. 2.3. C; 2.5 d-g, arrows). As in case K 369 labeled climbing fibers are also found in the caudal part of folium p. The labeling appears as patches in the molecular layer and cannot be associated with any of the floccular zones or compartments (fig. 2.5 i-k).

The distribution of labeling in the XC_1 and XC_4 compartments and the XZ_I and XZ_{IV} zones of the nodulus is similar to the previous case (figs. 2.5 l; 2.6 b). Climbing fiber labeling was present in the A and B zones of the anterior vermis and in the lateral A zone of Buisseret-Delmas (1988) in the hemisphere of the posterior lobe.

The distribution of tritiated leucine-labeled climbing fibers in case C 914, with an injection in the caudal dc and the subnucleus ß (fig. 2.14 A) is similar to the previous two cases (fig. 2.6 C; 2.7 H).

fig. 2.5 Drawings of adjacent AChE-stained and HRP-reacted transverse sections through brain stem and cerebellum in case K 314. Note the presence of labeled fibers in compartments FC_2 and FC_4, which terminate as climbing fibers in corresponding zones in the molecular layer of the flocculus. Some labeled fibers are present in compartment FC_1, terminating in FZ_I (arrowheads in d-f). Labeling in lobule X is present in compartments XC_1 and XC_4. For symbols indicating compartments in AChE-stained sections see fig. 2.3.

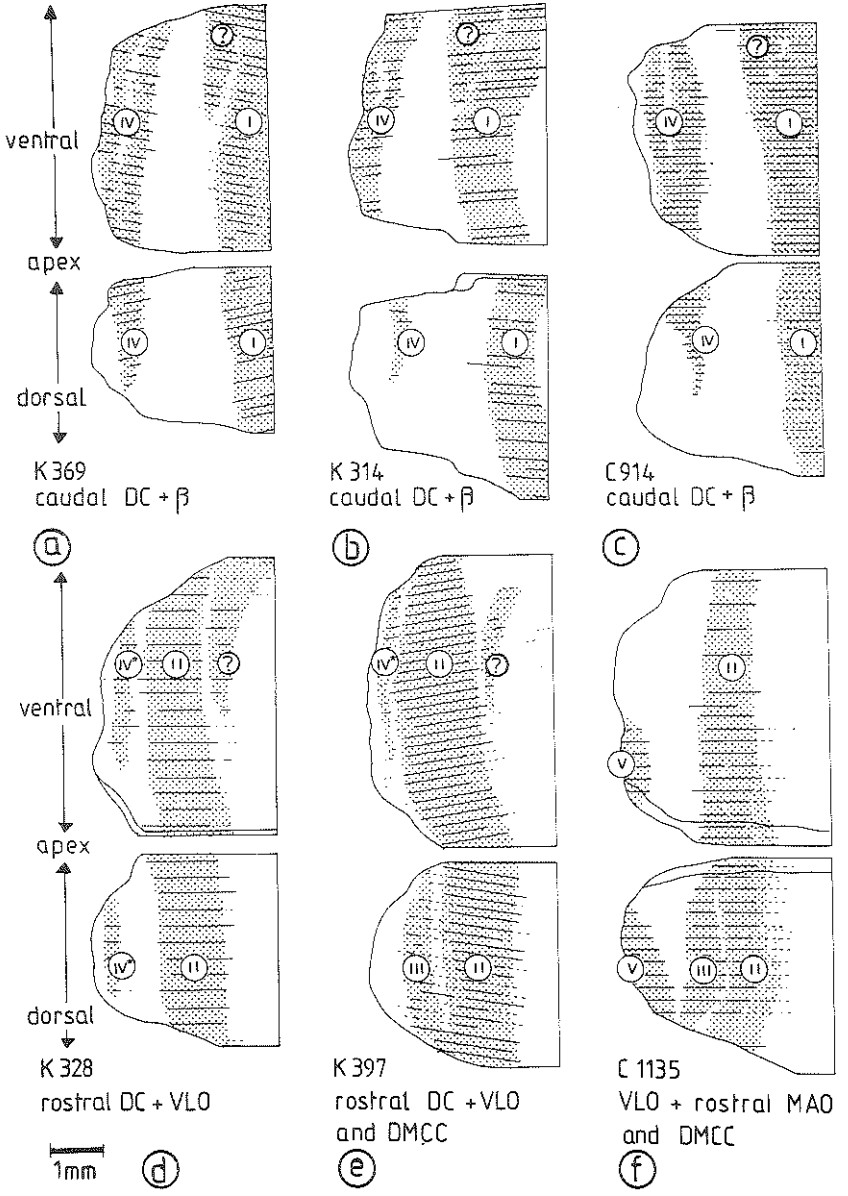
ventral
apex
dorsal
K 369
caudal DC + β
K 314
caudal DC + β
C 914
caudal DC + β
a
b
c
ventral
apex
dorsal
K 328
rostral DC + VLO
K 397
rostral DC + VLO
and DMCC
C 1135
VLO + rostral MAO
and DMCC
1mm
d
e
f

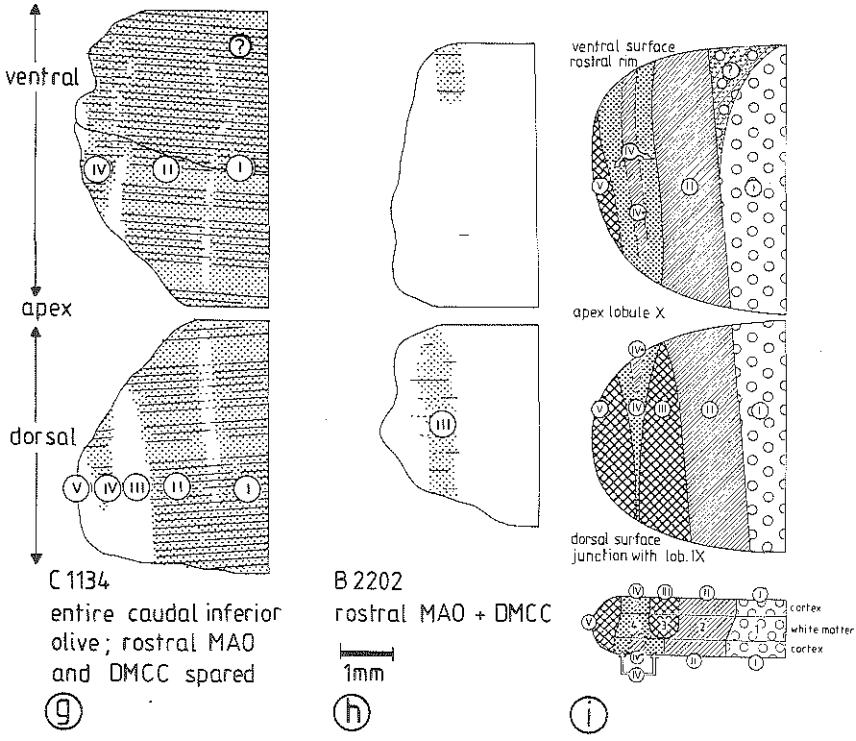

fig. 2.6 Maps of the climbing fiber distribution on the ventral and dorsal surface of lobule X. The presence of labeled climbing fibers in the sections used to prepare the maps is indicated by lines. Climbing fiber zones are numbered I-V and indicated by dots. The intermediate, rostral dc/vlo-innervated strip in XZ_{IV} is indicated as XZ_{IV}*. Arabic numerals refer to the white matter compartments XC_1-XC_4 illustrated in the bottom diagram in fig. 2.6 i. The ventromedial compartment indicated with a questionmark was labeled after injections including the group ß, the caudal and rostral dorsal cap (a-d) and in one of the cases involving the ventrolateral outgrowth (e). A summarizing diagram of the compartments and the climbing fiber zones of the nodulus is shown under i. The white matter compartment corresponding to XZ_V cannot be distinguished in AChE-stained sections and is not indicated in i.

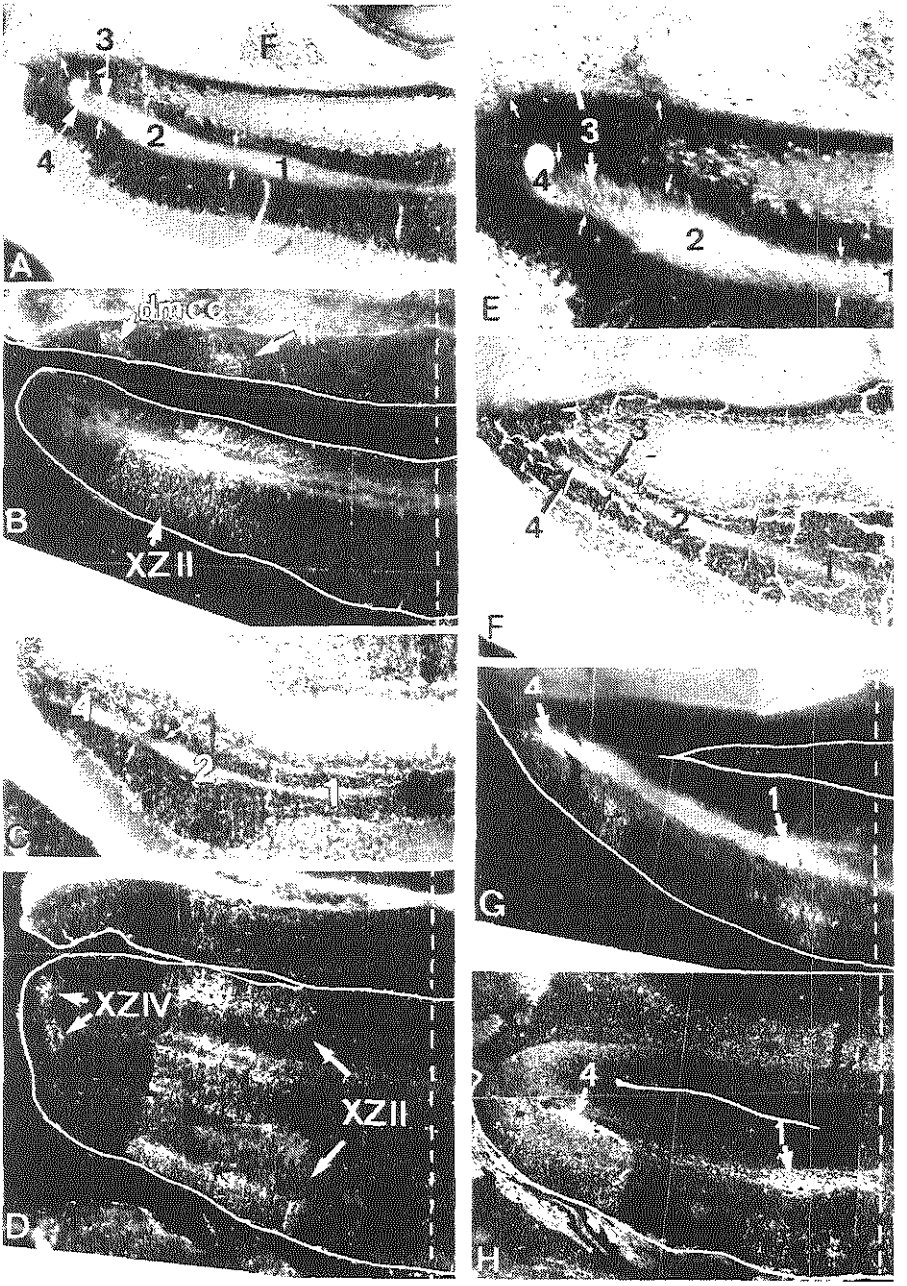
A
3
F
4
2
1
B
dmcc
XZII
C
4
2
1
D
XZIV
XZII
E
3
4
2
1
F
3
4
2
1
G
4
1
H
4
1

2.3.2 *The projection of the rostral dorsal cap and ventrolateral outgrowth (rostral dc/vlo).*

In five rabbits (K 327, K 328, K 333, K 397 and C 1135) the injection site involved the rostral dc/vlo. Three of these cases (K 328, K 397 and C 1135) will be presented.

The injection site in case K 328 is limited to the rostral dc and vlo (fig. 2.9 B). Retrogradely labeled neurons in the AOS nuclei are only present in the VTRZ (fig. 2.8 B). Labeled olivocerebellar fibers, located along the dorsolateral border of the contralateral restiform body, enter the floccular peduncle, where they ramify among the cells of group y (fig. 2.11 g-i). Next they occupy compartment FC_3 and, arching over FC_2, also distribute to compartment FC_1 (Fig. 2.11 f-g). They can be traced through FC_1 and FC_3 to terminate as climbing fibers in the FZ_I and FZ_{III} zones (fig. 2.9 A). FZ_I occupies a lateral position, but remains separated from the lateral margin of the flocculus by an unlabeled stretch of molecular layer, corresponding to the C2 zone (see below), which broadens more caudally. The C_2 compartment of the flocculus also does not contain any labeled fibers (fig. 2.9 A; 2.11 e-g). FZ_{III} is separated from FZ_I by an empty strip, corresponding to FZ_{II} (fig. 2.11 a-h). FZ_I and FZ_{III} extend into folium p, enclosing the dorsal tip of FZ_{II} (fig. 2.12 e,

Fig. 2.7 Photomicrographs of AChE-stained sections and darkfield exposures of sections containing labeled fibers in lobules IX and X.
A,B,F: case K 397. A,B: AChE. The raphes bordering compartment 3, which is present in dorsal lobule X and occupies the lateral white matter of lobule IX and the raphe between the compartments XC_1 and XC_2 are indicated with small, white arrows in A and E. The compartments are indicated with arabic numerals. WGA-HRP labeled fibers from the rostral dc and the vlo are present in XZ_{II} and XC_2. Labeled climbing fibers from the dmcc are present in XC_3 and terminate laterally in lobule IX (arrow).
C,D: case K 328. WGA-HRP labeled fibers from rostral dc and vlo are present in compartments XC_2 and XC_4 and corresponding zones.
F,G: case K 369. WGA-HRP labeled fibers after an injection in caudal dc and subnucleus ß are present in XC_1 and XC_4.
H: Case C 914, with an injection of tritiated leucine in caudal dc and subnucleus ß. Distribution as in previous case K 369.

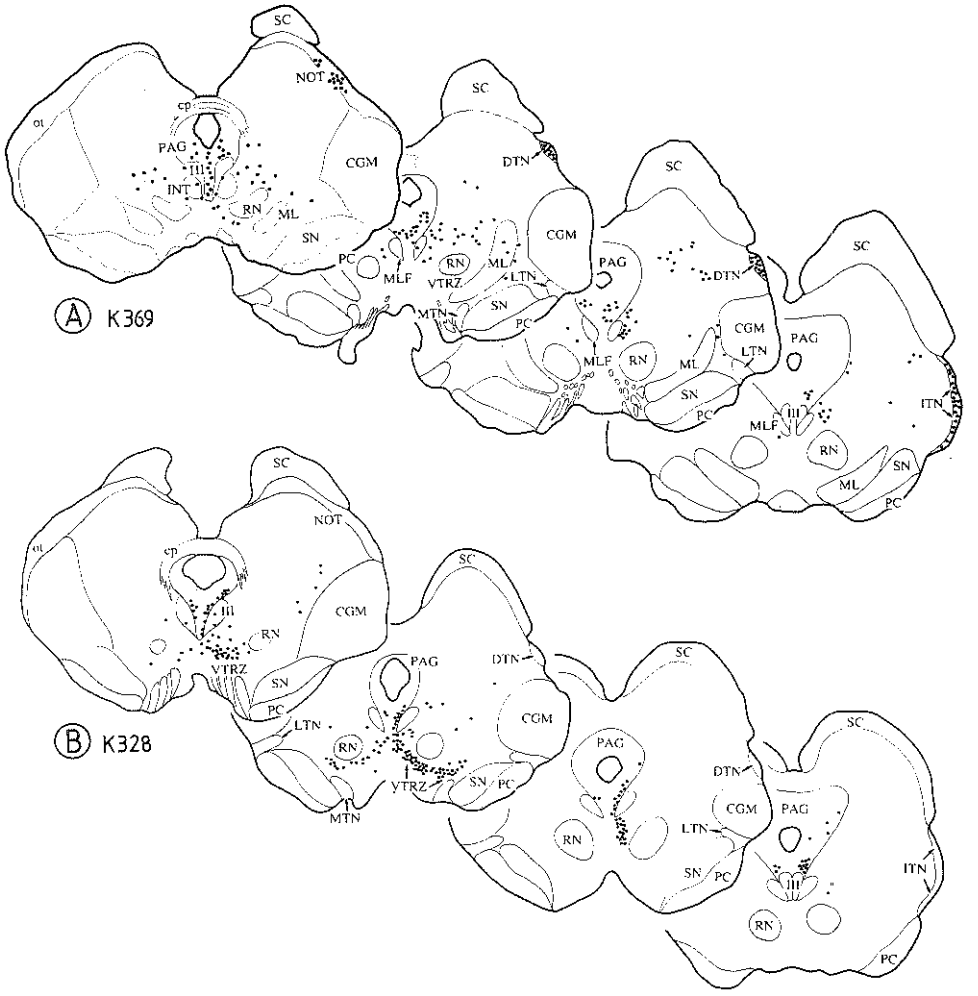

fig. 2.8 Drawings of transverse sections through the mesencephalon in cases K 369 (A) with an injection involving the cdc and K 328 (B) with an injection involving the rdc/vlo. Black dots indicate retrogradely labeled cells. The VTRZ is labeled in case K 328; the nucleus of the optic tract (NOT), the dorsal and interstitial nuclei of the accessory optic tract (DTN, ITN) in case K 369.

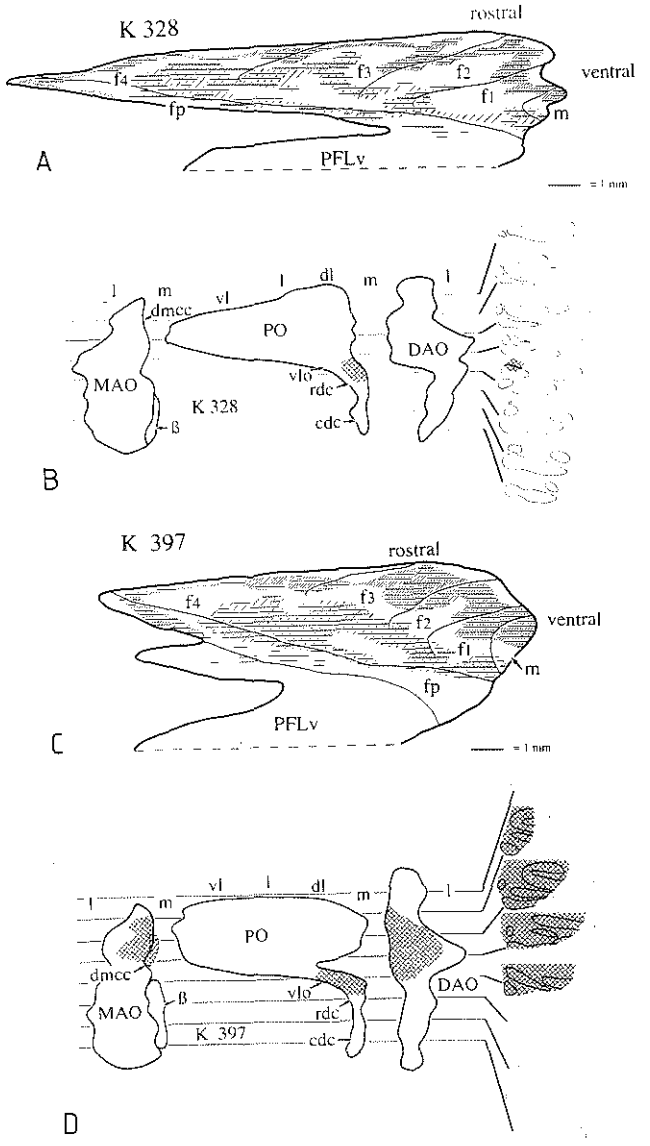

fig. 2.9 Diagrams of the distribution of climbing fibers in the unfolded flocculus and ventral paraflocculus and diagrams of the inferior olive showing injection sites including the rostral dorsal cap and ventrolateral outgrowth, in cases K 328 (A,B) and K 397 (C,D). Labeled climbing fibers in sections used to prepare the unfolded flocculus are indicated with horizontal lines. Labeling in FZ_I is indicated with coarse hatching and in FZ_{III} with fine hatching.

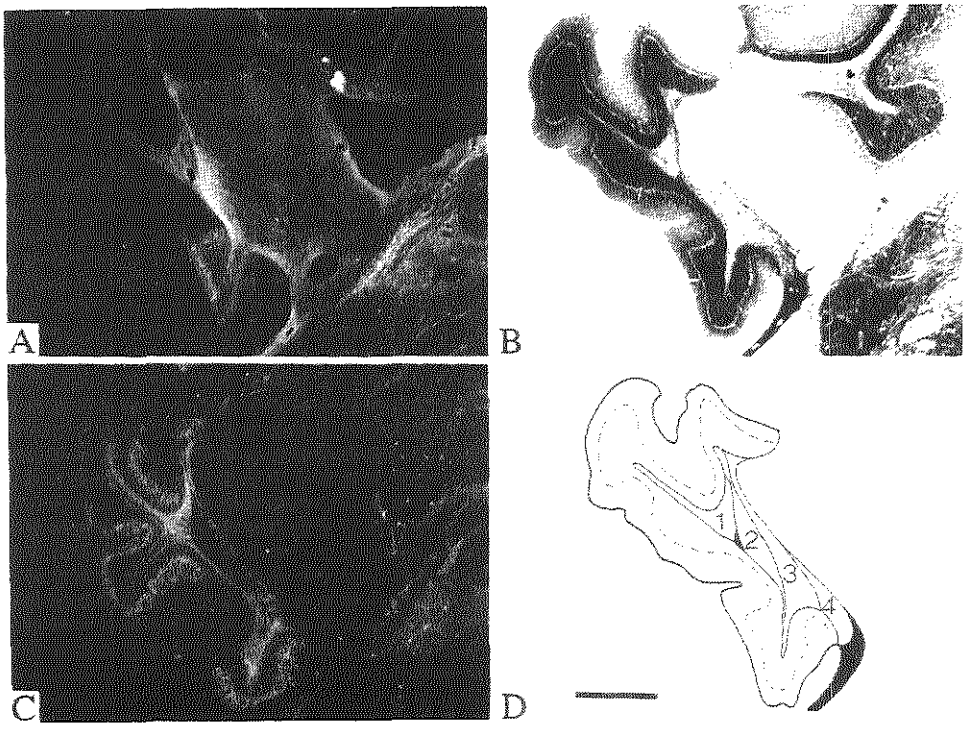

fig. 2.10 Darkfield photomicrographs of corresponding TMB-processed sections through the flocculus in K 314 (A) with an injection in the caudal dorsal cap and K 327 (C) with an injection in the rostral dorsal cap. Raphes and white matter compartments are depicted in B and D. Note that the labeled parts of the white matter and associated floccular cortex in K 314 (FC_2, FC_4 and FZ_{II}) are not labeled in K 327 which shows prominent labeling in FC_1, FC_3 and FZ_I and FZ_{III}.

arrow). Patchy climbing fiber labeling is present in the molecular layer of the central part of folium p (fig. 2.11 f-i), and it cannot be correlated to any of the FC or FZ.

Labeling in compartment FC_3 can be traced caudally, ventral to the lateral cerebellar nucleus and medially along the attachment of the roof of the fourth ventricle (fig. 2.11 j). These fibers subsequently enter lobule X. Here they occupy compartments XC_2 and XC_4, which can be delineated in adjacent AChE stained sections (fig. 2.11 k-l). Fibers from XC_2 terminate

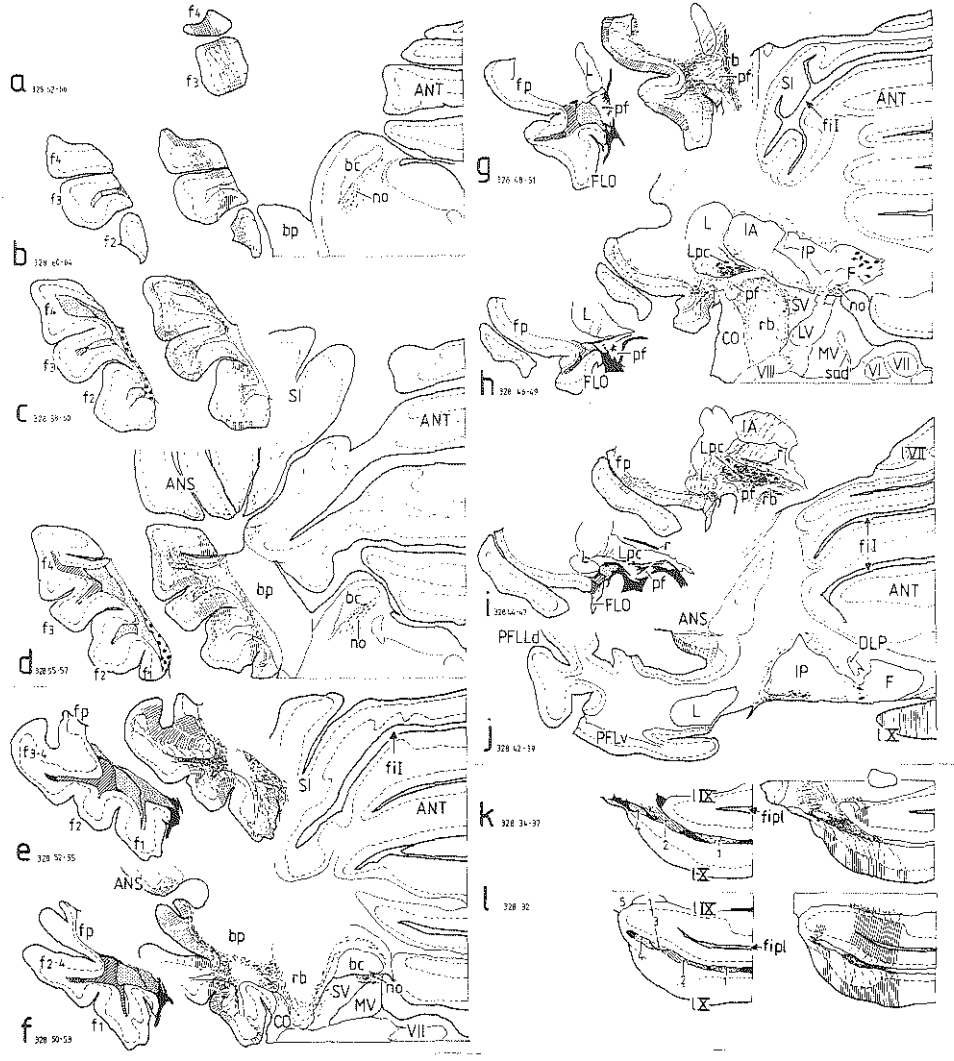

fig. 2.11 Drawings of adjacent AChE and HRP-reacted transverse sections through brain stem and cerebellum in case K 328. Note the presence of labeled fibers in FC_1 and FC_3 and FZ_I and FZ_{III} in the flocculus and in compartments and zones XZ_I and XZ_{IV} of lobule X. For symbols indicating compartments in AChE-stained sections see fig. 2.3.

as climbing fibers in the intermediate part of XZ_{II}, which is continuous in the bottom of the posterolateral fissure with a similar zone in lobule IX (fig. 2.6 d; 2.7 D). Labeled fibers in compartment FC_4 terminate in a narrow lateral strip on the ventral and dorsal aspect of this lobule. The medial compartment XC_1 and the medial cortex do not contain labeled fibers.

A heavy concentration of retrogradely labeled cells is present in the Lpc (fig. 2.11 h-i), a few labeled cells are found in the fastigial nucleus. Neurons of dorsal group y, lying within the floccular peduncle or ventral group y, capping the restiform body are not labeled. Labeled fibers pass medially from the Lpc in the rostral wall of the lateral recess and the lateral angle of the fourth ventricle (no, fig. 2.11 h). They ascend in a bundle located ventral and ventrolateral to the superior cerebellar peduncle (fig. 2.11 b-f) which enters the decussation of the superior cerebellar peduncle. Their localization corresponds to the nucleo-olivary fibers (Légendre and Courville, 1987), which were retrogradely labeled in this experiment.

The injection site in K 397 is larger than in K 328 and in addition to the rostral dc and vlo, it also involves the dmcc and the rostromedial parts of the DAO and MAO, except for their rostralmost poles (fig. 2.9 D). It also extends into the contralateral olive. Retrogradely labeled cells are present in the VTRZ, but they were absent from the NOT, DTN, and ITN (fig. 2.8 B). Hardly any labeled cells were found in the MTN and LTN. Labeled fibers enter the flocculus via the floccular peduncle (fig. 2.12 i-l), pass through group y and the anterior interposed and lateral cerebellar nuclei. The distribution of labeled olivocerebellar fibers in the flocculus is very similar to the previous case (K 328). The labeled climbing fibers of FZ_I and FZ_{III} merge in the rostral molecular layer of folium p, surrounding a small unlabeled area, corresponding to the FZ_{II} zone (Fig. 2.12 e, arrow). Caudally patchy labeling extends into the central part of folium p and into other parts of the ventral paraflocculus (fig. 2.12 g-j). The labeling in lobule X also resembles the previous case. In addition, some labeled fibers are present in compartment XC_3 (fig. 2.12 n) and

they terminate in XZ_{III} in the lateral half of the dorsal molecular layer of lobule X, adjacent to XZ_{II} and the ventral molecular layer of lobule IX (figs. 2.6 e; 2.12 m-n). Labeling in the hemisphere of the anterior and posterior lobes is fairly extensive. In the white matter of the caudal vermis labeled olivocerebellar fibers surround an empty compartment (fig. 2.12 l, asterisk), which contained the fibers from the lateral A-zone in experiments with injections involving the caudal and medial MAO (figs. 2.3 k; 2.5 k-l).

Extensive retrograde labeling is present among neurons of the cerebellar nuclei, including the Lpc (fig. 2.12 i-l; 2.13 D). The neurons of dorsal group y located between the fibers of the floccular peduncle and of the ventral group y located ventral to the peduncle and dorsal to the restiform body are not labeled. Some labeled cells are located in the medial and descending vestibular nuclei. The nucleo-olivary fiber bundle situated in the lateral recess of the fourth ventricle and ventral to the superior cerebellar peduncle is heavily labeled (no, fig. 2.12 d-h; 2.13).

In one case (C 1135, fig. 2.14 B) an injection of tritiated leucine was made in the rostral dc and vlo, but it also extended widely into other parts of the inferior olive, including the rostral pole of the MAO, which is thought to contain neurons projecting to the C_2 zone, and the dmcc. In the rostral dc/vlo the injection site was situated somewhat more rostrally than in the previous two cases (K 328 and K 397). The distribution of fibers in the floccular cortex is similar to them except for the presence of labeled climbing fibers in the cortex lateral and caudal to FZ_I, corresponding to the C_2 zone, which was unlabeled in K 328 and K 397. In C 1135 labeling in the C_2 zone continues into the medial part of the ventral paraflocculus and the dorsomedial and lateral part of the dorsal paraflocculus. Some labeled fibers are present in the fastigial and posterior interposed nucleus. Most are located in and dorsal to the anterior interposed and the medial part of the lateral cerebellar nucleus.

The white matter of the nodulus contains bundles of labeled fibers in an intermediate and a lateral position. They terminate as climbing fibers in a central zone corresponding in position to the XZ_{II} zone of the

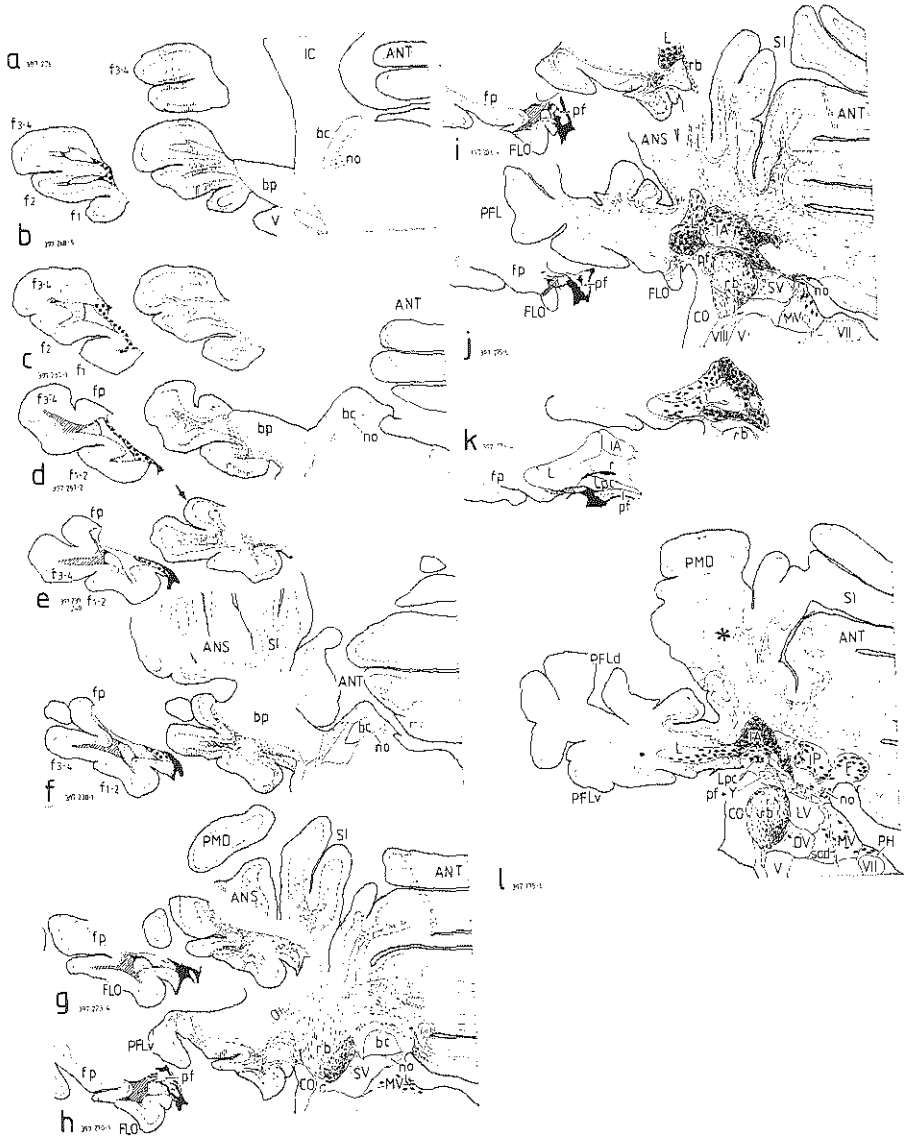
a
f3-4
IC
ANT
f3-4
bc
no
bp
f2
f1
V
b
c
f3-4
f2
f1
ANT
d
f3-4
fp
bp
bc
no
f1-2
e
fp
f3-4
f1-2
ANS
SI
ANT
f
fp
bp
bc
no
f3-4
f1-2
g
PMD
SI
ANT
ANS
fp
FLO
PFLv
pf
rb
bc
SV
no
CO
MV
h
fp
pf
FLO
i
L
rb
SI
fp
pf
ANT
FLO
ANS
PFL
IA
pf
fp
pf
rb
SV
no
FLO
FLO
CO
MV
VII
V
VII
j
k
rb
IA
L
fp
Lpc
pf
l
PMD
SI
ANT
PFLd
IA
L
IP
Lpc
PFLv
pf + r
no
CO
rb
LV
DV
MV
PH
V
VII

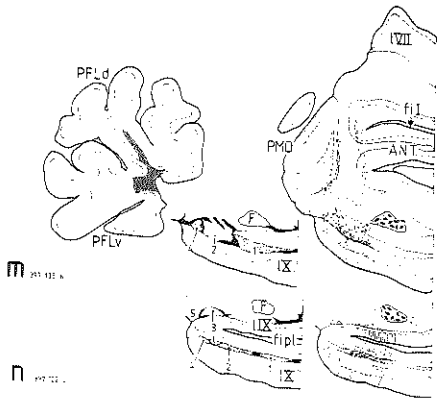

fig. 2.12 Drawings of adjacent AChE and HRP-reacted transverse sections through brain stem and cerebellum in case K 397. Asterisk (in l) indicates the position of the lateral A zone and the corresponding compartment of Buisseret-Delmas (1988), which was labeled in K 369/314 (figs 2.3 and 2.9). Arrow in e indicates extension of non-labeled FZ_{II} in folium p. Labeled fibers occupy the compartments FC_1 and FC_3 and terminate in the corresponding zones. In the nodulus (m-n) labeling is present in XC_1, XC_3, and XC_4 and terminates in the corresponding zones. For symbols indicating compartments in AChE-stained sections see fig. 2.3

previous cases. In addition an extremely lateral strip of molecular layer surrounding the lateral pole of the lobule (XZ_V) and a strip on the dorsal surface of the lobule (XZ_{III}) contain labeled climbing fibers. These fibers presumably take their origin from the rostral MAO and/or the dmcc. Regions of the molecular layer corresponding to XZ_I and XZ_{IV} remain virtually empty (figs. 2.6 f; 2.15 A).

Retrograde labeling of cells in the cerebellar nuclei does not occur with injections of tritiated leucine in the inferior olive. No labeled fibers are observed in the position of the nucleo-olivary tract.

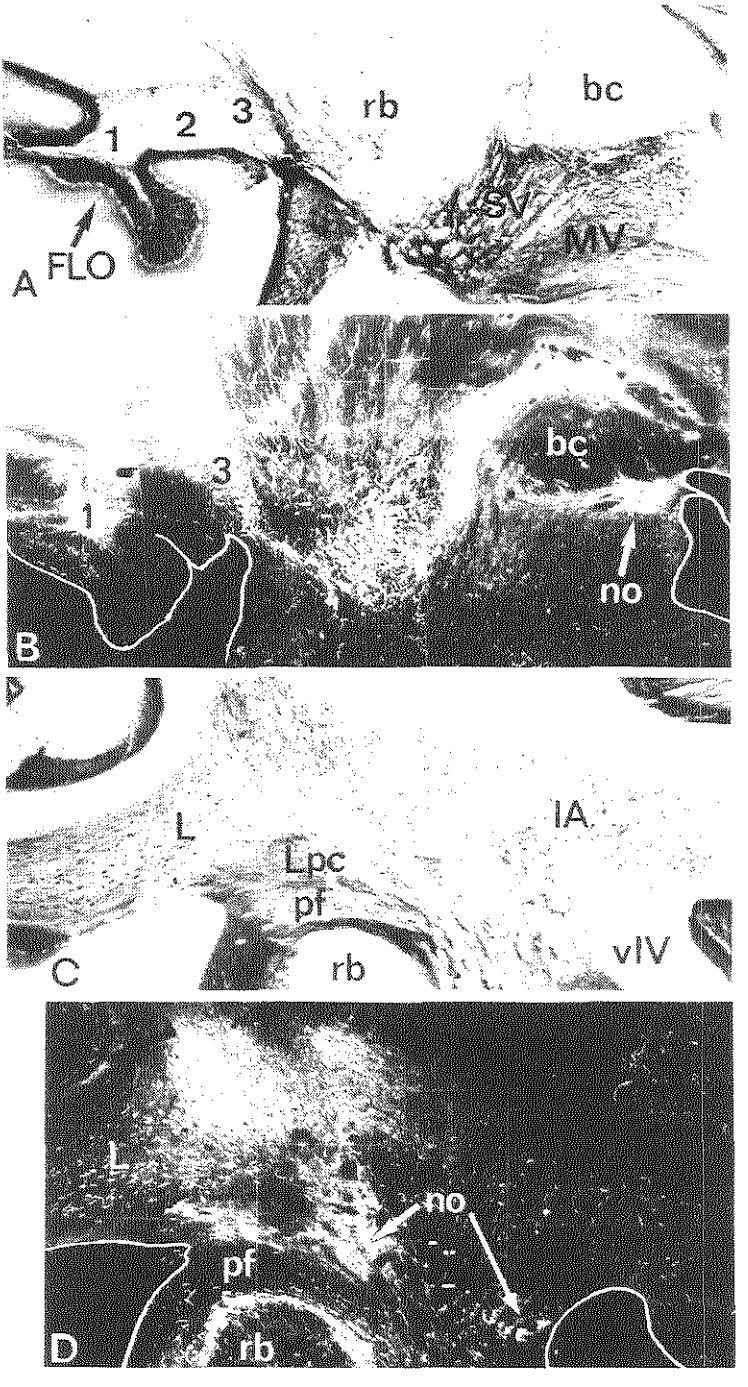
1
2
3
rb
bc
SV
MV
A
FLO
bc
3
1
no
B
L
IA
Lpc
pf
C
rb
vIV
L
no
pf
rb
D

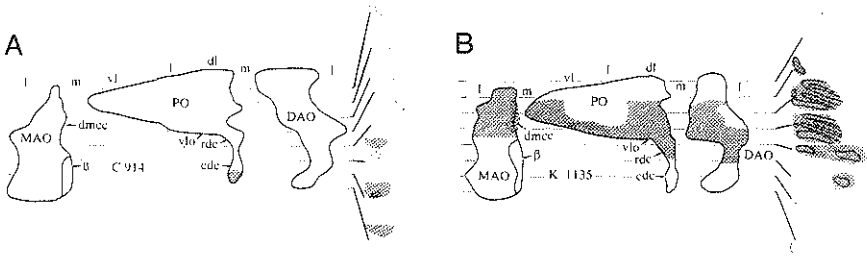

fig. 2.14 Diagrams of the injection sites in the inferior olive of cases C 914 and C 1135.

2.3.3 *The projection of the rostral pole of the medial accessory olive (MAO) and the dorsomedial cell column (dmcc).*

In one case a small injection of WGA-HRP was confined to the rostromedial part of the MAO and the dmcc (B 2202, fig. 2.16 D). In another rabbit large parts of the inferior olive, including the caudal dc, the rostral dc and the vlo, were injected with tritiated leucine, but the rostral pole of the MAO and the dmcc were spared (C 1134, fig. 2.16 B).

Labeled climbing fibers in case B 2202 (fig. 2.16 C; 2.17) travel through the ventromedial part of the restiform body to enter the cerebellum rather caudally. They curve medially towards the midline over the anterior interposed nucleus and accumulate in the posterior interposed nucleus. From this fiber bundle labeled fibers detach to enter the stalk of the paraflocculus. They terminate in a distinct C_2 zone extending over the dorsal and the ventral paraflocculus and the caudal part of the flocculus (fig. 2.17 b-h). In the white matter of the flocculus

fig. 2.13 Brightfield (A,C) and darkfield (B,D) photomicrographs of transverse sections through brainstem and flocculus in K 397.
A,B: anterograde labeling is present in compartments FC_1 and FC_3 and retrograde labeling in the nucleo-olivary pathway (no).
C,D: Fibers of the nucleo-olivary pathway (no) collect at this more caudal level near the lateral angle of the fourth ventricle. The floccular peduncle (pf) does not contain labeled fibers.

and the paraflocculus these fibers occupy a region corresponding to the C_2 compartment. Other labeled olivocerebellar fibers enter the caudal vermis, where they terminate in dorsal lobule X and ventral lobule IX in a position corresponding to the XZ_{III} zone (fig. 2.17 f-h). Retrogradely labeled cells are found in the posterior interposed nucleus and a small cell group ventral to it. A few retrogradely labeled fibers were observed in the nucleo-olivary tract in the lateral angle of the fourth ventricle (fig. 2.17 a-c).

In case C 1134 the injection with tritiated leucine involved the caudal dc, rostral dc and vlo (fig. 2.16 B). It extended into the caudal half of the MAO and DAO and subnucleus ß, but spared the rostral pole of the MAO, which contains the neurons projecting to the C_2 zone. Dense labeling was present over all parts of the white matter and the molecular layer of the flocculus except for a small area in the caudal pole, where all

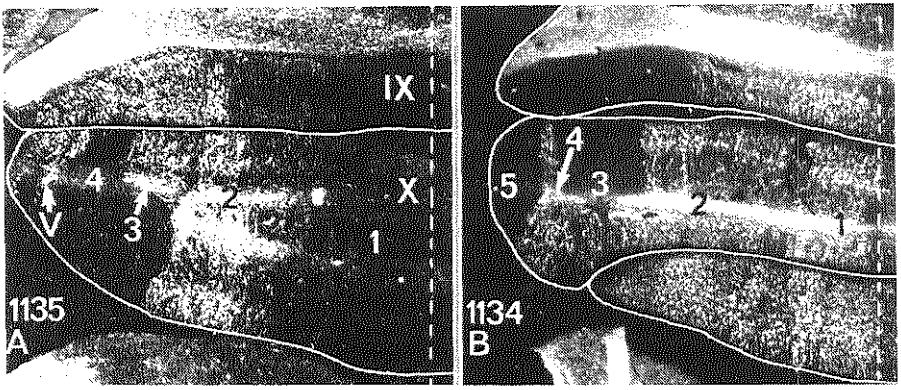

fig. 2.15 Darkfield photographs of autoradiograms of sections through the lobules IX and X.
A) C 1135. This injection involved the rdc, the vlo and the rostral MAO and labeled fibers in compartments XC_2 and XC_3 and the corresponding zones and in the extreme lateral pole of lobule X (XZ_V).
B) C 1134. This large injection spared the rostral MAO and the dmcc. No labeling is observed in compartment XC_3 zones XZ_{III} and XZ_V.

folia taper into a single folium (fig. 2.16 A). This area approximately corresponds with the lateral unlabeled area seen in the caudal flocculus of rostral dc/vlo injected cases and the labeled C_2 compartment in case B 2202. The labeling in the white matter of case C 1134 was characterized by the relatively sparse labeling at the borders between the compartments. These areas of sparse labeling seem to coincide with AChE-positive raphes (fig. 2.18). Labeling in the nodulus spared the XC_3 compartment and the XZ_{III} zone, and the molecular layer covering the lateral pole of the lobule, corresponding to XZv (fig. 2.15 B). Labeled olivocerebellar fibers are also found in the fastigial nucleus, the medial part of the vermis and paramedian lobule, the dorsal part of the simple lobule, and in several small bands in the ventral paraflocculus and the ventral part of the dorsal paraflocculus. This large injection of anterograde tracer caused no labeling in the nucleo-olivary tract (fig. 2.18).

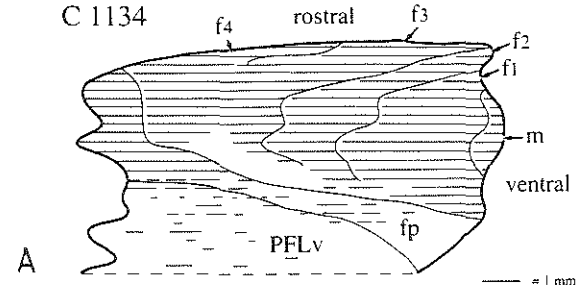
C 1134
f4
rostral
f3
f2
f1
m
ventral
fp
PFLv
A
≈ 1 mm

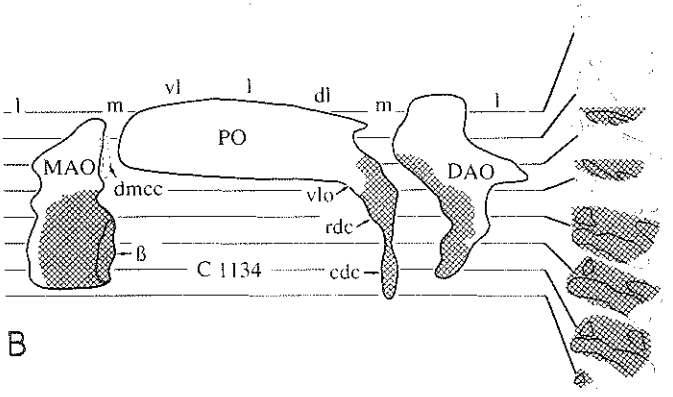
l
m
vl
l
dl
m
l
PO
MAO
DAO
dmcc
vlo
rdc
ß
C 1134
cdc
B

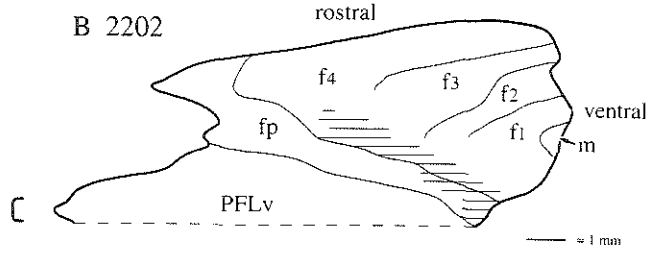
B 2202
rostral
f4
f3
f2
ventral
fp
f1
m
PFLv
C
≈ 1 mm

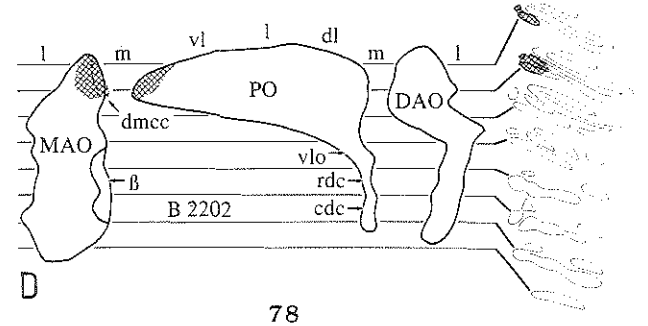
l
m
vl
l
dl
m
l
PO
DAO
dmcc
MAO
vlo
ß
rdc
B 2202
cdc
D

2.4 Conclusions

The olivocerebellar projection to the flocculus and nodulus is summarized in the diagrams of figs. 2.19 and 2.6 i.

1. Labeled olivocerebellar fibers in the flocculus from injections including the caudal dc (i.e. the region caudal to the constricted portion of this subnucleus, cases K 369, K 314, K 426 and C 914) become located in compartments FC_2 and FC_4 of the white matter of the flocculus, which are delineated by AChE-positive raphes in adjacent AChE-stained sections. They terminate in the corresponding cortical zones FZ_{II} and FZ_{IV} (fig. 2.19). Injections involving the rostral dc and vlo result in labeling fibers in compartments FC_1 and FC_3, which terminate in FZ_I and FZ_{III}. These zones extend into folium p and merge around the rostral tip of FZ_{II} (fig. 2.19). Some labeling in compartment FC_1 and the FZ_I is observed in K 314 where the caudal dc injection site encroaches on the most caudal part of the rostral dc. The C_2 compartment is located laterally and caudally in the white matter of the flocculus. It is continuous with a compartment in the medial white matter of the paraflocculus and contains labeled fibers that terminate in the corresponding C_2 zone after injections including the rostral pole of the MAO (C 1135, B 2202).

2. In the white matter of the nodulus four compartments (XC_1-XC_4) are delineated by accumulations of AChE at their borders. Injections in the caudal dc and subnucleus ß result in labeled fibers in compartments XC_1 and XC_4 that terminated as climbing fibers in the XZ_I and XZ_{IV} zones

fig. 2.16 Diagrams of the distribution of climbing fibers in the unfolded flocculus and ventral paraflocculus and diagrams of the inferior olive showing injection sites in cases C 1134 (A) with an injection including cdc, rdc, and vlo, and sparing rostral MAO (B) and case B 2202 (C) with an injection in rostral MAO (D). Note that in C 1134 almost all parts of the flocculus are labeled except for a caudolateral region corresponding to the C_2 zone, which receives climbing fibers in case B 2202.

(fig. 2.6 i). Zone XZ_{IV} is bisected by a central, empty strip of molecular layer and is wider on the ventral than on the dorsal side of lobule X. Injections in the rostral dc and vlo label zone XZ_{II} on the ventral and dorsal surface of lobule X and a central strip indicated as XZ_{IV}*. A rostrolateral area in the XZ_{I} contains labeled climbing fibers after injections of subnucleus β, the caudal dc, and the rostral dc and the vlo. This area is indicated with a question mark in figs. 2.6 i. Labeling in XZ_{III} and XZ_{V} is in accordance with the data from the retrograde labeling experiments of Katayama and Nisimaru (1988). XC_3 and XZ_{III} are labeled when the injection included the dmcc (K 397, B 2202, C 1135). Labeling is present in a lateral strip of climbing fibers covering the lateral rim of the nodulus (XZ_{V}) when the injection of the rostral MAO included its lateral border region (C 1135), but not when this region was spared (B 2202, C1134). Compartment XC_3 is wedged between compartments XC_3 and XC_4 and exists only in the dorsal cortex of the lobule. It is continuous with a distinct, much wider compartment in the lateral white matter of lobule IX.

2.5 Discussion

2.5.1 *The correlation of white matter compartments with climbing fiber zones in the flocculus.*

The present study showed that fibers from certain subnuclei of the inferior olive segregate into bundles that occupy specific compartments within the white matter of the flocculus and the nodulus. They travel within these compartments until they penetrate the granular layer to terminate in the molecular layer as climbing fibers on their target Purkinje cells. Climbing fibers projecting through these compartments constitute zones that are continuous across the folia of the flocculus and the nodulus and sometimes extend into adjacent lobules. The graphical reconstructions of the climbing fiber zones of the flocculus (figs. 2.2; 2.9; 2.16) exemplify the approximately orthogonal relation of the zones with

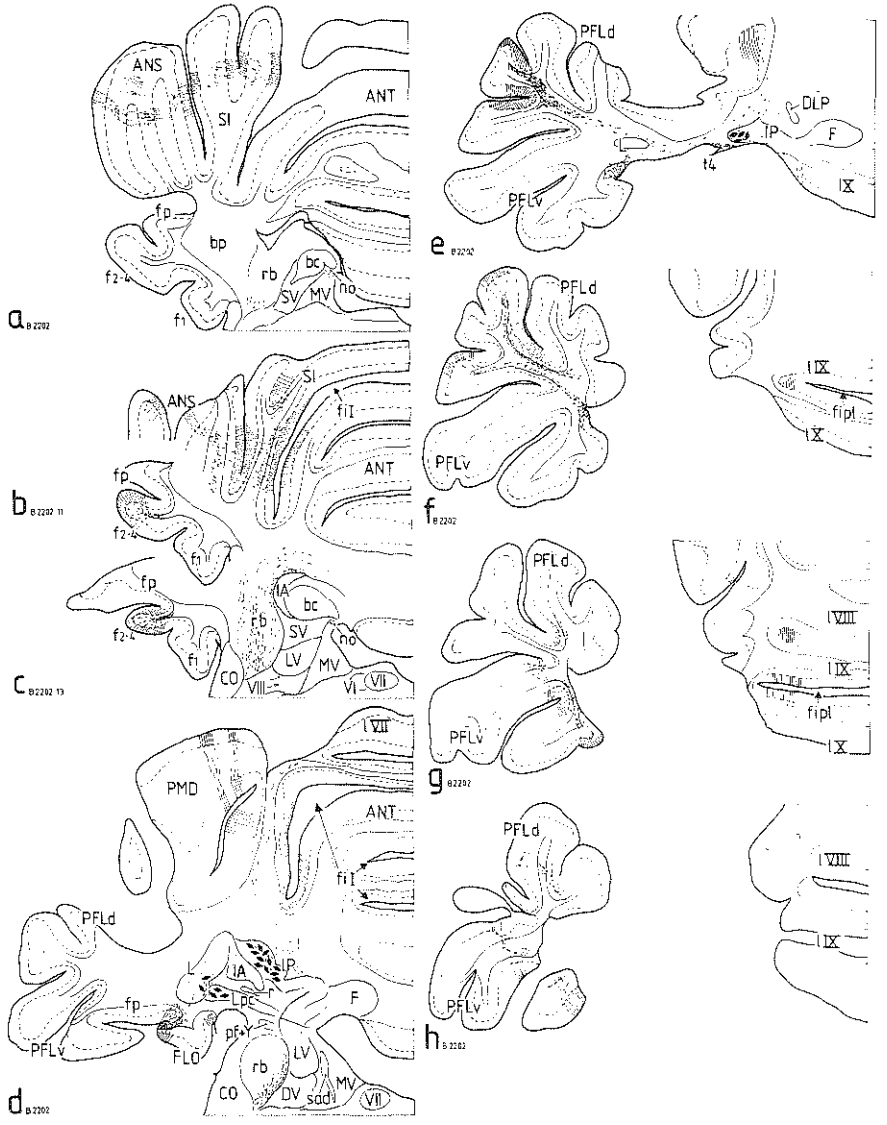

fig. 2.17 Drawings of labeled fibers in transverse sections through brain stem and cerebellum in case B 2202. Labeling is present in the C_2 compartment and zone and in a region corresponding to XC_3 in lobules IX and X.

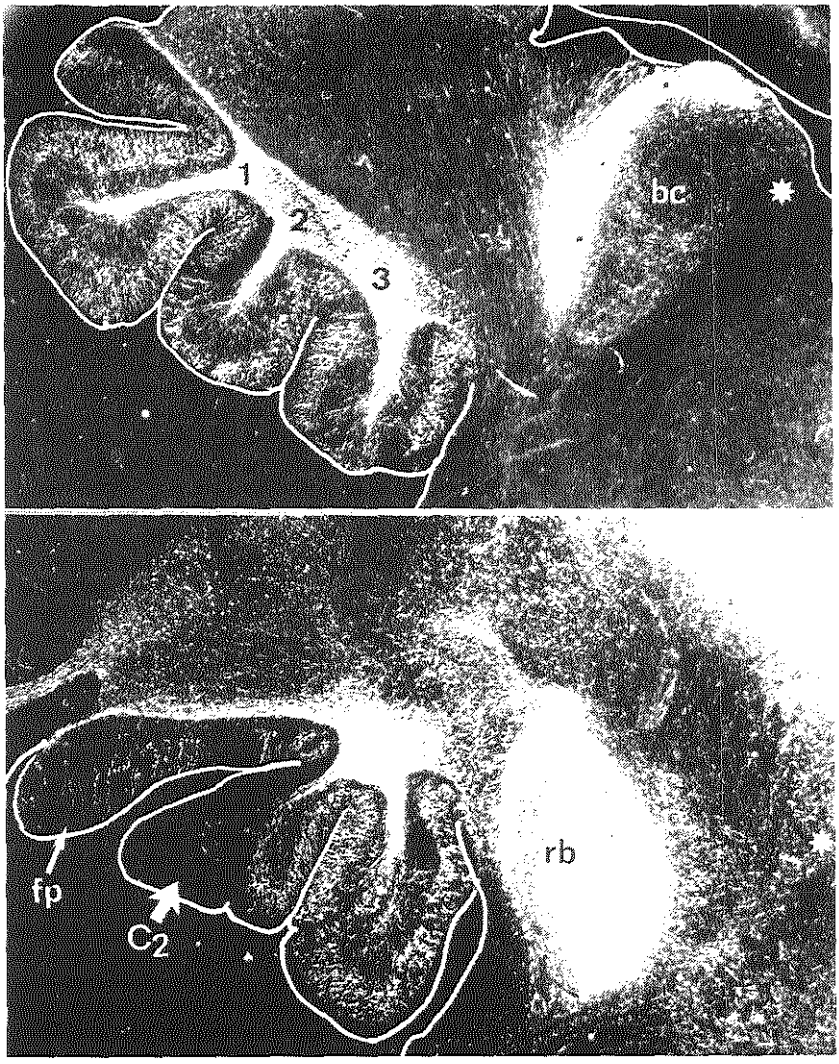

fig. 2.18 Darkfield photomicrographs of transverse sections through the flocculus in case C 1134. Note the relatively sparse number of labeled fibers at the borders of the white matter compartments FC_1, FC_2, and FC_3 and the dense labeling in the lateral part of compartment FC_2. Labeled fibers are absent from compartment C_2 (B). No labeling is present in the position of the nucleo-olivary tract (asterisk in A and B, compare fig. 2.14 B,D).

the transverse interfolial fissures. The AChE-positive raphes, which subdivide the floccular white matter into compartments (chapter 1) shift medially in the direction of the caudal pole of the flocculus. A similar shift was observed in the position of the climbing fiber zones FZ_I-FZ_{IV}.

The caudal dc, the rostral dc, and the vlo, first described by Kooy (1916), are segments of a continuous cell column located dorsomedial to the medial accessory olive. The borders between these segments were never precisely defined with anatomical methods, but they have been identified in the rabbit by recording field potentials in dc and vlo after flash stimulation of the ipsilateral and the contralateral eyes (Maekawa and Takeda, 1977; Takeda and Maekawa, 1980) and on the basis of the laterality and orientation of the best response axis for rotation of the visual surround (Simpson et al., 1981; Leonard et al., 1988). The border between the rostral and caudal dc was found to be located at the constriction of the cell column, which marked the transition between units in the caudal dc activated from the contralateral eye by temporal to nasal rotation around the vertical axis (vertical axis neurons) and the more rostral region comprising rostral dc and vlo, containing units activated by rotation around a horizontal axis. This horizontal axis enters the ipsilateral eye at an angle of about 45° with the midsagittal plane and leaves the contralateral eye at an angle of about 135°. This axis is approximately collinear with the axis perpendicular to the contralateral anterior semicircular canal. Stimulation of the ipsilateral eye dominates the response of most cells in the rostral dc (anterior (45°) axis neurons). Cells in the vlo and in the most rostral part of the rostral dc prefer stimulation of the contralateral eye (posterior (135°) axis neurons). The border between the caudal dc and the rostral dc is in accordance with the general pattern of afferent connections of the caudal dc from the NOT, the DTN and ITN, and of the rostral dc and the vlo from the MTN and the VTRZ. The electrophysiological and morphological criteria of Leonard et al. (1988) for the subdivision of the dc and vlo were applied in our studies to place our injections of the inferior olive.

Several previous anatomical studies found a zonal arrangement in the climbing fiber projection to the flocculus (Yamamoto, 1979a, Gerrits

and Voogd, 1982, Sato et al, 1983a; Ruigrok et al., 1992). Injections of HRP in the rabbit flocculus resulted in different patterns of retrograde labeling in the olive (Yamamoto, 1979a). A few small injections in the rostral and middle portions of the flocculus resulted in retrograde labeling mainly restricted to the rostral dc. Most injections that covered folia f1-f4 showed labeled cells in the rostral dc with the vlo and in the caudal dc, separated by an empty segment of the dc. This empty segment of the dc and the principal olive contained labeled cells when the injection included folium p.

Similar observations were made in the combined retrograde WGA-HRP and anterograde Phasaeolus vulgaris lectin tracing study of the olivocerebellar projection in the rat (Ruigrok et al., 1992). The caudal dc was found to project to paired FE/FE' zones in the flocculus. A more rostral segment of the dc, corresponding to the "empty segment" of Yamamoto (1979a), projected to the extension of the FE zone in the ventral paraflocculus. The vlo innervated two other zones (FD and FD'), which interdigitate with, and are situated, respectively, caudal to FE and FE' in the flocculus. More rostrally located cells in the PO projected to an extension of the FD and FD' in the ventral paraflocculus. FD and FD' fused around the end of the FE zone and continued as the D zone in the ventral paraflocculus. Both Yamamoto (1979a) and Ruigrok et al. (1992) recognized the projection of the rostral MAO to the caudal flocculus, which continues in the ventral paraflocculus as the C_2 zone. Yamamoto's (1979a) observations, therefore, indicate that cells projecting to more rostral segments of the zones FZ_I-FZ_{IV} are located more rostrally in the caudal dc and in the rostral dc/vlo/PO column. Such a shift was not observed with the relatively large injections in the dc/vlo in our experiments.

A more intricate pattern in the climbing fiber projection to the flocculus has been shown by Gerrits and Voogd (1982) in the cat. Using an anterograde autoradiographic technique they found that the caudal dc, rostral dc, and vlo each supplied two zones of Purkinje cells in the flocculus. Their medial F1 zone received a projection from the caudal dc and did not extend into the paraflocculus. Its lateral side was bordered by

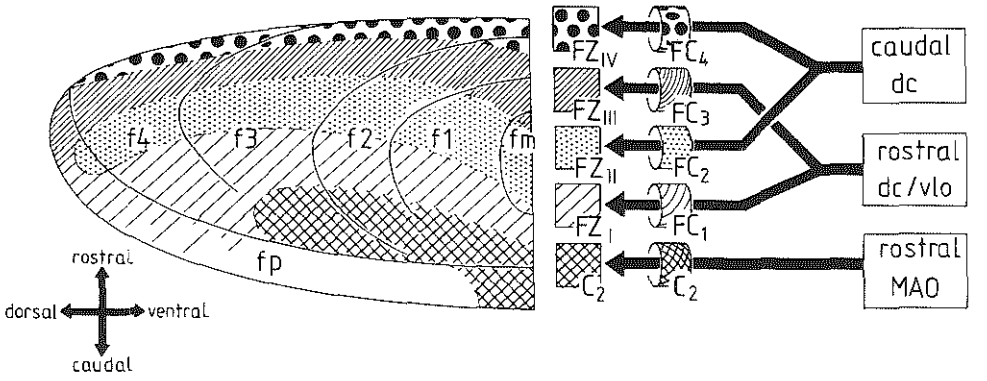

fig. 2.19 Summary diagram of the projection of the dc, vlo and rostral MAO through FC_1-FC_4 and C_2 to the corresponding zones (FZ) in the flocculus.

the F2 zone, which received fibers from the vlo. The F1/F2 border was considered as genuine because it separates climbing fibers from non-contiguous portions of the inferior olive. The F1 zone of the cat, therefore, is the equivalent of the FZ_{IV} zone in the rabbit and the FE' zone in the rat. The vlo-innervated F2 zone in the cat is bordered on its lateral side by F3, which receives a projection from the rostral dc. The same pattern is repeated more laterally, with the appearance of F4 (caudal dc), F5 (vlo) and F6 (rostral dc). The vlo and rostral dc zones continued across the posterolateral fissure into the adjoining medial extension of the ventral paraflocculus (ME), where they enclose the end of the caudal dc-innervated F4 zone. This pattern is very similar to the situation in the rabbit and the rat, and, consequently, F4 of the cat can be considered as the equivalent of our FZ_{II} zone and the combined F2/3 and F5/6 zones as the homologues of the FZ_{III} and FZ_{I} zones of the rabbit flocculus. A subdivision of the FZ_{I} and FZ_{III} zones was not observed in our material, although an additional AChE-positive raphe sometimes was present, which divided the FC_1 compartment over some of its extent (Chapter 1).

The studies of Yamamoto (1979a), Gerrits and Voogd (1982, 1989), Ruigrok et al., (1992) and our own observations lead to the conclusion

that an identical pattern of climbing fiber connections is present in the flocculus of different mammalian species and that this pattern finds its expression in the compartmental subdivision of the white matter of the flocculus of the rabbit as revealed in AChE-processed brain sections (Chapter 1).

Sato et al. (1983) distinguished three zones in the cat flocculus, with projections from the rostral dc and the vlo to rostral and caudal zones and projections from the caudal dc to a middle zone. These zones resemble our FZ_I, FZ_{II}, and FZ_{III}. They did not recognize the projection from the caudal MAO to the C_2 zone of the flocculus nor a second zone receiving from the caudal dc. A similar trizonal organization was also found in the flocculus of the monkey (Balaban et al., 1981)

2.5.2 *The correlation of white matter compartments and the climbing fiber projection to the nodulus.*

Our observations on the projection of the inferior olive to the nodulus confirm the description of Katayama and Nisimaru (1988), based on retrograde axonal transport of HRP and resemble the pattern reported by Balaban and Henry (1988), also in the rabbit. We distinguished four compartments in AChE-stained material in each half of the white matter of the nodulus. A paramedian, 1 mm wide XZ_I zone was innervated through compartment XC_1 by the subnucleus ß and the caudal dc. The contributions of these two subnuclei could not be distinguished in our experiments. Katayama and Nisimaru (1988) subdivided this zone into a medial ß-innervated zone and a lateral caudal dc-innervated zone. We distinguished a triangular rostrolateral area bordering on XZ_I on the ventral surface of the nodulus, which received projections from the caudal dc and/or the nucleus ß and the rostral dc/vlo. It was indicated with a question mark in figs. 2.6 i. Olivocerebellar fibers from the rostral dc/vlo occupy compartment XC_2 and innervate the XZ_{II} zone, which was also recognized by Balaban and Henry (1988) and Katayama and Nisimaru (1988). Compartment XC_3 and the XZ_{III} zone are only present on the

dorsal surface of lobule X and are innervated by the dmcc. XZ_{IV} receives projections from the caudal dc and, in a central strip, XZ_{IV}*, from the rostral dc/vlo. Our diagram differs from that of Katayama and Nisimaru (1988) because, on the dorsal surface of the nodulus, XZ_{IV} (corresponding to their zone iv) intervenes between XZ_{III} and XZ_{V} (their zones v and vi), which are innervated by the dmcc and the rostral MAO, respectively.

Climbing fibers to the flocculus and nodulus originate from different regions of the rostral MAO. Cells projecting to the flocculus of the rabbit are located in the rostral tip of the MAO (Alley et al., 1975). Projections to the nodulus of the rabbit are derived from cells located in the lateral margin of the rostral MAO (see fig. 2 D of Katayama and Nisimaru, 1988) The differential origin of projections to the C_2 zone in the flocculus and the XZ_{III} and XZ_{V} zones of the nodulus is supported by our experiments. Injections that spared the lateral half of the rostral MAO, but included the dmcc (K 397, B 2202) caused labeling in XZ_{III} but not in XZ_{V}. Injections that included the rostral tip of the MAO (C 1135, B 2202) labeled climbing fibers of the C_2 zone.

Descriptions of the zonal arrangement of the olivocerebellar projection to the nodulus in other species are less complete and will not be discussed. The continuity of the XZ_{I}, XZ_{II}, XZ_{III} and XZ_{IV} zones with similar zones in the uvula is obvious from studies of this lobule in different species (Brodal, 1976; Groenewegen and Voogd, 1977; Groenewegen et al., 1979; Kawamura and Hashikawa, 1979; Eisenman, 1984; Sato and Barmack, 1985, rabbit; Bernard, 1987; Kanda et al., 1989, cat; Apps, 1990, rat).

The anatomical and electrophysiological studies of Takeda and Maekawa (1984a,b; 1989a,b), Maekawa et al., (1989), Kusunoki et al., (1990) and Kano et al. (1990) in the rabbit showed branching of climbing fibers between flocculus and nodulus. Takeda and Maekawa (1989) found that 35.6% of the climbing fibers in the flocculus and 63.4% of the climbing fibers in the nodulus that could be driven by optokinetic stimuli could be activated by their collaterals, terminating in the complementary

lobule. Retrograde labeling from flocculus and nodulus with different fluorescent tracers resulted in double-labeling of 9-27% of the dc neurons and 12-18% of the cells of the vlo (Maekawa et al., 1989). There was no distinct spatial segregation of the cells projecting to the nodulus and the flocculus. Branching of olivocerebellar fibers could not be observed in our experiments, but a continuity was observed between the white matter of the flocculus and the nodulus. Fibers from the rostral dc/vlo, contained in FC_1, and from the caudal dc, contained in FC_2, continue from the flocculus, along the attachment of the roof of the fourth ventricle (t4 in fig. 2.3 k), into the nodulus. It seems likely that climbing fibers innervating the paired zones FZ_I/F_{III} and FZ_{II}/FZ_{IV} of the flocculus are branches from the same axon, but this has not been definitely proven.

2.5.3 *The lateral A-zone and the nucleo-olivary pathway in the rabbit.*

Additional observations in our study concern the presence of a lateral A zone in the medial hemisphere of the posterior lobe (simple, ansiform and paramedian lobules), innervated by the lateral part (group c) of the caudal MAO. The olivo-cerebellar fibers in the white matter collect around and probably innervate the dorsolateral protuberance of the fastigial nucleus (K 369 and K 314, figs. 2.3; 2.5) before they enter the white matter of the lobules. The lateral A zone and its climbing fiber projections from the group c of the caudal MAO were first distinguished by Buisseret-Delmas (1988) and Akaike (1986a,b, 1987, 1992) in the rat. The projection of the lateral A zone to the dorsolateral protuberance was substantiated by Buisseret-Delmas (1988).

The course of the nucleo-olivary fibers, first described by Légendre and Courville (1987) in the cat, could be confirmed because this tract was retrogradely labeled from WGA-HRP injections of the rostral dc, the vlo, and portions of the rostral MAO, DAO and the PO (but not from the caudal dc and the caudal MAO) in our experiments. The nucleo-olivary fibers could not be labeled with injections of tritiated leucine in the inferior olive. The nucleo-olivary fibers leave the nuclei and pass through and around the parvicellular part of the lateral cerebellar nucleus in the

rostral wall of the lateral recess. They ascend in the lateral angle of the fourth ventricle dorsal to and intermingling with the fibers of Löwy's bundle to become located ventromedial to the superior cerebellar peduncle. Subsequently they enter the decussation of this tract.

2.5.4 *Functional considerations.*

The differential projection of the dc/vlo complex to the different FZ in the flocculus is part of the neuronal circuitry that is responsible for the control of eye movements. With the use of microstimulation three functional zones (indicated as "microzones" by Ito, 1984) were distinguished in the rabbit flocculus either by recording of eye movements (Dufossé et al., 1977; Nagao et al., 1985, chapter 4) or by recording the effects of vestibulo-ocular reflexes on evoked eye muscle activity (Yamamoto, 1979b; Ito et al., 1982b). Stimulation of a narrow strip in the rostral flocculus resulted in horizontal eye movements or suppression of VOR's from the horizontal canal (Horizontal (H) zone II). Stimulation rostral and caudal to zone II inhibited VOR's from the anterior canal or provoked vertical eye movements (rostral and caudal, Vertical (V) zones I and III). Stimulation points of the H and V zones showed considerable overlap. Moreover, inhibition of the VOR for the contralateral inferior oblique muscle (Ito et al., 1982b) and rotatory eye movements could be produced by stimulation from an area in the ventral flocculus that ran obliquely through zones I-III (Rotatory (R) zone, Nagao et al., 1985). Zone II corresponds to the more caudal of two strips of Purkinje cells in the rabbit flocculus that project to the medial vestibular nucleus (Yamamoto and Shimoyama (1977). Zones I and III correspond to the Purkinje cell strips projecting to the superior vestibular nucleus (Note that the rostralmost zone of Purkinje cells, projecting to the medial vestibular nucleus and described earlier by these authors was no longer mentioned in their later work (Ito, 1984)).

A zonal pattern has also been indicated by local electrical stimulation in the rabbit flocculus. Four zones have been identified in this way (Nagao et al., 1985): one dorsoventrally elongated zone from which

horizontal eye movements were evoked (H zone) and two flanking zones from which vertical eye movements were elicited (V zones). An R zone from which rotatory eye movements were evoked ran almost perpendicularly through the H and V zones. It was asserted that the zones of Purkinje cells controlling relay cells of different VORs matched the eye movement zones. In chapter 4 the relationship between the white matter compartmentation, climbing fiber zones and eye movements will be demonstrated in detail. Also in this study three zones were associated with eye movements, but these ran parallel and did not intertwine.

Climbing fiber responses (complex spikes) to optokinetic stimulation were recorded from Purkinje cells of the flocculus (Kusunoki et al., 1990) and the nodulus (Kano et al., 1990) of the rabbit. Cells that preferred horizontal movement were activated by a temporally to nasally moving optokinetic stimulus presented to the ipsilateral eye (Ipsi F cells). These cells were located in a single, 1 mm wide strip along the caudal part of the rostral one third of the flocculus. Some Ipsi F cells were found scattered in folium p. There is a good correspondence between this strip and the projection of the caudal dc, which contains the vertical axis neurons of Leonard et al. (1988), to the FZ_{II} zone. The rostral and medial FZ_{IV} zone, with a similar climbing fiber input, was not noticed by Kusunoki et al. (1990).

Most of the cells that preferred vertical optokinetic stimulation were excited by upward movement presented to the ipsilateral eye (Ipsi U cells) or downward movement presented to the contralateral eye (Contra D cells). Cells with a preference for vertical movement were located in two strips, one rostral and one caudal to the Ipsi F cells. These strips correspond to the FZ_{I} and FZ_{III} zones, which receive climbing fiber projections from the rostral dc and the vlo. The optokinetic stimulus activating the Ipsi U cells appears to be equivalent to the rotation that activated the posterior (135°) units in the vlo in the experiments of Leonard et al. (1988). The Contra D stimulus probably was relayed by the anterior (45°) units of Leonard et al. (1988) located in the rostral dc. There is a tendency for Ipsi U cells to be located more rostrally and medially in the flocculus than the Contra D cells (Kusunoki et al., 1990,

their Fig. 10 B,C). Similarly, the projection of the vlo to the F2 and F5 zones is medial with respect to the projection of the rostral dc to F3 and F6, as noticed by Gerrits and Voogd (1982) for the flocculus of the cat. Such a gradient could not be observed in the corresponding zones in the rat (Ruigrok et al., 1992) or the rabbit.

The Purkinje cell zones in the rabbit flocculus, defined by retrograde labeling (Yamamoto and Shimoyama, 1977), microstimulation (Dufossé et al., 1977; Yamamoto, 1979b; Ito et al., 1982a,b; Nagao et al., 1985) or optokinetic stimulus-induced complex spikes activity (Kusunoki et al., 1990) overlap considerably, especially in the ventral folia of the flocculus. In this respect they differ from the discrete climbing fiber projections identified in this study on the basis of the compartmental subdivision of the floccular white matter.

Purkinje cells responding with complex spikes to optokinetic stimulation have also been identified in the nodulus of the rabbit cerebellum (Simpson and Alley, 1974; Kano et al., 1990). Ipsi F cells were found in medial and lateral strips on the ventral surface of the nodulus. These two strips flanked a strip of Ipsi U and Contra D cells, which extended to the dorsal surface of the lobule (Kano et al., 1990). This arrangement approximately corresponds to the pattern of two caudal dc (and/or subnucleus ß-) innervated zones, flanking a single zone of climbing fibers from the rostral dc/vlo, as found by Katayama and Nisimaru (1988: zones ii, iii and iv), Henry and Balaban (1988) and by us (lateral part of XZ_I, XZ_{II} and XZ_{IV^*} zones). A few Purkinje cells of the Ipsi D or Contra U type were found in the medial, subnucleus ß-innervated part of zone XZ_I of the nodulus and the uvula (Kano et al., 1990).

Our data indicate that the pattern of terminal zonation of the climbing fiber projection to the flocculus is rooted in the anatomical compartmentation found with AChE histochemistry. This compartmentation provides an intrinsic, independent framework that is a useful tool for correlating anatomical and physiological data. This compartmentation is apparently the basis of the modular organization of differential control by the flocculus of eye muscle activity.

Chapter 3

Zonal organization of the flocculo-vestibular nucleus projection in the rabbit. A combined WGA-HRP tracing and acetylcholinesterase histochemical study.

3.1 Introduction

The flocculus plays an important role in the control of eye movements by processing visual and vestibular information (Robinson, 1976; Ito et al., 1982a; Nagao 1983; Ito, 1984). Via their projections to the vestibular nuclei Purkinje cells of the flocculus inhibit certain groups of vestibulo-ocular relay cells (Ito et al., 1970; Fukuda et al., 1972; Baker et al.,1972; Highstein, 1973; Kawaguchi, 1985; Sato and Kawasaki, 1987, 1990a,b, 1991; Sato et al., 1988). The projection of the flocculus to the vestibular nuclei has been known since the studies of Dow (1936, 1938a,b, 1939) with the Marchi method in rat, cat and monkey. Recent studies using modern tracing techniques showed that the flocculus sends major projections to the superior (SV) and medial vestibular nucleus (MV), group y, lateral cerebellar nucleus (LCN), basal interstitial nucleus and minor projections to the descending vestibular nucleus (DV) and the nucleus prepositus hypoglossi (Jansen and Brodal, 1940; Voogd, 1964; Angaut and Brodal, 1967; Alley, 1977; Haines, 1977; Yamamoto and Shimoyama, 1977; Balaban et al., 1981; Sato et al., 1982a and b; Carpenter and Cowie, 1985; Langer et al., 1985b; Epema, 1990). Some of these studies have indicated that the Purkinje cell population of the flocculus consists of subsets, which are arranged in zones that cross the folia of the flocculus and project to different vestibular nuclei.

Yamamoto and Shimoyama (1977) found Purkinje cells of the rabbit flocculus that project to the MV and SV to be distributed in a striped pattern. They distinguished two Purkinje cell zones projecting to MV and two zones to SV. The two zones projecting to MV interdigitate with and are located rostral to the zones projecting to SV. Purkinje cells of a fifth

zone, located in the caudal flocculus and also extending in folium p. were labeled from injections of HRP in the cerebellar lateral nucleus (Yamamoto, 1978). In her later publications (Yamamoto, 1978, 1979a,b) the presence of the rostral MV zone no longer was mentioned. A single MV zone, flanked by two SV-projecting zones also was distinguished in monkeys (Balaban et al., 1981). A different pattern of efferent connections was described for the three zones in the flocculus of the cat by Sato et al. (1982a and b). Their rostral zone was connected with SV, their middle zone with MV and the caudal zone projected to group y and sparsely to the ventromedial, parvicellular lateral cerebellar nucleus.

Similar zonal patterns were revealed by microstimulation of the rabbit flocculus and recording of the inhibition of specific vestibulo-ocular reflex pathways (Yamamoto, 1979b; Ito et al., 1982b). Local electrical stimulation elicited eye movements (Dufossé et al., 1977; Balaban and Watanabe, 1984; Sato et al., 1984, 1990a, 1991; Nagao et al., 1985; Belknap and Noda, 1987). In the rabbit microstimulation in the Purkinje cell layer of the flocculus resulted in horizontal, vertical and rotatory eye movements located in four zones (Dufossé et al., 1977; Nagao et al., 1985). An H-zone, in which electrical stimulation elicited horizontal eye movements was flanked by two V-zones in which stimulation elicited vertical eye movements. This trizonal organization of eye movement control has also been found in cat (Sato and Kawasaki, 1984, 1987, 1990a,b, 1991; Sato et al., 1982a, b, 1983a, 1984, 1988) and monkey (Balaban and Watanabe, 1984). In the rabbit the zonal organization was complicated by the presence of rotatory eye movements on stimulation of an R-zone which overlapped large parts of the H- and V-zones (Ito et al., 1982b, Nagao et al., 1985).

The functional representation of eye movements in zones probably reflects the zonal arrangement in the efferent and afferent (climbing fiber) connections of the Purkinje cells. Precise correlations of the functional and anatomical properties of the floccular zones are hindered by inconsistencies between the different anatomical and physiological studies on the number and extent of the zones, by large individual variations in the number and size of the folia of the flocculus and by

differences in zonal organization between different species.

Recently, a morphological zonation in the rabbit flocculus has been demonstrated using acetylcholinesterase (AChE) histochemistry (Tan et al., 1989, see also chapter 1). AChE-positive raphes subdivide the white matter of the flocculus into 5 compartments. In the previous study (Chapter 2) the AChE-compartmentation was used as an independent framework to correlate data from experiments on the olivocerebellar projection to the rabbit flocculus. The climbing fibers terminate in 5 zones, FZ_I-FZ_{IV} and C_2, each of which is associated with a particular white matter compartment (FC_1-FC_4, C_2). The rostral dorsal cap (rdc) and adjacent ventrolateral outgrowth (vlo) supply climbing fibers to FZ_I and FZ_{III} via compartments FC_1 and FC_3, the caudal dorsal cap (cdc) supplies FZ_{II} and FZ_{IV} via FC_2 and FC_4, and the rostral medial accessory olive innervates zone C_2 via compartment C_2.

In this study we investigated with anterograde and retrograde transport methods the differential projection of Purkinje cells of the floccular zones FZ_I-FZ_{IV} to the vestibular and cerebellar nuclei and the relation of their axons to the white matter compartmentation, as described in chapter 1 and Tan et al. (1989). Recently, Purkinje cell axons from identified zones were also traced with biocytin by De Zeeuw et al. (1992).

3.2 Materials and methods

3.2.1 *Retrograde studies.*

HRP (33%) dissolved in phosphate buffered saline was pressure injected within the vestibular nuclei of rabbits with a 1 µL Hamilton syringe with a 25 gauge needle (Epema, 1990). Two of these cases will be presented: one with an injection of SV (case C 253 (0.1 µL)) and one in the MV (C 480 (1.0 µL)). After a survival time of two days the animals were heparinized and transcardially perfused under deep anaesthesia with 0.5 L saline, followed by 1.5 L citrate buffer (0.1 M, pH 7.4) containing 1% formaldehyde and 1.25% glutaraldehyde and subsequently washed with 0.5 L citrate buffer (0.1 M, pH 7.4) containing 8% sucrose (Mesulam, 1978). The brains were removed, embedded in 10% gelatin (Voogd and Feirabend, 1981), and transversely sectioned at 40 µm. A series containing one out of every four sections was incubated with diaminobenzidine (DAB; Graham and Karnovsky, 1966) and counterstained with cresyl violet.

3.2.2 *Anterograde studies.*

In 9 pigmented Dutch belted rabbits (K 227, 244, 301, 305, 340, 355, 358, 360, 370) small quantities (5-15 nl) of a 7% solution of horseradish peroxidase coupled to wheat germ agglutinin (WGA-HRP, Sigma type VI) were injected with air pressure into the flocculus. Further processing of the transversely sectioned brains for TMB, DAB and AChE has already been described in chapter 2.2 and 3.2. In some cases (K 301, 305, 340, 355, 360, 370) the injection sites were determined by recording climbing fiber responses of the Purkinje cells to rotating random dot patterns (Graf et al., 1988; Leonard et al., 1988). Injection sites are indicated in diagrams of the unfolded flocculus (see fig. 3.1). When the flocculus was unfolded, the length of the Purkinje cell layer in a single transverse section was indicated as a straight line. The sections were aligned using the distance from the most ventromedial point of the

floccular Purkinje cell layer (B in fig. 3.1) to the midline (M). The distance between the sections (t) correspond to the true distance between the reconstructed sections multiplied by the magnification factor (fig. 3.1). The location and extent of the injection sites, the interfolial fissures and the approximate position of the climbing fiber zones (FZ_I-FZ_{IV}, C_2), estimated by extrapolating the AChE raphes to the Purkinje cell layer, were indicated in these diagrams (figs. 3.6; 3.8). The labeled fibers in the cerebellum and brain stem were plotted. In the white matter of the flocculus the raphes were identified in adjacent AChE sections. The subdivision and nomenclature of the vestibular complex used in the present study is according to Epema et al. (1988).

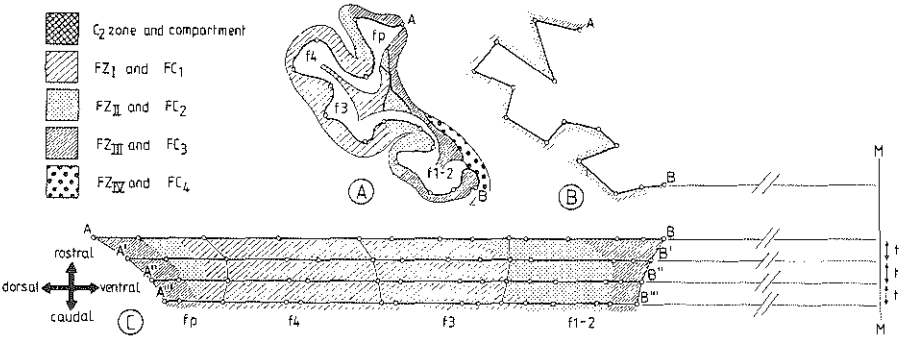

fig. 3.1 Diagram of the method used to unfold the cortex in preparing maps of the unfolded surface of the flocculus showing the approximate extent of the floccular zones. The Purkinje cell is straightened; the position of the injection site and the approximate position of the cortical zones FZ_I- FZ_{IV} and C_2 is indicated. Sections are aligned using the distance between the midline (M) and the most ventromedial point of the Purkinje cell layer (B). Four sections (A-B to A'''-B''') are reconstructed in C. The distance between the reconstructed sections (t) is obtained by multiplying the distance between the reconstructed sections by the magnification factor. Symbols indicating the floccular zones and compartments are shown on the right.

3.3 Results

3.3.1 *Retrograde experiments.*

In C 480 the HRP injection involved all parts of the MV and the ventromedial portion of the LV. Retrogradely labeled Purkinje cells are found in all folia of the flocculus (fig. 3.2). Two distinct zones of Purkinje cells were labeled. The one located rostrally and medially contained only a few labeled cells. The second zone was located more laterally and caudally and remained separated from the rostromedial zone by a band of unlabeled cells. It extended into the rostral tip of folium p (Fig. 3.2 d-e). More caudally, scattered groups of labeled Purkinje cells were present in folium p. Mossy fibers and climbing fibers in the flocculus remained unlabeled. Thick, retrogradely labeled Purkinje cell axons could be traced from the labeled Purkinje cells, through the granular layer into the white matter. Each Purkinje cell zone was associated with labeling in a certain part of the white matter. Labeled axons associated with the medial zone of labeled Purkinje cells were present along the rostromedial border of the flocculus with the brachium pontis (figs. 3.2 b-c; 3.4). More caudally, they assembled in a bundle at the ventromedial tip of the flocculus, dorsal to the cochlear nuclei (fig. 3.2 d-e). Fibers associated with the lateral zone of labeled Purkinje cells extended from folium p dorsally into folium f2 ventrally (fig. 3.2 d). More caudally they collected into a triangular bundle, with its base resting on the cortex of f1 (figs. 3.2 e; 3.4 B). The topography of the labeled compartments corresponds with the FC_4 and FC_2 compartments delineated in AChE-incubated tissue sections (chapter 1.3). In the caudal flocculus the labeled fibers no longer could be distinguished as two separate compartments. They entered the floccular

fig. 3.2 Drawings of retrogradely labeled Purkinje cells and their axons in transverse sections through the flocculus and floccular peduncle of case C 480 with an HRP injection site involving the rostral part of the medial vestibular nucleus. Most fibers occupy compartment FC_2 and FC_4, with labeled cells in the corresponding zones FZ_{II} and FZ_{IV}.

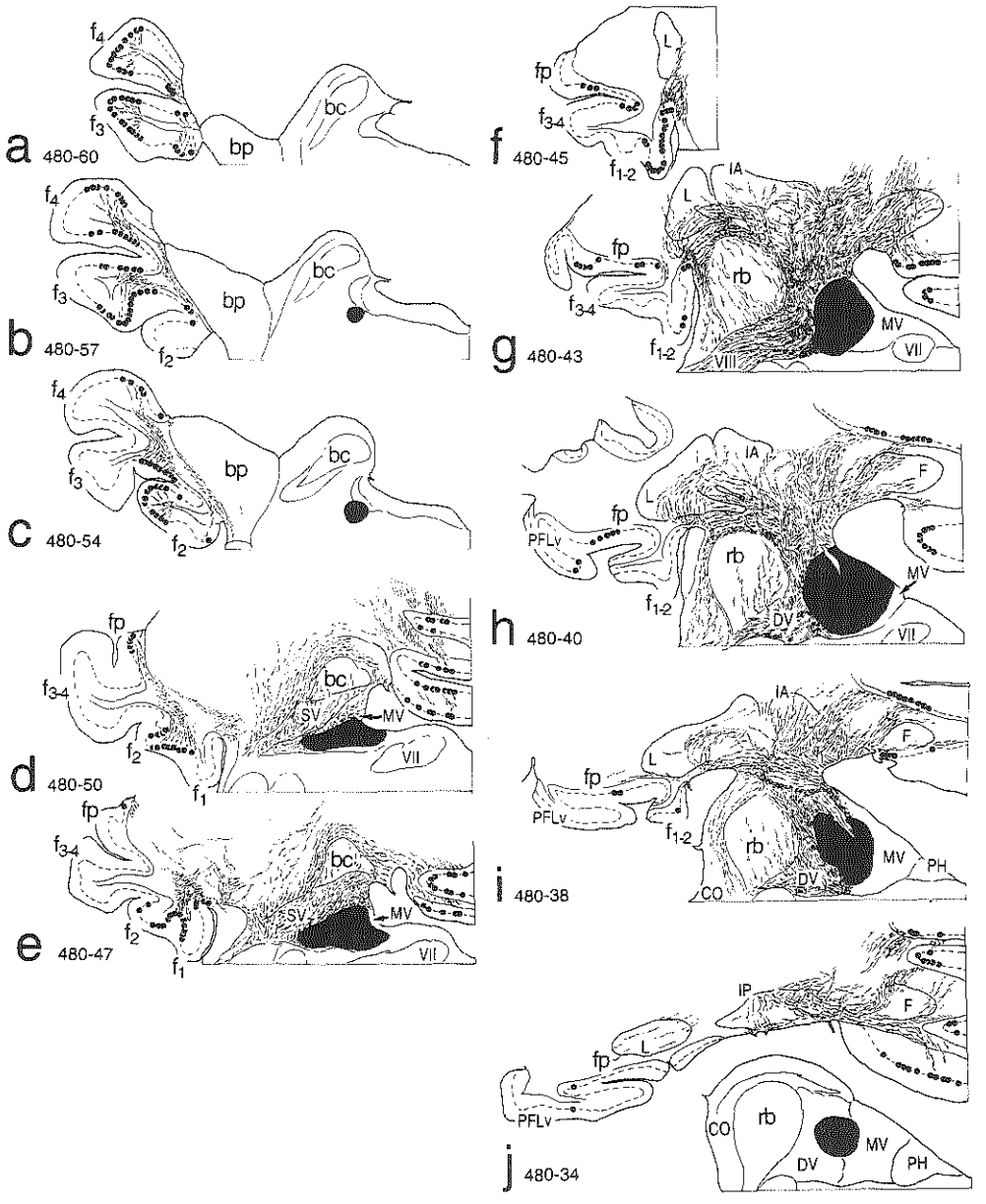
a
480-60
f4
f3
bp
bc
b
480-57
f4
f3
f2
bp
bc
c
480-54
f4
f3
f2
bp
bc
d
480-50
fp
f3-4
f2
f1
bc
SV
MV
VII
e
480-47
fp
f3-4
f2
f1
bc
SV
MV
VII
f
480-45
fp
f3-4
f1-2
L
g
480-43
fp
f3-4
f1-2
L
IA
rb
MV
VII
VIII
h
480-40
fp
PFLv
f1-2
L
IA
F
rb
MV
DV
VII
i
480-38
fp
PFLv
f1-2
L
IA
F
rb
MV
PH
CO
DV
j
480-34
fp
PFLv
L
IP
F
CO
rb
MV
DV
PH

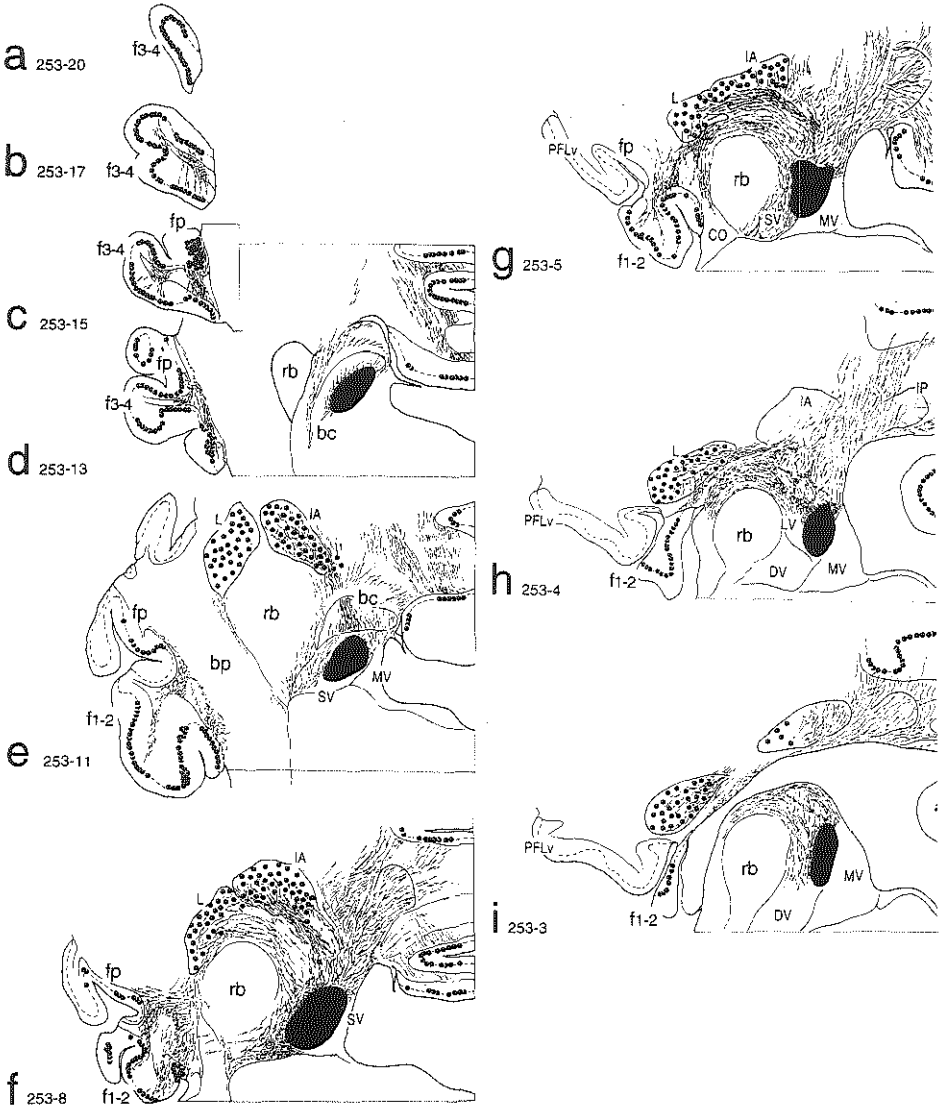
a 253-20
f3-4
b 253-17
f3-4
fp
f3-4
c 253-15
fp
f3-4
rb
bc
d 253-13
L
IA
fp
rb
bc
bp
MV
SV
f1-2
e 253-11
IA
L
rb
SV
fp
f1-2
f 253-8
IA
L
fp
rb
SV
PFLv
fp
f1-2
g 253-5
IA
L
rb
CO
SV
MV
IP
IA
L
PFLv
rb
LV
DV
MV
f1-2
h 253-4
PFLv
rb
MV
DV
f1-2
i 253-3

peduncle in bundles, passing between unlabeled Purkinje cell axons of other compartments. The majority of the retrogradely labeled fibers could be traced, through the floccular peduncle and group y, to the injection site in the MV nucleus. Labeled fibers in the ventral part of the floccular peduncle, immediately dorsal to the restiform body, were tightly packed while the rest of the fibers in the floccular peduncle were more loosely arranged. Some of these fibers entered the dorsal part of the cochlear nucleus. Other bundles of labeled fibers arched through the ventral part of the lateral cerebellar nucleus (fig. 3.4 C). Most of these fibers passed dorsal to the parvicellular part of the lateral nucleus. More medially they turned sharply ventrally to reach the MV through the caudal pole of the SV. A great number of retrogradely filled axons from labeled Purkinje cells in the anterior and posterior vermis passed through the fastigial nucleus and the medial portion of the anterior and posterior interposed nuclei in the direction of the injection site (fig. 3.2 f-j).

In case C 253 the injection site was situated in SV and LV, touching upon the MV (fig. 3.3 d-i). The injection extended into the ventral part of the superior cerebellar peduncle. Retrogradely labeled Purkinje cells in the flocculus were distributed in two wide zones, separated by an empty strip (fig. 3.5). Purkinje cells located along the rostromedial edge of the flocculus remained unlabeled. Labeling of Purkinje cells of both zones extended into folium p (fig. 3.3 c-f). Retrogradely filled Purkinje cell axons traveled in two bundles in the rostral white matter of the flocculus (fig. 3.3 c). The medial bundle remained separated from the medial border of the flocculus by an empty space, corresponding to FC_4 which contained labeled axons in the previous case with an injection of MV. Dorsally in the white matter of folium p the two bundles became fused,

fig. 3.3 Drawings of retrogradely labeled Purkinje cells and their axons in transverse sections through the flocculus and floccular peduncle of C 253 with an HRP injection site involving the superior vestibular nucleus. Most Purkinje cell axons occupy compartments FC_1 and FC_3 with labeled neurons in zones FZ_I and FZ_{III}. An extension of the injection site, involving the superior cerebellar peduncle (d) causes retrograde labeling of many neurons in the cerebellar nuclei (e-i).

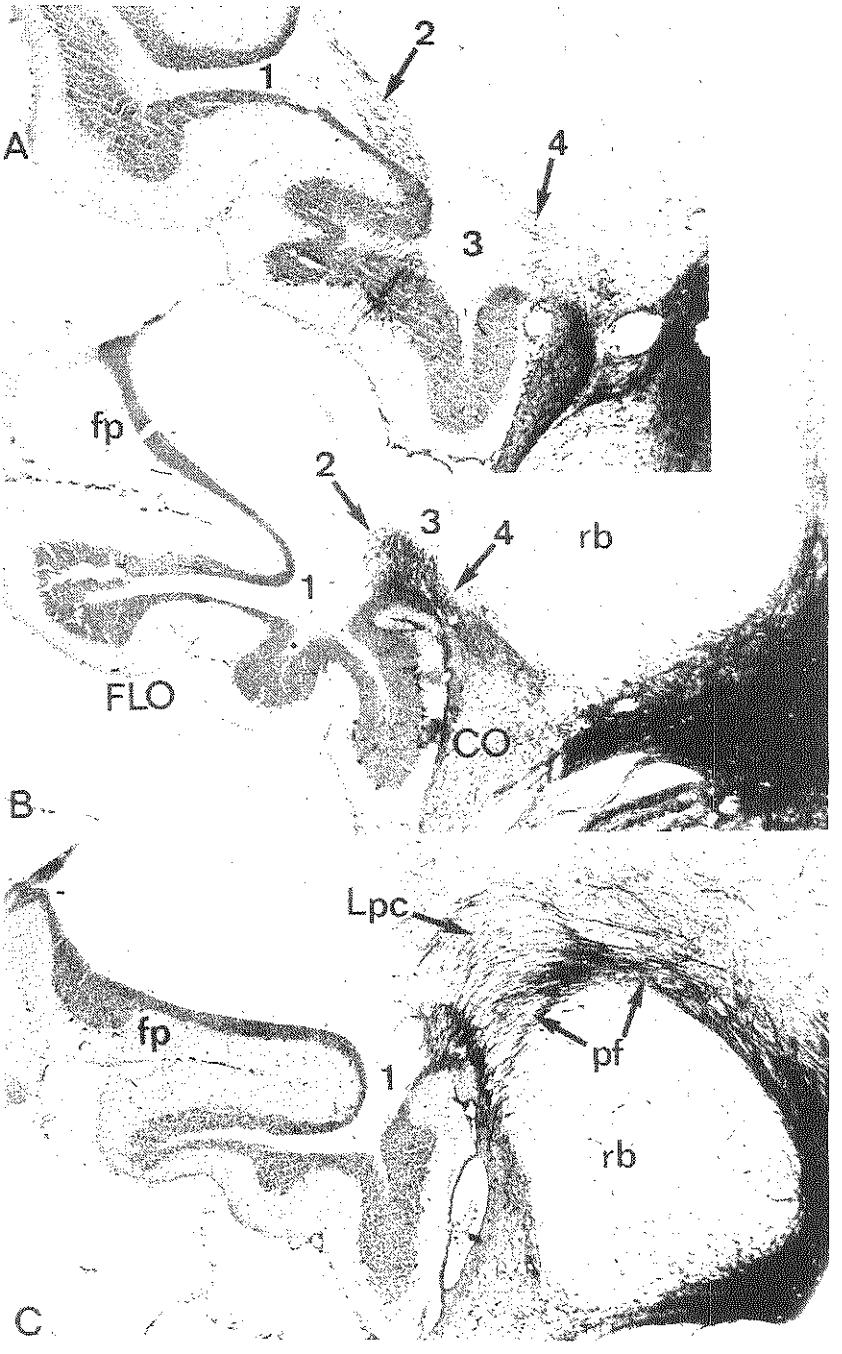
A
1
2
3
4
fp
B
1
2
3
4
rb
FLO
CO
C
Lpc
fp
1
pf
rb

ventrally they were separated by a triangular area containing a few labeled fibers and corresponding to the FC_2 compartment (fig. 3.3 d-g; 3.5 C). The most lateral parts of the white matter of the folia f1-f2 remained free of labeled axons (fig. 3.3 e-g). This region corresponds to the C_2 compartment. From the caudal flocculus labeled fibers proceeded in the floccular peduncle in bundles, passing between unlabeled fibers of the floccular white matter. They passed through dorsal group y to reach the injection site in SV (fig. 3.5 C). Other fibers followed a dorsal route, through the lateral cerebellar nucleus. Their final course was difficult to establish, because thick, retrogradely filled axons of the superior cerebellar peduncle and retrogradely labeled cells dominate the picture of the lateral and interposed nuclei. Purkinje cells of the vermis and their axons were also retrogradely labeled from this injection site.

3.3.2 *Anterograde experiments.*

The cases were grouped together according to the white matter compartment in which the labeled fibers were located and according to the extent and location of the injection sites in the flocculus compared with the predicted position of the FZ bands.

Group 1 (K 244, K 355, K 358, K 360)

In this group small injections of WGA-HRP in the cortex of the flocculus resulted in labeled fibers which clearly grouped together in compartment FC_1 (figs. 3.7 A-B; 3.9; 3.11). The injection sites in K 244 and K 355 are situated within the predicted borders of FZ_I (fig. 3.8 B-C), the injections in K 358 and K 360 encroach upon FZ_{II} (figs. 3.6 C; 3.8 D).

The injection site in K 244 is located in f3-f4 and extends more caudally than in the other three cases (figs. 3.8 B; 3.9 c). The labeled

fig. 3.4 Brightfield photomicrographs of transverse sections through the flocculus in C 480. Compare fig. 3.2, d, e and g.

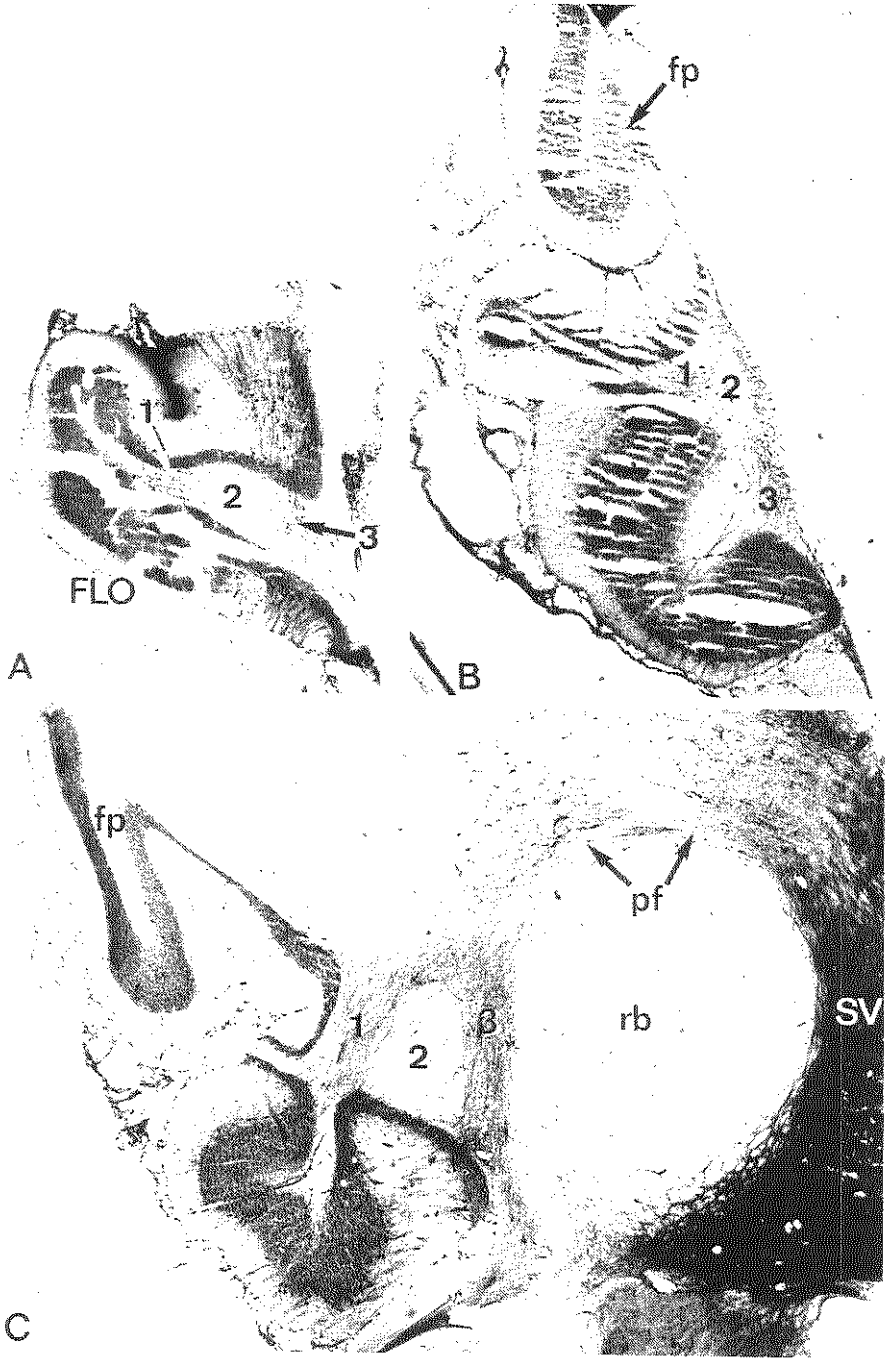
fp
1
2
3
FLO
A
B
fp
pf
1
2
β
rb
SV
C

fibers are located in the lateral half of compartment FC_1. No labeled fibers were present in any of the other compartments. Labeled neurons in the inferior olive are almost restricted to the vlo and the rdc (fig. 3.16). In the caudal flocculus fibers in this compartment pass medially, dorsal to compartment FC_2, where they subdivide into two fiber streams. One stream curves dorsalwards through the lateral cerebellar nucleus, turning medially and caudally along the dorsal border and through the parvicellular lateral cerebellar nucleus. Within the anterior interposed nucleus they turn abruptly ventrally to enter the caudal pole of the superior vestibular nucleus (SV) (fig. 3.9 e-f). A few fibers continue along the lateral vestibular nucleus (LV) and the descending vestibular nucleus (DV), close to the restiform body. The second stream remains in a ventral position and enters the floccular peduncle. It comprises the bulk of fibers of compartment FC_1. Labeled fibers ramify among the cells of group y located between the white matter of the flocculus, restiform body and the cochlear nucleus (fig. 3.9 f; 3.10 B, C) and between other cells of the dorsal group y, situated between the fibers of the floccular peduncle. Due to the great number of labeled fibers traversing through dorsal group y it cannot be established with certainty, whether the axons actually terminate on these neurons. Labeled fibers are scarce in ventral and dorsal parts of the floccular peduncle. A few labeled fibers pass through the ventral group y, along the dorsal border of the restiform body. Very few fibers passing through the caudal pole of SV enter Löwy's bundle. Labeled fibers of the second stream intersect with fibers arching through the lateral and interposed nuclei in the region of the caudal pole of SV (fig. 3.9 e). Most labeled fibers terminate mainly in the dorsolateral and central parts of SV, and in its caudal pole (fig. 3.9 b-e). A few fibers can be traced into MV and DV. Retrogradely labeled cells of different size are bilaterally present in SV, MV and PH. Some retrogradely labeled cells are present caudally in the ipsilateral dorsal group y and in the region

fig. 3.5 Brightfield photomicrographs of transverse sections through the flocculus in C 253. Compare fig. 3.3, b, e and f.

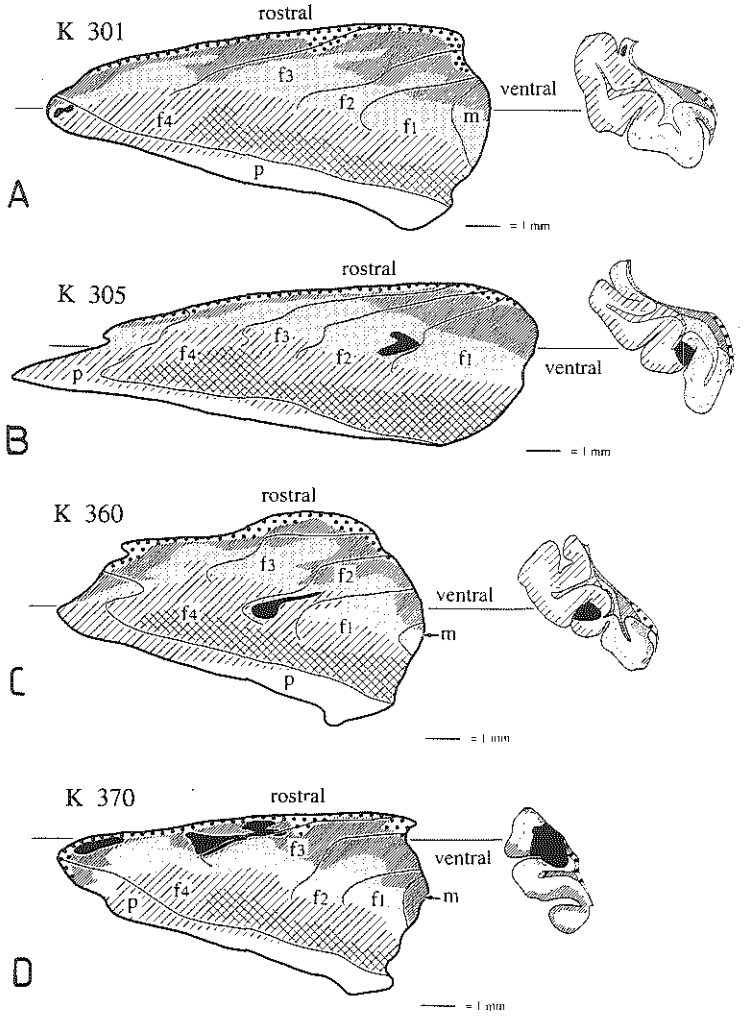

fig. 3.6 Diagrams of the unfolded flocculus (left) and a transverse section through the flocculus at the level of the injection site (right) in cases K 301, K 305, K 360, K 370. The extent of the injection sites is shown in relation to the floccular compartments and zones. For explanation of the symbols indicating zones and compartments, see fig. 3.1.

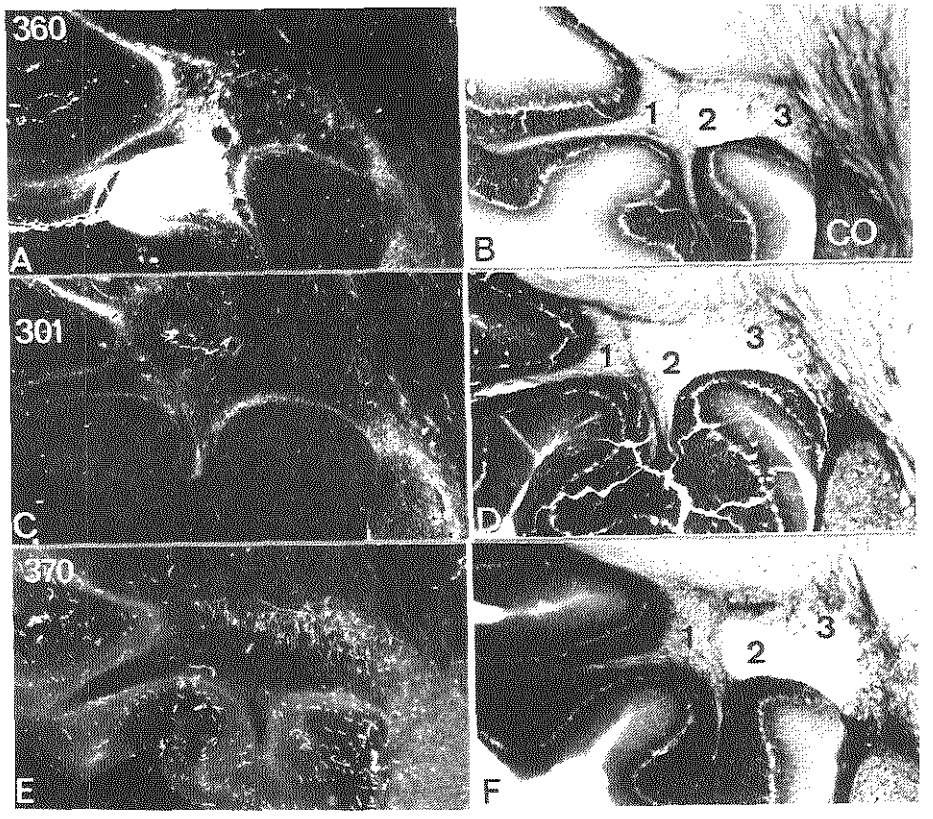

fig. 3.7 Darkfield and brightfield photomicrographs of TMB processed (A,C,E) and adjoining AChE processed sections through the flocculus showing the position of labeled fibers in the different white matter compartments. K 360 with an injection site in FZ_I and anterogradely labeled fibers in FC_1, K 301 with an injection site in FZ_{II} and labeled fibers in FC_2, K 370 with an injection site in FZ_{III} and labeled fibers in FC_3.

caudal and dorsal to the parvicellular lateral cerebellar nucleus. Retrogradely labeled cells extend in the roof of the fourth ventricle to the lateral border of the nodulus.

The injection site in K 355 is located in f3 in the center of the estimated FZ_I zone (fig. 3.8 C). The majority of the retrogradely labeled cells in the inferior olive is located in the vlo and rdc (fig. 3.16). Labeled

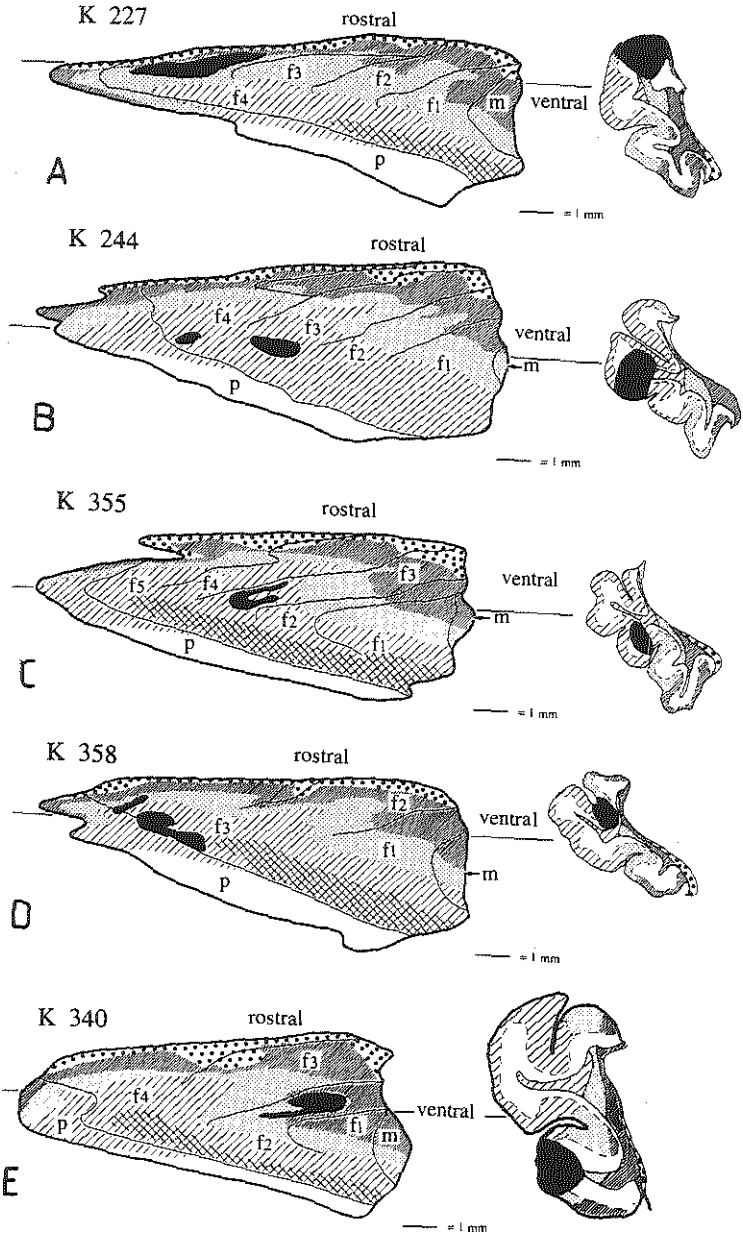
K 227
rostral
f3
f2
f4
f1
m
ventral
p
A
= 1 mm
K 244
rostral
f4
f3
f2
ventral
f1
m
p
B
= 1 mm
K 355
rostral
f5
f4
f3
ventral
f2
m
p
f1
C
= 1 mm
K 358
rostral
f2
f3
ventral
f1
m
p
D
= 1 mm
K 340
rostral
f3
f4
p
ventral
f1
m
f2
E
= 1 mm

fibers in the cerebellar white matter are mainly located in the medial half of compartment FC_1 with a few fibers in FC_2. The course of the labeled fibers is the same as in case K 244.

The injection sites in K 360 (fig. 3.6 C) is situated in FZ_I, but encroaches upon FZ_{II}. The majority of the retrogradely labeled cells in the olive is located in vlo and rdc, but a substantial number is found in the cdc. Labeled fibers are located in FC_1 and central FC_2 (figs. 3.7 A, B; 3.11 c-e). Two fiber streams, one arching through the lateral and interposed nuclei and one passing through the floccular peduncle can be distinguished. Most fibers terminate in dorsolateral, central, and caudal parts of SV (fig. 3.11 d-f). Other fibers, passing between LV and the restiform body, Löwy's bundle and dorsal DV distribute to MV (fig. 3.11 g-j). They terminate in the parvicellular part of MV, dorsolateral to the acoustic stria, among larger cells of MV, ventrolateral to the stria, and in more caudal parts of this nucleus. Very few labeled fibers can be seen in the nucleus prepositus hypoglossi. Diffuse labeling is present in the medial part of the dorsal cochlear nucleus (fig. 3.11 h-i). Retrogradely labeled neurons are present bilaterally in the vestibular nuclei except for LV. The ipsilateral dorsal group y contains a substantial number of retrogradely labeled neurons, very few are present contralaterally (fig. 3.11 f-g). Similar observations were made in K 358 (fig. 3.8 D)

Group 2 (K 301, K 305, K 340)

The injection sites of group 2 are located in FZ_{II} and labeled Purkinje cell axons travel in compartment FC_2. In case K 301 and K 340 retrograde labeling in the contralateral inferior olive prevails in the cdc (fig. 3.16). The caudal pole of the inferior olive in K 305 was not

fig. 3.8 Diagrams of the unfolded flocculus (left) and a transverse section containing the injection site (right) in cases K 227, K 244, K 355, K 358, K 340. The extent of the injection sites are shown in relation to the floccular compartments and zones. For explanation of symbols indicating zones and compartments see fig. 3.1.

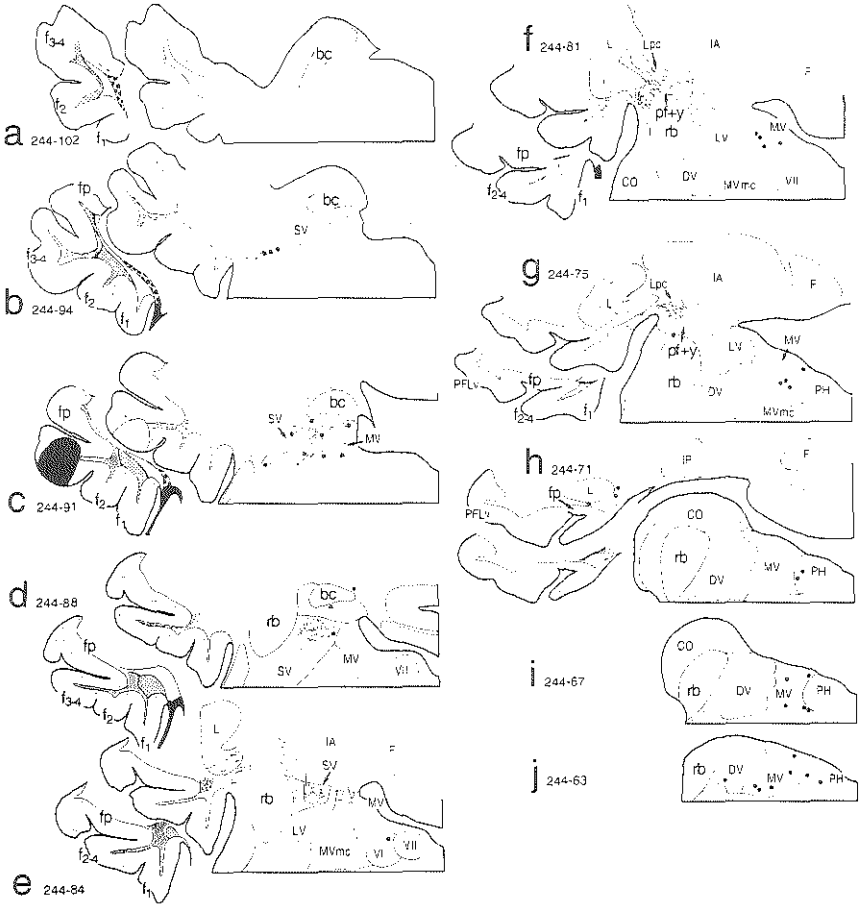

fig. 3.9 Drawings of labeled fibers and neurons in transverse sections through the flocculus and brain stem in case K 244 with an injection in FZ_I. Note the location of efferent fibers in FC_1. Fibers follow two routes, one through the floccular peduncle and group y, the other passing more dorsally through the lateral and anterior interposed cerebellar nuclei. Fibers terminate in mainly the superior vestibular nucleus (SV).

sectioned, but no labeled cells were present in the vlo in this case.

The injection site in K 301 in the rostral pole of folium p (figs 3.6 A; 3.12 d) labels a small number of fibers in dorsal FC_2 (fig. 3.7 C, D). They pass dorsal to the parvicellular part of the lateral nucleus or ventral to it, through the floccular peduncle (fig. 3.12 e-f). In the vestibular nuclei they terminate in MV, medial and lateral to the acoustic stria (fig. 3.12 f-h). A few labeled cells are present bilaterally in dorsal and ventral group y (fig. 3.12 f).

The injection site in K 305 is located in the FZ_{II} zone of f_2 (fig. 3.6 B, 3.13 C). The labeled fibers occupy most of the compartment FC_2 except for a dorsal triangle (fig. 3.13 c-e). This triangle becomes filled after an injection in FZ_{II} in folium p (K 301, figs. 3.7 C; 3.12 d). A few labeled fibers are present in FC_3. At the level of the floccular peduncle these fibers follow a similar course as fibers in the previous experiments. Two fiber streams can be observed. A small number of fibers curves through the lateral cerebellar and anterior interposed nuclei and enters the vestibular nuclei through the caudal SV, lateral to LV. The majority of the fibers accumulate in the floccular peduncle and travel medially in Löwy's bundle to the lateral angle of the fourth ventricle where they bend sharply in a ventral direction to enter MV. Labeled fibers in the floccular peduncle traverse the dorsal and ventral divisions of group y, but no distinct signs of termination could be observed. The majority of the labeled fibers terminates in MV. They are present in the rostral MV, ventral to SV, and more caudally they are especially numerous dorsomedial and ventrolateral to the acoustic stria (fig. 3.13 c-i). Labeled fibers extend beyond the stria into the caudal MV. Some fibers enter SV. Diffuse labeling is present in the medial part of the dorsal cochlear nucleus (fig. 3.13 h). A few labeled fibers were observed in the nucleus prepositus hypoglossi. Some retrogradely labeled neurons are present bilaterally in all vestibular nuclei, with the exception of LV. Ventral and dorsal group y contains some labeled neurons, a few labeled neurons are present in contralateral group y. Identical observations were made in case K 340 (fig. 3.8 E).

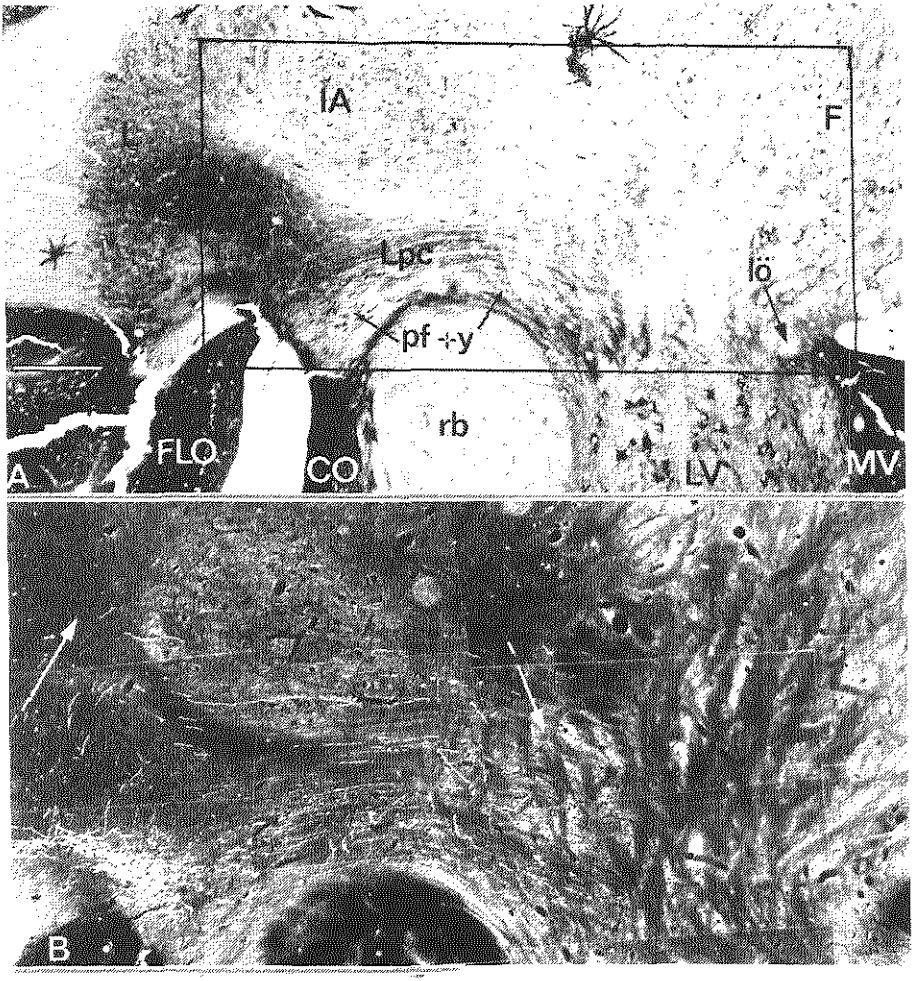
lA
F
Lpc
pf
y
lö
rb
FLO
CO
LV
MV
A
B
C

Group 3 (K 227, K 370).

The injection sites in both cases are located in FZ_{III} (figs. 3.6 D; 3.8 A). In K 227 the injection extends into FZ_{II} and also involvement of FZ_{IV} cannot be excluded. Labeling in the olive prevails in the vlo and the rdc in K 370. In K 227 retrogradely labeled cells ares almost equally distributed over the cdc and the rdc with the vlo (fig. 3.16).

Labeled fibers in K 370 are almost restricted to FC_3 (fig. 3.7 E, F). In the caudal flocculus these fibers enter the floccular peduncle as a single compact bundle. They ramify among cells of dorsal group y. Labeled fibers are also present in ventral and caudal parts of the floccular peduncle, a few fibers travel through ventral group y, bordering on the restiform body (fig. 3.14 e-g; 3.15 C-D). Most fibers enter and terminate in the dorsolateral, central, and caudal parts of SV (fig. 3.15 A-B). Few fibers travel through Löwy's bundle and through DV towards MV, where they terminate in the region surrounding the acoustic stria, and in more caudal parts of MV. A considerable number of labeled fibers appears to terminate in the dorsal cochlear nucleus (fig. 3.14 h-i). A few labeled fibers were seen in the nucleus prepositus hypoglossi. Retrogradely labeled cells are present bilaterally in SV, DV and MV. The dorsal and ventral group y contain a few retrogradely labeled cells; more labeling is observed around and caudal to the parvicellular lateral nucleus. A few labeled cells are present in the contralateral group y. Small labeled neurons in the roof of the fourth ventricle extend, ventral to the cerebellar nuclei, into the white matter of the nodulus (fig. 3.14 g-h).

Labeling in case K 227 is a combination of the distributions in groups 2 and 3. Fibers terminate in SV, MV and DV.

fig. 3.10 Brightfield (A,C) and darkfield photomicrographs (B,D) of the floccular peduncle in K 244. Note the course of the labeled fibers through the floccular peduncle containing the cells of dorsal group y (pf+y) and the presence of fibers arching through the cerebellar nuclei (arrows in B). Labeled fibers ramify among cells of dorsal group y (C). Bar in A = 500 μm, in C = 33 μm.

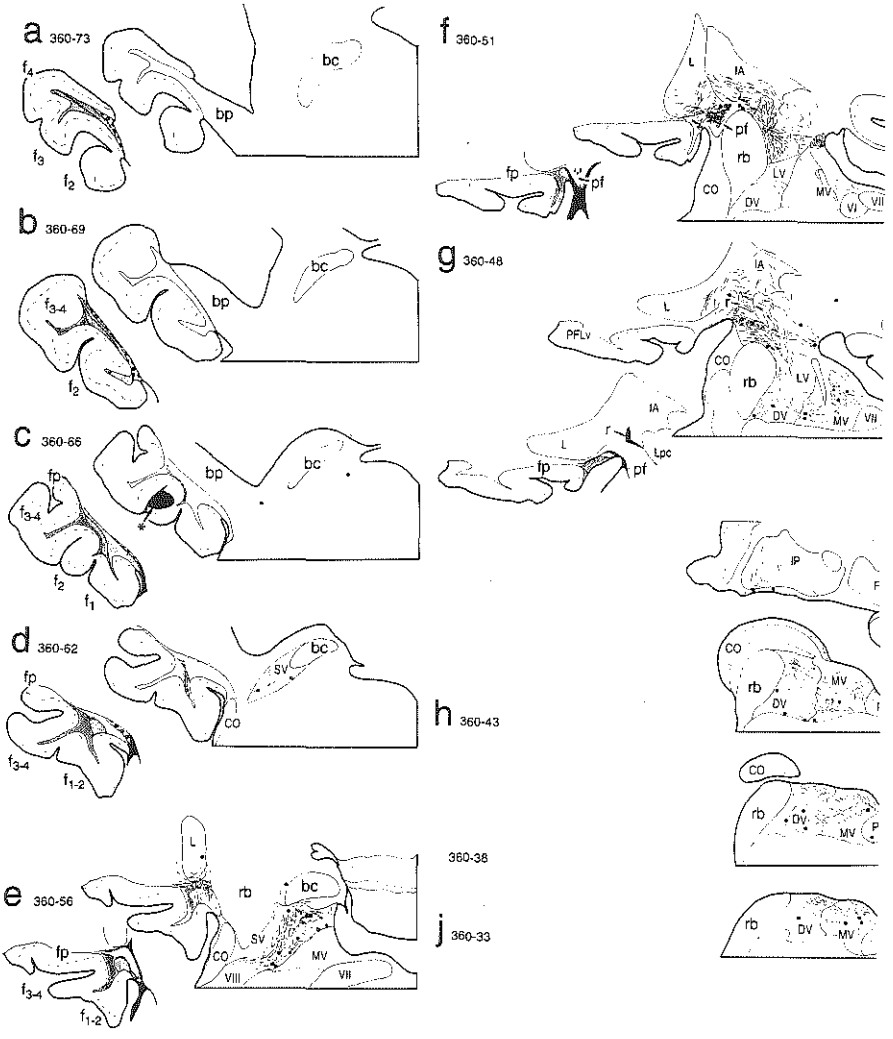

fig. 3.11 Drawings of labeled fibers and neurons in transverse sections through the flocculus and brain stem in case K 360 with an injection mainly located in FZ_I, encroaching upon FZ_{II}. Note the efferent fibers in FC_1, scattered fibers in FC_2, and their termination in the superior (SV), medial (MV) and descending vestibular nuclei (DV).

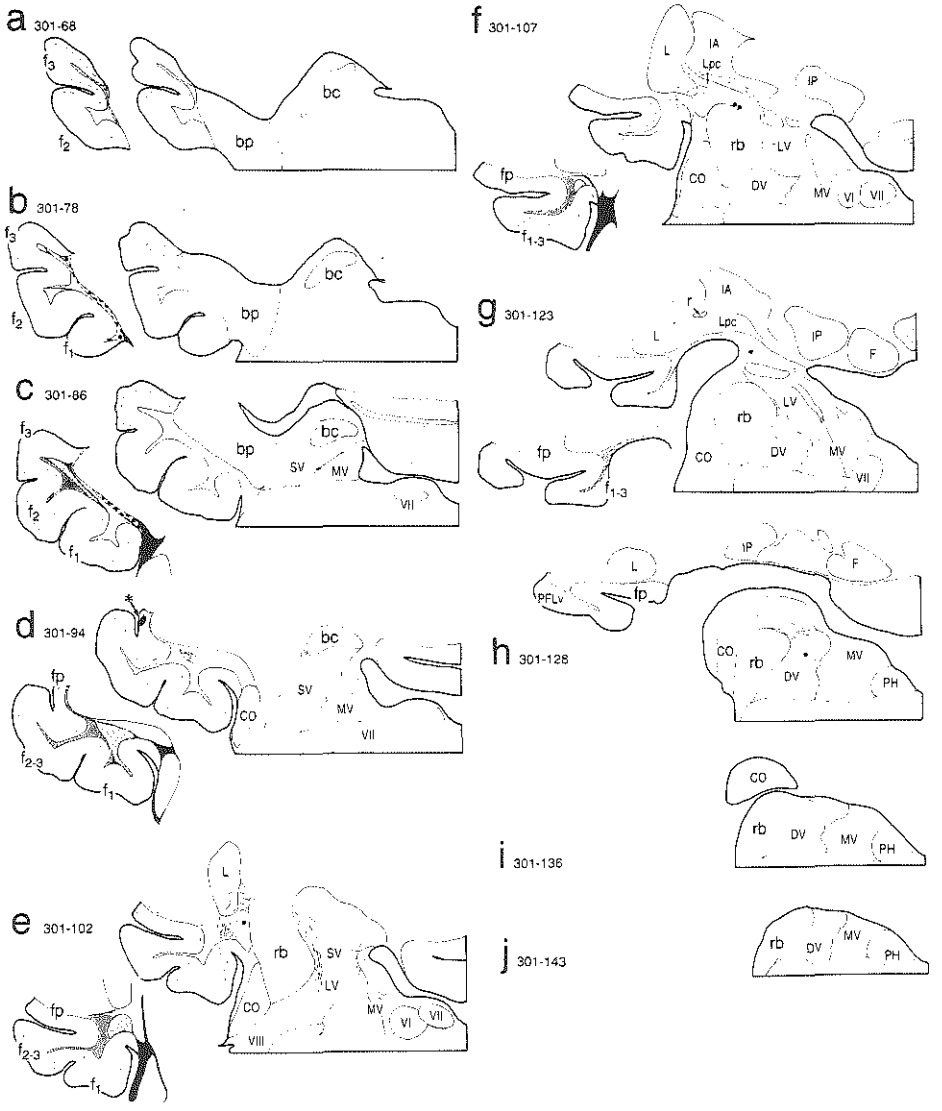

fig. 3.12 Drawings of labeled fibers and neurons in transverse sections through the flocculus and brain stem in case K 301 with an injection in FZ_{II}. Note the location of efferent fibers in the laterodorsal part of FC_2 and terminating in the medial vestibular nucleus (MV).

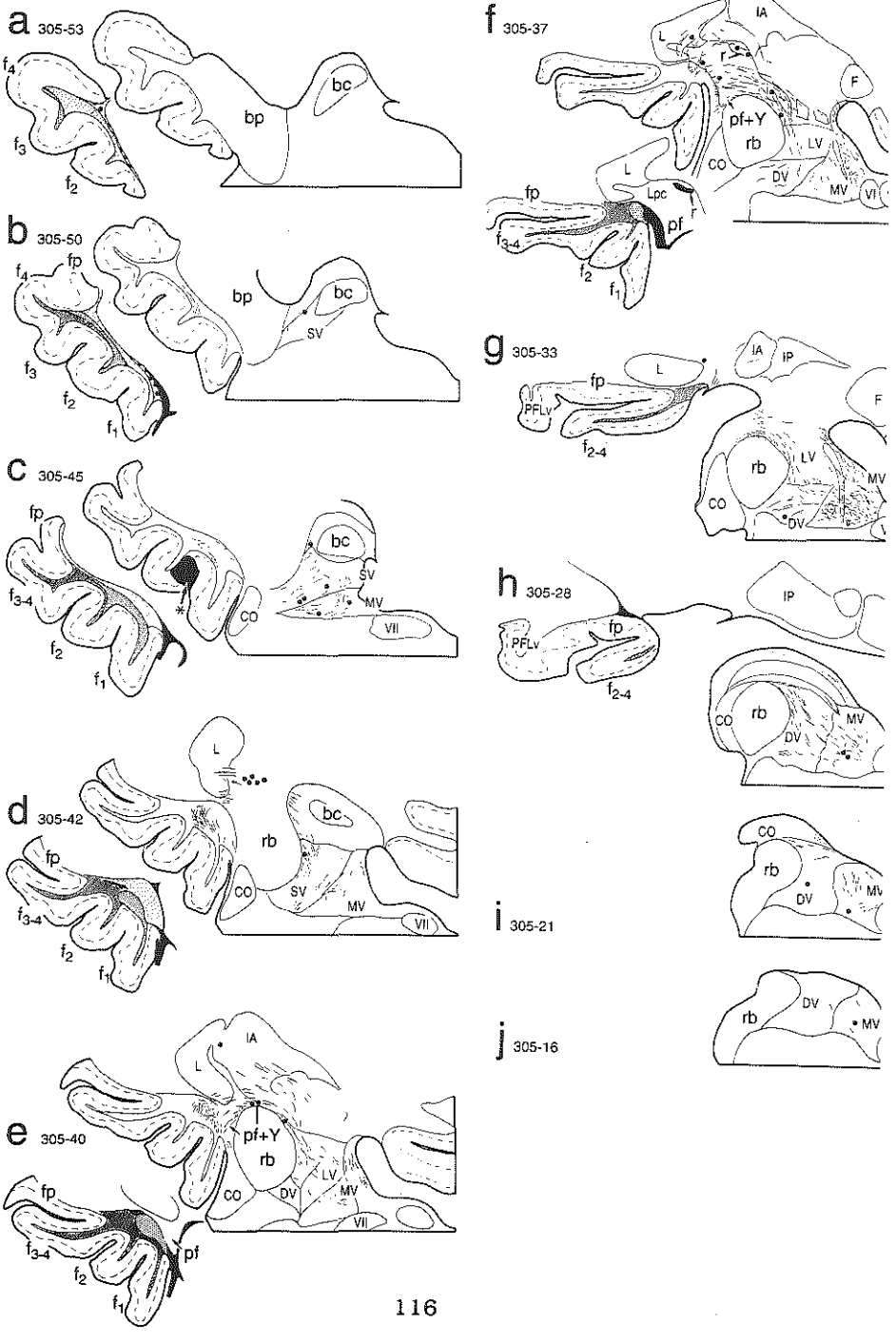
a 305-53
f4
f3
f2
bp
bc
b 305-50
f4
fp
f3
f2
f1
bp
bc
SV
c 305-45
fp
f3-4
f2
f1
*
CO
bc
SV
MV
VII
d 305-42
L
fp
f3-4
f2
f1
rb
bc
CO
SV
MV
VII
e 305-40
IA
L
pf+Y
rb
fp
f3-4
f2
f1
CO
DV
LV
MV
VII
pf
f 305-37
IA
L
r
F
pf+Y
rb
LV
CO
DV
MV
VI
L
fp
Lpc
r
pf
f3-4
f2
f1
g 305-33
IA
IP
L
fp
PFLv
f2-4
F
rb
LV
MV
CO
DV
h 305-28
IP
PFLv
fp
f2-4
CO
rb
MV
DV
i 305-21
CO
rb
DV
MV
j 305-16
rb
DV
MV

3.3.3 Conclusions

Retrograde labeling of Purkinje cells from HRP-injections in their vestibular target nuclei confirmed the localization of the MV-projecting cells in two zones, located rostral to, and interdigitating with two zones projecting to SV (Yamamoto and Shimoyama, 1977). The axons of these Purkinje cells collect in four bundles that correspond to the white matter compartments FC_1-FC_4 delineated in the previous studies (Tan et al., 1989; chapters 1 and 2).

Anterograde WGA-HRP tracing combined with AChE histochemistry demonstrates that Purkinje cells of climbing fiber zones project to specific parts of the vestibular complex (fig. 3.17). FZ_I and FZ_{III} mainly project to the dorsolateral, central, and caudal parts of the SV, with possible minor projections to DV, MV, and prepositus hypoglossi (PH). FZ_{II} and FZ_{IV} project to MV, with possible minor projections to SV and PH. Strong terminations were consistently found in the MV region surrounding the acoustic stria. Most labeled fibers in DV seem to pass through this nucleus on their way to MV rather than to terminate there. The possible minor projections are likely due to spread to neighbouring Purkinje cell zones.

Termination of fibers passing through group y could not be definitely established. Ramifications of labeled fibers around neurons of dorsal group y were observed in cases with injections of FZ_I and FZ_{III}, but not with injections in the FZ_{II} zone. Terminations of arciform fibers from FZ_I and FZ_{II} passing through the cerebellar nuclei and along Lpc cannot be excluded. No arciform fibers were observed in the cases with injections in FZ_{III}.

fig. 3.13 Drawings of labeled fibers and neurons in transverse sections through the flocculus and brain stem in case K 305 with an injection in FZ_{II}. Note the location of efferent fibers in FC_2 terminating almost exclusively in the medial vestibular nucleus (MV).

Fine labeling was present in the dorsal cochlear nucleus in some of the cases with injections in zones FZ_I-FZ_{III}, but not in all of them. No experiments with small injections in C_2 and FZ_{IV} were available.

3.4 Discussion

The present study shows that the Purkinje cells of the flocculus are partitioned in zones. Purkinje cell axons of each zone collect in a white matter compartment and project to specific parts of the vestibular nuclear complex. The data on pathways of Purkinje cell axons demonstrated with anterograde tracing with WGA-HRP are supported by the findings in our retrograde HRP experiments.

3.4.1 *The retrograde and anterograde tracing methods used in this study.*

Two methods have been used in this study to trace the efferent pathways and connections of the flocculus: retrograde axonal transport of HRP injected into the vestibular nuclei and anterograde axonal transport of WGA-HRP injected into the flocculus.

Retrograde filling with HRP of Purkinje cells and their axons demonstrated with DAB as a substrate has been used before to map the corticonuclear and -vestibular projections (Voogd and Bigaré, 1980; Voogd, 1989; Voogd et al., 1987). Anterograde transport in vestibulo-cerebellar mossy fibers that would have hindered the identification of labeled axons as belonging to the retrogradely labeled Purkinje cells, was never observed in these or in the present experiments.

WGA-HRP demonstrated with trimethyl benzidine (TMB) is a more sensitive method. Moreover, WGA-HRP is transported both anterogradely and retrogradely (Lechan et al., 1981; Trojanowski et al., 1981). The injections with very small amounts of WGA-HRP in the cortex of the flocculus, used for anterograde tracing of the Purkinje cell axons, also caused retrograde labeling of neurons in the vestibular nuclei bilaterally and in the contralateral inferior olive. This raises the question whether

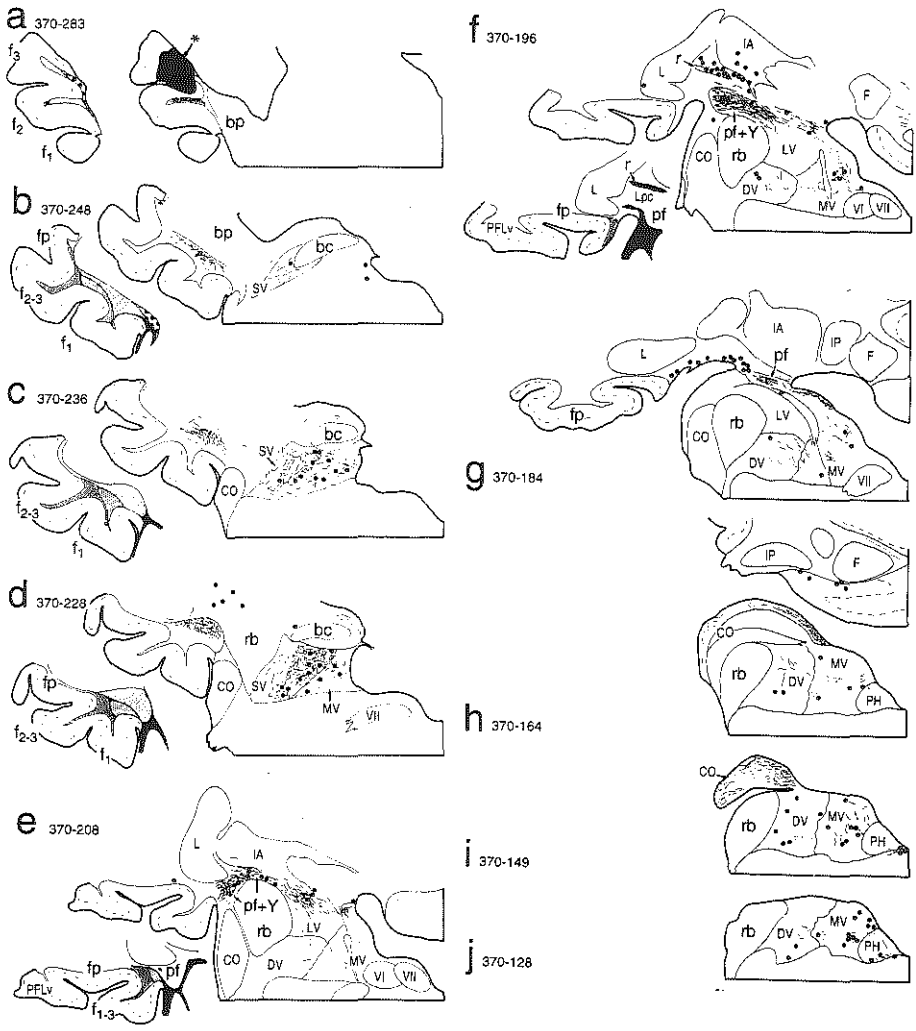

fig. 3.14 Drawings of labeled fibers and neurons in transverse sections through the flocculus and brain stem in case K 370 with an injection in FZ_{III}. Note the location of efferent fibers in FC_3, their passage through the floccular peduncle and dorsal group y, and their termination in the superior vestibular nucleus (SV). Note the absence of fibers passing through the lateral cerebellar nucleus in comparison with cases K 360 and K 244 (figs. 3.9 and 3.11).

some of the axonal labeling observed in our experiments could have been due to retrograde transport in the axons of these labeled cells. This is unlikely because few, if any vestibulocerebellar or olivocerebellar fibers appear to be retrogradely labeled in these cases. Labeled olivocerebellar axons were not observed in the olivary decussation or the restiform body. No labeled fibers could be traced from labeled cells in the contralateral vestibular nuclei to the flocculus. Moreover, the distribution of labeled axons in the ipsilateral vestibular nuclei varies systematically with the localization of the injection site, whereas the distribution of labeled cells was roughly the same in all experiments (see Magras and Voogd (1985); Thunnissen (1990) and Sato et al. (1983b) for experiments showing lack of zonal differentiation in terminations of secondary vestibulocerebellar mossy fibers). Anterograde transport of WGA-HRP of Purkinje cell axons can, therefore, be used to study their distribution.

3.4.2 *Zonal organization of Purkinje cells projecting to the medial and superior vestibular nuclei and group y.*

The overall distribution of the floccular Purkinje cell axons is similar to earlier reports on the rabbit (Epema, 1990) and other species (Voogd, 1964; Angaut and Brodal, 1967, cat; Haines, 1977, Galago; Langer et al., 1985b, macaque monkey). Epema (1990) noticed the two routes followed by these fibers. One runs ventrally, through the floccular peduncle, between the Lpc and the restiform body. Some of its fibers proceed dorsal to LV to Löwy's bundle near the lateral corner of the fourth ventricle. The second route consists of arciform fibers, curving dorsally and caudally through the lateral and anterior interposed

fig. 3.15 Darkfield and brightfield photomicrographs of adjacent AChE-stained (A,C) and HRP-reacted sections (B,D) through the superior vestibular nucleus (A,B) and the floccular peduncle (C,D) in K 370 showing accumulation of terminating fibers in the dorsolateral part of SV (B). More caudally labeled fibers are almost exclusively located just dorsal to the restiform body in the floccular peduncle (D).

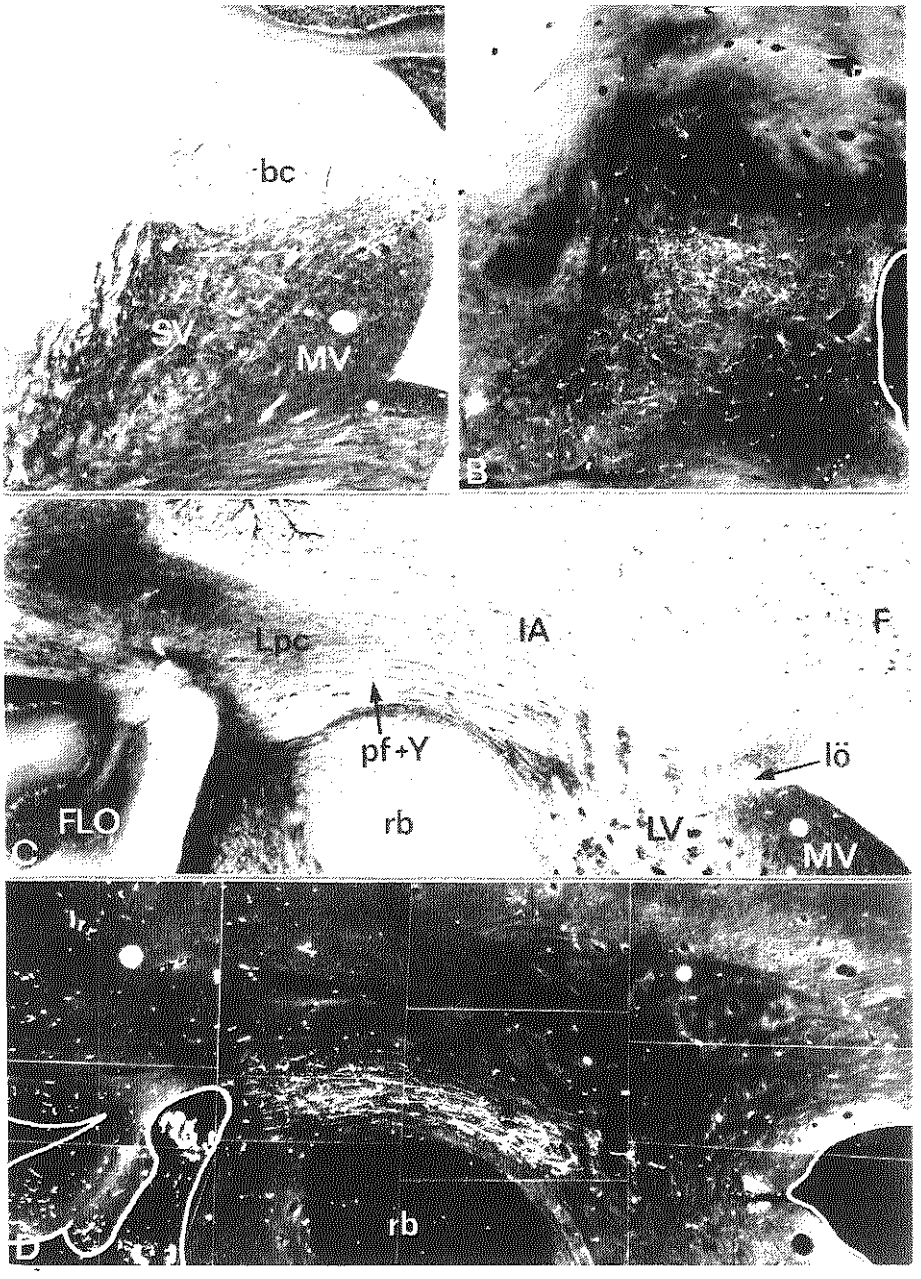
bc
SV
MV
B
Lpc
IA
F
pf+Y
lö
FLO
C
rb
LV
MV
rb
B

cerebellar nuclei. Medial to Lpc and lateral to LV they rejoin the fibers of the floccular peduncle. Arciform fibers, passing through the lateral cerebellar nucleus were observed in cat and Galago, but not in the macaque monkey (Langer et al., 1985b).

Our experiments with retrograde labeling of HRP show that Purkinje cell axons of FZ_{II} and FZ_{IV}, contained in the compartments FC_2 and FC_4, project to MV and those from FZ_I and FZ_{III}, located in FC_1 and FC_3 project to SV. These experiments confirm and extend the observations of Yamamoto and Shimoyama (1977) in the rabbit, especially with respect to the presence of a medial FZ_{IV} zone and a corresponding FC_4 compartment, projecting to MV. Judging from the localization of the injection sites, the distribution of the labeled Purkinje cell axons over the white matter compartments and the retrograde labeling in the inferior olive, most of the injections of WGA-HRP in the cerebellar cortex were focussed on a single floccular zone with encroachment on neighbouring zones in some experiments. No experiments with injections limited to the FZ_{IV} and C_2 zones were available.

Our experiments demonstrate that FZ_I and FZ_{III} project strongly to the SV, especially to its dorsolateral, central, and caudal parts, and that FZ_{II} projects to the MV. Terminations in regions traversed by labeled fibers such as group y, the lateral and anterior interposed cerebellar nuclei, and DV are difficult to establish with certainty. In cases with injections of FZ_I and FZ_{III} labeled fibers ramified among the cells of dorsal group y, but no such ramifications were observed in cases with injections in FZ_{II}. A few labeled fibers extended into nucleus prepositus hypoglossi in cases with injections in FZ_{II} and FZ_{III}. Projections to the dorsal cochlear nucleus previously found by Epema (1990) were observed in some, but not in all experiments with injections in FZ_I and FZ_{III}. Fibers from FZ_I and FZ_{II} travel both along the ventral route through the floccular peduncle and group y, and the dorsal route, curving through the lateral and anterior interposed cerebellar nuclei and the Lpc. Terminations of Purkinje cell axons in these nuclei cannot be excluded.

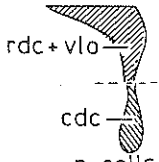

	I				II			II-III	III
	K244	K355	K358	K360	K301	K340	K305	K227	K370
rdc + vlo	93%	85%	82%	67%	11%	15%	-	55%	85%
cdc	7%	15%	18%	33%	89%	85%	-	45%	15%
n cells	250	81	78	86	46	35	-	186	150
in N sections	49	12	18	14	28	25	-	19	18

fig. 3.16 Distribution of labeled cells over the caudal dorsal cap (cdc) and the rostral dorsal cap with the ventrolateral outgrowth (rdc + vlo) in cases with injections of WGA-HRP in the floccular zones FZ_I-FZ_{III}.

Fibers from FZ_{III} pass exclusively through the floccular peduncle. Our observations are in accordance with the results of De Zeeuw et al. (1992), who traced axons from individual Purkinje cells of the flocculus with biocytin. They found projections from Purkinje cells of FZ_I and FZ_{III} to SV, and from FZ_{II} to parvicellular and magnocellular parts of MV. In addition, they observed terminals from FZ_I and FZ_{III} Purkinje cell axons in group y, and for FZ_I also in the ventral dentate nucleus. FZ_{II} did not project to group y or the dentate nucleus.

Our findings are in good agreement with earlier studies (Yamamoto and Shimoyama, 1977; Yamamoto, 1978; Balaban et al., 1981; Sato et al., 1982a, 1982b). Our zone FZ_{II} and FZ_{III} correspond to the middle and rostral zones of the flocculus of the cat (Sato et al., 1982a) and the monkey (Balaban et al., 1981), which also project to MV and SV, respectively. By the absence of a projection to SV the caudal zone of the cat flocculus differs from the FZ_I zone of the rabbit (Sato et al., 1982b). It is still possible that zones equivalent to FZ_I and C_2 exist in the caudal cat flocculus, and that the injections of the lateral cerebellar nucleus and

group y labeled fibers of passage of FZ_I and C_2 on their way to SV and the posterior interposed nucleus. A caudal zone, which projects to SV and corresponds to FZ_I was found in the monkey (Balaban et al., 1981).

The vestibular nuclei contain excitatory and inhibitory relay neurons for the vestibulo-ocular reflexes that convey input from semicircular canals activated by head movements (Ito et al., 1973). Purkinje cells of the flocculus innervate horizontal and anterior canal relay cells, but do not terminate on relay cells of the posterior canal (Ito et al., 1973, 1977, 1982a,b). Fibers from FZ_I and FZ_{III} terminate mainly in the dorsolateral, central, and caudal parts of the SV. Excitatory anterior canal relay cells that innervate contralateral motoneurons innervating the superior rectus and the inferior oblique muscles, are located in dorsolateral SV. Inhibitory anterior canal relay cells, which innervate inferior rectus and superior oblique motoneurons of the ipsilateral oculomotor and trochlear nerve nuclei, occupy the central part of SV (Highstein, 1973; Ito et al., 1977; Yamamoto et al., 1978; Highstein and Reisine, 1979; Sato and Kawasaki, 1990b; Labandeira-Garcia et al., 1991). Since floccular stimulation inhibits the VOR pathway from the anterior canal (Ito et al., 1977, 1982a,b) it is likely that it is conveyed through the FZ_I/FZ_{III} projection to the central and dorsolateral SV. These vestibular neurons are also active during vertical smooth pursuit eye movements (Chubb and Fuchs, 1982; Chubb et al., 1984).

The heaviest projection of FZ_{II} is found in the parvicellular MV, dorsomedial to the acoustic stria, and among the larger cells of MV, ventrolateral to this bundle. Fewer fibers terminate in the most rostral part of MV, ventral to SV, and in caudal parts of this nucleus. No fibers were traced to LV or to the interstitial nucleus of the vestibular nerve.

Of the vestibulo-ocular relay neurons located in MV, only horizontal canal cells receive inhibitory projections from the flocculus (Ito et al., 1973; 1977). Kawaguchi (1985) distinguished medial and lateral groups of horizontal canal cells that received inhibition from the rabbit flocculus. The medial group was located medial to the acoustic stria, and the lateral group in the ventrolateral part of LV (i.e. in the magnocellular part of MV

in our terminology). Cells of both groups projected to the ipsilateral medial rectus subdivision of the oculomotor nucleus, but in addition the medial group contained cells that presumably projected to the ipsilateral abducens nucleus. These cells correspond to the inhibitory neurons intercalated in the inhibitory vestibulo-ocular pathway to the ipsilateral abducens nucleus that is under inhibitory control of the flocculus (Highstein, 1973; Ito et al., 1977; Sato et al., 1988; Sato and Kawasaki, 1991). The projection of the flocculus extends beyond the acoustic stria into caudal MV and DV and, therefore, may include neurons with other connections that the oculomotor nuclei (see also Epema, 1990).

The accumulation of fibers from FZ_I, FZ_{II} and FZ_{III} in the area of group y indicates that some of these fibers may also terminate in this cell group. Cytoarchitectonically it consists of dorsal and ventral parts (Highstein and Reisine, 1979, cat; chapter 1, rabbit). The ventral group y is formed by a thin layer of tightly packed small fusiform neurons immediately dorsal to the restiform body. Neurons of ventral group y receive primary vestibular afferents (Sato and Kawasaki, 1987) from the sacculus (Lorente de No, 1933; Gacek, 1969; Carleton and Carpenter, 1984; Kevetter and Parachio, 1984). They do not respond to antidromic stimulation from the oculomotor nuclei (Sato and Kawasaki, 1987). The dorsal part of group y consists of larger, fusiform, and multipolar neurons which gradually blend into the parvicellular part of the lateral cerebellar nucleus. In the cat these neurons that receive polysynaptic input from both VIIIth nerves are the primary target for floccular Purkinje cells in the caudal zone (Sato and Kawasaki, 1987). Some of these target neurons were also found in the adjacent ventral part of the LCN (Lpc). They project to the caudal half of the contralateral oculomotor nucleus (Highstein, 1971, 1973; Graybiel and Hartwieg, 1974; Highstein and Reisine, 1979; Stanton, 1980; Carpenter and Cowie, 1985; Sato and Kawasaki, 1987; Labandeira-Garcia et al., 1991). This part of the oculomotor nucleus harbours the motoneurons innervating the inferior oblique muscle ipsilateral to the motoneuron and the contralateral superior rectus muscle (Gacek, 1977; Naito et al., 1974; Akagi, 1978). In our cases with injections of FZ_I and FZ_{III} labeled fibers ramified around

cells of dorsal group y that were not labeled retrogradely (figs 3.10; 3.15). No such evidence was available for the projections of FZ_{II}.

3.4.3 *Correspondence of cortico-vestibular with climbing fiber zones in the rabbit flocculus.*

The zonal pattern described in the present study corresponds well with the zonation of climbing fibers demonstrated with anterograde WGA-HRP tracing in rabbit (chapter 2) and Phasaeolus leucagglutinin transport in the rat (Ruigrok et al., 1992) and the autoradiographic study of Gerrits and Voogd (1982) in the cat. In the previous chapter we compared the climbing fiber projection to the flocculus with the compartmentation in adjacent AChE-stained sections as a reference. We found close correlations between particular subsets of olivary neurons and certain white matter compartments. The cdc projected through compartments FC_2 and FC_4 to floccular zones FZ_{II} and FZ_{IV}, while rdc/vlo neurons projected through compartments FC_1 and FC_3 to floccular zones FZ_I and FZ_{III}. Our observations on retrograde labeling of cells of the dorsal cap and the ventrolateral outgrowth in experiments with small injections of individual floccular zones generally support this conclusion.

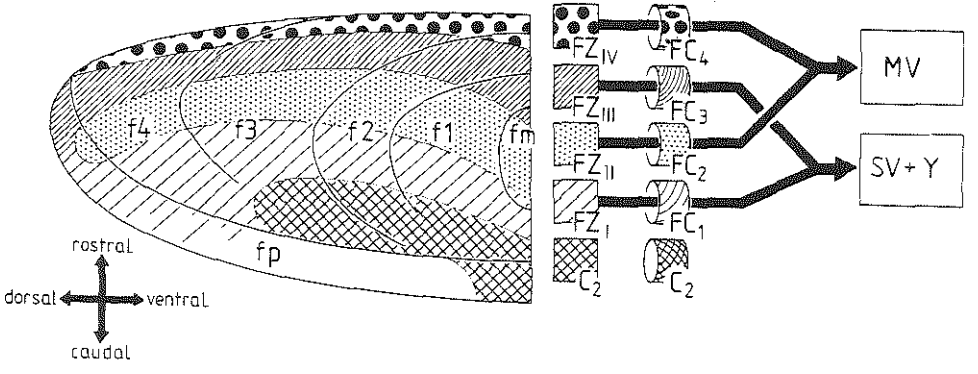

fig. 3.17 Diagram of the projections of the floccular zones FZ_I-FZ_{IV} through compartments FC_1-FC_4 to the vestibular nuclei.

3.4.4 *Functional considerations.*

The efferent flocculo-vestibular projection forms part of the neuronal circuitry that is the basis of oculomotor control (Ito et al., 1973). Through these connections Purkinje cells in the flocculus can inhibit the activity of vestibular neurons (Highstein, 1971; Baker et al., 1972; Fukuda et al., 1972; Ito et al., 1977). An imbalance of vestibular discharge activities would result in eye muscle activity. Indeed, local electrical stimulation in the flocculus elicits eye movements (Ron and Robinson, 1973; Dufossé et al., 1977; Sato and Kawasaki, 1984, 1990a, 1990b; Nagao et al., 1985; Belknap and Noda, 1987; Chapter 4). Some of these studies indicated that a particular type of eye movement could only be elicited by stimulating within a confined area of the flocculus (Sato and Kawasaki, 1984, 1990a, 1990b; Nagao et al., 1985; Simpson et al., 1989; Chapter 4). Recent studies (Simpson et al., 1989, Van der Steen et al., 1991, Chapter 4) demonstrated that optimum responses were obtained by stimulating the white matter of the flocculus. They verified the stimulation sites histologically, compared them with the AChE compartmentation, and found that in three of the five white matter compartments (compartments FC_1, FC_2 and FC_3) clear eye movements could be elicited. The relatively small size of compartments C_2 and FC_4 made it difficult to be sure that the stimulation was confined to them and no conclusion was reached about their relationship to eye movements (see also chapter 4). Stimulation in compartments FC_1 and FC_3 resulted in rotatory conjugate eye movements around axes in the horizontal plane; the ipsilateral (left) eye moved counterclockwise around an axis at about 135° to the midsagittal plane, the contralateral (right) eye moved clockwise around an axis at about 45° to the midsagittal plane. These compartments flanked compartment FC_2, in which electrical stimulation resulted in horizontal eye movements (i.e. rotation around the vertical axis) towards the stimulated side. The results of the present study and that of Van der Steen et al. (1991, see also Chapter 4) indicate that each floccular zone controls the activity of specific extra-ocular muscle pairs

through the compartmentalized flocculo-vestibular nucleus projection to specific vestibulo-ocular relay neurons in the vestibular nuclei.

Chapter 4

Functional and anatomical organization of three-dimensional eye movements in rabbit cerebellar flocculus

4.1 Introduction

The flocculus of the cerebellum is part of the compensatory eye movement control system that stabilizes gaze during involuntary head rotations. Because head rotations can occur about any axis in space, signal processing in the flocculus has to support eye rotations having three degrees of freedom. Understanding this signal processing requires detailed knowledge of how three-dimensional eye movements are represented in the flocculus.

One approach to this question has been to use electrical stimulation of the flocculus while recording eye movements or eye muscle activity (rabbit; Ito et al., 1977; Dufossé et al., 1977; Ito et al., 1982a,b; Nagao et al., 1985; monkey: Balaban and Watanabe, 1984; Belknap and Noda, 1987; cat: Sato and Kawasaki, 1990a). Another approach has been to determine the geometry of the floccular climbing fiber (CF) signals of retinal image slip (Maekawa and Simpson, 1973; Simpson and Alley, 1974; Simpson et al., 1981; Leonard et al., 1988; Graf et al., 1988; Kano et al., 1990; Kusunoki et al., 1990). From the electrical stimulation studies, a topographical representation in the form of zones emerged from the distribution of sites where microstimulation evoked different classes of eye movements or influenced different vestibulo-ocular reflex (VOR) pathways. A zonal representation is also indicated from the CF studies showing that the different classes of CFs that signal retinal slip in reference to specific axes of visual world rotation arise from different parts of the dorsal cap and ventrolateral outgrowth of the inferior olive. When this relation is combined with the general anatomical and physiological finding (Voogd, 1969; Groenewegen and Voogd, 1977; Voogd and Bigaré, 1980; Brodal and Kawamura, 1980; Gerrits and Voogd,

1982; Oscarsson, 1969, 1979) that the inferior olive can be subdivided such that each subdivision's terminal field in the cerebellar cortex has the form of a parasagittal zone, then the importance of a zonal configuration in the floccular representation of eye movements is further apparent. Even so, the reported localization and extent of these zones within or between species has not been consistent. The variable and sometimes conflicting results have arisen for at least two reasons. First, the techniques used to measure the evoked eye movements did not permit precise, dynamic three-dimensional measurements. Second, no independent anatomical delineation of the zones was available for comparison with the physiology on an animal by animal basis. To overcome the first limitation, three-dimensional search coils can be used to obtain the required measurements (Van der Steen and Collewijn, 1984). An opportunity to overcome the second limitation has been provided by the finding of Hess and Voogd (1986) that acetylcholinesterase (AChE) histochemistry can be used to reveal distinct compartments in the cerebellar white matter. With AChE histochemistry five compartments have been demonstrated within the floccular white matter of the rabbit (Tan et al., 1989; Van der Steen et al., 1989; see chapter 1).

This paper reports that in the rabbit implanted with three-dimensional search coils only a small number of different classes of short latency eye movements are evoked by electrical stimulation of the floccular white matter and that they are differentially associated with anatomically distinguishable compartments revealed by AChE histochemistry. Furthermore, these eye rotations are organized in a coordinate system like that of the visual CFs. In view of the similarity of the orientation of the preferred axes of the CFs and the rotation axes of the extra-ocular muscle pairs, a relatively simple geometrical relationship is suggested between each class of CFs and the eye rotations produced by the activation of the Purkinje cells upon which that class of CFs synapse. Some of the results were presented previously in brief (Van der Steen et al., 1989, 1991).

4.2 Materials and methods

4.2.1 *Eye movement recordings.*

Eye movements in response to electrical microstimulation in the flocculus were recorded in 44 awake, pigmented rabbits. The three-dimensional movements of both eyes were recorded with the scleral search coil technique (Van der Steen and Collewijn, 1984). One week before the experiment two search coils, one horizontal on top of the superior rectus muscle and one vertical, parallel to the limbus, were implanted using general anaesthesia (initial intramuscular dose: 32 mg/kg ketamine, 0.6 mg/kg acepromazine, 5 mg/kg xylazine; supplement each 45 min.: 18 mg/kg ketamine, 0.32 mg/kg acepromazine, 4 mg/kg xylazine) and aseptic techniques. The vertical axis (horizontal) component of eye rotation was measured with the vertical coil using the phase-angle detection technique (Collewijn,1977; Van der Steen and Collewijn, 1984), while the rotation components about the 45° and 135° axes (see below) were measured with the horizontal coil using the amplitude detection technique (Robinson, 1963). The vertical coils had absolute calibration, whereas the horizontal coils were calibrated prior to implantation. The three eye position components for each eye were recorded on a polygraph and stored on magnetic tape. To generate eye position plots, the components were digitized off-line on a minicomputer (DEC, PDP11/73) at a sampling frequency of 125 Hz with a resolution of 10 seconds of arc. The latencies of the eye movement components were taken from selected trials throughout the experimental series. The latencies were determined from eye position signals digitized at a rate of 500 Hz by a CED-1401 data-acquisition system (Cambridge Electronic Design) connected to a personal computer. Each axial component was displayed at its optimal resolution and its latency from stimulus onset was determined from the display by judging where the eye displacement first exceeded the noise level. Because of the variations in the shape of the initial eye movements following electrical stimulation, a visual inspection procedure was chosen rather than an automatic fitting procedure.

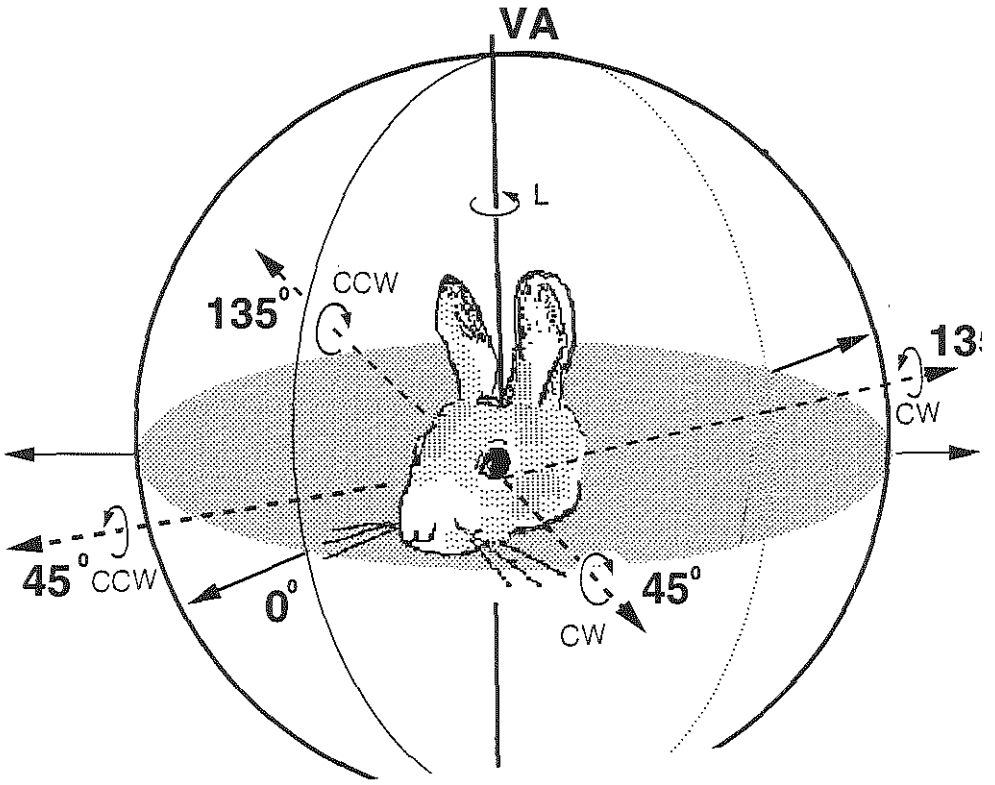

fig. 4.1 The orthogonal coordinate system used in measuring the angular displacements of the eyes. For explanation see text.

4.2.2 *The coordinate system for measuring the eye movements.*

The orthogonal coordinate system used to measure the eye rotations is shown in fig. 4.1. It consisted of a vertical axis and two horizontal axes oriented at 45° and 135° azimuth. The 0° azimuth reference was defined as rostral in the midsagittal plane and the azimuthal coordinate was taken to increase to each side of the reference direction. The three components of the rotation of each eye were named after their respective axis of measurement (i.e. vertical axis (VA), 45° axis, and 135° axis). The sense of rotation was defined as left and right for the vertical axis and clockwise (CW) and counterclockwise (CCW) for the

45° and 135° axes according to how the respective eye movement components would appear to an observer looking along each axis of rotation towards the rabbit's eye. With these conventions, the 135° axis of one eye is oriented parallel to the 45° axis of the other eye, and a CW rotation of one eye is conjugate, with respect to sense of rotation to a CCW rotation of the contralateral eye.

4.2.3 *Electrophysiology.*

Several days before the experiment the rabbit was anaesthetized (as above) and under aseptic conditions a craniectomy was made to expose the paramedian lobe on each side of the cerebellum. A small chamber of dental acrylic was constructed around each opening in the skull. The dura was covered with an antibiotic gel and a thin sheet of silicon rubber, and the chamber was filled with bonewax and paraffin. On the day of the experiment, the rabbit was comfortably restrained in a hammock with the head held with the nasal bone at 57° to the horizontal. The dura was opened under local anaesthesia and a recording microelectrode (glass or metal) was lowered into the cerebellum. The flocculus was identified by monitoring the modulation of the Purkinje cell CF activity in response to a handheld moving visual pattern (Simpson and Alley, 1974; Graf et al., 1988). With the animal in darkness, the flocculus was stimulated along the electrode track at 200 μm intervals with electrical pulses (200 Hz, 2-20 μA, negative polarity, 0.2 msec pulse width, 1 sec train duration). A stimulation site was regarded as an effective site when electrical stimulation, not exceeding 20 μA, produced an eye movement with an amplitude of at least 0.5° about at least one of the six axes of rotation. When metal electrodes were used, selected sites effective for evoking eye movements were marked by small electrical lesions (5 μA, 5 sec duration DC current, tip positive). Experiments were carried out using both the right and left flocculi, but for clarity of presentation all results are represented in reference to stimulation of the left flocculus.

4.2.4 *Histology.*

See chapter 2.2.

4.3 Results

4.3.1 *Classification of eye movement responses.*

Prior to the availability of the AChE staining showing white matter compartments, experiments were conducted in 26 rabbits to determine the characteristics of the three-dimensional eye movements evoked by electrical stimulation of the flocculus. In this series of experiments about 90% of the flocculus was explored; only the most rostral and the most caudal parts were not included. Eye movements were more readily evoked by stimulation in the deep granular layer and in the white matter than from the molecular and Purkinje cell layers. Typically the responses consisted of slow eye movements with an amplitude varying between 1° and 8°. On occasion, slow eye movements with amplitudes up to 20° were observed and these larger movements were sometimes interrupted by resetting saccades. The onset of the prominent components of the eye movement responses usually occurred between 8-48 ms after stimulus onset. Peak speed occurred 100-200 msec after movement onset and reached a maximum value of 20°/s. After cessation of the stimulus the eyes usually returned within 4-10 seconds to the position held before the stimulus began. In a few instances, however, the eyes remained in an eccentric position and successive 1 sec periods of stimulation then produced successively smaller displacements. The eye movements were classified according to the largest component of the response. Of the 12 possible classes (2 eyes x 3 axes x 2 senses of rotation), two of the classes accounted for 78% of the responses.

4.3.2 *135° axis eye movement responses.*

For 59% (82/140) of the effective stimulation sites, the largest

response component was a CCW rotation of the left (ipsilateral) eye about its 135° axis. Three examples of this class of eye movements, each from a different animal, are shown in fig. 4.2. The 135° axis class showed three variations: In about 50% (42/82) of the cases the response was conjugate in that the largest response component for the contralateral (right) eye was a CW rotation about its 45° axis. The amplitude of this component was always smaller than the conjugate component about the 135° axis of the ipsilateral (left) eye. In 13% (10/82) of the cases, the conjugate component of the contralateral eye was virtually absent. The third variation (37%, 30/82) consisted of cases where, in addition to the CCW 135° axis response of the ipsilateral (left) eye (which was the largest of all components), the CW component of the contralateral (right) eye about its 45° axis was accompanied by an equally large or larger CCW component about the 135° axis (see e.g. fig. 4.7 A). For each of the three variations of the 135° axis class, disjunctive rotations of both eyes about the vertical axis were sometimes present, as shown by the VA traces in fig. 4.2.

4.3.3 *Vertical axis eye movement responses.*

For 19% (26/140) of the effective stimulation sites the largest response component was an abduction of the ipsilateral eye (a leftward rotation of the left eye about its vertical axis). Fig. 4.3 shows three examples, each from a different animal, in which the ipsilateral VA component was the largest of all components. The VA component of the contralateral eye was conjugate in direction, but showed considerable variation in magnitude. In the example of fig. 4.3 A the evoked eye movement was virtually restricted to the ipsilateral eye. In other cases (fig. 4.3 B-C) stimulation resulted in rotation of both eyes about the vertical axis, although the VA component of the contralateral eye was always smaller than that of the ipsilateral eye. In addition to the major component of rotation about the vertical axis, smaller rotations about the 45° and 135° axes sometimes occurred.

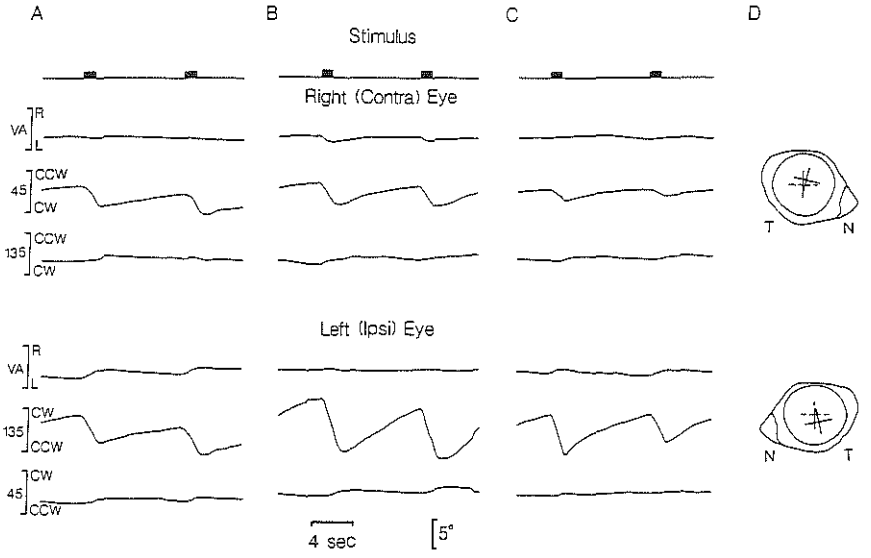

fig. 4.2 Examples from three different animals of the class of evoked eye movements for which the largest component was a CCW rotation of the ipsilateral (left) eye about its 135° axis. In these examples (A-C) the largest component of the contralateral (right) eye movement was a conjugate (CW) rotation about its 45° axis. For this class of eye movements, an accompanying disjunctive (vergence) movement about the vertical axis was often present. In this and other similar figures, the three traces for each eye show the angular displacement about the indicated axes (L, leftward; R, rightward; CW, clockwise; CCW, counterclockwise). A downward deflection indicates a leftward rotation of each eye about its vertical axis (VA), a clockwise rotation of the right (contralateral) eye about its 45° and 135° axes, and a counterclockwise rotation of the left (ipsilateral) eye about its 45° and 135° axes. The periods of electrical stimulation are indicated by the solid blocks at the top. The drawings to the right of the eye position traces in this (D) and other similar figures show how the net rotation of the eye would appear if a cross had been placed on the cornea (dashed cross: initial position, solid cross: position at the end of the stimulation. T, temporal; N, nasal).

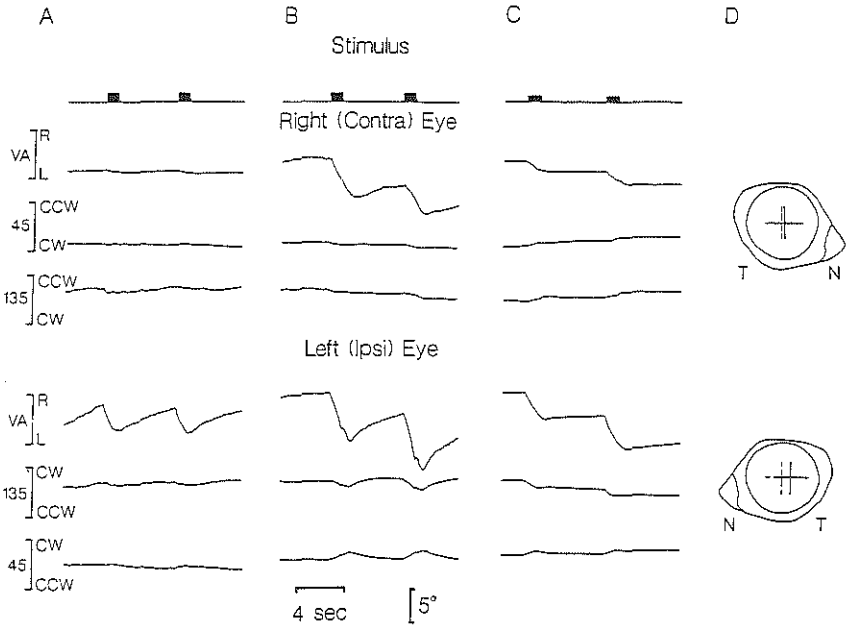

fig. 4.3 Examples from three different animals of the class of evoked eye movements for which the largest component was an abduction of the ipsilateral (left) eye. In the left panel (A) the response was virtually restricted to the ipsilateral eye, whereas in panels B and C the responses were bilateral. For explanation of symbols and abbreviations see fig. 4.2.

4.3.4 *Other response types.*

Although the majority of the responses fell into one of the two classes described above, in the remaining 22% (32/140) of the cases other types of responses were recorded. These responses comprised, in part (10/140), cases in which the largest component was a CCW rotation about the contralateral (right) 135° axis in combination with a smaller CW rotation about the contralateral (right) 45° axis. In other cases (16/140) a CW 135° axis rotation of the ipsilateral (left) eye was the largest component.

The remaining 6 cases consisted of vergence eye movements for which the disjunctive contralateral VA component was the largest component.

4.3.5 *Latencies of the response components.*

A further distinction between the different types of eye movement responses was made on the basis of the latency of each of the components. For this purpose, examples were drawn from throughout the experimental series. Using the larger amplitude responses facilitated the latency measurements, which revealed short and long latencies among the different components.

The CCW 135° axis and abducting ipsilateral components, which defined the two main classes, all had short latencies. Of these, the latencies of the 135° class were the shortest and had the sharpest onset. A typical example of the onset of both the ipsilateral CCW 135° and contralateral CW 45° axis components is shown with an expanded time and position scale in fig. 4.4 C. Fig. 4.4 A shows the latency distribution for the population of analyzed 135° class responses. The mean latency of the CCW rotation of the ipsilateral (left) eye about its 135° axis was 15 msec (S.D. ± 11 msec, n=65). When both eyes moved there was also a measurable CW rotation of the contralateral (right) eye about its 45° axis. The mean latency of this response was 28 msec (S.D. ± 18 msec, n=35). This difference in the onsets of the ipsilateral CCW 135° and contralateral CW 45° axis responses was not significant (p=0.74, Kolmogorov-Smirnov test).

The latencies of the VA components of the VA class responses were also short (fig. 4.4 B-C). The mean latency of the ipsilateral abducting VA response was 27 msec (S.D. ± 15 msec, n=27), while the mean latency of the contralateral adducting VA component was 49 msec (S.D. ± 25 msec, n=19). These latency differences were not significant (p=0.5, Kolmogorov-Smirnov test).

The latencies of the other relatively large response components were also measured. In one of the three variations of the 135° axis class, stimulation evoked a CW rotation of the contralateral (right) eye about its

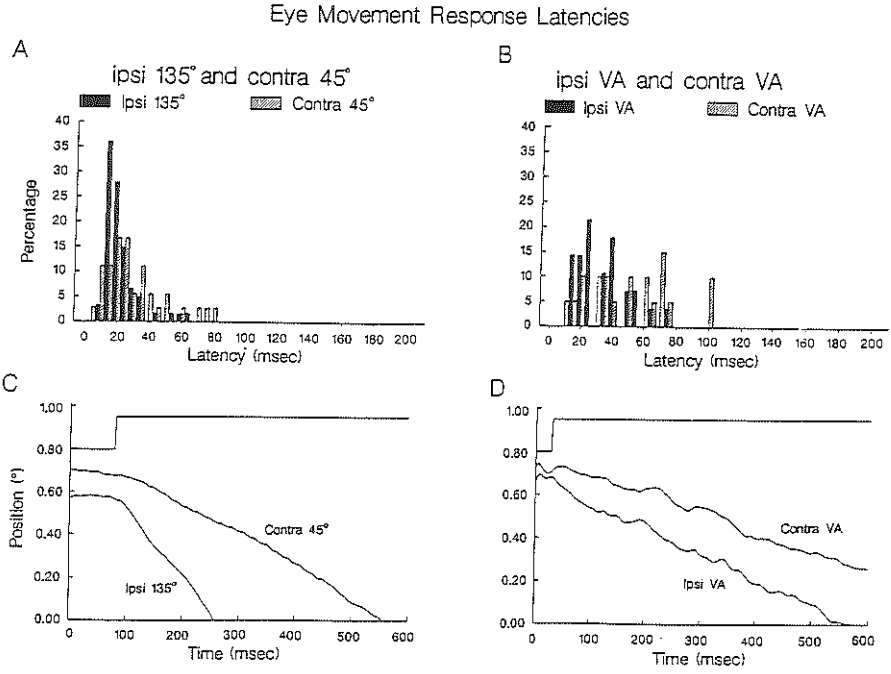

fig. 4.4 Latency histograms (top panels) and examples (lower panels) for the predominant component and the conjugate component for the 135° axis (A and C) and VA axis (B and D) classes of evoked eye movements. For each class the ipsilateral and the contralateral conjugate components are indicated by solid and hatched bars, respectively. In the histograms the number of ipsilateral cases is greater than the number of contralateral cases because in some instances there was no accompanying response component for the contralateral conjugate axis.The latencies were grouped in 5 msec bins and two bins, one for the ipsilateral component and one for the contralateral component, are displayed for each latency interval. The top trace in C and D shows the onset of the stimulation period. Further explanation in the text.

45° axis along with a comparably sized CCW rotation about its 135° axis. The latencies of the CCW rotation about the contralateral (right) 135° axis and the CW rotation about the contralateral (right) 45° axis were clearly different (fig. 4.5 A, C). The component about the 135° axis had a

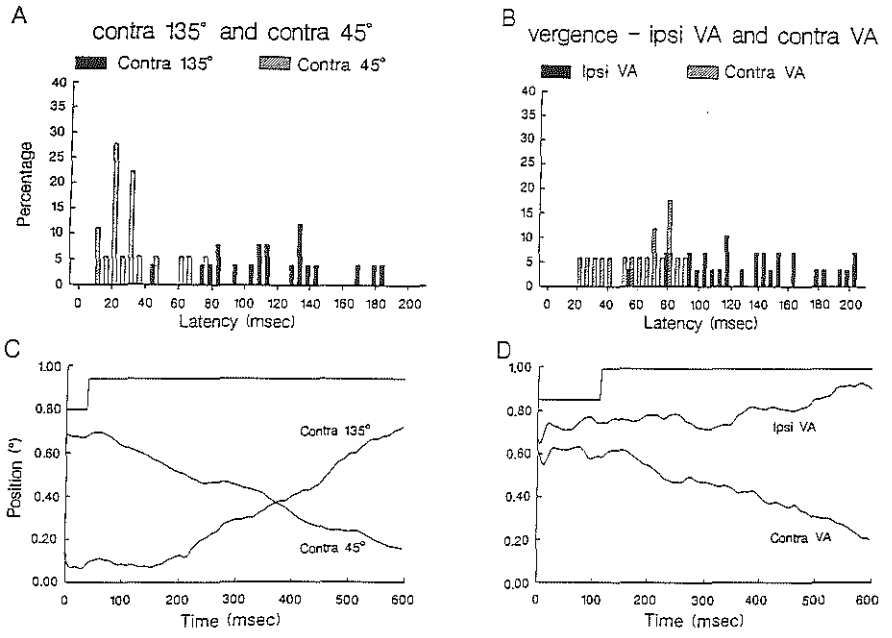

fig. 4.5 Latency histograms (top panels) and examples (lower panels) for evoked eye movements for which (A and C) rotation of the contralateral eye occurred with nearly equal amplitude components about the 45° and 135° axes, or for which (B and D) vergence occurred with adduction of both the ipsilateral and contralateral eye about the vertical axis. The format for the latency histograms in A and B is similar to that used for Fig. 4 A and B. For the example in C, the latency of the contralateral CCW 135° axis component was 90 msec longer than that of the contralateral CW 45° axis component. For the example in D, the latency of the ipsilateral adducting component was 125 msec longer than that of the contralateral adducting component.

substantially longer mean latency (121 msec, S.D. ± 46 msec, n=22) than that of either the accompanying CW 45° axis component (27 msec, S.D. ± 16 msec, n=22) or the ipsilateral accompanying CCW 135° axis component (14 msec, S.D. ± 7 msec, n= 22). As can be appreciated from the latency distribution shown in Fig. 4.5 A, the latency differences between the contralateral CW 45° and the contralateral CCW 135° axis

components were statistically highly significant ($p<0.001$, Kolmogorov-Smirnov). It should be noted that for this variation of the 135° axis class the movements of the two eyes were far from conjugate. The net response of the contralateral eye was approximately "vertically" upward, whereas the response of the ipsilateral eye was predominantly a CCW rotation about its 135° axis.

Some eye movements of the 135° axis class included an adduction of both the ipsi- and contralateral eyes about the vertical axis, producing a disconjugate (vergence) movement. The latencies of the accompanying ipsilateral CCW 135° axis and contralateral CW 45° axis components were short, as described above. However, the latencies of the disconjugate VA components of the two eyes differed considerably (fig. 4.5 B, D). The onset of the ipsilateral VA response in the adducting direction was considerably later (142 ms, S.D. ± 53 msec, n=29) than that of the contralateral adduction (59 msec, S.D. ± 20 msec, n=13). The two latency distributions, shown in fig. 4.5 B, were significantly different ($p< 0.01$, Kolmogorov-Smirnov).

In those instances in which the ipsilateral eye rotated about the 135° axis in the CW sense rather than in the far more commonly found CCW sense, the latencies of the CW component were significantly longer (106 msec, S.D. ± 16 msec, n=13, $p<0.001$, Kolmogorow-Smirnov).

4.3.6 *Anatomically delineated compartments.*

In the course of the experiments, the AChE histochemistry technique introduced by Hess and Voogd (1986) became available for use in the rabbit. With this technique, the floccular white matter was seen to be subdivided into five compartments separated by darkly stained raphes (Tan et al., 1989; Van der Steen et al., 1989; chapter 1). Following the convention described in chapter 1, the compartments were labeled from lateral to medial as C_2, FC_1, FC_2, FC_3 and FC_4. Fig. 4.6 A and B show AChE stained transverse sections through the rostral and caudal thirds of the flocculus, respectively. A complete series of transverse sections taken at 80 µm intervals through the entire flocculus of one animal was digitized

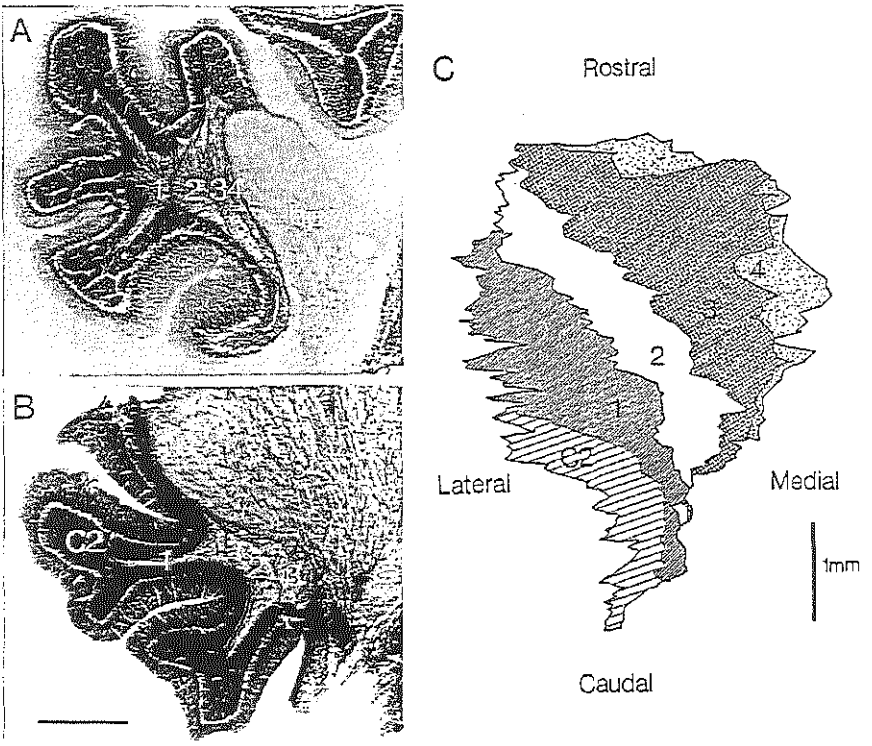

fig. 4.6 Anatomically delineated compartments in the floccular white matter. A and B, AChE-stained transverse sections, showing the different compartments separated by darker staining raphes. A is from the rostral third of the left flocculus, and from lateral to medial the compartments are labeled (FC)1, 2, 3, and 4. B is from the caudal third of the left flocculus. Because the compartments run obliquely from caudomedial to rostrolateral, compartment 4, which is the most medial one, is not yet clearly visible in this relatively caudal section, whereas C_2 is present only in the most lateral part of the white matter. The scale bar in B represents 1 mm and applies also to A. bp: brachium pontis. The full extent of the floccular white matter compartments, in C, is based on a three-dimensional reconstruction of the white matter. The reconstructed floccular white matter is shown as a projection onto a horizontal plane below the flocculus with the observer looking down on the plane.

and a three-dimensional reconstruction of the white matter was made using a graphical computer program (Hillman et al, 1990; Mahoney et al., 1990).The reconstruction (fig. 4.6 C) shows the five compartments forming a set of strips running obliquely in a caudomedial to rostrolateral direction.

4.3.7 *Classes of eye movements in relation to anatomical compartments.*

The relation between the different classes of three-dimensional eye movement responses and the anatomically distinguishable compartments was elucidated in a second series of experiments performed on 18 awake, pigmented rabbits. In this series, the electrical stimulation and eye movement recordings were combined with AChE histochemistry. The eye movements were evoked by electrical stimulation with tungsten microelectrodes and small electrolytic lesions were placed at sites producing different classes of eye movements. In the AChE-stained serial sections the lesions and electrode tracks were located with respect to the anatomically distinguishable compartments. With this technique a clear relation was found between compartments FC_1, FC_2 and FC_3 and the different classes of eye movements. Because the most caudolateral and most rostromedial compartments (C_2 and FC_4, respectively) are comparatively small, it was not possible to determine the eye movements evoked by stimulating only the fibers in the white matter or granular layer within these two compartments.

Eye movements whose largest component was a CCW rotation about the ipsilateral (left) 135° axis were evoked by stimulation of the most lateral of the three large compartments (FC_1). An example with two stimulation sites in FC_1 is shown in fig. 4.7. In this particular case, the electrode passed through folium p (Yamamoto and Shimoyama, 1977; Yamamoto, 1978) in addition to the more ventral part of FC_1. At both lesion sites (A and B) the largest component of the eye movement response was a CCW rotation about the 135° axis of the ipsilateral (left) eye, accompanied by a smaller CW rotation of the contralateral eye (right)

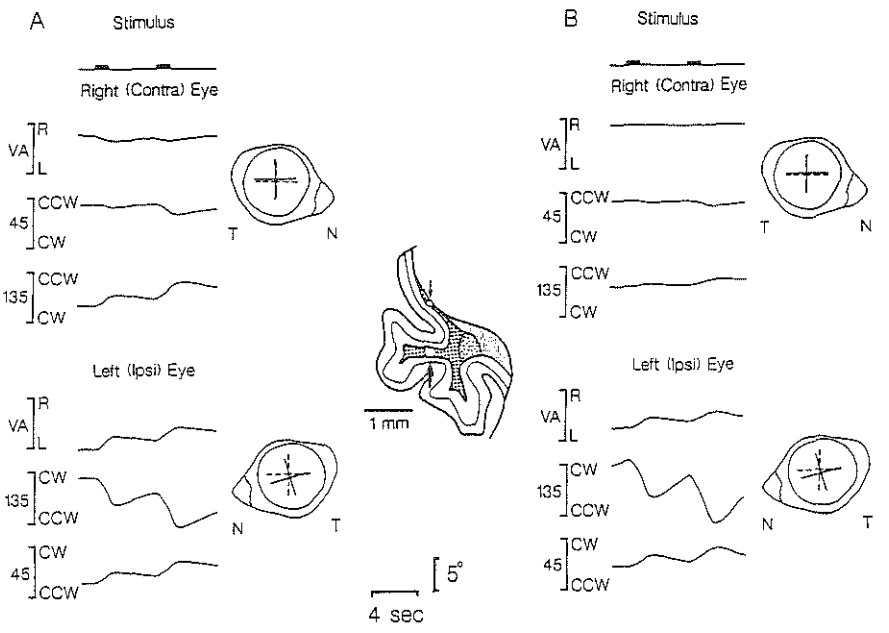

fig. 4.7 Eye movements evoked by electrical stimulation in compartment FC_1. The drawing in the center panel depicts a transverse section of the flocculus; white matter compartments FC_1, FC_2 and FC_3 are indicated by large, medium and small dots, respectively. The eye movements in A resulted from stimulation in the ventral part of compartment FC_1 (marking lesion indicated by large arrow). The responses in B were evoked by stimulation in the extension of compartment FC_1 into folium p (marking lesion indicated by small arrow). In both cases, the largest response component was a CCW rotation of the ipsilateral (left) eye about its 135° axis.

about its 45° axis. These movements were accompanied by vergence components about the vertical axis and, as shown clearly in fig. 4.7 A, also by a CCW rotation about the contralateral 135° axis.

Fig. 4.8 illustrates the eye movements evoked by stimulation of compartment FC_3. The eye movements produced by stimulation of FC_3 were on aggregate indistinguishable from those produced by stimulation

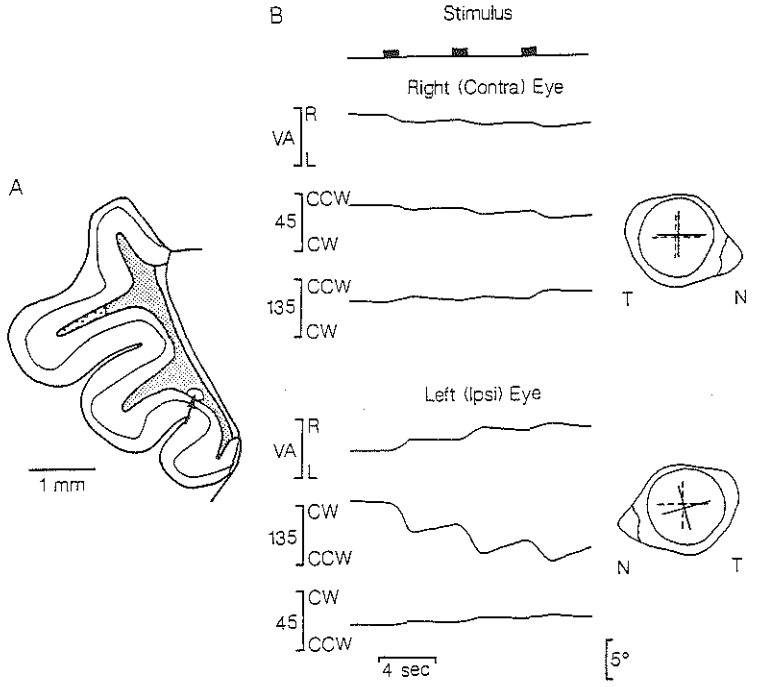

fig. 4.8 Eye movements evoked by electrical stimulation in compartment FC_3. The largest response component was a CCW rotation of the ipsilateral (left) eye about its 135° axis (B). Also note the small disjunctive rotations of the eyes about the vertical axis. The drawing of the transverse section in A shows the marking lesion (arrow) at the stimulation site in compartment FC_3 (small dots), which at this relatively rostral level comprises the majority of the white matter. The laterally located compartment FC_2 is indicated by medium dots and the thin, medially located compartment FC_4 is undotted.

of FC_1; the largest component was a CCW rotation about the 135° axis of the ipsilateral (left) eye. The variations of the 135° axis class found for compartment FC_1 stimulation were also found for FC_3 stimulation,

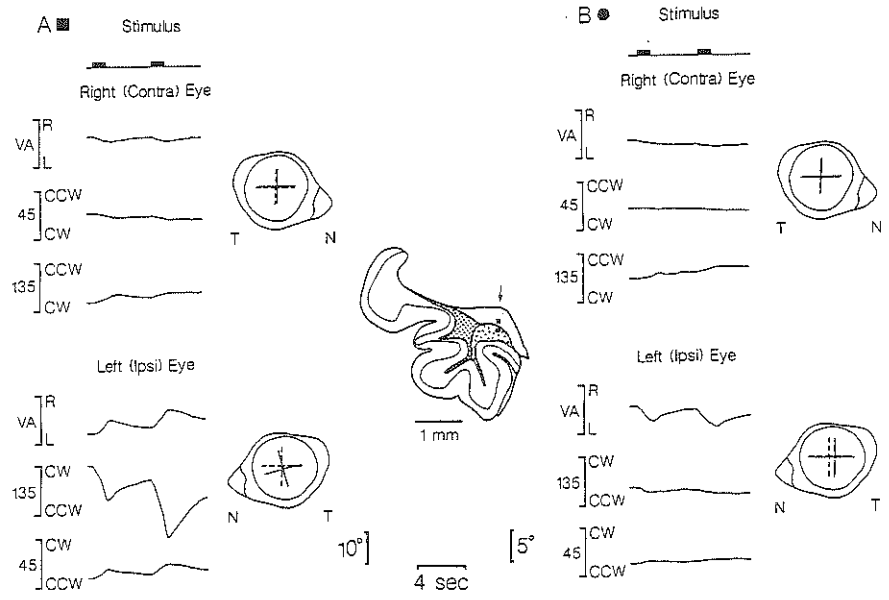

fig. 4.9 Example of the sharp change in the class of eye movement responses occurring when the stimulating electrode passed from one compartment to the other along the direction indicated by the arrow. The center panel shows the stimulation sites in compartment FC_3 (filled square, fine dots) and in compartment FC_2 (filled circle, medium dots). The eye movements produced at the two locations are shown in the two bordering panels.
A) For the eye movements evoked from compartment FC_3 the largest component was a CCW rotation of the ipsilateral (left) eye about its 135° axis. Note that the vertical axis rotation is disjunctive and that the ipsilateral VA component is an adducting (rightward) rotation.
B) Stimulation 200 μm deeper than in (A) and in compartment FC_2 produced VA class eye movements. The largest component of the ipsilateral eye movement was an abducting (leftward) rotation.

including disjunctive VA (vergence) movements.

The raphes form distinct anatomical boundaries between the different white matter compartments. If these compartments also represent functional subunits, then one would expect to find marked

changes in the eye movement responses when the stimulating electrode passed from one compartment to the other. The presence of such a relation between anatomical and functional compartmentation is shown in figs. 4.9 and 4.10. Fig. 4.9 illustrates a case in which the electrode passed through the white matter of FC_3 and then entered the white matter of FC_2, as depicted in the central panel. The two different classes of eye movements shown in fig. 4.9 A and B were evoked from stimulation sites only 200 μm apart. Fig. 4.9 A shows the eye movements obtained with the electrode tip located in FC_3 (black square in central panel). The dominant rotation component was a CCW rotation about the ipsilateral (left) 135° axis, accompanied by some vergence about the vertical axis. When the electrode was advanced 200 μm into FC_2 (filled circle in central panel) a sharp transition of the eye movement responses occurred. The dominant response component became an abduction of the ipsilateral eye (fig. 4.9 B).

Stimulation of FC_2 invariably resulted in eye movements whose largest component was an abduction of the ipsilateral eye, as illustrated in figs. 4.9 B and 4.10. In the case illustrated in fig. 4.10, two electrode tracks were made at the same rostrocaudal level. The more lateral track passed into FC_1, while the more medial track passed into FC_2. Stimulation in FC_1 evoked eye rotations whose largest component was a CCW rotation about the ipsilateral (left) 135° axis (fig. 4.10 A), and accompanying disjunctive movements about the vertical axis. In contrast, stimulation in the adjacent compartment (FC2) evoked eye rotations whose largest component was an abduction of the ipsilateral eye (fig. 4.10 B). The sharp transitions in the responses evoked by electrical stimulation in relation to the floccular white matter compartments indicate that they are in correspondence to the physiologically distinguishable classes of eye movements.

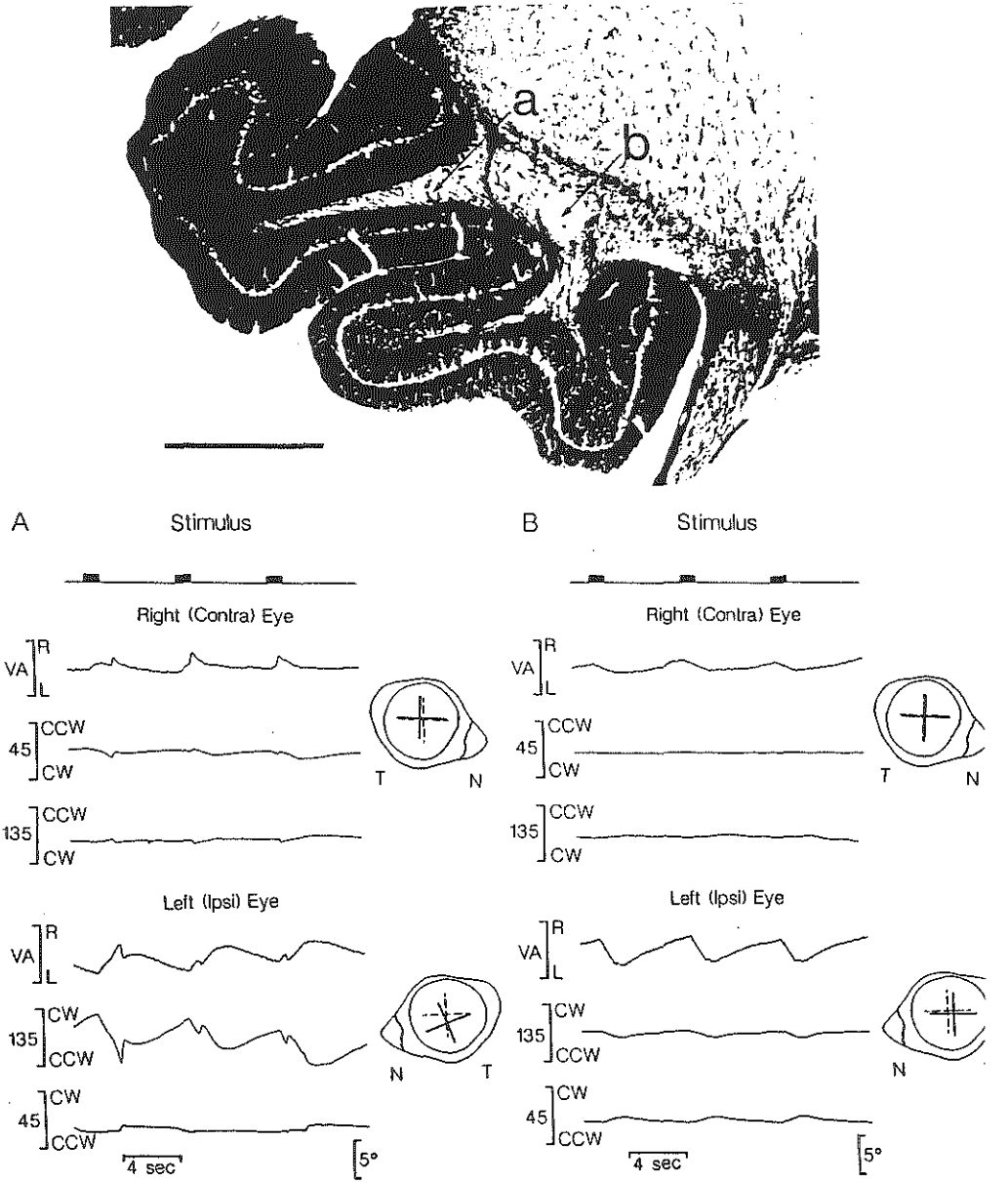
a
b
A
Stimulus
Right (Contra) Eye
VA
R
L
45
CCW
CW
135
CCW
CW
T
N
Left (Ipsi) Eye
VA
R
L
135
CW
CCW
45
CW
CCW
N
T
4 sec
5°
B
Stimulus
Right (Contra) Eye
VA
R
L
45
CCW
CW
135
CCW
CW
T
N
Left (Ipsi) Eye
VA
R
L
135
CW
CCW
45
CW
CCW
N
4 sec
5°

4.4 Discussion

This study provides a direct demonstration of a correspondence between anatomically identified floccular zones and different patterns of evoked eye movements. In previous studies using electrical stimulation of the flocculus, a correspondence could only be inferred because no independent anatomical identification of floccular zones was available for the animals actually used in the stimulation experiments. In those studies, the anatomically based zonal structure of the flocculus was compiled from a number of different animals using retrograde HRP labeling techniques to delineate differential projections of floccular Purkinje cells to the vestibular nuclear complex (Yamamoto and Shimoyama, 1977; Yamamoto, 1978 ; Sato et al., 1982a,b; Balaban et al., 1981). In the present study, however, the floccular zones could be determined in each stimulated animal by staining for AChE.

Previous investigators have pointed out that the wide variations among animals makes it difficult to use standardized maps (Nagao et al., 1985; Kusunoki et al., 1990). Attempts to superpose results from a number of animals have led to the impression that the zones are more interdigitated than is seen using AChE staining. With an independent anatomical marker of floccular subdivisions available for each animal, a more accurate and reliable comparison between physiological and anatomical maps of the rabbit flocculus can now be made. To this end, we will first discuss the present findings on the classes of evoked eye movements and compare them to previous findings in the rabbit. Second, we will discuss the correspondence between the present anatomical and

fig. 4.10 Association of different classes of eye movements with different anatomically delineated floccular white matter compartments. Top panel: AChE stained transverse section showing electrolytic marking lesions in two adjacent compartments of the floccular white matter. Electrical stimulation in the white matter of compartment FC_1 at the site marked by the more lateral lesion (a) evoked 135° class eye movements, as shown in A. In this particular case, the accompanying adduction of the ipsilateral eye was unusually large. Stimulation in compartment FC_2 at the site marked by the more medial lesion (b) evoked VA class eye movements as shown in B. The scale bar represents 1 mm.

physiological floccular maps and compare them to previous attempts to chart the flocculus structurally and functionally.

4.4.1 *Classes of evoked eye movements.*

The sense of rotation and the orientation of the rotation axes of the short latency classes of evoked eye movements are in line with the effects of flocculus stimulation in rabbit on the various semicircular canal vestibulo-ocular reflex (VOR) pathways (Ito et al., 1973, 1977, 1982b). Floccular Purkinje cells monosynaptically inhibit vestibular nuclei neurons that are part of the three-neuron arc of the VOR (e.g. Ito et al., 1970; Fukuda et al., 1972; Baker et al.,1972; Highstein, 1973; Kawaguchi, 1985; Sato and Kawasaki, 1987, 1990b; Sato et al., 1988), but only some of these VOR pathways are directly influenced by the flocculus. The specificity of the inhibition for particular pathways was shown by determining whether electrical stimulation of the flocculus depressed individual canal-ocular reflexes. These experiments demonstrated that the rabbit flocculus influences six specific canal-ocular pathways (Ito et al., 1973, 1977, 1982a,b). Two of these pathways link the horizontal canal with the ipsilateral medial and lateral recti muscles. Increased activity of the related floccular Purkinje cells would result in increased activity of the lateral rectus muscle and decreased activity of the medial rectus muscle, causing abduction of the ipsilateral eye. In our experiments, such eye movements formed one class of the short latency responses. The four other canal pathways under direct floccular control arise from the anterior canal. They excite the ipsilateral superior rectus and the contralateral inferior oblique muscles and inhibit their antagonists, the ipsilateral inferior rectus and contralateral superior oblique muscles. The eye movements expected as a result of increased activity of the Purkinje cells influencing the anterior canal pathways would be, for a rabbit, a combination of depression, intorsion and abduction of the ipsilateral eye and a combination of intorsion, elevation and adduction of the contralateral eye. In our experiments such eye movements constituted the majority of the short latency responses.

The short latency eye movements produced by floccular stimulation in our study are in agreement with the results of Ito et al. (1977) who showed, using electromyographic and muscle tension measurements, that floccular stimulation produced depression of the excitatory and inhibitory three neuron arc pathways originating from only the horizontal and anterior canals. The posterior canal pathways were not inhibited by floccular stimulation. In agreement with this finding we never observed an eye rotation that had as its main component a rotation about the ipsilateral 45° axis, which would have implicated the posterior canal pathways. Ito et al. (1977) proposed four separate groups of flocculus inhibited neurons in the anterior canal pathways: two groups of excitatory neurons, one projecting to ipsilateral superior rectus motoneurons and the other projecting to contralateral inferior oblique muscle motoneurons; and two groups of inhibitory neurons, one projecting to ipsilateral inferior rectus motoneurons and the other projecting to contralateral superior oblique motoneurons. Graf et al. (1983) showed, however, that rabbit posterior canal VOR relay neurons branch to both oblique and vertical rectus motor pools. If a similar branching pattern applies to anterior canal VOR relay neurons,as was suggested for cat by Sato and Kawasaki (1991), then the number of distinct groups of anterior canal pathway neurons receiving inhibitory input from the flocculus would be two rather than four. On the other hand, in our experiments in rabbit quantitative differences were found between the amplitude of the rotations of the ipsilateral and contralateral eyes. Often movement of the contralateral eye was virtually absent, which indicates that the projection pattern of floccular receiving neurons is probably not uniform and that some flocculus receiving neurons in the rabbit vestibular nucleus project to the motoneurons of only one extra-ocular muscle.

Although there is general agreement between the predicted eye movements and those evoked in the present study, there are some important differences with previous reports on eye movements evoked by electrical stimulation of the rabbit flocculus. In experiments by Dufossé et al. (1977) and Nagao et al. (1985) the eye movements were classified as horizontal, rotatory, and vertical. The eye rotation axes of the horizontal

and rotatory classes, as defined in these earlier investigations, are consistent with the eye rotations expected from combining the electromyographic studies of Ito et al. (1973, 1977, 1982a,b) with the measurements of the pulling directions of the individual extra-ocular muscles in the rabbit (Graf and Simpson, 1981; Simpson and Graf, 1985). The VA class of eye movement responses found in the present study is consistent with the previously defined horizontal class (Dufossé et al., 1977) and can be explained by the known influence of the flocculus on the lateral and medial recti muscle activity.

In the present study, the most common response was a CCW rotation of the ipsilateral (left) eye about its 135° axis, frequently accompanied by a smaller CW rotation of the contralateral (right) eye about its 45° axis. This class is similar to the rotatory class of Dufossé et al. (1977) and Nagao et al. (1985), except that the contralateral eye movement was previously found to be either larger than the ipsilateral eye movement (Nagao et al., 1985) or to occur without an accompanying ipsilateral eye movement (Dufossé et al., 1977). In those studies the rotatory class movements of the contralateral eye were considered to result from the inhibitory influence of the flocculus on the pathways from the ipsilateral anterior canal to the contralateral oblique muscles. No explanation, however, was offered for the ipsilateral eye movement about the 135° axis. The present study indicates that the short latency ipsilateral "rotatory" eye movements are essentially the result of floccular inhibition of the anterior canal pathways to the ipsilateral vertical recti.

A short latency "vertical" class of eye movements was not found in the present study and such a class should not, in fact, be expected. The presence of a "vertical" class of eye movements (rotation about a nasal-occipital axis) indicates that the flocculus stimulation influenced both anterior and posterior canal pathways, since rotations about a nasal-occipital (roll) axis requires the action of both the vertical recti and the obliques of each eye. Because of the geometrical arrangement of the vertical recti and oblique muscles, it is not possible to produce a "vertical" eye movement by inhibition of only the pathways from the ipsilateral anterior canal.

The contralateral "vertical" eye movements found in the present study as nearly equal, but opposite rotations of the contralateral eye about its 45° and 135° axes are apparently the same as the contralateral eye movements in the vertical class of Dufossé et al. (1977) and Nagao et al. (1985), but, as shown here, the latency of the contralateral 135° axis component was significantly longer than that of the contralateral 45° axis component. This difference implies that the effect on the posterior canal pathways was less direct and possibly not the result of a direct stimulation of Purkinje cells. Also, in the present study, the ipsilateral eye movement accompanying the "vertical" contralateral eye movement was not "vertical", but consisted predominantly of a larger CCW rotation about the 135° axis. While a combination of short and longer latency responses of the contralateral eye can account for previous observations of contralateral "vertical" eye movements, such an explanation for the ipsilateral "vertical" eye movements reported previously is not available from our observations.

4.4.2 *Latency considerations.*

The range of average latencies for the short latency classes of eye movements (15-49 msec) are comparable to those reported in other studies of eye movements evoked by low intensity stimulation of the flocculus (39 msec in cat, Sato et al., 1984; 24 msec in monkey, Belknap and Noda, 1987; 30-40 msec in one rabbit, Dufossé et al., 1977). These values are larger than those derivable from electrophysiological studies on the influence of flocculus stimulation on VOR pathways, but the difference can be reasonably ascribed to the requirement for temporal summation of the inhibitory influence of Purkinje cells before the behavioral consequence of low intensity flocculus stimulation is manifest. In previous studies in the rabbit, the methods of eye movement measurement (photographs and TV tracking systems) precluded obtaining accurate latency measures. Therefore, some of the discrepancies between the reported "vertical" eye movements and the directions of eye movements expected from the actions of the vertical recti and oblique muscles could be due to a confounding of responses with differing latencies.

Whereas the shorter latency responses can be explained in terms of previous findings on flocculo-vestibulo-ocular connectivity, the basis of the longer latency responses is not known. They could originate from axon reflex activity of antidromically activated afferents or they could arise from influences of Purkinje cells on vestibular circuits of a higher order than the three neuron arc canal-ocular paths. Of the several longer latency eye movements, the most intriguing is the ipsilateral adduction, which in combination with the accompanying contralateral adduction, results in a vergence movement. It seems odd that the evoked ipsilateral adduction should arise from stimulation of floccular compartments FC_1 and FC_3, which are associated with the ipsilateral vertical recti and contralateral obliques and not from compartment FC_2, which is associated with eye movements about the vertical axes. The finding of long latency eye movements that differ from those predicted from studies conducted in anaesthetized animals is not surprising since the absence of anaesthesia permits activity to traverse more complicated polysynaptic pathways. Some of these pathways may not reflect the normal operation of the nervous system because of the artifice of electrical stimulation, while others may be normally used, but were not revealed in the anaesthetized animal. Only future studies will reveal which of the long latency responses reflect normal signal processing.

4.4.3 *Topographical organization of the flocculus.*

The anatomical organization of the floccular white matter into compartments separated by raphes, as revealed by AChE histochemistry, is directly related to the physiologically distinguishable classes of eye movements and probably to specific VOR pathways. The existence of a zonation of the rabbit flocculus has been proposed by Ito and colleagues (Dufossé et al.,1977; Ito et al., 1982b; Nagao et al., 1985) on the basis of the distribution of sites where microstimulation evoked either different patterns of eye movements or influenced specific VOR pathways. Throughout the years, however, the localization and the extent of these different areas has shown a considerable variability. In addition, the

proposed organization of the zonation was contrary to the basic principle of cerebellar zonation because the "rotatory" zone ran sharply across the "horizontal" and "vertical" zones (Ito et al., 1982b; Nagao et al., 1985).

The present anatomical findings show that the floccular white matter is subdivided into five compartments, the three largest of which can be related to particular canal-ocular pathways on the basis of the short latency evoked eye movements and the relation of the underlying eye muscles to particular canals. Since the largest eye movement evoked from stimulation in FC_2 is abduction of the ipsilateral eye, it can be concluded that this compartment is coupled to the horizontal canal pathway linking the horizontal canal with the horizontal recti muscles. Similarly, floccular compartments FC_1 and FC_3 are coupled to the ipsilateral anterior canal pathways since the short latency components of the evoked eye movements are largely the consequence of a combination of an increase in the activity of the ipsilateral inferior rectus and the contralateral superior oblique muscles and a decrease in the activity of the ipsilateral superior rectus and the contralateral inferior oblique muscles. The relations between the three largest floccular white matter compartments and the eye movements evoked at short latency are summarized in fig. 4.11 and 4.12.

4.4.4 *Comparison of eye movement and climbing fiber response axes.*

The present microstimulation experiments show that the short latency eye rotations occur about axes that closely correspond to the best response axes of the ipsilateral horizontal and anterior semicircular canals and to the rotation axes of the ipsilateral horizontal and vertical recti and the contralateral oblique muscles (Ezure and Graf, 1984a,b; Graf et al, 1988). Moreover, the spatial organization of these eye rotation axes is also similar to that of the preferred axes characterizing the optic flow signals reaching the flocculus through the CFs from the dorsal cap and ventrolateral outgrowth of the inferior olive (Simpson et al., 1981; Graf et al., 1988; Kusunoki et al., 1990; Kano et al., 1990). One class of CFs is most strongly modulated by rotational optic flow about the vertical axis

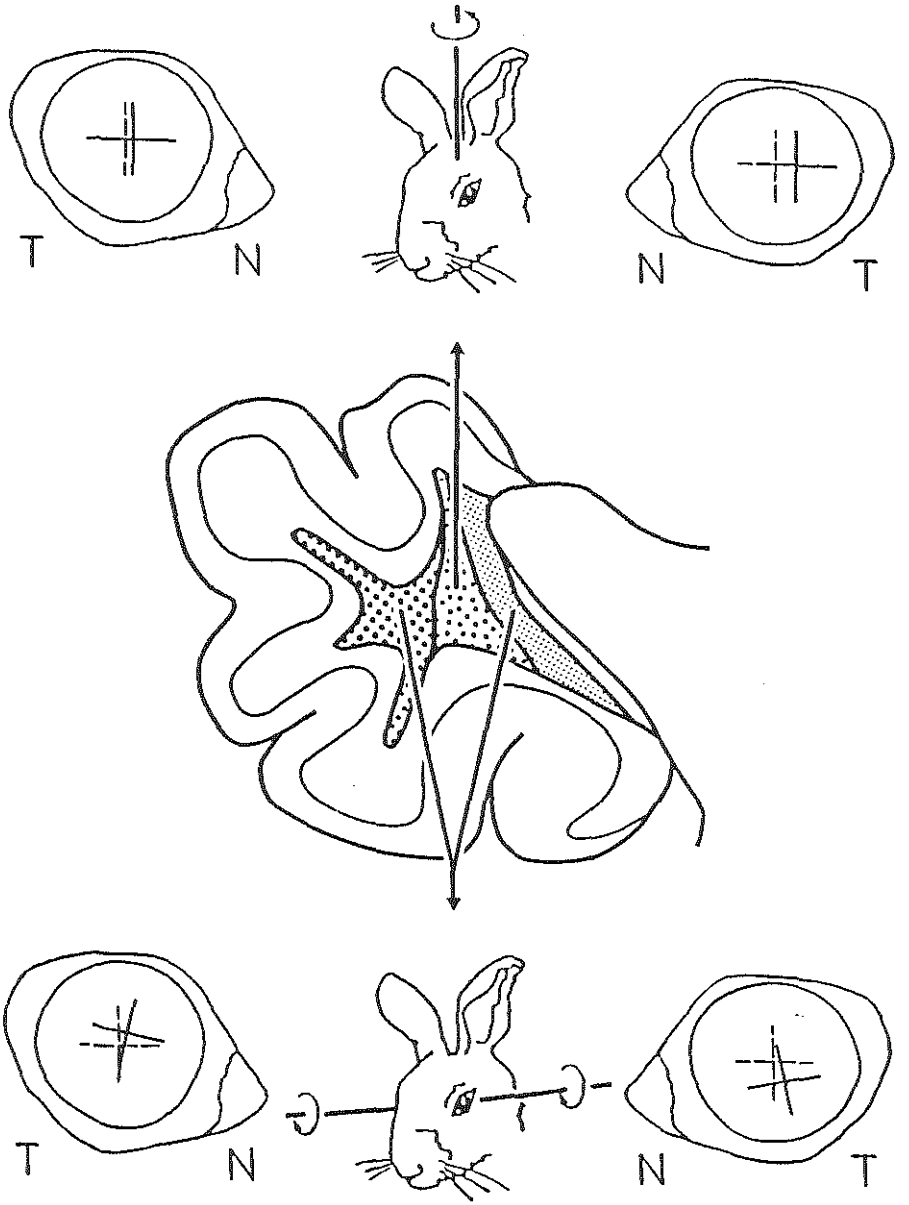
T
N
N
T
T
N
N
T

and is activated predominantly from the ipsilateral eye. The two other classes of CFs have their axis of best modulation close to the horizontal plane at an azimuthal angle of either about 135° to the ipsilateral (dominant) eye, or about 45° to the contralateral (dominant) eye. Consequently, the short latency abduction movement of the ipsilateral eye evoked by stimulation in FC_2 would result in a strong activation of the vertical axis class of CFs if the rabbit viewed a stationary world, whereas the short latency eye movements evoked by stimulation in FC_1 and FC_3 would result in a strong activation of the ipsilateral 135° axis and the contralateral 45° axis CF classes.

In this study no distinction was evident between FC_1 and FC_3 with regard to the evoked eye movement patterns. For both compartments electrical stimulation resulted in eye movements whose largest short latency component was a CCW rotation of the ipsilateral (left) eye about its 135° axis. Also, the range of amplitudes of the accompanying CW 45° axis component of the contralateral (right) eye was similar for the two compartments. Although the absence of differences between FC_1 and FC_3 indicates that they both receive input from both the ipsilateral 135° and the contralateral 45° classes of CFs, the possibility of a finer organizational structure in FC_1 and FC_3 exists because these two classes of CFs have their origin in different parts of the rostral dorsal cap and ventrolateral

fig. 4.11 Summary diagram of the topographical organization of the three largest compartments delineated by AChE staining and the classes of short latency eye movements evoked by electrical stimulation in the left flocculus. Stimulation of the middle compartment (compartment FC_2, medium dots) evoked abduction of the ipsilateral eye with a varying amount of adduction of the contralateral eye. Stimulation of the two compartments on either side of the middle compartment (FC_1, large dots, and FC_3, small dots) produced ipsilateral eye movements consisting of a combination of depression, intorsion and abduction, and contralateral eye movements consisting of a combination of elevation, intorsion and adduction. With stimulation of compartments FC_1 and FC_3 the movements of the ipsilateral eye are those produced by the vertical recti (inferior rectus contracting), whereas the movements of the contralateral eye are those produced by the oblique muscles (superior oblique contracting).

outgrowth of the inferior olive. In fact, Gerrits and Voogd (1982) have concluded that in the cat the rostral dorsal cap and the ventrolateral outgrowth project differentially within the homologous compartments of FC_1 and FC_3.

In contrast to the projections of the different climbing fiber classes, which match the anatomically delineated compartmental organization, the mossy fiber projections appear to be far less compartmentalized (Yamamoto, 1979a; Sato et al., 1983a,b). In addition, one would expect the mossy fiber input to be distributed across compartments by parallel fibers whose length is sufficient to traverse 3-4 compartments (Brand et al., 1976; Mugnaini, 1983). Therefore, it is surprising that the best-response axes for visually induced climbing fiber and simple spike modulation of floccular Purkinje cells are often found to be closely aligned (Graf et al., 1988; Kano et al., 1991). This observation reveals that despite the absence of an anatomical compartmentation, the mossy fiber input, as reflected in the simple spike activity of Purkinje cells, can be functionally compartmentalized.

The existence of only a small number of classes of both climbing fiber afferents and evoked eye rotations and their correspondence with the anatomically distinguishable compartments suggests that the compartments are the structural correlate of a coordinate system in which eye movements are represented. Any particular eye rotation can be synthesized from components taken in this coordinate system, but it remains to be determined how these components are computed from the diffusely organized mossy fiber inputs.

4.4.5 *Comparison with eye movements evoked by floccular stimulation in cat*

In the present study on the flocculus of the awake rabbit, the classes of short latency evoked eye movements and the distribution of the respective stimulation sites are in close agreement with the results obtained by Sato and Kawasaki (1990a,b;1991) with microstimulation in the flocculus of the anesthetized cat. In their study, division of the flocculus into three zones (rostral, middle and caudal) emerged from the

distribution of stimulation sites that elicited different classes of eye movements. In both species the zones or compartments form oblique strips running, when viewed from above, from caudomedial to rostrolateral. Electrical stimulation of the middle zone in the cat flocculus evoked abduction of the ipsilateral eye and adduction of the contralateral eye, as in the rabbit with stimulation of FC_2. Stimulation of the caudal and rostral zones of the cat flocculus produced a downward movement of both eyes in combination with an intorsion of the contralateral eye and a small extorsion of the ipsilateral eye. At first glance, these movements in the cat appear to differ from those produced by stimulation of FC_1 and FC_3 in the rabbit, but because of differences in the eye ball referenced kinematics of eye muscles in frontal- and lateral-eyed animals, they, in fact, result from the action of the same muscles (Simpson and Graf, 1981; Graf and Simpson, 1981). In both species the movement of the ipsilateral eye is due to the action of the vertical recti, with the inferior rectus contracting, whereas the movement of the contralateral eye is due to the action of the obliques, with the superior oblique contracting. These similarities between cat and rabbit suggest that in both lateral-eyed and frontal-eyed species the preferred axes of the visual CF input and the floccular Purkinje cell output are similarly organized in a coordinate system whose spatial orientation bears a close resemblance to that of the semicircular canals and the extra-ocular muscles.

As in the cat, electrical stimulation of the rabbit flocculus delineated three compartments on the basis of eye movement patterns. While the AChE staining in rabbit shows that two additional compartments are present, their relatively small size precluded localization of the stimulus to them. A similar limitation was likely present for stimulation of the cat flocculus because the anatomical study by Gerrits and Voogd (1982) of the cat flocculus showed CF projection zones that are comparable not only to the three compartments stimulated in the rabbit, but also to the two smaller compartments, C_2 and FC_4. On the basis of the source (caudal dorsal cap, see chapter 2) of the CF projection to FC4 in the rabbit and its corresponding zone in the cat (F1), it is likely that this zone is related to

horizontal eye movements. The C_2 compartment in rabbit (see chapter 2) and its corresponding zone in the cat (C_2) receive from the rostral part of the medial accessory olive. This part of the flocculus may not be directly related to eye movement control (Ito et al., 1982a,b). A recent anatomical study (Ruigrok et al., 1992) has shown that the compartmental pattern of the CF projection to the rat flocculus is like that of rabbit and cat, which increases the likelihood that the geometrical relation between floccular compartments, their CF inputs, and particular eye muscles described above is fundamental to compensatory eye movement control.

fig. 4.12 Summary diagram of the classes of eye movements elicited from the various zones (FZ) in the flocculus.

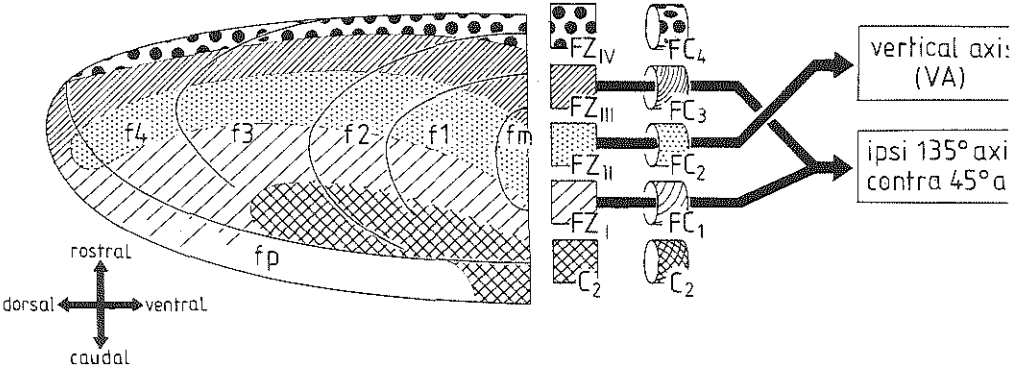

5. General conclusions

This study demonstrates a reproducible compartmentation in the white matter of the rabbit flocculus and nodulus with AChE histochemistry (chapters 1 and 2). Compact sheets of thin myelinated AChE-positive fibers, the so-called raphes, separate compartments of coarser fibers staining less intensely for AChE. In the flocculus the white matter was subdivided in 5 compartments, indicated as C_2, FC_1-FC_4 from laterally to medially. The nodulus consisted of 4 compartments, XC_1-XC_4. The organization of raphes and compartments was then used to study the interrelations of afferent climbing fibers and efferent Purkinje cell axons from different subsets of olivary neurons and Purkinje cells. In chapters 2 and 3 the results of combined anterograde and retrograde tracing experiments with HRP, WGA-HRP, tritiated leucine, and AChE histochemistry are reported. They indicate that Purkinje cell populations in the flocculus and nodulus are portioned into zones that receive their afferent climbing fiber input from certain subnuclei of the inferior olive and send efferent projections to specific vestibular and cerebellar neurons (see diagrams figs. 2.19 and 3.17). The C_2 zone projects to the posterior interposed nucleus and receives climbing fibers from the rostral pole of the medial accessory olive. The FZ_I and FZ_{III} zones project to the superior vestibular nucleus and receive their climbing fiber input from the rostral dorsal cap (rdc) and the ventrolateral outgrowth (vlo). The FZ_I and FZ_{III} zones alternate with another pair of zones. These zones FZ_{II} and FZ_{IV} project to the medial vestibular nucleus and receive climbing fibers from the caudal dorsal cap (cdc). Physiological experiments using microstimulation of the Purkinje cell axons contained in the compartments showed that two main classes of eye movements can be linked to two sets of the white matter compartments.

Thus two main functional modules can be distinguished in the flocculus, each with its own neuronal circuit. Each consists of two Purkinje cell zones. The VA module controls eye movements around a vertical axis by the lateral and medial rectus muscles. It consists of the

FZ_{II} and most likely also the FZ_{IV} zones and their projections to vestibulo-ocular relay cells of the horizontal semicircular canal in the medial vestibular nucleus. It receives climbing fibers from the caudal dorsal cap, which convey optokinetic information about movements of the surround around a vertical axis. The 135° axis module consists of the FZ_I and FZ_{III} zones and their projections to vestibulo-ocular relay cells of the anterior semicircular canal, located in the superior vestibular nucleus which controls movement of the eyes around a horizontal, 135° axis via the ipsilateral vertical recti muscles and the contralateral oblique muscles. It receives a climbing fiber projection from the rostral dorsal cap and the ventrolateral outgrowth. These climbing fibers carry optokinetic information about rotations of the surround around a 135° horizontal axis.

The functional significance of floccular zones C_2 and FZ_{IV} remains unclarified because the relatively small size of compartments C_2 and FC_4 made it difficult to restrict the stimulation to them.

6. Abbreviations

A	= zone A
ANS	= ansiform lobule
ANT	= anterior lobule
ß	= nucleus beta
bc	= brachium conjunctivum
bp	= brachium pontis
CI	= crus I
CII	= crus II
cc	= commissura cerebelli
cdc	= caudal dorsal cap
CGM	= medial geniculate body
CO	= cochlear nucleus
DAO	= dorsal accessory olive
DC,dc	= dorsal cap
dl	= dorsal lamella
DLP	= dorsolateral protuberance
dlp	= lateral A zone of Buisseret-Delmas (1988)
dmcc	= dorsomedial cell column
DTN	= dorsal terminal nucleus
DV	= descending vestibular nucleus
F	= fastigial nucleus
FC	= floccular compartment
FZ	= floccular zone
fil	= primary fissure
fipl	= posterolateral fissure
fm, m	= folium m of the flocculus
fp, p	= folium p ,, ,,
f1	= folium 1 ,, ,,
f2	= folium 2 ,, ,,
f3	= folium 3 ,, ,,
f4	= folium 4 ,, ,,
f5	= folium 5 ,, ,,
FLO	= flocculus
g	= genu of the facial nerve
IA	= anterior interposed nucleus
IP	= posterior interposed nucleus
ITN	= interstitial terminal nucleus
l	= lateral
l VII	= lobule VII
l IX	= lobule IX, uvula
l X	= lobule X, nodulus
L	= lateral cerebellar nucleus
lö	= Löwy's fiber bundle
Lpc	= parvicellular part of the lateral cerebellar nucleus
LTN	= lateral terminal nucleus
LV	= lateral vestibular nucleus
m	= folium m
MAO	= medial accessory olive
ML	= medial lemniscus

mlf = medial longitudinal fascicle
MTN = medial terminal nucleus
MV = medial vestibular nucleus
MVmc = magnocellular medial vestibular nucleus
no = nucleo-olivary tract
p = folium p
PAG = periaqueductal grey
PC = cerebral peduncle
pf = floccular peduncle
PFL = paraflocculus
PFLd = dorsal paraflocculus
PFLv = ventral paraflocculus
PH = nucleus prepositus hypoglossi
PMD = paramedian lobule
PO = principal olive
r = nucleus r,
rb = restiform body
rdc = rostral dorsal cap
RN = red nucleus
rIV = lateral recess of the fourth ventricle
sad = dorsal acoustic stria
SI = simplex lobule
SN = substantia nigra
SV = superior vestibular nucleus
t IV = taenia of fourth ventricle
vl = ventral lamella
vlo = ventrolateral outgrowth
VTRZ = visual tegmental relay zone
u = uncinate fascicle
XC = compartment of the nodulus
XZ = zone of the nodulus
y = group y
III = oculomotor nucleus
V = trigeminal complex
VI = abducens nucleus
VII = facial nerve
VIII = vestibulocochlear nerve

7. References

Akagi, Y. (1978) The localization of the motor neurons innervating the extraocular muscles in the oculomotor nuclei of the cat and rabbits, using horseradish peroxidase.
J. Comp. Neurol. 181:745-762

Akaike, T. (1986a) Electrophysiological analysis of the tecto-olivo-cerebellar (crus II) projection in the rat.
Brain Res. 378:186-190

Akaike, T. (1986b) Differential localization of inferior olivary neurons projecting to the tecto-olivo-recipient zones of lobule VII or crus II in the rat cerebellum.
Brain Res. 386:400-404

Akaike, T. (1987) Electrophysiological analysis of the tecto-olivo-cerebellar (lobulus simplex) projection in the rat.
Brain Res., 417:371-376

Akaike, T. (1992) The tectorecipient zone in the inferior olivary nucleus in the rat.
J. Comp. Neurol. 320:398-414

Alley, K.A. (1977) Anatomical basis for interaction between cerebellar flocculus and brainstem. In R. Baker and A. Berthoz (eds): Control of Gaze by Brain Stem Neurons. Amsterdam: Elsevier, pp.109-117

Alley, K.A., R. Baker, and J.I. Simpson (1975) Afferents to the vestibulo-cerebellum and the origin of the visual climbing fibers in the rabbit.
Brain Res. 98:582-589

Altman, J., and G.D. Das (1970) Postnatal changes in the concentration and distribution of cholinesterase in the cerebellar cortex of rats.
Exp. Neurol. 28:11-34

Andersson, G., and O. Oscarsson (1978a) Projections to lateral vestibular nucleus from cerebellar climbing fiber zones.
Exp. Brain Res. 32:549-564

Andersson, G., and O. Oscarsson (1978b) Climbing fiber microzones in the cerebellar vermis and their projection to different groups of cells in the lateral vestibular nucleus.
Exp. Brain Res. 565-579

Angaut, P., and A. Brodal (1967) The projection of the "vestibulocerebellum" onto the vestibular nuclei in the cat.
Arch. Ital. Biol. 105:441-479

Appleyard, M., and H. Jahnson (1992) Actions of acetylcholinesterase in the guinea pig cerebellar cortex in vitro.
Neuroscience, 47:291-301

Apps, R. (1990) Columnar organization of the inferior olive projection to the posterior lobe of the rat cerebellum.
J. Comp. Neurol. 302:236-254

Baker, R., Precht, W., and R. Llinas (1972) Cerebellar modulatory action on the vestibulotrochlear pathway in the cat.
Exp. Brain Res. 15:364-385

Baker, R., and R.F. Spencer (1981) Synthesis of horizontal conjugate eye movement signals in the abducens nucleus.

Jap. J. EEG. EMG 31:49-59
Baker, R., N. Mano, and H. Shimazu (1969) Postsynaptic potentials in abducens motoneurons induced by vestibular stimulation.
Brain Res. 15:577-580
Balaban, C.D. (1984) Olivo-vestibular and cerebello-vestibular connections in albino rabbits.
Neuroscience 12, 129-149
Balaban, C.D., and R.T. Henry (1988) Zonal organization of olivo-nodulus projections in albino rabbits.
Neurosci. Res. 5:409-425
Balaban, C.D., and E. Watanabe (1984) Functional representation of eye movements in the flocculus of monkeys (Macaca fuscata).
Neurosci. Lett. 49:199-205
Balaban, C.D., M. Ito, and E. Watanabe (1981) Demonstration of zonal projections from the cerebellar flocculus to vestibular nuclei in monkeys (Macaca fuscata).
Neurosci. Lett 27:101-105
Barmack, N.H., R.W. Baughman, and F.P. Eckenstein (1992a) Cholinergic innervation of the cerebellum of rat, cat, and monkey as revealed by choline acetyltransferase activity and immunohistochemistry.
J. Comp. Neurol. 317:233-249
Barmack, N.H., R.W. Baughman, F.P. Eckenstein, and H. Sjojaku (1992b) Secondary vestibular cholinergic projection to the cerebellum of rabbit and rat as revealed by choline acetyltransferase immunohistochemistry.
J. Comp. Neurol. 317:250-270
Barmack, N.H., M. Fagerson, and P. Errico (1993) Cholinergic projection to the dorsal cap of the inferior olive of the rat, rabbit, and monkey.
J. Comp. Neurol. 328:263-281
Barth, F., and M.S. Ghandour (1983) Cellular localization of butyrylcholinesterase in adult rat cerebellum determined by immunofluorescence.
Neurosci. Lett. 39:149-153
Belknap, D.B., and H. Noda (1987) Eye movements evoked by microstimulation in the flocculus of the alert macaque.
Exp. Brain Res. 67:352-362
Bernard, J.F. (1987) Topographical localization of olivocerebellar and corticonuclear connections in the rat - a WGA-HRP study.
I. Lobules IX, X, and the flocculus.
J. Comp. Neurol. 263:241-258
Bigaré, F. (1980). De efferente verbindingen van de cerebellaire schors van de kat. Thesis
Blanks, R.H.I. (1990) Afferents to the cerebellar flocculus in cat with special reference to pathways conveying vestibular, visual (optokinetic) and oculomotor signals.
J. Neurocytol. 19:628-642
Blanks, R.H.I., W. Precht, and Y Torigoe (1983) Afferent projections to the cerebellar flocculus in the pigmented rat demonstrated by retrograde transport of horseradish peroxidase.
Exp. Brain Res. 52:293-306

Boegman, R.J., A. Parent, and R. Hawkes (1988) Zonation in the rat cerebellar cortex: patches of high acetylcholinesterase activity in the granular layer are congruent with Purkinje cell compartments.
Brain Res. 448:237-251

Bolk, L. (1906). Das Cerebellum der Säugetiere: Eine vergleichende anatomische Untersuchung. Jena/Haarlem, Fischer.

Brand, S. A..-L. Dahl, and E. Mugnaini (1976) The length of parallel fibers in the cat cerebellar cortex. An experimental light and electron microscopic study.
Exp. Brain Res. 26, 39-58.

Brodal, A. (1940) The cerebellum of the rabbit. A topographical atlas of the folia as revealed in transverse sections.
J. Comp. Neurol. 72:63-81

Brodal, A. (1976) The olivocerebellar projection in the cat as studied with the method of retrograde axonal transport of horseradish peroxidase. II. The projection to the uvula.
J. Comp. Neurol. 166:417-426

Brodal, P., and A. Brodal (1981) The olivocerebellar projection in the monkey. Experimental studies with the method of retrograde tracing of horseradish peroxidase.
J. Comp. Neurol. 201:375-393

Brodal, P., and A. Brodal (1982) Further observations on the olivocerebellar projections in the monkey.
Exp. Brain Res. 45:71-83

Brodal, A., and K. Kawamura (1980) Olivocerebellar projection: a review.
Adv. Anat. Embryol. Cell Biol. 64:1-137

Brodal, A., and O. Pompeiano (1957) The vestibular nuclei in the cat.
J. Anat. 91:438-454

Brown, W.J., and S.L. Palay (1972) Acetylcholinesterase activity in certain glomeruli and Golgi cells of the granular layer of the rat cerebellar cortex.
Z. Anat. Entwickl.-Gesch. 137:317-334

Buisseret-Delmas, C. (1988) Sagittal organization of the olivocerebello-nuclear pathway in the rat. I. Connections with the nucleus fastigii and the nucleus vestibularis.
Neurosci. Res. 5:475:493

Cajal, S. Ramon y (1911) Histologie du système nerveux de l'homme et de vertebres. Vol. II. Paris: Maloine, p. 24

Carleton, S.C., and M.B. Carpenter (1984) Distribution of primary vestibular fibers in the brain stem and cerebellum of the monkey.
Brain Res. 294:381-298

Carpenter, M.B., and R.J. Cowie (1985) Connections and oculomotor projections of the superior vestibular nucleus and cell group 'y'.
Brain Res. 336:265-287

Chambers, W.W., and J.M. Sprague (1955a) Functional localization in the cerebellum. I. Organization in longitudinal cortico-nuclear zones and their contribution to the control of posture, both extrapyramidal and pyramidal.
J. Comp. Neurol. 103: 105-130

Chambers, W.W., and J.M. Sprague (1955b) Functional localization in the cerebellum. II. Somatotopic organization in cortex and nuclei.

Arch. Neurol. Psychiat. 74:653-680
Chan-Palay, V., G. Nilaver, S.L. Palay, M.C. Beinfeld, E.A. Zimmerman, J.Y. Wu, and T.L. O'Donohue (1981) Chemical heterogeneity in cerebellar Purkinje cells: Existence and coexistence of glutamic acid decarboxylase-like and motilin-like immunoreactivities.
Proc.Natl.Acad.Sci.USA 78:7787-7791
Chan-Palay, V., S.L. Palay, and J.Y. Wu (1982) Sagittal cerebellar microbands of taurine neurons: Immunocytochemical demonstration by using antibodies against the taurine synthetizing enzyme cysteine sulfinic acid decarboxylase.
Proc.Natl.Acad.Sci.USA 79:4221-4225
Chubb, M.C., and A.F. Fuchs (1982) Contribution of y group of vestibular nuclei and dentate nucleus of cerebellum to generation of vertical smooth eye movements.
J. Neurophysiol. 48:75-99
Chubb, M.C., A.F. Fuchs, and C.A. Scudder (1984) Neuron activity in monkey vestibular nuclei during vertical vertical vestibular and eye movements.
J. Neurophysiol. 52:724-742
Collewijn, H (1977) Eye and head movements in freely moving rabbits.
J. Physiol 266:471-498
Courville, J., F. Faraco-Cantin, and N. Diakiw (1974) A functionally important feature of distribution of the olivocerebllar climbing fibers.
Can. J. Physiol. Pharmacol. 52:1212-1217
Csillik, B., F. Joo and P. Kasa (1963) Cholinesterase activity of archicerebellar mossy fiber apparatus.
J. Histochem. Cytochem. 11, 103-113.
DeLacalle, S., L.B. Hersch, and C.B. Saper (1993) Cholinergic innervation of the human cerebellum.
J. Comp. Neurol. 328:364-376
De Zeeuw, C.I., P.L. DiGiorgi, D.R. Wylie, D. Wang, E. Marsh, and J.I. Simpson (1992) Projections of individual Purkinje cells of identified zones in the rabbit flocculus to the vestibular and cerebellar nuclei.
Soc. Neurosci. Abstr. 18:854
De Zeeuw, C.I., P. Wentzel, and E. Mugnaini (1993) Fine structure of the dorsal cap of the inferior olive and its GABAergic and non-GABAergic input from the nucleus prepositus hypoglossi in rat and rabbit.
J. Comp. Neurol. 327:63-82
Dow, R.S. (1936) The fiber connections of the posterior parts of the cerebellum in the cat and rat.
J. Comp. Neurol. 63:527-548
Dow, R.S. (1938a) Efferent connections of the flocculonodular lobe in Macaca mulatta.
J. Comp. Neurol. 68:297-305
Dow, R.S (1938b) Effects of lesions in the vestibular part of the cerebellum in primates.
Arch. Neurol. Psychiat. 40:500-520
Dow, R.S. (1939) Cerebellar action potentials in response to stimulation of various afferent connections.

J. Neurophysiol. 2:543-555
Dufossé, M., M. Ito, and Y. Miyashita (1977) Functional localization in the rabbit's cerebellar flocculus determined in relationship with eye movements.
Neurosci. Lett. 5:273-277
Eisenman, L.M. (1984) Organization of the olivocerebellar projection to the uvula in the rat.
Brain Behav. Evol. 24:1-12
Epema, A.H. (1990) Connections of the vestibular nuclei in the rabbit.
Thesis, Rotterdam
Epema, A.H., N.M. Gerrits, and J. Voogd (1988) Commissural and intrinsic connections of the vestibular nuclei in the rabbit: a retrograde tracer study.
Exp. Brain Res. 71:129-146
Epema, A.H., N.M. Gerrits, and J. Voogd (1990) Secondary vestibulocerebellar mossy fiber projections to the flocculus and uvulonodular lobule in the rabbit: a study using HRP and double fluorescent tracer techniques.
Exp. Brain Res. 80:72-82
Friede, R.L., and L.M. Fleming (1964) A comparison of cholinesterase distribution in the cerebellum of several species.
J. Neurochem. 11:1-7
Fukuda, J., S.M. Highstein, and M. Ito (1972) Cerebellar inhibitory control of the vestibulo-ocular reflex investigated in rabbit IIIrd nucleus.
Exp. Brain Res. 14:511-526
Furber, S.E., and C.R.R. Watson (1983) Organization of the olivocerebellar projection in the rat.
Brain Behav. Evol. 22:132-152
Gacek, R.R. (1977) Location of brain stem neurons projecting to the oculomotor nucleus in the cat.
Exp. Neurol. 57:725-749
Gacek, R.R. (1979) Location of abducens afferent neurons in the cat.
Exp. Neurol. 64:342-353
Geneser-Jensen, F.A., and T.W. Blackstad (1971) Distribution of acetylcholinesterase in the hippocampal region of the guinea-pig.
I. Entorhinal area, parasubiculum and presubiculum.
Z. Zellforsch. Mikrosk. Anat. 114:460-481
Gerebtzoff, M.A. (1959) Cholinesterases: A histochemical contribution to the solution of some functional problems.
Internat. Series of Monographs on Pure and Applied Biology, Vol.3.
Oxford: Pergamom Press.
Gerrits, N.M., and J. Voogd (1982) The climbing fiber projection to the flocculus and adjacent paraflocculus in th cat.
Neuroscience 7: 2971-2991
Gerrits, N.M., and J. Voogd (1986) The nucleus reticularis tegmenti pontis and the adjacent paramedian pontine reticular formation: differential projections to the cerebellum and the caudal brainstem.
Exp. Brain Res. 62:29-45
Gerrits, N.M., and J. Voogd (1989) The topographical of climbing and mossy fiber afferents in the flocculus and the ventral paraflocculus

in rabbit, cat and monkey. In: P. Strata (ed): The Olivocerebellar System in Motor Control.
Exp. Brain Res. Series Vol. 17. Amsterdam: Elsevier, pp. 26-29

Gerrits, N.M., A.H. Epema, A. van Linge, and E. Dalm (1989) The primary vestibulocerebellar projection in the rabbit: absence of primary afferents in the flocculus.
Neurosci. Lett. 290:262-277

Gerrits, N.M., J. Voogd, and I.N. Magras (1985) Vestibular afferents of the inferior olive and the vestibulo-cerebellar climbing fiber pathway to the flocculus in the cat.
Brain Res. 332:325-336

Gibson, A.R., D.I. Hansma, J.C. Houk, and F.R. Robinson (1984) A sensitive low artifact TMB procedure for the demonstration of WGA-HRP in the CNS.
Brain Res. 298:235-241

Giolli, R.A., R.H.I. Blanks, and Y. Torigoe (1984) Pretectal and brain stem projections of the medial terminal nucleus of the accessory optic system of the rabbit and rat as studied by anterograde and retrograde neuronal tracing methods.
J. Comp. Neurol. 227:228-251

Giolli, R.A., R.H.I. Blanks, Y. Torigoe, and D.D. Williams (1985) Projections of medial accessory optic nucleus, ventral tegmental nuclei, and substantia nigra of rabbit and rat as studied by retrograde axonal transport of horseradish peroxidase.
J. Comp. Neurol. 232:99-116

Giolli, R.A., Y. Torigoe, R.H.I. Blanks, and H.M. McDonald (1988) Projections of the dorsal and lateral terminal accessory optic nuclei and of the interstial nucleus of the superior fascicle (posterior fibers) in the rabbit and rat.
J. Comp. Neurol. 277:608-620

Goodman, D.C., R.E. Hallett, and R.B. Welch (1963) Patterns of localization in the cerebellar cortico-nuclear projection of the albino rat.
J. Comp. Neurol. 121:51-67

Gorenstein, C., N.C. Bundman, J.L. Bruce, and A. Rotter (1987) Neuronal localization of pseudocholinesterase in the rat cerebellum: saggital bands of Purkinje cells in the nodulus and uvula.
Brain Res. 418:68-75

Graf, W., and J.I. Simpson (1981) The relations between the semicircular canals, optic axis, and the extraocular muscles in lateral-eyed and frontal-eyed animals. In A. Fuchs and W. Becker (eds): Progress in Oculomotor Research. Amsterdam: Elsevier, pp. 411-420

Graf, W., J.I. Simpson, and C.S. Leonard (1988) Spatial organization of visual messages of the rabbit's cerebellar flocculus.
II. Complex and simple spike responses of Purkinje cells.
J. Neurophysiol. 60:2091-2121

Graham, R.C., and M.J. Karnovsky (1966) The early stages of absorption of injected horseradish peroxidase in the proximal tubules of the mouse kidney. Ultrastructural cytochemistry by anew technique.
J. Histochem. Cytochem.14:291-302

Graybiel, A.M., and E.A. Hartwieg (1974) Some afferent connections of the oculomotor complex in the cat: an experimental study with tracer techniques.
Brain Res. 81:543-551

Greenfield, S.A (1984) Acetylcholinesterase may have novel functions in the brain.
Trends in Neurosci. 7:364-368

Groenewegen, H.J., and J. Voogd (1977) The parasagittal zonation within the olivocerebellar projection.
I. Climbing fiber distribution in the vermis of the cat cerebellum.
J. Comp. Neurol. 174:417-488

Groenewegen, H.J., J. Voogd, and S.L. Freedman (1979) The parasagittal zonation within the olivocerebellar projection.
II.Climbing fiber distribution in the intermediate and hemispheric parts of the cat cerebellum.
J. Comp. Neurol. 183: 551-602

Gulya, K., and P. Kása (1983) Structural localization of the elements of the acetylcholine system in the rat cerebellum.
Acta Biol. Hung. 34:155-161

Häggqvist, G. (1936) Analyse der Faserverteilung in einem Rückenmarkquerschnitt (Th. 3).
Z. mikr. anat. Forschung 29:1-34

Haines, D.E. (1977) Cerebellar corticonuclear and corticovestibular fibers of the flocculonodular lobe in a prosimian primate (Galago senegalensis).
J. Comp. Neurol. 174:607-630

Hawkes, R., and N. Leclerc (1987) Antigenic map of the rat cerebellum: distribution of parasagittal bands as revealed by monoclonal anti-Purkinje cell antibody mabQ 113.
J. Comp. Neurol. 256:29-41

Hess, D.T., and J. Voogd (1986) Chemoarchitectonic zonation of the monkey cerebellum.
Brain Res. 369:383-387

Highstein, S.M. (1971) Organization of the inhibitory and excitatory vestibulo-ocular reflex pathways to the third and fourth nuclei in rabbit.
Brain Res. 32:218-224

Highstein, S.M. (1973) The organization of the vestibulo-ocular and trochlear reflex pathways in the rabbit.
Exp. Brain Res. 17:285-300

Highstein, S.M., and H. Reisine (1979) Synaptic and funtional organization of vestibulo-ocular reflex pathways.
Prog. Brain Res. 50:431-442

Hoddevik, G.H. and A. Brodal (1977) The olivo-cerebellar projections studied with the method of retrograde axonal transport of horseradish peroxidase. V. The projection to the flocculo-nodular lobe and the paraflocculus in the rabbit.
J. Comp. Neurol. 176: 269-280

Holstege, G., and H. Collewijn (1982) The efferent connections of the nucleus of the optic tract and the superior colliculus in the rabbit.
J. Comp. Neurol. 209:139-175

Hunt, S., and J. Schmidt (1978) Some observations on the binding pattern of α-bungarotoxin in the central nervous system of the rat. Brain Res. 157:213-232

Ikeda, M., T. Houtani, T. Ueyama, and T. Sugimoto (1991) Choline acetyltransferase immunoreactivity in the cat cerebellum. Neuroscience, 45:671-690

Illing, R.-B. (1990) A subtype of cerebellar Golgi cells may be cholinergic. Brain Res. 522:267-274

Ingram, V.M., M.P. Ogren, C.L. Chatot, J.M. Gossels, and B.B. Owens (1985) Diversity among Purkinje cells in the monkey cerebellum. Proc. Natl. Acad. Sci. USA 82:7131-7135

Ito, M. (1972) Neural design of the cerebellar motor control system. Brain Res. 40:81-84

Ito, M. (1982) Cerebellar control of the vestibulo-ocular reflex-around the flocculus hypothesis. Ann. Rev. Neurosci. 5:275-296

Ito, M. (1984) The cerebellum and neuronal control. Raven, New York.

Ito, M. (1990) A new physiological concept on cerebellum. Rev. Neurol. 146:564-569

Ito, M., S.M. Highstein, and J. Fukuda (1970) Cerebellar inhibition of the vestibulo-ocular reflex in rabbit and cat andits blockage by picrotoxin. Brain Res. 17:524-526

Ito, M., P.J. Jastreboff, and Y. Miyashita (1982a) Specific effects of unilateral lesions in the flocculus upon eye movements in albino rabbits. Exp. Brain Res. 45:233-242

Ito, M., Y. Miyashita, and A. Ueki (1978) Functional localization in the rabbit's inferior olive determined in connection with the vestibulo-ocular reflex. Neurosci. Lett. 8:283-287

Ito, M., N. Nisimaru, and M. Yamamoto (1973) Specific neural connections for the cerebellar control of vestibulo-ocularreflexes. Brain Res. 60:238-243

Ito, M., N. Nisimaru, and M. Yamamoto (1977) Specific patterns of neuronal connections involved in the control of the rabbit's vestibulo-ocular reflexes by the cerebellar flocculus. J. Phys. (Lond.) 265:833-854

Ito, M., I. Orlov, and M. Yamamoto (1982b) Topographical representation of vestibulo-ocular reflexes in rabbit cerebellar flocculus. Neurosci. 7: 1644-1657

Jansen, J., and A. Brodal (1940) Experimental studies on the intrinsic fibers of the cerebellum. II. The cortico-nuclear projection. J. Comp. Neurol. 73:267-321

Jansen, J. and Brodal, A. (1942) Experimental studies on the intrinsic fibers of the cerebellum. III. Cortico-nuclear projection in the rabbit and the monkey. Norske Vid. Akad. Avh.I. Math. Nat.Kl. No.3: 1-30.

Kan, K.S.K., L.P. Chao, and L.S. Forno (1978) Immunohistochemical localization of choline acetyltransferase in rabbit spinal cord and

cerebellium.
Brain Res. 146:221-229
Kan, K.S.K., L.P. Chao, and L.S. Forno (1980) Immunohistochemical localization of choline acetyltransferase in the humancerebellum.
Brain Res. 193:165-171
Karczmar, A.G. (1969) Is the central cholinergic nervous system overexploited ?
Fedn. Proc. Fedn. Am. Socs. Exp. Biol. 28:147-157
Kanda, K-I., Y. Sato, K. Ikarashi, and T. Kawasaki (1989) Zonal organization of climbing fiber projections to the uvula in the cat.
J. Comp. Neurol. 279:138-148
Kano, M-S., M. Kano, and K. Maekawa (1990) Receptive field organization of climbing fiber afferents responding to optokinetic stimulation in the cerebellar nodulus and flocculus of the pigmented rabbit.
Exp. Brain Res. 82:499-512
Katayama, S., and W. Nisimaru (1988) Parasagittal zonal pattern of olivo-nodular projections in rabbit cerebellum.
Neurosci. Res. 5:424-438
Kaufman, G.D., J.H. Anderson and A. Beitz (1991) Activation of a specific vestibulo-olivary pathway by centripetal acceleration in rat.
Brain Res. 562: 311-317.
Kawaguchi, Y (1985) Two groups of secondary vestibular neurons mediating horizontal canal signals, probably to the ipsilateral medial rectus muscle, under inhibitory influences from the cerebellar flocculus in rabbits.
Neurosci. Res. 2:434-446
Kawamura, K., and T. Hashikawa (1979) Olivocerebellar projections in the cat studied by means of anterograde axonal transport of labeled amino acids as tracers.
Neurosci. 4:1615-1633
Kevetter, G.H., and A.A. Perachio (1984) Central projections of vestibular afferents innervating the macula of the saccule ingerbil.
Neurosci. Lett. 51:7-12
Kimura, H., P.L. McGeer, J.H. Peng, and E. McGeer (1981) The central cholinergic system studied by choline acetyltransferase immuno-histochemistry in the cat.
J. Comp. Neurol. 200:151-201
Komei, I., T. Hajai, P.L. McGeer, and E.G. McGeer (1983) Evidence for an intracerbellar acetylcholinesterase-rich but probably non-cholinergic flocculonodular projection in the rat.
Brain Res. 258:115-119
Korneliussen, H.K. (1968) On the ontogenic development of the cerebellum (nuclei, fissures, and cortex) of the rat, with special reference to regional variations in corticogenesis.
J. Hirnforsch. 10:379-412
Kooy, F.H. (1916) The inferior olive in vertebrates.
Thesis.Haarlem: Bohn.
Kuhar, M.J., and H.I. Yamamura (1975) Light autoradiographic localization of cholinergic muscarinic receptors in rat brain by specific binding of a potent antagonist.
Nature 253:560-561

Kusunoki, M., M. Kano, M.-S. Kano, and K. Maekawa (1990) Nature of optokinetic response and zonal organization of climbing fiber afferents in the vestibulocerebellum of the pigmented rabbit.
I. The flocculus.
Exp. Brain Res. 80:225-237

Labandeira-Garcia, J.L., M.J. Guerra-Seijas, J.A. Labandeira-Garcia, and F.J. Jorge-Barreira (1991) Distribution of the vestibular neurons projecting to the oculomotor and trochlear nuclei in rabbits.
Brain Behav. Evol. 37:111-124

Langer, T. (1985) Basal interstitial nucleus of the cerebellum: cerebellar nucleus related to the flocculus.
J. Comp. Neurol. 235:38-47

Langer, T., A.F. Fuchs, C.A. Scudder, and M.C. Chubb (1985a) Afferents to the flocculus of the cerebellum in the Rhesus Macaque as revealed by retrograde transport of horseradish peroxidase.
J. Comp. Neurol. 235:1-25

Langer, T., A.F. Fuchs, M.C. Chubb, C.A. Scudder, and S.G.Lisberger (1985b) Floccular efferents in the Rhesus Macaque as revealed by autoradiography and horseradish peroxidase.
J. Comp. Neurol. 235:26-37

Larsell, O. (1934) Morphogenesis and evolution of the cerebellum. Arch. Neurol. Psychiat. (Chic.), 31: 373-395.

Larsell, O (1937) The cerebellum, a review and interpretation.
Arch. Neurol. Psychiatr. 38:580-607

Larsell, O (1952) The morphogenesis and adult pattern of the lobules and fissures of the cerebellum of the white rat.
J. Comp. Neurol. 97:281-356

Larsell, O. (1970) The Comparative Anatomy and Histology of the Cerebellum from Monotremes through Apes. J. Jansen (ed.). Minneapolis, University of Minnesota Press.

Larsell, O., and J. Jansen (1972) The comparative anatomy and histology of the cerebellum. In: The Human Cerebellum, Cerebellar Connections, and The Cerebellar Cortex. Minneapolis, University of Minnesota Press.

Lechan, R.M., J.L. Nestler, and S. Jacobson (1981) Immunohistochemical localization of retrogradely andanterogradely transported wheat germ agglutinin within the central nervous system of the rat: application to immunostaining of a second antigen within the same neuron.
J. Histochem. Cytochem. 29:1255-1262

Légendre, A. and J. Courville (1987) Original trajectory of the cerebello-olivary projection: an experimental study with radioactive and fluorescent tracers in the cat.
Neurosci. 21:877-891

Leonard, C.S., J.I. Simpson, and W. Graf (1988) Spatial organization of visual messages of the rabbit's cerebellar flocculus.
I. Typology of inferior olive neurons of the dorsal cap of Kooy.
J. Neurophysiol. 60:2073-2090

Lorente de No, R. (1933) Anatomy of the eight nerve.
The Laryngoscope, XLIII:1-38

Löwy, R. (1928) Über die Faseranatomie und Physiologie der Formatio vermicularis cerebelli.
Arb. Neurol. Inst. Univ. Wien. 21:359-382
Maekawa, K., and J.I. Simpson (1972) Climbing fiber activation of Purkinje cells in the flocculus by impulses transferred through the visual pathway.
Brain Res. 39:245-251
Maekawa, K., and J.I. Simpson (1973) Climbing fiber responses evoked in the vestibulocerebellum of rabbit from the visual system.
J. Neurophysiol. 36:649-666
Maekawa, K. and T. Takeda (1976) Electrophysiological identification of climbing and mossy fiber pathways from the rabbit's retina to the contralateral cerebellar flocculus.
Brain Res. 109:169-174
Maekawa, K. and T. Takeda (1977) Afferent pathways from the visual system to the cerebellar flocculus in the rabbit. In R.Baker and A. Berthoz (eds): Control by Gaze of Brain Stem Neurons. Amsterdam: Elsevier, pp. 187-195
Maekawa, K., and T. Takeda (1979) Origin of descending afferents to the rostral part of the dorsal cap of inferior olive which transfers contralateral optic activities to the flocculus. A horseradish peroxidase study.
Brain Res. 172:393-405
Maekawa, K., T. Takeda, M. Kano, and M. Kusunoki (1989) Collateralized climbing fiber projection to the flocculus and the nodulus of the rabbit.
Exp. Brain Res. Ser. 17:30-45
Magras, I.N., and J. Voogd (1985) Distribution of secondary vestibular fibers in the cerebellar cortex. An autoradiographic study in the cat.
Acta Anat. (Basel) 123:51-57
Mallol, J., M.C. Sarraga, M. Bartolome, M.S. Chandour, and G. Gombos (1984) Muscarinic receptor during postnatal development of rat cerebellum: an index of cholinergic synapse formation ?
J. Neurochem. 42:1641-1649
Marani, E. (1982) Topographic Enzyme Histochemistry of the Mammalian Cerebellum 5'-nucleotidase and Acetylcholinesterase.
Thesis, Leiden.
Marani, E. (1986) Topographic histochemistry of the cerebellum.
Prog. Histochem. Cytochem. Vol. 16
Marani, E., and J. Voogd (1977a) An acetylcholinesterase bandpattern in the molecular layer of the cat cerebellum.
J. Anat. 124:335-345
Marani, E., and J. Voogd (1977b) A longitudinal pattern of acetylcholinesterase in the molecular layer of the cerebellum of the cat.
Acta Morphol. Neerl. Scand. 15:332-333
Martin, G.F., J. Culberson, C. Laxson, M. Linauts, M. Panneton, and I. Tschismadia (1980) Afferent connections of the inferior olivary nucleus with preliminary notes on its development: Studies using the North American opossum. In J. Courville, C.C. de Montigny, and Y. Lamarre (eds): The Inferior Olivary Nucleus: Anatomy and

Physiology. New York: Raven Press, pp. 35-72
Mash, D.C., and L.T. Potter (1986) Autoradiographic localization of M1 and M2 muscarine receptors in the rat brain.
Neurosci. 19:551-564
McCrea, R.A., and R. Baker (1985) Anatomical connections of the nucleus prepositus hypoglossi of the cat.
J. Comp. Neurol. 237:377-407
Mesulam, M.M. (1978) Tetramethylbenzidine for horseradish peroxidase neurohistochemistry: a non-carcinogenic blue reaction-product with superior sensitivity for visualizing neural afferents and efferents.
J. Histochem. Cytochem. 26:106-117
Mizuno, N., K. Mochizuki, C. Akimoto, and R. Matsushima (1973) Pretectal projection to the inferior olive in the rabbit.
Exp. Neurol. 39:498-506
Mizuno, N., Y. Nakamura, and N. Iwahori (1974) An electronmicroscopic study of the dorsal cap of the inferior olive in the rabbit, with special reference to the pretecto-olivary fibers.
Brain Res. 77:385-395
Mugnaini, E. (1983) The length of cerebellar fibers in chicken and rhesus monkey.
J. Comp. Neurol. 220, 7-15
Nagao, S. (1983) Effects of vestibulocerebellar lesions upon dynamic characteristics and adaptation of vestibulo-ocular and optokinetic responses in pigmented rabbits.
Exp. Brain Res. 53:36-46
Nagao, S. (1988) Behavior of floccular Purkinje cells correlated with adaptation of horizonatal optokinetic eye movement response in pigmented rabbits.
Exp. Brain Res. 73:489-497
Nagao, S., M. Ito, and L. Karachot (1985) Eye field in the cerebellar flocculus of pigmented rabbits determined with local electrical stimulation.
Neurosci. Res. 3:39-51
Naito, H., K. Tanimura, N. Taga, and Y. Hosoya (1974) Microelectrode study on the subnuclei of the oculomotor nucleus in the cat.
Brain Res. 81:215-231
Nelson, B.J., N.H. Barmack, and E. Mugnaini (1986) GABAergic projection from vestibular nuclei to rat inferior olive.
Soc. Neurosci. Abstr. 71:15
Nelson, B.J. and E. Mugnaini (1989) Origins of GABAergic inputs to the inferior olive. In: P. Strata (ed): The Olivocerebellar System in Motor Control.
Exp. Brain Res. Series Vol. 17. Amsterdam: Elsevier, pp. 86-107.
Neustadt, A., A. Frostholm, and A. Rotter (1988) Topographical distribution of muscarinic cholinergic receptors in the cerebellar cortex of the mouse, rat, guinea pig, and rabbit: a species comparison.
J. Comp. Neurol. 272:317-330
Nilaver, G., R. Defendini, K.A. Zimmerman, M.C. Beinfeld, and T.L. O'Donohue (1982) Motilin in the Purkinje cell of the cerebellum.

Nature 295:597-598
Ojima, H., S.I. Kawajiri, and T. Yamasaki (1989) Cholinergic innervation of the rat cerebellum: Qualitative and quantitative analyses of elements immunoreactive to a monoclonal antibody against choline acetyltransferase.
J. Comp. Neurol. 290:41-52
Ono, M., and H. Kato (1938) Zur Kenntnis des Kleinhirnkerne des Kaninchens.
Anat. Anz. 86:245-259
Oscarsson, O (1969) The sagittal organization of the cerebellar anterior lobe as revealed by the projection patterns of the climbing fiber system. In R. Llinas (ed): Neurobiology of Cerebellar Evolution and Development. Chicago, Illinois, AMA, pp. 525-537
Oscarsson, O. (1973) Functional organization of spinocerebellar paths. In A. Iggo (ed) Handbook of Sensory Physiology. Vol. III. Somatosensory System. New York: Springer, pp. 339-380
Oscarsson, O (1979) Functional units of the cerebellum-sagittal zones and microzones.
Trends Neurosci. 2:143-145
Robertson, L.T., and K. Logan (1986) Relationship of parasagittal bands of acetylcholinesterase activity to the climbing fiber representation.
Neurosci. Lett. 72:128-134
Robinson, D.A. (1963) A method of measuring eye movement using a scleral search coil in a magnetic field.
IEEE Trans. Biomed. Electron. B.E. 10:137-145
Robinson, D.A. (1976) Adaptive gain control of vestibulo-ocular reflex by the cerebellum.
J. Neurophysiol. 39:954-969
Ron, S., and D.A. Robinson (1973) Eye movements evoked by cerebellar stimulation in the alert monkey.
J. Neurophysiol. 36:1004-1022
Rotter, A., N.J.M. Birdsall, A.S.V. Burgen, P.A. Field, A. Smolen, and G. Raisman (1979a) Muscarinic receptors in the central nervous system of the rat. IV. A comparison of the effects of axotomy and deafferentation on the binding of 3H-propylbenzilcholine mustard and associated synaptic changes in the hypoglossal and pontine nuclei.
Brain Res. Rev. 1:207-224
Rotter, A., N.J.M. Birdsall, P.M. Field, and G. Raisman (1979b) Muscarinic receptors in the central nervous system of the rat.
II. Distribution of binding of 3H-propylbenzilcholine mustard in the midbrain and hindbrain.
Brain Res. Rev. 1:167-183
Ruigrok, T.J.H., and J. Voogd (1990) Cerebellar nucleo-olivary projections in the rat: an anterograde tracing study with Phaseolus vulgaris-leucoagglutinin (PHA-L).
J. Comp. Neurol. 298:315-333
Ruigrok, T. J. H., R.J. Osse, and J. Voogd (1992) Organization of inferior olivary projections to the flocculus and ventral paraflocculus of the rat cerebellum.
J. Comp. Neurol. 316:129-150

Saint-Cyr, J.A., and J. Courville (1979) Projection from the vestibular nuclei to the inferior olive in the cat. An autoradiographic and horseradish peroxidase study.
Brain Res. 165:189-200
Sato, Y., and N.H. Barmack (1985) Zonal organization of olivocerebellar projections to the uvula in rabbits.
Brain Res. 359:281-292
Sato, Y., and T. Kawasaki (1984) Functional localization in the three zones related to eye movement control in the cat.
Brain Res. 290:25-31
Sato, T., and T. Kawasaki (1987) Target neurons of floccular caudal zone inhibition in y-group nucleus of vestibular nuclear complex.
J. Neurophysiol. 57:460-480
Sato, Y., and T. Kawasaki (1990a) Eye movement evoked by stimulation of Purkinje cell zones of the cerebellar flocculus in the cat.
Acta Med. Biol. 38:27-35
Sato, Y., and T. Kawasaki (1990b) Operational unit responsible for plane-specific control of eye movement by cerebellar flocculus in cat.
J. Neurophysiol. 64:551-564
Sato, Y., and T. Kawasaki (1991) Identification of the Purkinje cell/climbing fiber zone and its target neurons responsible for eye-movement control by the cerebellar flocculus.
Brain Res. Rev. 16: 39-64
Sato, Y., T. Kawasaki, and K. Ikarashi (1982a) Zonal organization of the floccular Purkinje cells projecting to the vestibular nucleus in cats.
Brain Res. 232:1-15
Sato, Y., T. Kawasaki, and K. Ikarashi (1982b) Zonal organization of the floccular Purkinje cells projecting to group y of the vestibular complex and the lateral cerebellar nucleus in cats.
Brain Res. 234:430-434
Sato, Y., T. Kawasaki, and K. Ikarashi (1983a) Afferent projections from the brainstem to the three floccular zones in cats.
I. Climbing fiber projections.
Brain Res. 272:27-36
Sato, Y., T. Kawasaki, and K. Ikarashi (1983b) Afferent projections from the brainstem to the three floccular zones in cats.
II. Mossy fiber projections.
Brain Res. 272:37-48
Sato, Y., F. Yamamoto, H. Shojaka, and T. Kawasaki (1984) Pathway from floccular caudal zone contributing to vertical eye-movements in cats. Role of group y nucleus of vestibular nuclei.
Brain Res. 294: 375-380
Sato, Y., K. Kanda, and T. Kawasaki (1988) Target neurons of floccular middle zone inhibition in the medial vestibular nucleus.
Brain Res. 446:225-235
Scott, T.G. (1963) A unique pattern of localization in the cerebellum.
Nature 200:793
Scott, T.G. (1964) A unique pattern of localization within the cerebellum of the mouse.
J. Comp. Neurol. 122:1-8

Silver, A. (1967) Cholinesterases of the central nervous system with special reference to the cerebellum.
Int. Rev. Neurobiol. 10:57-109
Silver, A. (1974) The Biology of Cholinesterases. Amsterdam: Elsevier, pp. 355-388
Simpson, J.I., and K.E. Alley (1974) Visual climbing fiber input to rabbit vestibulo-cerebellum: a source of direction-specific information.
Brain Res 82:302-308
Simpson, J.I., W. Graf, and C. Leonard (1981) The coordinate system of visual climbing fibers to the flocculus. In W. Becker and A. Fuchs (eds): Progress in Oculomotor Research. Amsterdam: Elsevier, pp. 475-484
Simpson, J.I., and W. Graf (1985) The selection of reference frames by nature and its investigators. In A. Berthoz and G. Melvill Jones (eds): Adaptive Mechanisms in Gaze Control. Amsterdam, Elsevier, pp. 3-16
Simpson, J.I., W. Graf, and C.S. Leonard (1989) Three-dimensional representation of retinal image movement by climbing fiber activity. In P. Strata (ed): The Olivocerebellar System in Motor Control. Exp. Brain Res. suppl:17, New York, Springer, pp. 323-327
Simpson, J.I., C.S. Leonard and R.E. Soodak (1988) The accessory optic system of rabbit. II. Spatial organization of direction selectivity.
J. Neurophysiol. 60:2055-2072
Simpson, J.I., J. Van der Steen, J. Tan, W. Graf, and C.S. Leonard (1989) Representations of ocular rotations in the cerebellar flocculus of the rabbit. In J.H.J. Allum and M. Hulliger (eds): Progress in Brain Research. Vol. 80. Amsterdam: Elsevier, pp. 213-223
Simpson, J.I., J. Van der Steen, and J. Tan (1992) Eye movements and the zonal structure of the rabbit flocculus. In T. Llinas and C. Sotelo (eds.): The Cerebellum. Springer Verlag, pp. 255-266
Soodak, R.E. and J.I. Simpson (1988) The accessory system of rabbit.
I. Basic visual response properties.
J. Neurophysiol. 60:2037-2054
Spaçek, J. , L. Parizek, and A.R. Lieberman (1973) Golgi cells, granule cells and synaptic glomeruli in the molecular layer of the rabbit cerebellar cortex.
J. Neurocytol. 2:407-428
Stanton, G.B. (1980) Afferents to oculomotor nuclei from area "y" in Macaca mulatta: an anterograde degeneration study.
J. Comp. Neurol. 192:377-385
Stroud, B.B. (1895) The mammalian cerebellum.
J. Comp. Neurol. 5:71-118
Takeda, T., and K. Maekawa (1976) The origin of the pretecto-olivary tract.
Brain Res. 117:319-325
Takeda, T., and K. Maekawa (1980) Bilateral visual inputs to the dorsal cap of the inferior olive: differential localization and inhibitory interactions.
Exp. Brain Res. 39:461-471
Takeda, T, and K. Maekawa (1984a) Collateralized projection of visual climbing fibers to the flocculus and nodulus of the rabbit.

Neurosci. Res. 2:125-132
Takeda, T. and K. Maekawa (1984b) Dorsal cap neurons projecting to the flocculus, nodulus and uvula with axonal branches.
Neurosci. Lett. Suppl. 17: S73
Takeda, T., and K. Maekawa (1989a) Olivary branching projections to the flocculus, nodulus and uvula in the rabbit.
I. An electrophysiological study.
Exp. Brain Res. 74:47-62
Takeda, T., and K. Maekawa (1989b) Olivary branching projections to the flocculus, nodulus and uvula in the rabbit.
II. Retrograde double labeling study with fluorescent dyes.
Exp. Brain Res. 76:323-332
Tan, J., L.M. Eisenman, N.M. Gerrits, R. Hawkes, and J. Voogd (1989) Compartmentalization within the rabbit flocculus. A mab Q113 immunohistochemical, acetylcholinesterase and anatomical tracing study.
Eur. J. Neurosci. Suppl. 2:33
Tan, H., and N.M. Gerrits (1992) Laterality in the vestibulo-cerebellar mossy fiber projection to flocculus and caudal vermis in the rabbit: a retrograde fluorescent double-labeling study.
Neuroscience, 47:909-919
Thunnissen, I.E. (1990) Vestibulocerebellar and vestibulo-oculomotor relations in the rabbit.
Thesis, Rotterdam.
Thunnissen, I.E., A.H. Epema, and N.M. Gerrits (1989) Secondary vestibulocerebellar mossy fiber projection to the caudal vermis in the rabbit.
J. Comp. Neurol. 290:262-277
Trojanowski, J.Q., J.O. Gonatas, and N.K. Gonatas (1981) Conjugates of horseradish peroxidase (HRP) with cholera toxin and wheat germ agglutinin are superior to free HRP as orthogradely transported markers.
Brain Res. 223:381-385
Trott, J.R., and D.M. Armstrong (1987a) The cerebellar corticonuclear projection from lobule Vb/c of the cat anterior lobe: a combined electrophysiological and autoradiographic study.
I. Projection from the intermediate region.
Exp. Brain Res. 66:318-338
Trott, J.R., and D.M. Armstrong (1987b) The cerebellar corticonuclear projection from lobule Vb/c of the cat anterior lobe: a combined electrophysiological and autoradiographic study.
II. Projection from the vermis.
Exp. Brain Res. 68:339-358
Van der Steen, J., and H. Collewijn (1984) Ocular stability in the horizontal, frontal and sagittal planes in the rabbit.
Exp. Brain Res. 56:263-274.
Van der Steen, J., J.I. Simpson, and J. Tan (1989) Eye movements evoked from histochemically distinguished compartments of the rabbit flocculus.
Soc. Neurosci. Abstr.15:613. (abstract).

Van der Steen, J., J.I. Simpson, and J. Tan (1991) Representation of three-dimensional eye movements in the cerebellar flocculus of the rabbit. In R. Schmid and D. Zambarbieri (eds): Oculomotor Control and Cognitive Processes. Amsterdam: Elsevier, pp 63-77

Van Rossum, J (1969) Corticonuclear and corticovestibular projections of the cerebellum.
Thesis, Leiden. Assen: Van Gorcum

Voogd, J. (1964) The Cerebellum of the Cat.
Thesis, Leiden

Voogd, J. (1969) The importance of fibre connections in the comparative anatomy of the mammalian cerebellum. In R. Llinas(ed): Neurobiology of Cerebellar Evolution and Development. Chicago: A.M.A., pp.493-514

Voogd, J. (1975) Bolk's subdivision of the mammalian cerebellum. Growth centres and functional zones.
Acta Morphol. Neerl. Scand. 13:35-54

Voogd, J. (1982) The olivocerebellar projection in the cat. In S.L. Palay and V. Chan-Palay (eds): The Cerebellum: New Vistas. NewYork: Springer Verlag, pp 135-161

Voogd, J. (1989) Parasagittal zones and compartments of the anterior vermis of the cat cerebellum. In P. Strata (ed): The Olivocerebellar System in Motor Control. Exp. Brain Res. Suppl.17. New York: Springer Verlag, pp 3-19

Voogd, J., and F. Bigaré. 1980. Topographical of olivary and corticonuclear fibers in the cerebellum. A review. In J.Courville, C.C. de Montigny, and Y. Lamarre (eds): The Inferior Olivary Nucleus: Anatomy and Physiology. New York: Raven Press,pp. 207-234.

Voogd, J. and H.K.P. Feirabend (1981) Classic methods in neuroanatomy. In R. Lahue (ed): Methods in Neurobiology, Vol. 2. New York: Plenum, pp 207-234

Voogd, J., N.M. Gerrits, and E. Marani (1985) The cerebellum of the rat. In G. Paxinos (ed.): The Rat Nervous System. Vol. 2: Hindbrain and Spinal cord. London, Academic Press, pp. 251-291

Voogd, J., N.M. Gerrits, and D.T. Hess (1986) Parasagittal zonation of the cerebellum in macaques: an analysis based on acetylcholinesterase histochemistry. In M. Glickstein, C. Yeo,and J. Stein (eds): Cerebellum and Neuronal Plasticity. New York: Plenum, pp. 15-39

Voogd, J., D.T. Hess, and E. Marani (1987) The parasagittal zonation of the cerebellar cortex in cat and monkey. In J.S.King (ed): New Concepts in Cerebellar Neurobiology. Neurology and Neurobiology Vol. 22. New York: Alan R. Liss Inc., pp. 183-220

Walberg, F., N. Kotchabhakdi and G.H. Hoddevik (1979) The olivocerebellar projections to the flocculus and paraflocculus inthe cat, compared to those in the rabbit. A study using horseradish peroxidase as tracer.
Brain Res. 161:389-398

Walberg, F., T. Nordby, and E. Dietrichs (1987) The olivonodular projection: a re-examination based on folial cerebellar implants.
Neurosci. Lett. 81:82-87

Whitworth, R.H. Jr., D.E. Haines, and G.W. Patrich (1983) The inferior olive of a Prosimian primate, Galago senegalensis. II. Olivocerebellar projections to the vestibulocerebellum.
J. Comp. Neurol. 219:228-240

Yamamoto, F., Y. Sato, and T. Kawasaki (1986) The neuronal pathway from the flocculus to the oculomotor nucleus:
an electrophysiological study of group y nucleus in cats.
Brain Res. 371:350-354

Yamamoto, M. (1978) Localization of rabbit's flocculus Purkinje cells projecting to the lateral cerebellar nucleus and the nucleus prepositus hypoglossi investigated by means of the horseradish peroxidase retrograde axonal transport.
Neurosci. Lett. 7:197-202

Yamamoto, M. (1979a) Topographical representation in rabbit cerebellar flocculus for various afferent inputs from the brainstem investigated by means of retrograde axonal transport of horseradish preoxidase.
Neurosci. Lett. 12:29-34

Yamamoto, M (1979b) Vestibulo-ocular reflex pathways of rabbits and their representation in the cerebellar flocculus. In Granit, R, Pompeiano, O (eds.) : Reflex Control of Posture and Movement.
Progr. Brain Res. 50: 451-457 Amsterdam: Elsevier/North-Holland.

Yamamoto, M., and I. Shimoyama (1977) Differential localizationof rabbit's flocculus Purkinje cells projecting to the medial and superior vestibular nuclei, investigated by means of the HRP retrograde axonal transport.
Neurosci. Lett. 5: 279-283

Yamamoto, M., I. Shimoyama and S.M. Highstein (1978) Vestibular nucleus neurons relaying excitation from the anterior canal to the oculomotor nucleus.
Brain Res. 148: 31-42

Yamamura, H.I., and S.H. Snyder (1974) Muscarinic cholinergic binding in rat brain.
Proc. Natl. Acad. Sci. 71:1725-1729

8. Summary

This thesis describes the subdivision of the white matter of the rabbit flocculus and the nodulus on the basis of acetylcholinesterase (AChE) histochemistry (chapter 1), the compartmental organization of afferent pathways from the inferior olive to the flocculus and nodulus (chapter 2), the efferent pathways from the zonally organized Purkinje cells of the flocculus to the vestibular and cerebellar nuclei (chapter 3), and the characteristics of eye movements evoked by microstimulation of the rabbit flocculus (see chapter 4).

The flocculus of the cerebellum is involved in eye movement control. Several anatomical and electrophysiological studies have already indicated that the flocculus is subdivided into zones, each of which controls specific eye muscle activity. However, the zones delineated in the various studies differ in number and extent. Some of these differences are undoubtedly due to individual variations in size and number of the floccular folia. If an internal frame of reference was available to compare the histological and physiological data from individual experiments, then the problems caused by the individual variations in the morphology of the flocculus would be solved.

Our study has demonstrated that AChE reveals the presence of raphes (sheets of thin myelinated fibers) that subdivide the cerebellar white matter into compartments containing coarser fibers. The compartments in the white matter of the flocculus were studied in transverse, horizontal and sagittal sections processed for AChE. This survey included the morphology of the nodulus, the ventral paraflocculus, the floccular peduncle and the associated vestibular and cerebellar nuclei (chapter 1).

The granular layer stains most densely with AChE, while the Purkinje cells are AChE-negative. The molecular layer consists of two regions. The inner region, located close to the Purkinje cell layer stains more densely for AChE than the outer two-thirds of the molecular layer which hardly contains any AChE. This subdivision of the molecular layer is characteristic for the flocculus and the ventral paraflocculus and it

suddenly disappears at the border of the ventral and dorsal paraflocculus. The white matter of the flocculus is subdivided by 4 raphes into 5 compartments, called C_2, FC_1-FC_4 from caudolateral to rostromedial. Medially the white matter of the flocculus is delineated from the brachium pontis by a densely staining raphe, which at more caudal levels becomes less clear. The compartments FC_1-FC_4 blend together caudally and travel through group y as the floccular peduncle. Group y contains intensely AChE-stained neurons. It consists of a ventral portion of closely packed cells, forming a cap over the restiform body and a dorsal more loosely arranged portion with larger cells. Medially group y merges with the caudal pole of the superior vestibular nucleus. The ventromedial extension of the lateral cerebellar nucleus, consisting of small- and medium-sized cells (Lpc) is located dorsal to the floccular peduncle and group y.

Despite variations in number and extent of the floccular folia, the location of the raphes in the floccular white matter follows a strict pattern. This compartmentation can serve as the intrinsic framework that is required to accurately match data from anatomical tracing (see chapters 2 and 3) and electrophysiological experiments (see chapter 4) instead of using the folia and interfolial fissures as landmarks.

The flocculus receives climbing fiber input from the dorsal cap, ventrolateral outgrowth, and the rostral pole of the medial accessory olive. Visual signals are relayed via the dorsal cap and adjoining ventrolateral outgrowth. In chapter 2 WGA-HRP anterograde tracing combined with AChE histochemistry was used to find out whether the climbing fiber projection to the flocculus and the nodulus is zonally organized according to the intrinsic reference frame as described in chapter 1. Injections were placed in subsets of olivary neurons, which were identified by their electrophysiological characteristics.

The afferent climbing fiber bundle to the flocculus separates into five smaller bundles in the white matter, each of which becomes located within a compartment delineated by AChE-positive raphes. The caudal part of the dorsal cap sends its climbing fibers through compartments FC_2 and FC_4 to terminate on Purkinje cells located in longitudinal strips

of molecular layer (floccular zones FZ_{II} and FZ_{IV} respectively). Afferent fibers from the rostral part of the dorsal cap and ventrolateral outgrowth course through compartments FC_1 and FC_3 and terminate in FZ_I and FZ_{III}. Compartment C_2 contains climbing fibers from the rostral pole of the medial accessory olive (rMAO) which terminate in floccular zone C_2. The boundaries between the floccular zones are sharp and are in line with the raphes. A similar pattern is observed in the nodulus, the white matter of which is subdivided into 4 compartments, XC_1-XC_4. Injections in the caudal dorsal cap and subnucleus ß label fibers in compartments XC_1 and XC_4, which terminate as climbing fibers in the XZ_I and XZ_{IV} zones. Climbing fibers from the rostral dorsal cap and ventrolateral outgrowth terminate in zone XZ_{II} on the ventral and dorsal surface of lobule X and a central strip in XZ_{IV} (called XZ_{IV}*) via compartments XC_2 and XC_4. Injections involving the rostral MAO label XC_3 and XZ_{III} on the dorsal side of lobule X and the ventral side of lobule IX. These results show the close correspondence between the white matter compartments (FC and XC) and the Purkinje cell zones (FZ and XZ).

In chapter 3 the efferent projection of the floccular zones to the vestibular nuclei was studied with HRP retrograde tracing, WGA-HRP anterograde tracing and AChE histochemistry. As in chapter 2 the injection site was identified by the physiological properties of the different Purkinje cell zones. FZ_I and FZ_{III} project via compartments FC_1 and FC_3 to the dorsolateral part of the superior vestibular nucleus. Fibers from these compartments also appear to terminate on cells of dorsal group y. FZ_{II} and FZ_{IV} project to the medial vestibular nucleus via FC_2 and FC_4. No injections were made in zone C_2. The results are compared to observations in the previous chapter.

Chapters 1-3 show that specific subsets of olivary neurons are connected with specific Purkinje cell zones, which in turn project to specific parts of the vestibular nuclei. Furthermore, these zones correlate well with the AChE white matter compartmentation. This zonally organized pathway may serve as the basic neuronal circuitry for

differential control of eye muscle activity. Indeed, local electrical stimulation in different parts of the flocculus does elicit specific types of eye movements. The published results of earlier microstimulation studies are hampered by the variations in the morphology of the flocculus.

In chapter 4, AChE histochemistry has also been used to verify the position of stimulation sites marked by small lesions. The three-dimensional, binocular eye movements evoked by electrical microstimulation of the cerebellar flocculus of alert, pigmented rabbits were recorded using the magnetic induction coil technique. Search coils were implanted on both eyes. A voltage was induced in the coils by placing them in a alternating magnetic field and changes in the induced voltage indicated the displacement of the eyes. Eye movements were registered with reference to an orthogonal coordinate system consisting of a vertical axis and two horizontal axes at 45° and 135° azimuth. The azimuth coordinate was taken to increase to both sides from the 0° reference in the direction of the nose. Eye movements were most readily evoked by stimulation (0.2 msec pulses at 200 Hz for 1 sec, intensity 20 μA or less) at loci in the deep granular layer and the white matter. They consisted of slow (5-20°/sec) movements. The responses occurred either in both eyes, with the eye ipsilateral to the stimulated flocculus usually having the largest amplitude, or were restricted to the ipsilateral eye. The evoked responses were classified according to the combination of the largest measured component of rotation and its sense of rotation (clockwise, CW, or counterclockwise, CCW). Seventy-eight percent of the evoked eye movements could be placed in one of two classes. For one of these classes, the largest response component was an abduction of the ipsilateral eye about its vertical axis (19%), whereas for the other class the largest response component was a CCW rotation of the ipsilateral (left) eye about its 135° axis (59%).

The two main classes of three-dimensional eye movements are differentially associated with anatomical compartments revealed by acetylcholinesterase histochemistry. Eye movements were elicited with stimulation of the three largest compartments in the floccular white matter (FC_1, FC_2, and FC_3). The middle of these three compartments

(FC_2) is associated with the vertical axis class of movements, whereas the two adjacent compartments (FC_1 and FC_3) are associated with the 135° class of eye movements. The relation of the two other, smaller compartments (C_2 and FC_4) was not determined.

The orientations of the rotation axes of the two main classes of eye movements correspond to those of the preferred axes of the visual climbing fiber input to the flocculus, which suggests that both are organized in a similar coordinate system. The spatial orientation of the axes of this coordinate system bears a close resemblance to that of the axes of the semicircular canals and to that of the rotation axes of particular pairs of eye muscles.

The association of distinct classes of eye movements and climbing fiber afferents with the anatomically distinguishable compartments suggests that the rabbit flocculus consists of anatomically definable modules that constitute the structural correlate of a coordinate system used by the brain to control compensatory eye movements.

9. Samenvatting

Dit proefschrift beschrijft een onderzoek naar de indeling van de witte stof en de schors van de flocculus en de nodulus in het cerebellum van het konijn op grond van het voorkomen van het enzym acetylcholinesterase (AChE) (hoofdstuk 1), de organisatie van afferente verbindingen van de oliva inferior naar de flocculus en nodulus (hoofdstuk 2), de efferente verbindingen van de flocculus naar de vestibulaire en cerebellaire kernen (hoofdstuk 3), en de karakteristieken van oogbewegingen die door microstimulatie van de flocculus kunnen worden opgewekt (hoofdstuk 4).

De flocculus van het cerebellum speelt een belangrijke rol bij de controle van oogbewegingen. Diverse anatomische en elektrofysiologische studies hebben reeds aangetoond, dat de flocculus in anatomisch afgrensbare zones is verdeeld. Er bestaan echter grote verschillen in aantal en grootte van deze zones tussen de verschillende studies. Waarschijnlijk worden deze verschillen in de hand gewerkt door individuele variaties in het aantal folia en de grootte en vorm van de folia van de flocculus. Met behulp van een intrinsiek referentie kader zouden de anatomische en fysiologische data van verschillende experimenten kunnen worden vergeleken en zouden de problemen, die ontstaan door de individuele variatie in de morfologie van de flocculus zijn opgelost.

Hersenmateriaal, dat gekleurd wordt met een enzym histochemische methode voor acetylcholinesterase (AChE), laat een bijzonder patroon zien, waarbij dunne raphes, die uit dunne AChE-positieve vezels bestaan, de witte stof van het cerebellum verdelen in compartimenten, waarin dikkere vezels, die niet met AChE kleuren, zijn gelegen. In hoofdstuk 1 concentreerde het onderzoek zich op de vraag of de witte stof van de flocculus in het konijn met behulp van deze techniek in compartimenten verdeeld zou kunnen worden. Hiervoor werden hersenen van konijnen in transversale, horizontale en sagittale coupes gesneden en gekleurd voor AChE. Het onderzoek richtte zich tevens op de morfologie van de ventrale paraflocculus, de pedunculus van de flocculus en daaraan gerelateerde vestibulaire en cerebellaire kernen.

De sterkste aankleuring voor AChE wordt gezien in de granulaire laag, terwijl Purkinje cellen ongekleurd blijven. De moleculaire laag lijkt uit twee delen te bestaan, waarvan het binnenste eenderde deel, dat tegen de Purkinje cellaag is gelegen, relatief hard aankleurt in vergelijking met het buitenste tweederde deel, dat haast geen AChE bevat. Dit patroon wordt gevonden in de flocculus en de ventrale paraflocculus en verdwijnt abdrupt op de grens van de ventrale met de dorsale paraflocculus. De witte stof van de flocculus wordt van het brachium pontis gescheiden door een sterk AChE-positieve raphe, die caudaal minder duidelijk wordt. De witte stof zelf wordt door 4 raphes verdeeld in 5 compartimenten. Deze compartimenten worden van caudolateraal naar rostromediaal benoemd als C_2, FC_1-FC_4. Caudaal versmelten de compartimenten FC_1-FC_4 en vormen zij de pedunculus van de flocculus. Deze verloopt door groep y van de vestibulaire kernen in de richting van de caudale pool van de nucleus vestibularis superior. De celgroep y bestaat uit een ventrale, compacte laag van cellen, die een kapje vormen, over het corpus restiforme, en een dorsale subnucleus met grotere, spoelvormige cellen tussen de vezels van de pedunculus flocculi. Alle neuronen van de groep y kleuren sterk voor AChE. Groep y grenst aan de dorsale zijde aan de ventromediale uitloper van de laterale cerebellaire kern, die kleine en middelgrote cellen bevat (Lpc). Mediaal versmelt groep y met de superior vestibulaire kern.

Ondanks individuele verschillen in aantal en grootte van de folia van de flocculus behouden de raphes in de witte stof van de flocculus hun positie. Deze onderverdeling in compartimenten wordt in dit proefschrift als intrinsiek referentiekader gebruikt voor de vergelijking van topografische gegevens, verkregen via anatomische tracing (zie hoofdstukken 2 en 3) en elektrofysiologisch onderzoek (zie hoofdstuk 4). Deze methode is veel nauwkeuriger dan de plaatsbepaling ten opzichte van folia en interfoliale fissuren zoals tot dusver gebruikelijk was.

De flocculus ontvangt klimvezels afkomstig van de volgende subnuclei van de onderste olijf: de dorsal cap, de ventrolateral outgrowth en de rostrale pool van de mediale bijolijf. De dorsal cap en de ventrolateral outgrowth ontvangen optokinetische informatie uit de kern

van de tractus opticus en de kernen van de accessoire tractus opticus in het mesencephalon. In hoofdstuk 2 werd anterograde tracing met WGA-HRP, gecombineerd met AChE histochemie, gebruikt om na te gaan of de klimvezelprojectie naar de flocculus en de nodulus een zonale indeling kent, die zich houdt aan het in hoofdstuk 1 beschreven intrinsieke referentie kader. Bij het maken van de injecties met WGA-HRP werden de subnuclei van de oliva inferior geïdentificeerd aan de hand van hun fysiologische karakteristieken.

De hoofdbundel van klimvezels naar de flocculus splitst zich in 5 kleinere bundels. Elk van deze bundels bezet een compartiment, dat begrensd is door AChE-positieve raphes. Het caudale deel van de dorsal cap stuurt klimvezels via compartimenten FC_2 en FC_4, terwijl afferente vezels vanaf het rostrale deel van de dorsal cap en de ventrolateral outgrowth gebruik maken van compartimenten FC_1 en FC_3. Compartiment C_2 bevat klimvezels afkomstig van de rostrale mediale bijolijf (rMAO). De vezels binnen elk compartiment eindigen in een nauwkeurig af te bakenen longitudinale strook van de moleculaire laag (flocculus zones C_2, FZ_I-FZ_{IV}). De begrenzing van deze stroken is scherp en ligt in het verlengde van de raphes. Eenzelfde patroon is aanwezig in de nodulus met 4 compartimenten in de witte stof, compartimenten XC_1-XC_4. Injecties in het caudale deel van de dorsal cap en nucleus ß laten gelabelde vezels zien in compartimenten XC_1 en XC_4, welke als klimvezels eindigen in zones XZ_I en XZ_{IV} van de nodulus. Klimvezels uit het rostrale deel van de dorsal cap en de ventrolateral outgrowth eindigen via compartimenten XC_2 en XC_4 in zone XZ_{II} op het ventrale en dorsale gedeelte van lobulus X en in een centrale strip binnen zone XZ_{IV}. Injecties, die de rMAO meenemen, sturen hun vezels via compartiment XC_{III} naar zone XZ_{III} op de dorsale zijde van lobulus X en de ventrale zijde van lobulus IX. Deze bevindingen laten zien dat elk van de witte stof compartimenten (FC en XC) aan een bepaalde Purkinje cel zone (FZ en XZ) is gerelateerd.

In hoofdstuk 3 werd de efferente projectie van de zones in de flocculus naar de vestibulaire kernen bestudeerd met behulp van HRP

retrograde tracing, WGA-HRP anterograde tracing, en AChE histochemie. Evenals in hoofdstuk 2 werden de injectieplaatsen bepaald aan de hand van de fysiologische karakteristieken van de verschillende Purkinje cell zones. De zones FZ_I en FZ_{III} sturen axonen via compartiment FC_1 en FC_3 naar het dorsolaterale gedeelte van de nucleus vestibularis superior. Vezels behorende bij deze compartimenten lijken ook te eindigen in groep y. Op vergelijkbare wijze projecteren FZ_{II} en FZ_{IV} naar de mediale vestibulaire kern via FC_2 en FC_4. Geen van de injecties was gelokaliseerd binnen C_2. De resultaten werden vergeleken met die van het vorige hoofdstuk.

In hoofdstukken 1-3 wordt beschreven hoe subgroepen binnen de oliva inferior in contact komen met specifieke Purkinje cel zones, die op hun beurt projecteren naar subgroepen binnen de vestibulaire kernen. Deze zones zijn morfologisch geassocieerd met specifieke compartimenten in de witte stof. Deze zonale verbindingen zouden het neuronale substraat kunnen zijn van gedifferentieerde controle over oogspier activiteit door de flocculus. Lokale elektrische stimulatie in de flocculus veroorzaakt verschillende typen oogbewegingen. Alweer blijkt, dat een consistente interpretatie van de resultaten van dergelijke experimenten verstoord wordt door de variabele morfologie van de flocculus. Zodoende werd AChE histochemie ook in hoofdstuk 4 ingezet om de relatieve plaatsing van de stimuluslocaties, die gemerkt werden door kleine lesies, te verifiëren.

De drie-dimensionale, binoculaire oogbewegingen, die door electrische microstimulatie van de flocculus van het cerebellum in wakkere gepigmenteerde konijnen konden worden opgewekt, werden geregistreerd met behulp van de magnetische inductie methode. Op beide ogen werden inductiespoeltjes geïmplanteerd op de sclerae. Geplaatst in een homogeen magnetisch veld zal er bij een oogbeweging een spanning worden geïnduceerd binnen de spoeltjes. Veranderingen in deze spanning zijn direct gerelateerd aan de grootte en de richting van de oogbeweging.

Voor de beschrijving van de oogbewegingen werd een orthogonaal

referentiekader bestaande uit een verticale as en twee horizontale assen gebruikt. De horizontale assen maken een hoek van 45° en 135° met de rostraal gerichte 0° as.

Oogbewegingen konden het gemakkelijkst worden opgewekt door te stimuleren (0,2 msec pulsen bij 200 Hz gedurende 1 sec, ≤ 20 μA) in de diepe granulaire laag en de witte stof. De oogbewegingen waren vrij langzaam (5-20°/sec). Beide ogen reageerden op de stimulus, waarbij het oog, dat ipsilateraal was gelokaliseerd ten opzichte van de gestimuleerde flocculus, doorgaans de grootste amplitude had. Soms waren de oogbewegingen uitsluitend ipsilateraal gelokaliseerd. De oogbewegingen werden geclassificeerd aan de hand van de grootste oogbewegingscomponent en de richting van de rotatie (met de klok mee, CW, of tegen de klok in, CCW). Achtenzeventig procent van de geregistreerde oogbewegingen kon worden geplaatst in één van twee groepen. In één van de groepen bestond de grootste respons uit een abductie van het ipsilaterale oog rondom de verticale as (19%), terwijl voor de andere groep (59%) de grootste component een CCW rotatie was van het ipsilaterale (linker) oog rondom de ipsilaterale 135° as.

Deze twee voornaamste groepen van drie-dimensionale oogbewegingen zijn nauw geassocieerd met de anatomische compartimenten, die met behulp van AChE histochemie kunnen worden begrensd. Voor de drie grootste van de vijf compartimenten (FC_1, FC_2 en FC_3) zijn stimulatie gegevens beschikbaar. De middelste van deze 3 (FC_2) is gerelateerd aan de eerste groep, met rotaties rond de verticale as, de twee flankerende compartimenten (FC_1 en FC_3) zijn betrokken bij rotaties rond de 135° as uit de tweede groep. De functionele betekenis van de twee andere, kleinere compartimenten (C_2 en FC_4) kon niet worden vastgesteld.

De orientatie van de rotatie-assen voor oogbewegingen, opgewekt door stimulatie van een bepaald compartiment, komt overeen met de richting van de rotatie-assen voor bewegingen van de omgeving, die een optimale respons uitlokken in de klimvezels die eindigen op Purkinje cellen van de corresponderende zone. Dit suggereert, dat de flocculus uit

modules is opgebouwd die voor hun klimvezel input en hun output hetzelfde coordinaten systeem hanteren. De positie van deze assen komt goed overeen met de positie van de assen van de halfcirkelvormige kanalen en met die van bepaalde oogspier paren. Elke module, met zijn eigen set van aanvoerende en afvoerende verbindingen, representeert oogbewegingen rond een bepaalde as.

Het verband, dat werd aangetoond tussen bepaalde klassen oogbewegingen, klimvezel afferenten en Purkinje cel efferenten met anatomische compartimenten, maakt het waarschijnlijk dat de flocculus uit modules bestaat, die het structurele correlaat vormen van een coordinaten systeem, dat door de hersenen wordt gebruikt bij de controle van compensatoire oogbewegingen.

10. Dankwoord

Bij deze wil ik degenen bedanken, die de basis vormden van dit proefschrift.

Mijn vader, die tegen een ziekte opliep, die mijn interesse in hersenonderzoek opwekte. Zijn strijd tegen ziekte en zijn belangstelling voor onderwijs zullen in mij voortleven.
Mijn moeder met haar nimmer aflatende belangstelling en aanmoedigingen als er weer eens een dip naderde, een echte moeder.

Mijn promotoren,
Beste Jan, na een sputterende start en een langdurige inhaalmaneuvre is het er toch nog van gekomen. Je enorme anatomische kennis en niet te evenaren tekenkunsten zullen mij voor altijd bijblijven.
Dear Jerry, this research project gained momentum after you put your weight behind it. Without your physiological knowledge and your willingness to invest time to study the anatomical side, this project would have been less "functional". Your love for big and small ants stretched my patience, but really polished up the goods. I am glad we shared other interests, such as the visual, olfactory, and gustatory input to the brain. I hope we will be able to continue sharing these life events in the future.
Beste Hans, hoofdstuk 4 zou niet bestaan zonder jouw technische kwaliteiten, je nuchtere aanpak en de vele slaapverwekkende uren die we in het donker samen met Jerry hebben doorgebracht.
Beste Henk, dank voor het plaats nemen in de leescommissie en voor je suggesties om tegenstrijdigheden uit de weg te ruimen.

De analisten,
Eddie "De Walm" Dalm, zonder jouw operatieve en fotografische kwaliteiten en bereidheid om buiten kantooruren door te werken zou dit proefschrift nog jaren op zich hebben laten wachten. Meestal werden deze kwaliteiten begeleid door rookwolken. Zodoende zou ik zeggen, tot ziens bij de KNO.
Hans van der Burg, je geduld en technisch vernuft heeft ervoor gezorgd, dat peperdure onwerkzame fabrieksapparatuur vervangen kon worden door handzame eigenfabricaten, die wel voldoen. Zonder jouw "puff' geval zouden hoofdstukken 2 en 3 niet geschreven zijn.
Rob Boer, jouw speurtocht naar de juiste verhoudingen en ingredienten stond aan de basis om de AChE histochemie en de HRP-gel techniek van de grond te krijgen. Je plakwerk was perfect.
Hennie Klink, Peter Elfferich, Erika Goedknegt, jullie hebben samen met Rob tienduizenden coupes gesneden, geTMBd, geDABd, geAChEd, geHäggqvist, gedroogd, opgeplakt, ontwaterd, tegengekleurd met cresylviolet, neutraal rood, gexylold, gePermount, afgedekt enz. enz.....
De ware ruggegraat van dit proefschrift ligt in deze handelingen.
Paula van Alphen, de creatieve fotografe wiens werk altijd sublieme kwaliteit vertoonde
Corlinda Bongers, een te WOW afscheidscadeau.

Edith Klink, de elegante en charmante spil van de afdeling. Jouw typewerk en flexibele geest heeft me gelukkig veel tijd opgeleverd (die ik anders onder andere kwijt was geweest aan het ontcijferen van Jan's handschrift).

Gert Holstege, samen met wijlen Prof. H. Kuijpers, heeft hij mij toen ik studentassistent neuro-anatomie bij hem was, in de eerste plaats enthousiast gemaakt over het fenomeen hersenen. Zijn manier van lesgeven maakt hem uniek, wat deels in mijn stijl van onderwijs geven nog altijd doorklinkt.

Joan Holstege, als ik een beetje in de put zat was je er. Dank je voor je gezelschap, zeker voor de uren buiten de gebruikelijke kantoortijden.
Dr L. Eisenman, dear Len, I would like to thank you for your hospitality during my stay at your department in Philadelphia. It was the feeding time of my life. I will be back.

Verder wil ik alle vrienden en kennissen bedanken voor hun aandacht en steun, in het bijzonder Judith (paranimf), Thea (paranimf), Jacqueline, Rob, Harold, Astrid, Steven Jobs, Enzo Ferrari, Antonio Carlos Jobim en Star Trek.

Niet bedankt worden de makers van Tristan Pinball, Space Quest, Wolf3D, Sub, Spectre, Crystal Quest, Paratrooper, PacMan, Apache Strike Mission, F-16 Falcon, Chessmaster, The Fool's Errant, MS-DOS enz....

11. Curriculum vitae

De auteur van dit proefschrift werd geboren op 20 september 1962 te Jogjakarta in Indonesië. Het eindexamen gymnasium ß werd afgelegd in 1980 aan het Erasmiaans gymnasium te Rotterdam. Vervolgens studeerde hij geneeskunde aan de Erasmus Universiteit Rotterdam, alwaar in 1985 het doctoraal examen werd behaald. In 1983 koos hij neuro-anatomie als keuzeprakticum en bleef tot 1986 als student-assistent/wetenschappelijk onderzoeker aan de afdeling Anatomie verbonden. Vanaf 1986 tot 1991 was hij in dienst als AIO (assistent in opleiding) bij deze afdeling, waar het onderzoek werd verricht dat tot dit proefschrift heeft geleid. In de periode 1991-1992 doorliep hij alsnog de senior co-schappen. Dit werd afgerond met het behalen van de artsenbul in juli 1992. Sinds september 1992 is hij werkzaam als arts-assistent op de afdeling KNO/Hoofd-hals chirurgie van het Academisch Medisch Centrum te Amsterdam (sinds oktober 1993 in opleiding).

12. List of publications

- Mesencephalic projections to the facial nucleus in the cat.
  An autoradiographical tracing study. G. Holstege, J. Tan, J. J. van Ham, and A. Bos.
  Brain Research 311 (1984) 7-22
- Afferent projections to the orbicularis oculi motoneuronal cell group.
  An autoradiographical tracing study in the cat. G. Holstege, J. J. van Ham, and J. Tan.
  Brain Research 374 (1986) 306-320
- Anatomical observations on the afferent projections to the retractor bulbi motoneuronal cell group and other pathways possibly related to the blink reflex in the cat. G. Holstege, J. Tan, J.J. van Ham, and G. A. Graveland.
  Brain Research 374 (1986) 321-334
- Anatomical evidence that the pontine lateral tegmental field projects to lamina I of the caudal spinal trigeminal nucleus and spinal cord and to the Edinger-Westphal nucleus in the cat. J. Tan and G. Holstege.
  Neuroscience Letters 64 (1986) 317-322
- Supraspinal control of motoneurons innervating the striated muscles of the pelvic floor including urethral and anal sphincters in the cat. G. Holstege and J. Tan.
  Brain 110 (1987) 1323-1344
- Anatomic observations on afferent projections of orbicularis oculi and retractor bulbi motoneuronal cell groups and other pathways possibly related to the blink reflex in the cat. G. Holstege, J. Tan, and J.J. van Ham.
  In: Cellular Mechanisms of Conditioning and Behavioral Plasticity (C.D. Woody, D.L. Alkon, and J.L. McGaugh eds). New York, Plenum Publishing Corporation, pp. 273-286 (1988)
- Projections from the red nucleus and surrounding areas to the brain stem and spinal cord in the cat. An HRP and autoradiographical tracing study. G. Holstege and J. Tan.
  Behavioural Brain Research 28 (1988) 33-57
- Representations of ocular rotations in the cerebellar flocculus of the rabbit. J.I. Simpson, J. van der Steen, J. Tan, W. Graf, and C.S. Leonard.
  In: Progress in Brain Research Volume 80 (J.H.J. Allum and M. Hülliger (eds). Amsterdam, Elsevier, pp. 213-223 (1989)
- Representation of three-dimensional eye movements in the cerebellar flocculus of the rabbit. J. van der Steen, J.I. Simpson, and J. Tan.
  In: Oculomotor Control and Cognitive Processes (R. Schmid and D. Zambarbieri eds). Amsterdam, Elsevier, pp 63-77
- Eye movements and the zonal structure of the rabbit flocculus.
  J.I. Simpson, J. van der Steen, and J. Tan
  In: Cerebellum Revisited (R. Llinas, C. Sotelo eds). Springer, Heidelberg, pp. 255-266 (1992)

- Reference frames of the rabbit flocculus.
  J.I. Simpson, J. van der Steen, and J. Tan
  In: Vestibular and Brain Stem Control of Eye, Head, and Body Movements (H. Shimazu, Y. Shinoda, eds.). Karger, Tokyo, pp.301-313 (1992)
- Binding of the ligand 3H-MK 801 to the glutamate NMDA receptor during acute hepatic encephalopathy and during ammonia infusion simulating acute hepatic encephalopathy. R.J. de Knegt, S.W. Schalm, J. Kornhuber, P. Riederer, and J. Tan.
  Metabol. Brain Dis. 8:81-94

chapter 1= White matter compartmentation in the flocculus of the rabbit. An acetylcholinesterase histochemical study. J. Tan, J.I. Simpson, and J. Voogd
J. Comp. Neurol. submitted

chapter 2= Zonal organization of the climbing fiber projection to the rabbit flocculus. J. Tan, J.I. Simpson, R. Nanhoe, N.M. Gerrits, and J. Voogd
J. Comp. Neurol. submitted

chapter 3= Zonal organization of the flocculo-vestibular nucleus projection in the rabbit. J. Tan, J.I. Simpson, N.M. Gerrits, and J. Voogd
J. Comp. Neurol. submitted

chapter 4= The functional and anatomical organization of three-dimensional eye movements in rabbit cerebellar flocculus. J. van der Steen, J.I. Simpson, and J. Tan.
J. Neurophysiol. submitted